Graduate School Form 9
(Revised 7/94)

PURDUE UNIVERSITY
GRADUATE SCHOOL
Thesis Acceptance

This is to certify that the thesis prepared

By James J. Chambers

Entitled Use of Conformationally-Restricted Analogues and Homology Modeling to Provide Insight Into the Nature of the 5-HT_{2A} Receptor Agonist Binding Site

Complies with University regulations and meets the standards of the Graduate School for originality and quality

For the degree of Doctor of Philosophy

Signed by the final examining committee:

David E. Nichols, Chair

Mark Gilbert

Mark Cushman

Richard B. Silverman

Approved by: Richard B. Silverman 9/12/02
Department Head Date

☐ is
This thesis ☑ is not to be regarded as confidential. David E. Nichols
Major Professor

Format Approved by:

David E. Nichols or
Chair, Final Examining Committee Thesis Format Adviser

USE OF CONFORMATIONALLY-RESTRICTED ANALOGUES AND HOMOLOGY MODELING TO PROVIDE INSIGHT INTO THE NATURE OF THE 5-HT_{2A} RECEPTOR AGONIST BINDING SITE

A Thesis

Submitted to the Faculty

of

Purdue University

by

James Joseph Chambers

In Partial Fulfillment of the

Requirements for the degree

of

Doctor of Philosophy

May 2002

ProQuest Information and Learning Company
300 North Zeeb Road
P.O. Box 1346
Ann Arbor, MI 48106-1346

To Rebecca

ACKNOWLEDGEMENTS

I would like to extend deep gratitude to Dr. David E. Nichols for his support, guidance, understanding, and encouragement during my years of doctoral study. Being a member of the Nichols group has been a very intellectually rewarding experience. Also, I would like to thank the members of my thesis advisory committee, Drs. Mark S. Cushman, Richard F. Borch and Mark A. Lipton, for their time and helpful suggestions during my studies.

I would also like to thank all of the current and past members of the Nichols research group for their help, time, and understanding. Of this group, I am especially indebted to Dr. Deborah Kurrasch-Orbaugh, Jason Parrish, Dr. Danuta Marona-Lewicka, and Niels Jensen for their collective pharmacological and behavioral efforts to characterize my target compounds. I sincerely appreciate their efforts and sacrifice and wish them the best. I am also grateful for the suggestions and direction that I received from Dr. Carol Post and Elif Ozkirimli concerning molecular modeling studies.

Finally, I would like to thank Rebecca, my family, and my friends for their support and encouragement during the difficult times and reminding me that balance is a necessity to achieve in science and life alike.

TABLE OF CONTENTS

Page

LIST OF TABLES

LIST OF FIGURES

Figure Page

Figure Page

LIST OF ABBREVIATIONS

Å = Ångstrom(s)

AcOH = acetic acid

AIBN = 2,2'-azobisisobutyronitrile

Ar = aryl, aromatic

Bu = butyl

°C = degree centigrade

CIMS = chemical ionization mass spectrometry

CNS = central nervous system

conc. = concentrated

DDQ = 2,3-dichloro-5,6-dicyano-1,4-benzoquinone

dec. = decompose(d)

DMF = *N*,*N*-dimethylformamide

DMSO = dimethyl sulfoxide

Et = ethyl

Et_2O = diethyl ether

EtOH = ethanol

g = gram(s)

GDP = guanosine diphosphate

GTP = guanosine triphosphate

GPCR = G-protein-coupled receptor

h = hour(s)

HPLC = high performance liquid chromatography

5-HT = 5-hydroxytryptamine, serotonin

Hz = Hertz

IP_3 = inositol triphosphate

LSD = *d*-lysergic acid *N*,*N*-diethylamide

M = molar

MAO = *monoamine oxidase*

Me = methyl

MeOH = methanol

mg = milligram(s)

min = minute(s)

mL = milliliter(s)

μM = micromolar

mM = millimolar

mmol = millimole(s)

mol = mole(s)

mp = melting point

m/*z* = mass to charge ratio

N = normal

nM = nanomolar

nmol = nanomole(s)

NMR = nuclear magnetic resonance

ppm = parts per million

ps = picosecond(s)

psi = pounds per square inch

RMS = root mean squared

RMSD = root mean squared deviation

RT = room temperature

SAR(s) = structure-activity relationship(s)

SEM = standard error of the mean

THF = tetrahydrofuran

TLC = thin layer chromatography

TM = transmembrane

tosyl = *p*-toluenesulfonyl

μg/kg = microgram per kilogram of body weight

Key to one-letter amino acid abbreviations used in text:

A = ala = alanine

C = cys = cysteine

D = asp = aspartic acid

E = glu = glutamic acid

F = phe = phenylalanine

G = gly = glycine

H = his = histidine

I = ile = isoleucine

K = lys = lysine

L = leu = leucine

M = met = methionine

N = asn = asparagine

P = pro = proline

Q = gln = glutamine

R = arg = arginine

S = ser = serine

T = thr = threonine

V = val = valine

W = trp = tryptophan

Y = tyr = tyrosine

ABSTRACT

Chambers, James Joseph. Ph.D., Purdue University, May 2002. Use of Conformationally-Restricted Analogues and Homology Modeling to Provide Insight Into the Nature of the 5-HT_{2A} Receptor Agonist Binding Site. Major Professor: David E. Nichols.

Efforts to understand better the serotonin-2A (5-HT_{2A}) receptor were concentrated on the characterization of the structural and chemical features of the agonist binding site. Design and synthesis of conformationally-restricted analogues of known 5-HT_{2A} receptor agonists, coupled with a homology-based model of the 5-HT_{2A} receptor that was developed during these studies, has enabled a more detailed understanding of the site. Conformationally-restricted analogues **6** and **7**, designed to incorporate in their structure an oxygen-pattern that is atypical of hallucinogenic arylalkylamines, were synthesized and found to have K_i values for [^{125}I]-DOI-labeled 5-HT_{2A} cloned rat receptors of 6.3 and 1.8 nM, respectively. Next, a series of substituted tetrahydronaphthofurans was designed and synthesized in an attempt to constrain the 2-aminoalkyl substituent of arylalkylamines to an anti-periplanar orientation, hypothesized to be the physiologically relevant conformer for binding to the 5-HT_{2A} receptor. These compounds were tested using in vitro assays, for their affinity and efficacy at selected 5-HT receptors. The benzofuran-containing analogues, **11** and **14**, had significantly higher affinity for the serotonin receptors than the benzodihydrofuran-containing compounds, **9**, **10**, **12** and **13**.

The compound (8-bromo-6-methoxy-4,5-dihydro-3H-naphtho[1,8-*bc*]furan-5-yl)amino-methane, **14**, had K_i values for [^{125}I]-DOI-labeled 5-HT_{2A} and 5-HT_{2C} cloned rat receptors of 2.6 and 1.1 nM, respectively. Despite their high affinity, the compounds of this naphthofuran series were found to lack full intrinsic activity at the 5-HT_{2A} receptor.

A 5-HT_{2A} receptor homology model was produced utilizing an *in silico* activated form of the rhodopsin protein as the structural core for the homology model. The computer model has offered distinct binding modes for ergolines, tryptamines, and arylalkylamines, the three main drug families that affect this receptor, that are compatible with the known SARs of these drug classes. A conformationally-restricted analogue of mescaline was designed based on analysis of the computer model. The resulting compound **17**, (2,3-dihydro-4,5,6-trimethoxy-1H-inden-1-yl)aminomethane, was found to possess 3-fold higher affinity and equal efficacy at the 5-HT_{2A} receptor when compared to the parent compound, mescaline. This compound, **17**, was also tested in a drug discrimination paradigm and found to substitute fully for LSD, thus validating the predictive power of the receptor model.

INTRODUCTION

Over the past five decades, a body of research on the physiological role of serotonin (5-HT) has accumulated. Receptors for this endogenous neurotransmitter have been found in many tissues throughout the human body, with significant populations of receptors in the gastrointestinal tract and the central and peripheral nervous systems. Modern molecular biology techniques have led to the discovery of fourteen different receptor isoforms for 5-HT with the possibility of a different physiological role for each.[1] The number of different 5-HT receptors as well as the fact that 5-HT is found in a range of species, from archaic plants to humans, suggest that 5-HT is an evolutionarily old and important endogenous compound.[2]

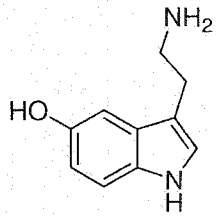

5-HT

In the 1930's, Erspamer's discovery that enterochromaffin cells could be stained with an indole-specific reagent marked the beginning of research into 5-HT, or *enteramine*, as it was known at the time. The highest concentrations of *enteramine* were found in cells of the gastrointestinal tract, platelets, and, to a lesser extent, cells of the

CNS.[3] A decade after the discovery of this endogenous compound, it was chemically identified by Rapport and Page and physiologically characterized as the major vasoconstrictor in blood.[4] *Enteramine* was renamed serotonin when the two compounds were shown to be identical.[5]

The interesting vasoconstricting properties of 5-HT garnered interest in the medical community, and soon after, the study of the physiological effects of 5-HT led to the hypothesis that the psychotic behaviors exhibited by certain intestinal tumor patients were caused by metabolites of 5-HT or naturally occurring 5-HT analogues. Synthetic variants of 5-HT were, at the time, known to exhibit a variety of central or peripheral pharmacological activities. The behaviors exhibited by these patients suggested that their symptoms were similar to hallucinogen-induced effects. Measurement of the excretion levels of the main 5-HT metabolite, 5-hydroxyindoleacetic acid, has shown that intestinal tumor patients overproduced 5-HT. Excreted levels of this metabolite for these patients was on the order of several hundred milligrams daily, a quantity in vast excess of the 2-10 mg excreted daily by healthy individuals.

In 1954, Wooley and Shaw observed that there were similarities between the chemical structures of 5-HT and LSD (*d*-lysergic acid *N*,*N*-diethylamide); in fact, most of the 5-HT structure can be found embedded within LSD (shown later as thick bonds).[6] Because a symptom of schizophrenia is hallucinations, these researchers proposed that the pathophysiology of schizophrenia might operate through a 5-HT-mediated mechanism. The finding that some patients with intestinal tumors exhibited tumor-induced psychoses supported the hypothesis that 5-HT might be utilized physiologically as a CNS neurotransmitter, in addition to its role as a vasoconstrictor.[7] Soon, the

biosynthetic and degradation pathways of 5-HT were identified and other researchers proposed similar involvement for 5-HT in schizophrenia, although it rapidly became clear that there were differences between LSD intoxication and the hallucinations experienced by schizophrenic patients.[8-11] Nevertheless, because most of the typical antipsychotic drugs of the time were thought to act through dopamine receptors, interest in a 5-HT-based pathophysiology for schizophrenia waned. Awareness of an underlying role for 5-HT in schizophrenia only resurfaced some years later after the discovery of Clozapine, an effective antipsychotic drug that was free of the extrapyramidal side effects common to the typical antipsychotic drugs of the day.[12] Clozapine was found to modulate 5-HT levels and also to down-regulate receptors of the 5-HT_2 subfamily.[13,14] Today, a large number of clinically efficacious psychotherapeutics for the treatment of schizophrenia, generally termed atypical antipsychotic drugs, are available and have markedly improved the treatment of schizophrenia. Many of these atypical antipsychotic drugs display high affinity for the 5-HT_2 receptor subfamily, consistent with the postulated role for 5-HT in the pathophysiology of schizophrenia.[15]

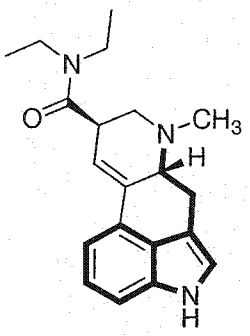

LSD

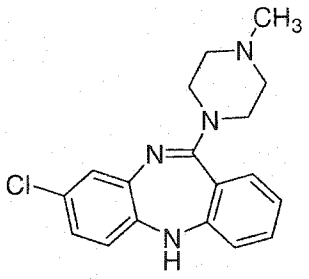

Clozapine

Serotonin and the Central Nervous System

Serotonin Synthesis and Metabolism

5-HT is produced in neurons from the essential amino acid L-tryptophan (Figure 1). Active transport of L-tryptophan into the brain is mediated by a carrier protein that also operates as the carrier for other large, branched, and neutral amino acids. Brain-levels of L-tryptophan are therefore influenced not only by the plasma concentration of L-tryptophan, but also by the concentrations of competing substrates for this carrier protein. Once L-tryptophan has gained entry to the brain, *tryptophan hydroxylase* adds a hydroxyl group to the 5-position of L-tryptophan to yield L-5-hydroxytryptophan. This hydroxylation process is the rate limiting step in the biosynthesis of 5-HT and has been the target of a few therapeutic agents.[16-18] L-*Aromatic amino acid decarboxylase* then transforms L-5-hydroxytryptophan into 5-HT.

The biological actions of 5-HT are terminated by either metabolism or reuptake into the neuron. Metabolic degradation is accomplished by *monoamine oxidase* (MAO), which acts to convert 5-HT to 5-hydroxyindoleacetaldehyde. This aldehyde is then

oxidized to 5-hydroxyindoleacetic acid by ubiquitous *aldehyde dehydrogenase*. The acid is actively transported out of the brain by a transporter protein and is quickly eliminated by excretion. Reuptake of 5-HT into a neuron occurs through an active transport mechanism mediated by a Na^+-dependent 5-HT-transporter protein. This transporter is localized on the outer membrane of the presynaptic axon terminal where it functions to remove 5-HT from the synapse following an action potential-mediated 5-HT release. Residual 5-HT that escapes degradation and reuptake by the presynaptic 5-HT transporter is taken up from the blood by platelets where it may accumulate.

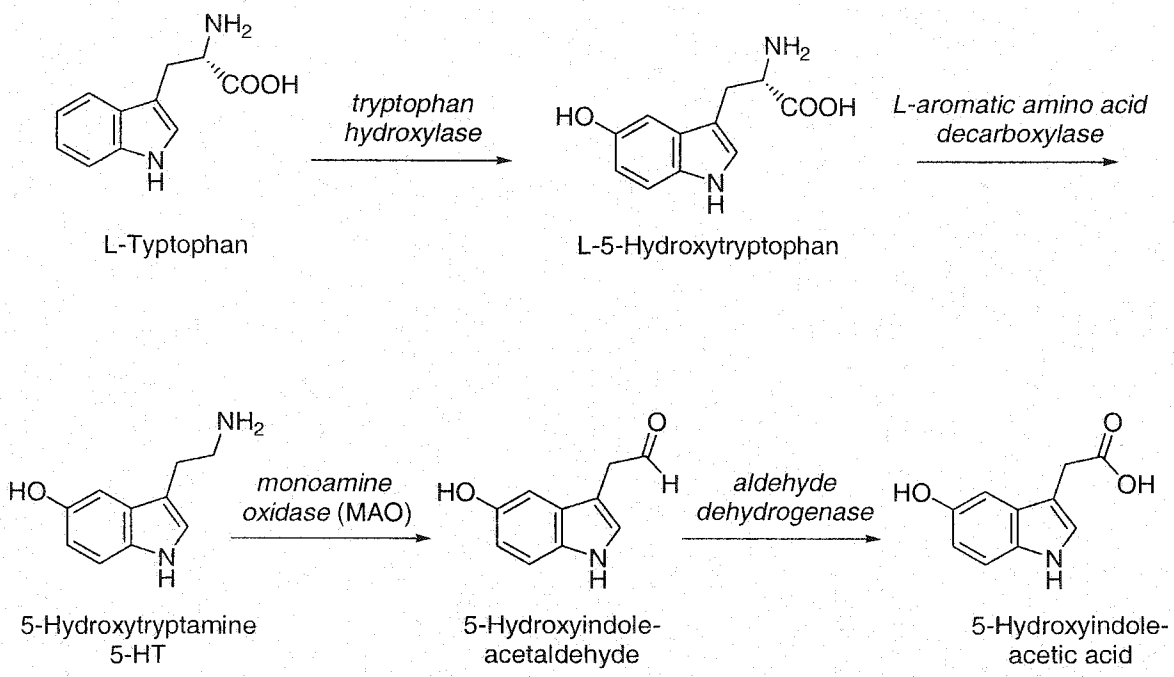

Figure 1. Biosynthesis and metabolism of 5-HT.

The Serotonergic System

In the periphery, the physiological effects of 5-HT can be generally categorized as vasoconstriction. Interestingly, the word serotonin, which was derived from "serum tonic factor," was coined to convey the properties of the compound.[18] In the CNS, however, 5-HT function is somewhat more complex and the elaborate system of neuronal communications that utilizes 5-HT is only poorly understood at the present time. Nonetheless, 5-HT and 5-HT receptors are thought to participate at some level in the underlying pathophysiology of a variety of CNS disorders including schizophrenia,[19] depression,[20-22] mania,[23,24] anxiety,[25] and migraine.[26,27]

There are also some brain processes that occur below the level of consciousness either affected or mediated by 5-HT including sleep, sensory perception, temperature, homeostasis, nociception, appetite, sexual behavior, and hormone secretion.[28,29] 5-HT is also thought to be involved at some level with higher brain functions including cognitive processes, learning and memory, and altered states of consciousness.[29-31]

The brain is profusely innervated by neurons that transmit signals through the release of 5-HT. The cell bodies, or soma, of all serotonergic neurons are located in the phylogenetically old raphe nuclei of the brain stem and send axonal projections throughout most of the brain and spinal cord. Besides 5-HT release into the synaptic cleft (Figure 2), the minute space between neurons, 5-HT is also released at non-synaptic areas called *varicosities*.[32] This non-synaptic release of 5-HT may explain the widespread influence and neuromodulatory effects of 5-HT. All serotonergic nerve terminals contain the enzymes necessary to convert L-tryptophan to 5-HT. Following biosynthesis, 5-HT is accumulated in synaptic vesicles that function as a means to 5-HT release as well as

storage containers for 5-HT where it is safe from the metabolizing effects of MAO. Upon nerve-impulse-prompted release into the synapse, 5-HT is promptly taken up by the presynaptic neuron through the Na^+-dependent 5-HT transporter. This reuptake effectively terminates the physiological action of 5-HT at the synapse. 5-HT that escapes the transporter either diffuses from the release site or is taken up by glial support cells.

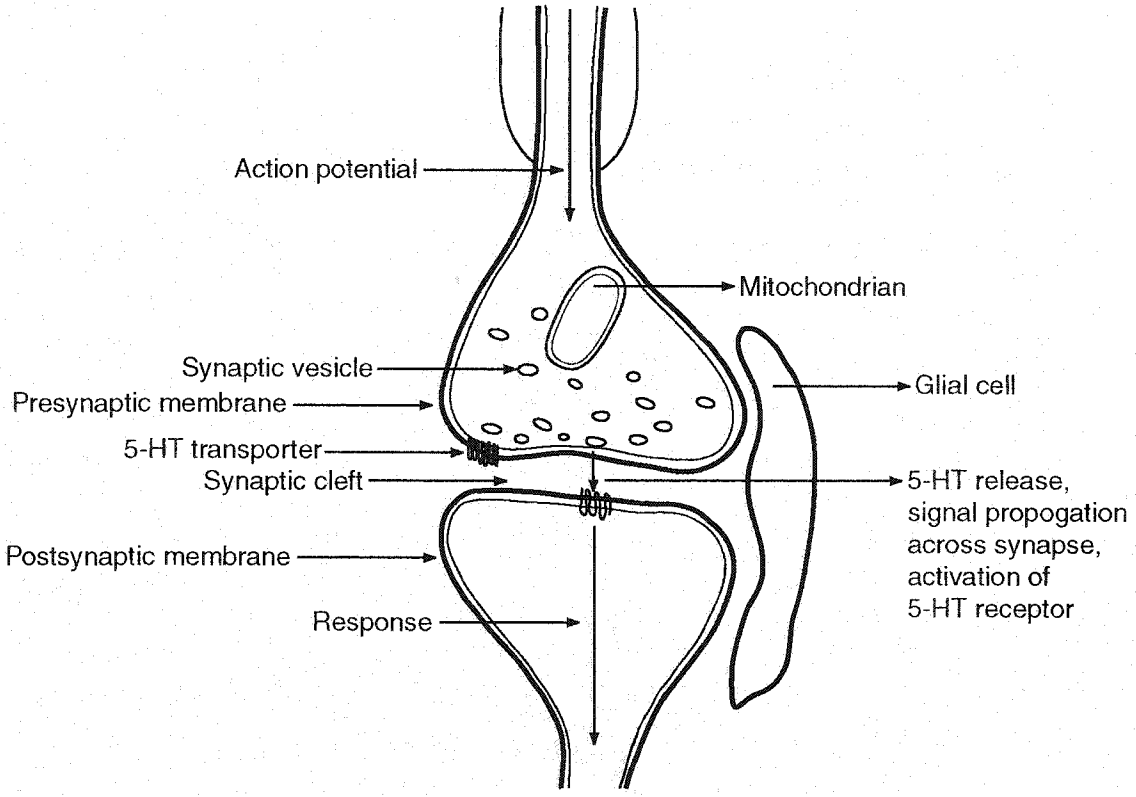

Adapted from Nieforth, et al.[33]

Figure 2. Schematic diagram of a synapse and 5-HT-mediated signal propagation.

Hallucinogens and the Serotonin-2A Receptor

Activation of the 5-HT_{2A} receptor subtype by an agonist drug is believed to be responsible for induction of the unique hallucinogenic intoxication that is produced by

drugs such as LSD, psilocin (4-hydroxy-*N*,*N*-dimethyltryptamine) and mescaline (3,4,5-trimethoxyphenethylamine).[34-37] Hallucinogenic drugs are defined by the altered psychological state that is induced following administration of the drug. The terminology that describes this altered state of consciousness has been the subject of debate and has ranged from psychotomimetic to psychedelic. Generally, the term "psychedelic" is adopted by authors who feel that hallucinogenic drugs possess inherently useful properties. This term has a positive connotation and is meant to describe these drugs as being "mind manifesting." Authors who oppose hallucinogen use or feel these drugs possess negative properties typically employ the term "psychotomimetic," interpreted to mean "mimicking psychosis," which elicits obvious negative connotations. The neutral terminology for members of this pharmacological class, and the one used in this text, is hallucinogen.

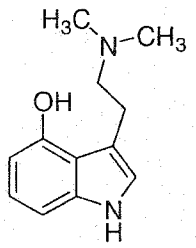

Psilocin

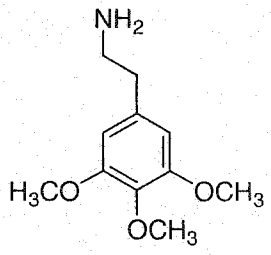

Mescaline

The psychological state that an individual experiences following hallucinogen administration can be characterized by some general terms, however, it appears that individual reactions to hallucinogens vary and that any one of, or combinations of, these indicators may be experienced by the user. Generally, hallucinogen intoxication results in alterations of normal perceptions of reality and time, changes in the processing of

sensory input, and modifications of body image and dimensions. Other experiences that have been described by users include changes in mood both during and after hallucinogen intoxication and a loss of one's ego.[30] Still more abstract experiences that are difficult to describe occur at a lower frequency. Users have reported experiences of religious exaltation and a feeling of union or "oneness" with mankind or with the universe. Still other users have reported achieving states of deep introspection otherwise achieved only by practiced masters of the art of meditation.[30,38,39]

The precise physiological mechanism of action by which hallucinogenic drugs operate is somewhat unclear. Activation of the 5-HT_{2A} receptor is a necessary but not necessarily sufficient condition to elicit hallucinogenic intoxication. In animal models, believed to reflect the subjective behavioral effects of hallucinogenic drugs such as LSD, activation of 5-HT_{2A} receptors by a drug appears to be the key pharmacological event.[40,41] Consistent with this finding, studies have shown that LSD and other hallucinogenic drugs act as full or partial agonists of the 5-HT_{2A} receptor-mediated generation of inositol triphosphate (IP_3). All hallucinogenic drugs, however, also exhibit high affinity and agonist activity at the 5-HT_{2C} receptor. The role of 5-HT_{2C} receptor activation in these behavioral alterations is presently unknown. LSD also interacts with many other 5-HT receptor subtypes including receptors whose functions have not yet been determined. Further complicating a simple mechanism for hallucinogenesis is the fact that LSD is an agonist at the 5-HT_{1A} autoreceptors on raphe cell bodies. Agonist activation of these receptors produces a slowed firing rate of serotonergic neurons and could be expected to affect consciousness through a 5-HT_{1A} receptor-mediated mechanism.[31,42] Despite the complex pharmacology of LSD, the hallucinogenic arylalkylamine class of drugs, of

which mescaline is a prototype, appear only to activate the 5-HT_{2A} and 5-HT_{2C} receptor isoforms.

Legitimate, or lawful, hallucinogen use at the present time remains highly restricted. Religious use of these drugs in the United States is constrained to only the Native American Church, a group that employs peyote as a religious sacrament. There have been some clinical investigations into the use of hallucinogens to treat mental illnesses and, with varying degrees of success, hallucinogenic drugs have been employed experimentally for the treatment of alcoholism and as an adjuvant to psychotherapy.[43-45] For these clinical uses, the hallucinogenic drug is employed not for the physiological response that is elicited by drug administration, but instead for the psychological response.[46] It has been hypothesized that psychotherapeutic treatment of destructive behaviors may be enhanced through controlled hallucinogen drug use. The psychological effects brought about by hallucinogens are thought to aid patients in bringing about positive life changes by enhancing analysis and introspection of the root causes of their problems. The sense of self is altered during hallucinogen intoxication, which may result in a reorganization of thought patterns, allowing patients to change destructive patterns of behavior. Underground or illegal hallucinogen use, by nature, is difficult to quantify and estimates of use vary widely. Surveys by the National Institutes of Health, however, have estimated that in 1997, 13.6% of high school seniors had experimented with LSD at least once in their lifetimes.[47] The level of LSD use has remained relatively constant in recent years.

Hallucinogenic drugs, aside from the associated CNS effects, have some limited peripheral physiological effects. These may include pupillary dilation, increased blood

pressure, mydriasis, tachycardia, tremor, nausea, piloerection, muscular weakness, and hyperthermia.[1] Some psychological complications associated with hallucinogenic drug use include paranoia, depersonalization, altered perception (visual, spatial and temporal), pain, anxiety, depression, and the emergence of latent psychoses.[30,48] Epidemiological studies of hallucinogen toxicity are confounded because the drugs are typically self-administered in doses that are unknown to the user.[49] The drugs are also sometimes administered as impure or adulterated samples.[30] Despite these factors, epidemiological studies have shown that hallucinogens have no withdrawal effects and that there are no documented toxic fatalities associated with LSD use.[30] Further, laboratory tests of pure hallucinogenic substances in models of toxicity have uncovered no adverse effects at concentrations that correspond to "normal" human doses, however, at much elevated doses, the data do suggest that LSD is mildly mutagenic in fungi and *Drosophila*.[33,50-52]

Ethnobotanical-Derived Hallucinogens

Ethnobotany is the study of the interrelation of "primitive" peoples and plants and has offered many interesting insights into the use of naturally occurring hallucinogens. Studies in this field have offered evidence that, throughout history, an assortment of plants known to contain hallucinogenic constituents has been used. That these plants or related species are still in use in some regions of the world suggests that this field of research may still have much to offer concerning the discovery of novel drug therapies. A handful of plants now known to contain psychoactive substances were typically employed by ancient cultures in divination rituals and ceremonies.[38,53] The physiological and psychological effects that were associated with these plants were particularly valued

by those cultures and, in many cases, the use of the plant products was restricted to a chosen few, typically the shaman or tribal leaders.[54,55] The experience and insight gained by those allowed to participate in the rituals, it is believed, was used to guide or heal the others of the tribe. In some cultures all members were able to use the psychoactive plant preparations at special times, such as in rites of passage-type rituals.[38]

The Aztec civilization used and worshiped a species of mushroom that they named teonanácatl, which translates to "flesh of the gods." So revered was this mushroom and the psychological effects that it brought about that the mushroom was the subject of numerous imaginative sculptures. Artifacts dating from around 1000 BC have been discovered that are believed to portray human and animal faces fused into the stalk of a giant mushroom. The western world learned of these sculptures and the mushrooms soon after the Aztec civilization was conquered by the Conquistadores. However, "modern" culture did not learn of the psychological effects of these mushrooms until the 1950's when R. Gordon Wasson, after traveling through Mexico and living amongst the indigenous peoples, published an article in Life magazine describing the use of mushrooms in divination ceremonies.[56] Samples of the mushrooms were subsequently forwarded to Albert Hofmann, the same chemist who discovered LSD. Soon after, the active constituent of the dried mushrooms was identified by cautious human sampling of chromatographic fractions as 4-phosphoryloxy-*N*,*N*-dimethyltryptamine, or psilocybin. Also present in the mushroom samples in small amounts and later found to be the biologically active constituent was the non-phosphorylated 4-hydroxy-*N*,*N*-dimethyltryptamine, named psilocin.[57]

Psilocin is a member of the tryptamine class of hallucinogenic drugs and is structurally very similar to 5-HT. This class of hallucinogens has been the subject of a great deal of scientific investigation. Psilocin also has recently been studied in clinical trials for the treatment of obsessive-compulsive disorder.[58] Clinical use, however, remains very controversial, but any positive results generated by these preliminary studies may lead to loosening of the restrictions on research with hallucinogens.

A variety of hallucinogenic tryptamines are found in nature. Bufotenine, the N,N-dimethyl analogue of 5-HT, is found in the toad *Bufo alvarius*, and, interestingly, the use of this hallucinogen source has been the subject of modern-day, popular culture comedy.[59] *N,N*-Dimethyltryptamine (DMT) is another naturally occurring tryptamine that is currently in use in a variety of forms. It is found in various species of plants but is not normally physiologically active when taken orally because it is rapidly metabolized in the liver by MAO. Ayahuasca, an interesting and effective preparation for the ingestion of DMT, was developed by the indigenous peoples of South America. It consists of a plant-derived DMT source, typically the *Psychotria viridis* bush, which is made orally available by the addition of a plant that contains harmala alkaloids for MAO inhibition.[38]

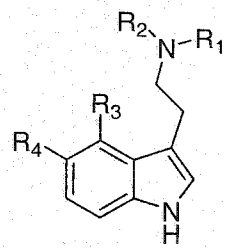

Typical Substitution Pattern:

$R_1 = R_2 = H$ or CH_3
$R_3 = H$ or OH
$R_4 = H$, OH, or OCH_3

Figure 3. General formula for hallucinogenic tryptamines.

Another substance that was employed by ancient cultures is mescaline, a member of the hallucinogenic arylalkylamine family. Mescaline is the hallucinogenic component of peyote cactus, *Lophophora williamsii.* This compound has been found in relatively high concentrations in other cacti including *Trichocereus bridgessi*, *T. pachanoi*, *T. peruvianus*, and *T. macrogenus*. Mescaline was used by the indigenous people of Mexico and the Southwestern United States before recorded history and is still used today by the Native American Church. For decades, mescaline has served medicinal chemists interested in hallucinogenic drugs as a lead compound. The mescaline structure has been extensively modified by Shulgin, et al. through the systematic synthesis and testing of positional isomers and diverse substitutions of the parent compound.[60,61] The hallucinogenic arylalkylamines are the main focus of this thesis and thus, a more detailed treatment of this pharmacological class will follow.

Another ethnobotanical of interest due to the hallucinogenic properties that it possesses is *Ipomoea violacea*, a member of the common morning-glory family.[54,62] This plant was used by the Aztecs and Mayans of Mexico in shamanism and divination ceremonies and has been found to contain ergot alkaloids, the chemical family to which LSD belongs. The indigenous peoples of Mexico have for centuries also used a sacred plant they called *ololiuhqui*. The seeds of this plant, the Mexican morning glory, *Rivea corymbosa*, were found to contain principally lysergic acid amide, a compound very similar to LSD. It was soon discovered that other plants produce similar derivatives. For example, another lysergic acid amide-producing plant is the baby Hawaiian woodrose, *Argyreia nervosa*, a climbing vine native to India, which has been used as a decorative plant in Hawaii and is still in use in modern India as a folk remedy.[63]

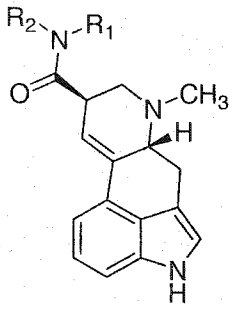

Typical Substitution Pattern:

$R_1 = R_2 =$ alkyl

Figure 4. General formula for hallucinogenic ergolines.

Synthetic Hallucinogens

Undoubtedly, the most well-known hallucinogenic drug is LSD, the N,N-diethylamide of lysergic acid. Lysergic acid is a hydrolysis product of ergot alkaloids produced naturally by the fungus *Claviceps purpurea*, a grain blight known to be responsible for the terrifying and sometimes deadly symptoms of ergot poisoning, or ergotism.[38] Ingestion of ergot alkaloids may cause hallucinations as well as induction of labor or strong and sometimes fatal vasoconstrictive effects. St. Anthony's fire, as poisoning by ergot was also known, was caused by contaminated grain baked into breads and resulted in thousands of deaths during the Middle Ages. Synthetic derivatives of the ergot alkaloids, the ergoline class of drugs, have been investigated in recent times for their powerful vasoconstrictive properties.[64]

Administration of LSD causes profound psychological alterations and hallucinations at doses as low as 1 μg/kg, making LSD one of the most potent drugs known. LSD was first synthesized as part of a semi-synthetic ergoline series in 1938 by Albert Hofmann who, quite by accident, discovered its hallucinogenic properties five years later through an accidental administration. The story surrounding the discovery is

very interesting and a small passage from Albert Hofmann's autobiographical description of his psychological state during the first accidental ingestion follows:[65]

> "I suddenly became strangely inebriated. The external world became changed as in a dream. Objects appeared to gain in relief; they assumed unusual dimensions; and colors became more glowing. Even self-perception and the sense of time were changed. When the eyes were closed, there surged upon me an uninterrupted stream of fantastic images of extraordinary plasticity and vividness and accompanied by an intense, kaleidoscope-like play of colors. After about two hours, the not unpleasant inebriation, which had been experienced whilst I was fully conscious, disappeared...
>
> The faces of those present appeared like grotesque colored masks; strong agitation alternating with paresis; the head, body and extremities sometimes cold and numb; a metallic taste on the tongue; throat dry and shriveled; a feeling of suffocation; confusion alternating with a clear appreciation of the situation...
>
> I lost all control of time; space and time became more and more disorganized and I was overcome with fears that I was going crazy. The worst part of it was that I was clearly aware of my condition though I was incapable of stopping it. Occasionally I felt as being outside my body. I thought I had died. My "Ego" was suspended somewhere in space and I saw my body lying dead on the sofa. I observed and registered clearly that my "alter ego" was moving around the room, moaning."

It could be argued that the discovery of LSD has changed the world in which we live. This subject, however interesting, is beyond the scope of this work.

Serotonin Receptors

The G-Protein Coupled Receptor Family

The family of guanine nucleotide-binding protein (G-protein) coupled receptors encompasses a large portion of present-day drug targets.[66] These cell membrane bound receptors receive extracellular signals in the form of photons, peptides, proteins, lipids, eicosanoids, purines, nucleotides, excitatory amino acids, ions, or small molecules such as 5-HT. The 5-HT receptors that have been identified to date (with the exception of the 5-HT_3 receptor subtype) are members of this G-protein coupled receptor (GPCR) family. The prototypical GPCR protein consists of seven transmembrane (TM) spanning segments arranged in a bundle and connected by intra- and extra-cellular loops. It has been established that the agonist binding site for the adrenergic, muscarinic, and serotonergic receptors is located in the TM regions of the receptor.[67] This site is analogous to the region in which light-sensitive retinal, the covalently-bound chromophore of opsin proteins, is found. Other members of the GPCR family have agonist binding sites putatively located in the extracellular loops (EL) that connect the TM helices. This externalized binding site permits larger effector molecules that would not be able to penetrate some distance into the helical bundle, such as peptides, to bind.

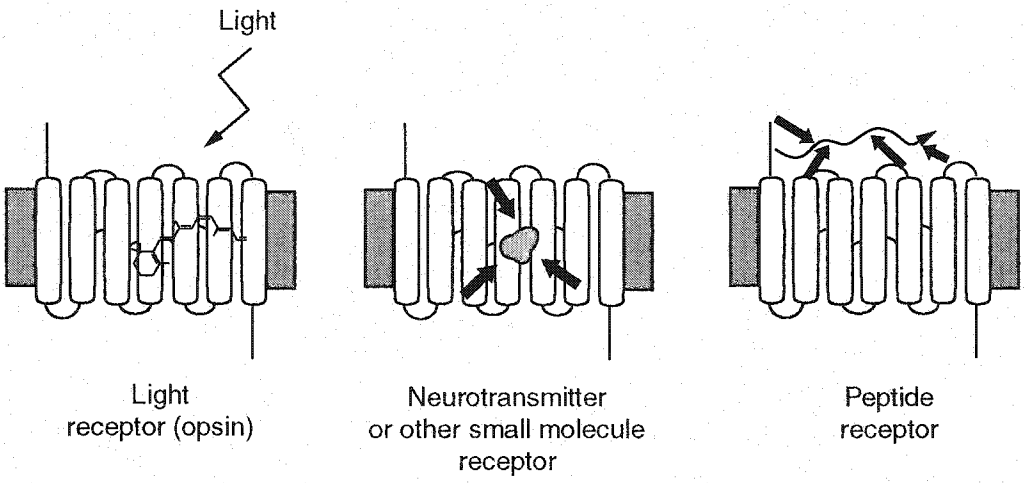

Figure 5. Modes of GPCR activation by light, small molecule, or peptide.

Like most proteins and enzymes, GPCRs are considered to be dynamic systems that may exist in a variety of conformational states. The fluid structure is hypothesized to exist in equilibrium between active and inactive forms of the receptor. In the absence of activating conditions (i.e., agonist binding and G-protein coupling) the structure lies at a potential energy minimum. Drugs that affect these receptors are thought to alter this equilibrium.[68] Compounds that behave as agonists alter the equilibrium in favor of an active receptor conformation. Antagonists, alternatively, are thought to stabilize the inactive form of the receptor and may block the actions of an agonist drug either by directly occupying part of the agonist binding site or by binding elsewhere and preventing conformational mobility of the receptor in an allosteric fashion.

An inactive GPCR exists between two distinct states that have been partially characterized in the 5-HT_{2A} receptor, the "low affinity" and "high affinity" state.[41,68,69] The term affinity, in this usage, refers to the affinity that an *agonist* drug has for the receptor. The "low affinity" state occurs when the GPCR is neither bound to an agonist

drug nor to an intracellular G-protein. The "high affinity" state occurs when a GPCR becomes bound to an intracellular G-protein, with no agonist bound. While the "high affinity" state alone does not cause intracellular signaling, this receptor state is believed to be the one that does bind an agonist molecule and propagate the agonist-induced signal. Upon productive binding of an agonist drug to a GPCR in the "high affinity" state, it is hypothesized that a conformational change within the TM domains occurs that converts the inactive receptor to an active form. This transient conformational shift, believed to be shared among all members of the GPCR family, is thought to be the key event in transduction of the extracellular, ligand-induced signal across the cellular membrane to the region of intracellular space. The associated G-protein complex, a heterotrimer consisting of an α, β, and γ subunit as well as a molecule of GDP, is activated and nucleotide exchange, GDP for GTP, is facilitated upon receptor activation. This exchange results in G-protein dissociation, with GTP bound to the α-subunit, separation from the $\beta\gamma$-complex, and subsequent modulation of downstream signaling proteins, thus triggering an intracellular signaling cascade that varies depending upon the subtype of the originally recruited G-protein.

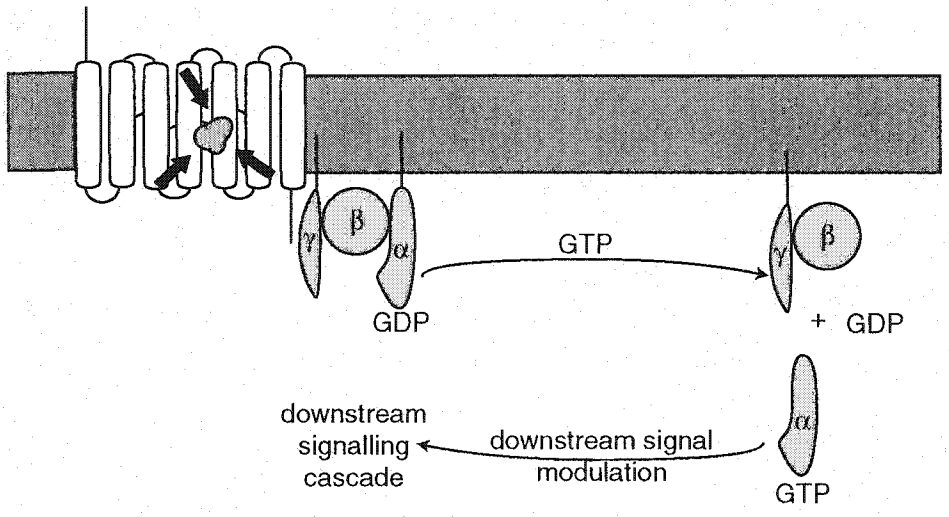

Figure 6. Schematic diagram of agonist-mediated G-protein complex activation.

Serotonin Receptor Subfamilies

To explain the multiple physiological actions of 5-HT, early hypotheses suggested that there were several pharmacologically distinct sites that bound 5-HT. Modern molecular biological techniques including cDNA cloning and pharmacological characterizations of drugs have shown there to be fourteen different 5-HT receptor isoforms. The current convention for 5-HT receptor classification and nomenclature segregates the receptors roughly into agonist-induced response and currently consists of seven 5-HT receptor subfamilies, 5-HT_1 – 5-HT_7.[70] Of the 5-HT receptor subfamilies, the 5-HT_1, 5-HT_2 and 5-HT_4 - 5-HT_7 are GPCRs. The 5-HT_3 receptor is part of a different structural family, the ligand-gated ion channels. Different 5-HT receptors exhibit varying degrees of primary sequence homology when compared to other 5-HT receptor family members and display, to a lesser extent, homology with the larger family of GPCRs.[71] Each 5-HT receptor subfamily is linked to varying intracellular signaling

mechanisms, believed to account for the variety of physiological effects that result from receptor activation by 5-HT. It remains plausible that each of these fourteen different 5-HT receptor subtypes may affect cellular biology in different ways; for instance, opposite effects have been observed upon activation of the 5-HT_{1A} and the 5-HT_{2A} receptor subtypes. Activation of the 5-HT_{1A} receptor results in an increase in K^+ conductance across the membrane[72] whereas activation of the 5-HT_{2A} receptor results in the opposite, a decrease in K^+ conductance.[73] That expression of multiple 5-HT receptor subtypes (or other receptors) may occur on a *single* neuron demonstrates that the cellular response to 5-HT may be almost infinitely diverse. The physiological summation of 5-HT-mediated receptor activation, it seems, may be tailored to each specific neuron.

The subfamily of 5-HT_2 receptors was initially identified by their relatively low affinity for [^{3}H]5-HT and high affinity for [^{3}H]spiperone, an antagonist at these receptors.[74,75] This subfamily of 5-HT receptors is now the target of a large range of psychopharmaceuticals, specifically atypical antipsychotic drugs, antidepressants, anxiolytics and, of most concern to this work, hallucinogens. There is a high degree of primary sequence identity within the 5-HT_2 receptor subfamily and across species, as shown by the dendrogram in Figure 7. This receptor subfamily consists of three members, 5-HT_{2A}, 5-HT_{2B}, and 5-HT_{2C}, all of which generate intracellular signals through phospholipase C activation. Activation of phospholipase C results in concomitant generation of two second messengers, diacylglycerol which serves to activate protein kinase C, and IP_3 which releases intracellular stores of Ca^{2+}.[76] The 5-HT_{2B} receptor subtype is largely found in peripheral regions of the body including the stomach fundus and vascular smooth muscle, but is also found in the CNS.[77-80] Based on

the observation that 5-HT induces mitogenic activity in cell preparations that express the 5-HT_{2B} receptor subtype, there have recently been suggestions that this receptor may be involved in the regulation of brain development.[81] The 5-HT_{2C} receptor isoform, formerly classified as the 5-HT_{1C} receptor, is found at high density in the choroid plexus, an epithelial tissue that is the main site of cerebrospinal fluid production, and on platelets where it is thought to promote clotting.[82] Although this subtype is populous in this tissue, the precise function of these receptors is still unknown. The 5-HT_{2C} receptor has also been found in other brain regions including the cortex, basal ganglia, hippocampus, and hypothalamus.[83,84] Observations based on in vitro studies have also suggested a role for 5-HT in addition to its role as a neurotransmitter. It was found that 5-HT may act as a growth factor for fibroblasts expressing high concentrations of the 5-HT_{2C} receptor isoform.[85] Because the focus of the present discourse is the 5-HT_{2A} receptor isoform, a more thorough description of this receptor is pertinent.

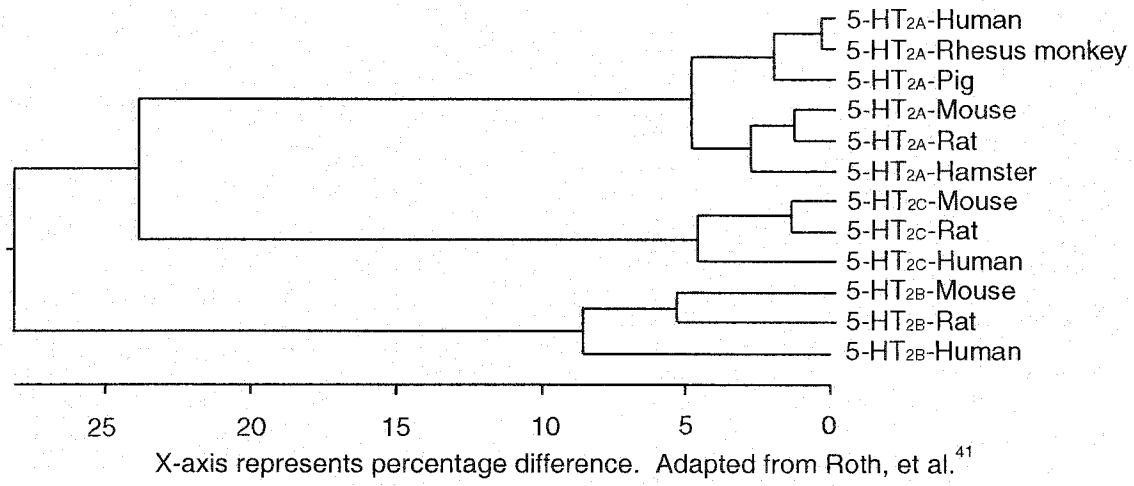

Figure 7. Dendrogram of a sample of 5-HT_2 receptors.

Serotonin-2A Receptor

The 5-HT_{2A} receptor is broadly distributed in the CNS, however, it is most populous in the terminal areas of serotonergic neurons. High populations of this receptor subtype are found in specific areas of the brain including the cortical regions, especially on pyramidal cells, the major output cells of the cortex, and at lower levels in the basal ganglia and hippocampus.[86-89] Populations of 5-HT_{2A} receptors also occur in platelets, vascular smooth muscle, uterine smooth muscle, and other tissues.[70,90-94] In most tissues, activation of the 5-HT_{2A} receptor promotes intracellular IP_3 formation.[91,92,95,96] These receptors may also regulate neurotrophin release in the brain.[97] In vascular smooth muscle, the 5-HT_{2A} receptor has also been implicated in activation of voltage-gated Ca^{2+} channels by a protein kinase C-mediated mechanism.[88,93,98,99]

Serotonin-2A Receptor Affinity and Efficacy

Affinity and efficacy at a receptor are two properties that may be measured for a given drug. Affinity can be defined as how well a drug "fits" into a binding site or the "attraction" that a drug possesses for a receptor. This is typically quantified by measuring the displacement of a radiolabeled compound, for example [^{3}H]DOB or [^{125}I]DOI in the case of the 5-HT_{2A} receptor, that has a known pharmacological profile. A drug, however, may bind to a receptor very tightly, but may or may not possess the ability to cause an action subsequent to binding. Receptor efficacy is the measure of receptor activation. Efficacy is typically determined by calculating the activation of a specific downstream signal, such as accumulation of a secondary messenger or gene

transcription, for example. Drugs that act as receptor agonists bind to the receptor and cause activation whereas drugs that act as antagonists bind to the receptor but cause no activation. Drugs that lie between the classification of full agonist and antagonist are commonly referred to as partial agonists.

Factors Influencing Affinity

The three main classes of agonist drugs that activate the 5-HT_{2A} receptor include certain substituted arylalkylamines, tryptamines, and ergolines. The orientations and structural conformations in which these different classes of 5-HT_{2A} receptor agonists bind to the receptor and exert their effects, however, remain the subject of conjecture. Structure-activity relationships (SARs) have been most thoroughly developed for the hallucinogenic arylalkylamines. Detailed descriptions of the ergoline and tryptamine drug class SAR are beyond the scope of this text, thus the reader is directed to several reviews that discuss these interesting hallucinogenic drug classes in depth.[65,100-102]

Arylalkylamine Agonists - General Considerations

An extensive body of research has been accumulating over the last 50 years concerning the study of hallucinogenic arylalkylamines, beginning with the studies of Benington, et al.[103] The now classical 2,4,5-substitution pattern of hallucinogenic arylalkylamines has evolved from SAR studies of the lead compound, mescaline.[60,104-108] Although this natural product is physiologically active and administration results in hallucinogenesis in humans, the drug is biologically active only at relatively high doses

and displays only modest affinity for the 5-HT_{2A} receptor. In general, the aryl-substitution pattern of the most potent hallucinogenic arylalkylamines consists of a 2,4,5-substitution pattern; alkoxy substituents at the 2- and 5-positions and a bulky, hydrophobic substituent at the 4-position. The 1-position of the phenyl ring is always substituted with a 2-aminoalkyl side chain, either a 2-aminoethyl or 2-aminopropyl group. The aromatic 2- and 5-substituents are typically methoxy and the 4-position, labeled as "X" in the generic arylalkylamine structure below, is classically a bromine, iodine, or methyl group. The hallucinogenic arylalkylamines are relatively free of conformational restriction and therefore the flexible elements may exist in numerous conformations at physiological conditions. As a result, efforts to understand the orientation in which arylalkylamines bind to the 5-HT_{2A} receptor have been confounded because there are multiple conformers that could possibly fit into the putative agonist binding site. To resolve this situation, arylalkylamine analogues in which distinct conformers of a parent molecule may be quantitatively investigated have been designed and tested.

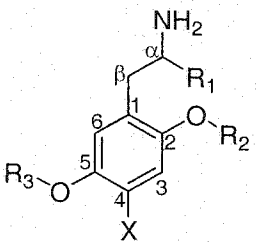

Typical Substitution Pattern:

R_1 = H or CH_3
R_2 = R_3 = CH_3
X = Br, I, or CH_3

Figure 8. General formula for hallucinogenic arylalkylamines.

2-Aminoalkyl Side Chain

The ubiquitous 2-aminoalkyl side chain of hallucinogenic arylalkylamines has been extensively investigated in past research endeavors. Alkylation of the basic amine group of arylalkylamines generally results in reduced affinity for the 5-HT_{2A} receptor as well as reduced hallucinogenic activity. Mono-N-methylation attenuates activity approximately 10-fold compared to the corresponding non-N-methylated arylalkylamine.[61,106] Furthermore, either di-N-substitution or mono-N-substitution with alkyl groups larger than methyl results in the complete loss of hallucinogenic activity.[61] A significant body of data has also indicated that, for optimum hallucinogenic activity, the 2-aminoalkyl side chain of arylalkylamines may either be a 2-aminoethyl or 2-aminopropyl group. Series of arylalkylamines in which the α-position was systematically substituted with sequentially larger alkyl groups have shown that groups larger than methyl at this position resulted in loss of hallucinogenic activity.[109] Also, 2-aminopropyl arylalkylamines are more potent in vivo than those in which the side chain is 2-aminoethyl.[106] The α-methyl group, it is surmised, prolongs the action of the drug by inhibiting side chain deamination. Further, addition of the α-methyl group results in an increase of the Log P value (1-octanol/water partition coefficient) of the drug, thereby aiding intestinal absorption, blood-brain barrier penetration, as well as partitioning into the hydrophobic 5-HT_{2A} receptor agonist binding site. The optimal Log P value for hallucinogenic arylalkylamines has been calculated to be 3.14 from correlations of hallucinogenic activity and calculated Log P.[110] In vitro studies of binding affinity at the 5-HT_{2A} receptor in which drugs containing either of these side chain congeners were compared, however, have shown that there is little difference between 2-aminopropyl and

2-aminoethyl. Introduction of an α-methyl group into the side chain results in a new stereochemical center that has also been the subject of some investigation. It has been shown that the *R*-enantiomer is more potent than the *S*-antipode both in binding affinity and efficacy studies at the 5-HT_{2A} receptor.[111,112] Interestingly, *R*-enantiomers of α-methylated arylalkylamines are typically equipotent to the corresponding analogue that does not contain the α-methyl group and are generally two- to five-fold more potent than the corresponding *S*-isomer.[111-114]

Conformational restrictions of the 2-aminoalkyl substituent that have been targeted in past research have generally favored an in-plane orientation with respect to the aromatic system.[115,116] By contrast, it has been observed by solution NMR studies that amphetamine likely exists in an anti-periplanar orientation under physiological conditions.[117] Compounds produced in our lab in which the 2-aminoalkyl substituent was constrained to an orientation in the plane of the phenyl ring resulted in reduced affinity for the 5-HT_{2A} receptor and were found to lack hallucinogen-like activity in an animal model.[116]

Para-substituents

A general requirement for potent hallucinogenic arylalkylamines is that the *para*-substituent, X in the previous structure, be a bulky, hydrophobic group. This requirement was observed in the extensive series of arylalkylamine analogues with varying *para*-substitutions that were synthesized and tested for their hallucinogenic activity by Shulgin and others.[61] It was also observed that polar substituents at the *para*-

position generally result in attenuated hallucinogenic activity.[118] Further, optimum chain length of *para*-alkylated arylalkylamines has been investigated and the results of these studies have shown that optimal chain length for straight chain 4-alkyl-substituted arylalkylamines is propyl.[118] Alkyl branching at the benzylic position of this substituent was not tolerated by the receptor; however, it has been shown that alkyl-branching at positions distal to the benzylic position may be accommodated.[118,119]

Recent studies by Nichols, et al. have suggested that a bulky substituent at the *para*-position of arylalkylamines may not be an absolute requirement to impart 5-HT_{2A} receptor binding affinity. Compound **1** has an extended aromatic system and lacks a substituent at the *para*-position. This compound possessed pharmacological properties of high affinity and efficacy at the 5-HT_{2A} receptor.[112] The results from the tests of this compound suggest that affinity for the receptor benefits from a hydrophobic substituent because, at least in part, it enhances partitioning of the drug into the hydrophobic receptor interior.

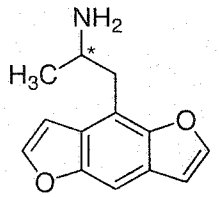

1

<u>*Ortho*- and *Meta*-substituents</u>

The methoxy groups of arylalkylamines have also been probed by extensive positional and chemical substitutions. It was discovered early on that the most potent substitution pattern for the arylalkylamine hallucinogenic drug class was one in which

methoxy groups were substituted at the 2- and 5-positions.[60,120] Recently, the incorporation of the O-substituents into tethered dihydrofuran ring structures has been utilized to investigate the optimal conformation of methoxy groups of prototype compounds. The tetrahydrobenzo[1,2-*b*;4,5-*b*']difuran heterocyclic scaffold has served to lock the *ortho*- and *meta*-substituents into an orientation that lies in the plane of the phenyl ring and has also served to impose directional restrictions on the lone pairs of oxygen electrons. These tetrahydrobenzodifuran-containing drugs (series **2**) proved to be extremely potent 5-HT_{2A} receptor agonists, suggesting that the methoxy group orientation that is mimicked by this structure is the optimal one for 5-HT_{2A} receptor binding and activation. These compounds further have shown that affinity, as well as efficacy, for the 5-HT_{2A} receptor could be enhanced significantly by the aromatization of the dihydrofuran rings (series **3**). The further increase in binding affinity could simply be the result of the increased aromatic surface area of the drug that is available for π-π-type or T-type edge-face interactions with the receptor.[112,121-123]

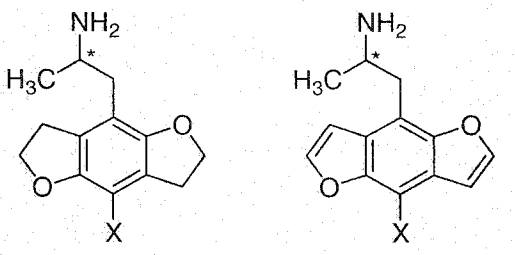

2 **3** X = Br, CF_3

GPCR and Serotonin-2A Receptor Features - General Considerations

A high resolution structure of the 5-HT_{2A} receptor has not been reported. Membrane-bound receptors have been very difficult to crystallize, primarily due to

complications arising from their hydrophobic properties and the lack of methods for producing large quantities of pure protein. In order to understand better the three-dimensional structure of the 5-HT_{2A} receptor, research in this area has been forced to rely on a combination of drug synthesis and SAR investigations, biochemical engineering techniques, and computational approaches to circumvent the absence of detailed structural information. An iterative procedure involving molecular modeling, site-directed mutagenesis, and ligand-binding experiments in which a model of the target receptor is incrementally improved appears, for now, to be the most efficacious way to learn details about the 5-HT_{2A} receptor. Recently, however, bovine rhodopsin, a prototypical GPCR was crystallized and has offered additional insight into this field of research.[124] Although the evolutionary relationship between bovine rhodopsin and the human 5-HT_{2A} receptor is a distant one, there are numerous primary sequence motifs that are shared by the pair.[125-128] The overall sequence similarity shared between bovine rhodopsin and the human 5-HT_{2A} receptor is ~15%, however, the similarity within the putative TM domains is ~25%.[127] Thus, a better understanding of the 5-HT_{2A} receptor may be gained by a detailed study of the bovine rhodopsin protein structure. As will be discussed in the latter portion of this work, this crystal structure has also furthered the evolution of a computer-generated model of the 5-HT_{2A} receptor.

Polar amino acid residues that lie within the putative TM regions of the 5-HT_{2A} receptor structure indicate residues that may be involved either in ligand binding regions, secondary or tertiary receptor structure stabilization, or agonist-mediated signal transduction. Site-directed mutagenesis, as well as molecular modeling studies that have attempted to explain the role of these charged and polar amino acids have met with

varying degrees of success. A productive technique to investigate possible roles for these polar residues, however, was to use primary sequence alignments. This method has allowed the characterization of residues conserved in all GPCR proteins or, conversely, residues conserved in only subfamilies of receptors. The former group of residues was generally thought to be involved either with receptor function or with structural stability of the tertiary structure because it is believed that all GPCR proteins are arranged almost identically and employ similar signal transduction mechanisms. The latter group of residues, those conserved only in subfamilies of GPCRs, could be assumed to be important for binding of specific effector molecules, such as residues specific for 5-HT or dopamine, or to be important for subfamily specific signal transduction nuances.

What follows now is an abbreviated treatment of the findings concerning charged or polar amino acid residues of GPCRs, focusing mainly on those residues that have been directly investigated in the 5-HT_{2A} receptor. While these exercises offered much insight into the structural details of the GPCR family, the crystallization of bovine rhodopsin and subsequent structural information that was derived by X-ray analysis has been a defining event for the field of GPCR research.[124]

The body of data concerning GPCR site-directed mutagenesis is rather extensive. Mutations specific to the 5-HT_{2A} receptor are, however, less common. Those studies have allowed insight into a few specific amino acid residues that contribute to agonist binding and a few other residues that have been implicated in receptor activation. The data derived from studies of the human 5-HT_{2A} receptor and species variants still leave many important questions unanswered. Furthermore, one must be cautions when interpreting site-directed mutagenesis-derived data and consider that the results are, by

nature, confounded by the unpredictable effects of the mutation. Well-designed control experiments must be done to be certain that the mutant protein is folded correctly and that the protein is targeted to the cellular membrane.[129]

The amino acid positional numbering system that will be used in this text is straightforward and allows direct comparison across cognate residues within the monoamine GPCR family. It follows the system proposed by Ballesteros, et al.[130] Three generalized numbers are associated with each amino acid position and are derived by beginning with the TM number (e.g., 2 for residues in TM2), followed by the position relative to a reference residue, the most conserved amino acid in that specific TM among the monoamine GPCR family. The reference residue has an arbitrary assignment of 50. For example, the most conserved residue in TM2 of monoamine GPCRs is an aspartate and therefore the identifier for this amino acid would be 2.50 (i.e., $D_{2.50}$). A proline residue located nine amino acids after $D_{2.50}$ is represented as $P_{2.59}$. To relate the numbering identifier to the amino acid sequence of the particular GPCR of discussion, each identifier is followed by the absolute sequential number in that particular sequence. For example, $D_{3.32}$ is residue number 155 in the human 5-HT_{2A} receptor and is represented as $D_{3.32(155)}$ when discussing that receptor. If an amino acid is located in a non-TM loop, it could, theoretically have two different identifiers relative to the two TM segments that it lies between, each uniquely identifying the same amino acid position. Table 1 lists the reference amino acids for each TM segment and illustrates the identifying numbers for the human 5-HT_{2A} receptor.

Table 1. Generalized numbering scheme for GPCR sequences.

TM	100% conserved in monoamine GPCRs	residue identifier	residue number in human 5-HT_{2A} receptor	residue identifier in human 5-HT_{2A} receptor
1	Asn	$N_{1.50}$	92	$N_{1.50(92)}$
2	Asp	$D_{2.50}$	120	$D_{2.50(120)}$
3	Arg	$R_{3.50}$	173	$R_{3.50(173)}$
4	Trp	$W_{4.50}$	200	$W_{4.50(200)}$
5	Pro	$P_{5.50}$	246	$P_{5.50(246)}$
6	Pro	$P_{6.50}$	338	$P_{6.50(338)}$
7	Pro	$P_{7.50}$	377	$P_{7.50(377)}$

Polar Residues Implicated in Affinity

There exists a large body of data indicating that $D_{3.32(155)}$, conserved among the family of monoamine GPCRs, is directly involved in agonist as well as antagonist binding to the 5-HT_{2A} receptor. This negatively charged residue is hypothesized to anchor the ubiquitous, positively charged amine moiety of ligands for monoamine receptors.[131-140] Other GPCRs with endogenous agonists that contain no such amine group generally lack this conserved, negatively charged residue. Site-directed mutagenesis of $D_{3.32(155)}$[135] has been used to investigate the precise role that this amino acid plays in the 5-HT_{2A} receptor. A mutation in which $D_{3.32(155)}$ was changed to an asparagine, $D_{3.32(155)}N$, resulted in diminished binding affinity of 5-HT, DOI, ketanserin,

mianserin and spiperone, and, to a lesser extent, LSD (ketanserin, mianserin, and spiperone are antagonists, Figure 9). This finding suggests that, although $D_{3.32(155)}$ is essential for ionic anchoring of 5-HT and related ligands, a somewhat different binding orientation exists for LSD with respect to $D_{3.32(155)}$ in which the importance of this residue is diminished slightly. Taken as a whole, these data suggest that $D_{3.32(155)}$ is important for ligand binding and the stabilization of the positively charged amine found in 5-HT and other ligands, however, residues in addition to this conserved aspartate must also be involved.

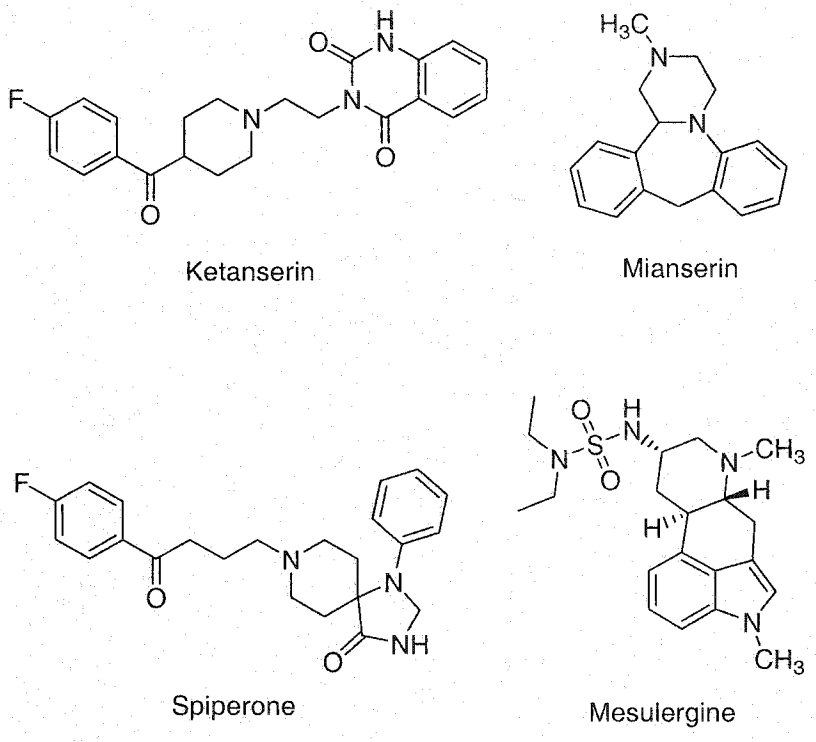

Figure 9. Several 5-HT_2 receptor antagonists.

Other polar amino acid residues conserved among the family of 5-HT receptors have also been specifically shown by mutagenesis studies to be essential for agonist

binding to the 5-HT_{2A} receptor. One of these residues is $S_{3.36(159)}$, located one helical rotation down from the conserved $D_{3.32(155)}$. Mutational studies of this residue have implicated it in binding of 5-HT and other 5-HT_{2A} receptor agonists.[140] Receptor binding data from receptors containing a mutation of this residue have shown that 5-HT exhibits an approximately 17-fold lower affinity for the $S_{3.36(159)}$A mutant than the wild type receptor, however, smaller changes in affinity were noted for bufotenine and LSD, both tertiary amine-containing drugs, 4-fold and 1.4-fold, respectively. These data could indicate that the N-methylated groups of the latter two ligands localize the protonated amine further away from $S_{3.36(159)}$ upon binding to the agonist binding site and therefore, this mutation results in a smaller effect on the binding affinity of these compounds. As will be discussed in more detail below, this residue may form hydrogen bonds with the oxygen substituents of arylalkylamine and tryptamine hallucinogens upon receptor binding.

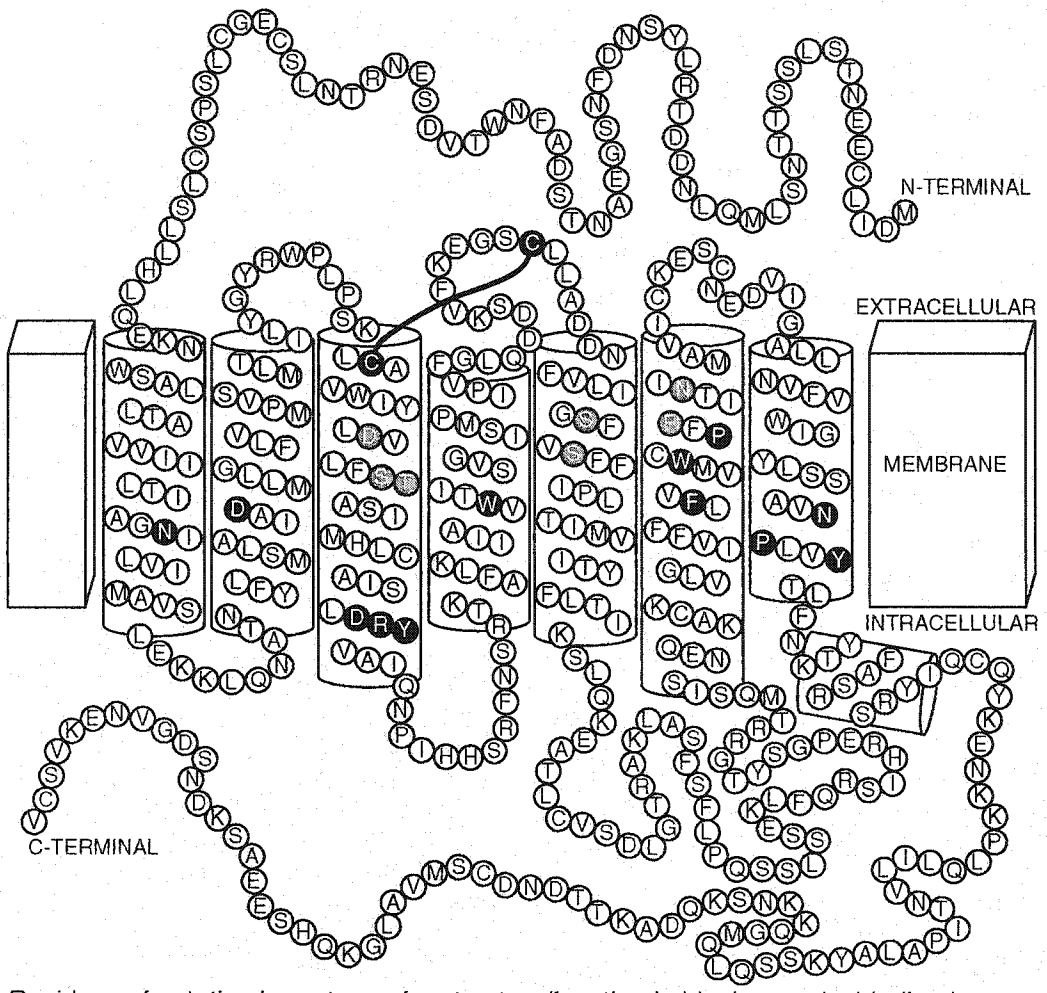

Figure 10. Schematic diagram of the 5-HT_{2A} receptor.

The advent of modern molecular biology techniques in which receptors were cloned and expressed stably in cell lines led to the discovery of species-specific binding differences for 5-HT_{2A} receptor ligands. It was observed that [^{3}H]mesulergine displays species-dependent differences in binding affinity – the drug bound with high affinity to the rat 5-HT_{2A} receptor but, interestingly, had low affinity at the human 5-HT_{2A} receptor.[141] Sequencing and cloning of the rat and human 5-HT_{2A} receptors revealed that

there were only three amino acid differences between these species homologs in the putative TM regions; one of these alterations was found to be a serine in the human 5-HT_{2A} receptor and an alanine in the rat orthologue.[142-144] Mutagenesis of the human to rat sequence at this position, $S_{4.47(242)}A$, resulted in a marked increase in the affinity of mesulergine.[144] This experiment confirmed that this residue was involved directly in the binding of mesulergine. These results indicated that very minor differences in primary amino acid sequence of these species homologs must account for the different pharmacological characteristics of these two receptors. Later, detailed SAR studies and mutagenesis experiments also suggested that $A_{4.47(242)}$ of the rat 5-HT_{2A} receptor was important for binding of drugs of the ergoline family. The rat 5-HT_{2A} receptor demonstrated higher affinity for N-1-substituted ergolines when compared directly to binding affinity data from the human receptor homolog.[145] Based on this evidence, Johnson, et al.[145] surmised that $S_{4.47(242)}$ of the human 5-HT_{2A} receptor likely serves as a hydrogen bond participant for N-1-*unsubstituted* ergolines. These ligands were observed to display a higher affinity for the human 5-HT_{2A} receptor than for the rat 5-HT_{2A} receptor. Furthermore, it was suggested that $S_{4.47(242)}$ of the human homolog may present steric hindrance to the N-1-*substituted* ligands resulting in a lower affinity for the human receptor when compared to the rat receptor. Thus, N-1-substituted ligands are more readily accommodated in the rat receptor which has a smaller, less polar alanine at this position. These results are illustrated in Figure 11. Thus, in addition to the data generated by the direct mutagenesis of $D_{4.47(242)}$, these data provided a secondary anchor point in the receptor which, upon binding, LSD must accommodate. This second anchor point for binding, as will be explained in detail in the Discussion section of this work, has

proven crucial for successful docking of ligands to a newly developed 5-HT_{2A} receptor model.

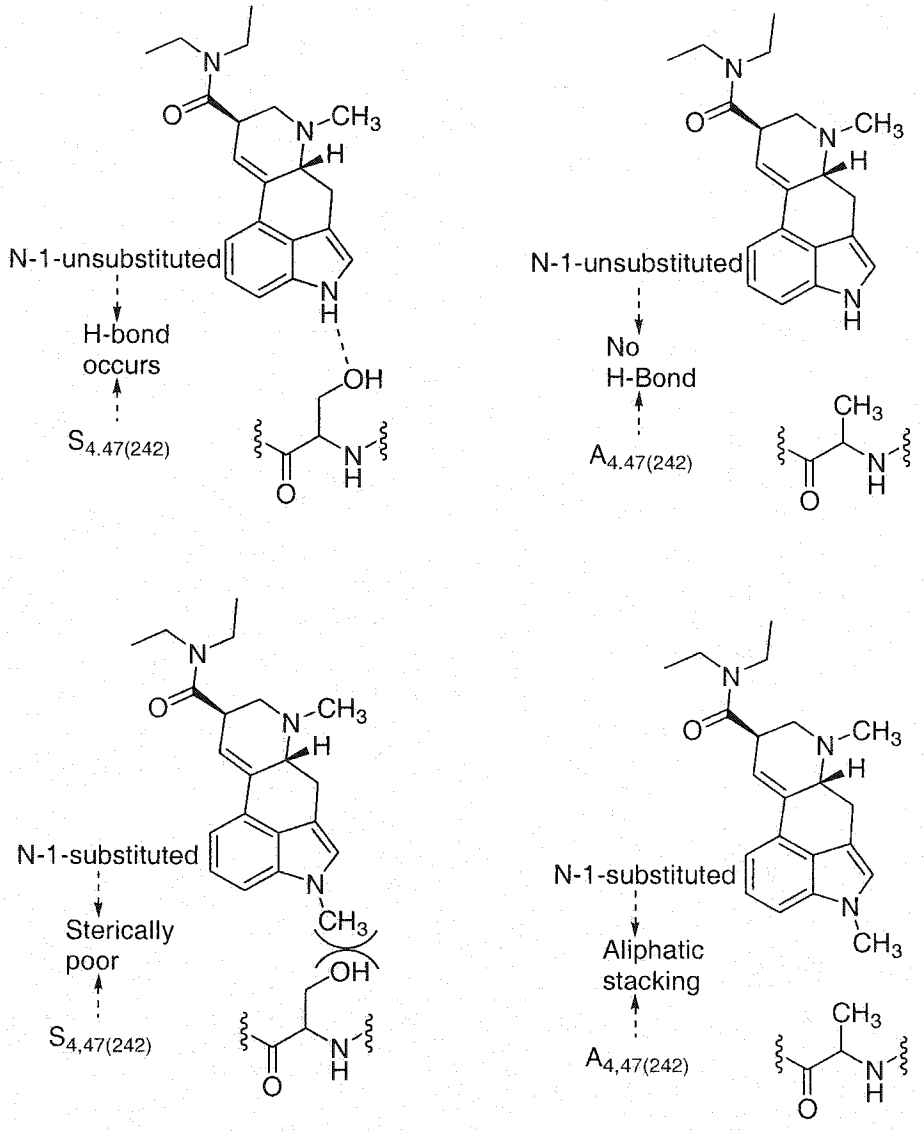

Figure 11. Schematic diagram of species- and N-1-alkylation-specific binding differences exhibited by ergolines.

Non-polar Residues Implicated in Binding Affinity

A conserved feature of all 5-HT_{2A} receptor agonist drugs is the presence of an aromatic moiety contained within the drug structure. This aromatic group, a phenyl ring in the case of arylalkylamines or an indole in the case of the tryptamines and ergolines, is invariably two methylene units (~4 Å) from the charged amine functionality. The steadfast presence of this aromatic moiety in potent 5-HT_{2A} receptor agonists suggests there to be at least one complementary aromatic amino acid residue present within the binding site. The aromatic nucleus of 5-HT_{2A} receptor ligands may have favorable contacts in the binding site by either π-π-type interactions or T-type edge-face interactions with an aromatic amino acid.[131,133,134,136,137,139,146-150] There are several conserved aromatic amino acids that may be involved directly with ligand binding to this receptor, although some of these residues could instead be involved with secondary or tertiary structure stabilization of the receptor protein.

Based on site-directed mutagenesis evidence, molecular modeling of the 5-HT_{2A} receptor, and inferences gained from multiple sequence alignment of GPCRs, a small number of conserved phenylalanine residues have been suggested to be involved in either binding of ligands or receptor activation. $F_{2.25(125)}$, $F_{5.47(243)}$, $F_{5.48(244)}$, $F_{6.51(339)}$, $F_{6.52(340)}$, and $F_{7.38(365)}$ alone or in various combinations, have been proposed to be important for agonist binding to the 5-HT_{2A} receptor.[131,133,134,137,139,147,148] Of this group of phenylalanine residues, a considerable body of direct mutagenesis data support the hypothesis that $F_{6.52(340)}$ is directly involved with agonist binding. A mutation in which $F_{6.52(340)}$ was replaced by leucine, $F_{6.52(340)}$L, displayed a marked decrease in binding affinity and efficacy for DOI, bufotenine, 5-HT, and other agonists tested at the mutant

5-HT_{2A} receptor.[146] The $F_{6.52(340)}L$ mutation also induced marked decreases in efficacy for the 5-HT-induced accumulation of IP_3, a measure of receptor activation, when compared to the wild-type receptor.[69] These latter functional mutagenesis studies offer support for the conclusion that $F_{6.52(340)}$ is essential for agonist recognition and for receptor activation. Mutation of an adjacent residue, $F_{6.51(339)}L$, did not effect agonist binding affinity or efficacy in a uniform manner, unlike the $F_{6.52(340)}L$ mutation, suggesting that $F_{6.51(339)}$ is not directly involved in agonist binding. Receptor binding assays using the $F_{6.51(339)}$ mutant found antagonists to be affected more profoundly than agonists, thus, it is possible that $F_{6.51(339)}$ is involved with antagonist binding.[146] Additionally, a $F_{2.55(125)}L$ mutation was constructed that also did not uniformly change agonist binding affinity or efficacy.[69] These results, taken as a whole, indicate that $F_{6.52(340)}$ is directly involved in agonist binding, however, $F_{6.51(339)}$ and $F_{2.25(125)}$ are most likely not involved. Other researchers have suggested that $F_{7.38(365)}$ has a role in agonist binding, however, a $F_{7.38(365)}L$ mutation displayed diminished agonist efficacy, but negligible effects on the binding affinity of agonists, supporting a role for this residue in either signal transduction or receptor activation mechanisms, but not agonist binding.[150]

In addition to the conserved phenylalanine residues implicated in the agonist binding mechanism, there is also a series of conserved tryptophan residues in the monoamine GPCR family thought to be essential.[131,133,134,136,139,148-150] Most 5-HT_{2A} receptor models that have been put forth have suggested the involvement of four specific tryptophan residues: $W_{3.28(151)}$, $W_{4.50(200)}$, $W_{6.48(336)}$, and $W_{7.40(367)}$.[131,133,139] Mutagenesis evidence for the role of $W_{4.50(200)}$ and $W_{6.48(336)}$ in agonist binding to the receptor has been found.[150] Mutations to alanine of these individual residues were found to markedly

reduce agonist affinity and efficacy and have thus been hypothesized to reside near the agonist binding site.[150]

Factors Influencing Efficacy

Evidence of Conserved Three-Dimensional Receptor Structure

A characteristic epitope at the area where TM3 ends and the second intracellular loop (IL2) begins is absolutely conserved in the entire family of GPCR proteins and has served as a partial GPCR-"fingerprint."[151] The primary sequence of this motif is $D_{3.49(172)}$-$R_{3.50(173)}$-$Y_{3.51(174)}$ in the 5-HT_{2A} receptor, however, it also appears as $E_{3.49}$-$R_{3.50}$-$Y_{3.51}$ or $D_{3.49}$-$R_{3.50}$-$F_{3.51}$ in some GPCRs. This conserved epitope is present in a majority of GPCR proteins at positions cognate to those in the 5-HT_{2A} receptor and, because of the ubiquity of this sequence in the GPCR family, is believed to be either structurally or functionally important for the GPCR family.[152] The precise role that it plays in either or both structure or function, however, is not well known.[135] Analysis of the bovine rhodopsin crystal structure has indicated an ionic interaction between residues $R_{3.50(135)}$ and $E_{3.49(134)}$ with the conserved $E_{6.30(247)}$.[41] This finding, in concert with recent results from mutant 5-HT_{2A} receptors,[153] offer direct evidence both for a structural and functional role for this group of conserved residues. Movement of the two TM segments in which this interhelical interaction occurs upon GPCR activation has been hypothesized to result in the exposure and protonation of $E_{3.49}$, thus allowing direct activation of an intracellular G-protein.[153-155]

There is definitive evidence for the spatial proximity of certain pairs of polar and charged residues in GPCR structure. The evidence is convincing for interhelical interactions between $D_{2.50(120)}$ and $N_{7.51(376)}$ as well as a functional role for this pair of residues. In one well-designed experiment, a $D_{2.50(120)}N$ mutation was constructed and was found to lack functional efficacy. However, receptor function was rescued by the reciprocal $N_{7.51(376)}D$ mutation.[156] This functional receptor, now the reciprocal mutant of the wild type receptor at these two positions, demonstrated that this pair of residues is surely involved in receptor function. Mutation of either member of this cognate pair in the β-adrenergic, α_{2a}-adrenergic, and muscarinic receptors also led to the loss of ability to stimulate second messenger formation.[157-159] Further examination of the crystal structure of bovine rhodopsin has indicated an interaction between $E_{3.37(122)}$ and $H_{5.46(211)}$ that we believe may be involved with receptor activation. This pair of amino acids correspond to residues known to be important for 5-HT_{2A} receptor agonist binding, $T_{3.37(160)}$ and $S_{5.46(242)}$.[41,160] The full implications of this inter-helical interaction have not been tested in bovine rhodopsin, thus no conclusion about the involvement of these residues in activation may presently be made.

The GPCR family had been hypothesized to contain a single, conserved disulfide bond. There is invariably a conserved cysteine residue at the extracellular side of TM3 and one located at varying positions of the second extracellular loop (EL2).[161,162] The data from the crystal structure of bovine rhodopsin have confirmed that this hypothesis is correct through the identification of a disulfide bond between $C_{3.25(110)}$ and $C_{4.76(187)}$. This bond covalently links the second extracellular loop (EL2) and TM3, however, the precise function and importance of this structural feature remains unknown.

RATIONALE

The underlying goal of this research project was to gain insight into the chemical and topological characteristics of the 5-HT_{2A} receptor agonist binding site. Initially, to probe this receptor, the research plan involved the design and synthesis of conformationally-restricted analogues of known 5-HT_{2A} receptor agonists. Significant advances in parallel fields of research occurred, however, during the course of our investigations that dictated changes in our research approach. The investigational method that resulted from these developments coupled rational drug design and organic synthesis with molecular modeling and ligand docking.

Alone, the design and synthesis of conformationally-restricted analogues of 5-HT_{2A} receptor agonists has resulted in much insight into the agonist binding site. Drug design coupled with a homology-based model of the 5-HT_{2A} receptor has, however, enabled the design of novel drugs based on a computationally-driven strategy. This two-tiered approach was not possible until recently when the crystal structure of bovine rhodopsin, a prototypical GPCR was published.[124] Bovine rhodopsin is a light receptor that is phylogenetically related to the 5-HT_{2A} receptor. The elucidation of its crystal structure has enabled more dependable computer-generated GPCR models. Prior to the publication of the bovine rhodopsin crystal structure, models were based either on the

crystal structure of bacteriorhodopsin, an unrelated proton pump, or on a low resolution X-ray projection map of frog rhodopsin, a member of the GPCR family.[163-165]

Conformationally-Restricted Arylalkylamines

Prior to development of a 5-HT_{2A} receptor model, hypothesis-driven drug design of conformationally-restricted analogues of known 5-HT_{2A} receptor agonists was employed to enhance our knowledge of the agonist binding site. Conformationally-restricted drugs allow for a qualitative exploration of distinct three-dimensional regions of the binding site by mimicking distinct rotational conformers of the parent compound. This methodology has enabled us to test specific hypotheses concerning the biologically active, or optimal, conformation of flexible moieties common to arylalkylamine agonists. This technique is limited only by the drug designer's creativity and the synthetic feasibility of the proposed compounds.

The optimal steric and electronic directionality of the 2- and 5-methoxy groups of typical arylalkylamines has been defined by past research. Various analogues of DOX (2,5-dimethoxy-4-X-amphetamine; DOB, X = Br; DOI, X = I; DOM, X = CH_3; etc.) that restrict the flexibility of the two methoxy groups have been synthesized and tested. The conformation found to be optimal for these methoxy substituents is exemplified by drugs that contain the tetrahydrobenzo[1,2-*b*;4,5-*b'*]difuran scaffold (**2**).

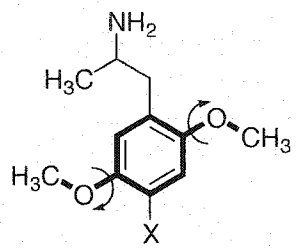

DOX

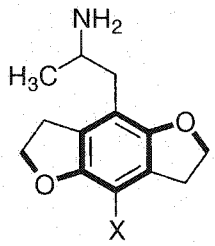

2

Early investigations that were conducted during the present work involved efforts to define further the optimal orientation for the 2- and 5-methoxy groups of arylalkylamines and to utilize this information to design a radioligand for the 5-HT_{2A} receptor. The main thrust of this body of work, however, was toward delineation of the optimal conformation of the flexible 2-aminoalkyl side chain of arylalkylamine agonists. Specifically, the aims of this work were to:

1) Integrate results of past research to design and synthesize a novel 5-HT_{2A} receptor radioligand that incorporates the highly potent tetrahydrobenzo-[1,2-*b*;4,5-*b'*]difuran molecular scaffold.[112,121-123]

2) Investigate the effects on 5-HT_{2A} receptor binding affinity of transposition of the typical arylalkylamine 5-oxygen substituent to the 6-position of the phenyl ring:
   i. methoxy group rigidification by incorporation into a tetrahydro-benzo[1,2-*b*;5,4-*b'*]difuran heterocycle;
   ii. aromatization of the tetrahydrobenzo[1,2-*b*;5,4-*b'*]difuran scaffold.

3) Delineate the active conformation of the 2-aminoalkyl side chain of arylalkylamines through the design and synthesis of tetrahydronaphthofurans:
   i. selective aromatization of the dihydrofuran component of the tetrahydronaphthofuran heterocycle.

ii. aromatic bromination at the 8-position, the substituent that corresponds to the *para*-substituent of classical arylalkylamines.

4) Create a homology-based model of the human 5-HT_{2A} receptor that utilizes the crystal structure of bovine rhodopsin as a foundation:

i. employ the 5-HT_{2A} receptor model to explain in vitro pharmacological data for known ligands.

ii. design novel drugs for the receptor based on receptor model-derived information.

Benzodifurans

Previous work in the field of 5-HT_{2A} receptor agonist design has established that constraint of the two methoxy substituents of DOX analogues into a tetrahydro-benzo[1,2-*b*;4,5-*b'*]difuran heterocycle results in an increase in binding affinity and increased efficacy at the 5-HT_{2A} receptor compared to the parent DOX compounds.[112,121-123] Compounds that incorporate this nucleus, series **2**, have been found to exhibit up to a 40-fold increase in binding affinity compared to the corresponding, non-rigid DOX drugs. It was also shown that aromatization of the appended dihydrofuran rings, series **3**, further increased binding affinity three- to 1500-fold relative to the corresponding non-rigid DOX compounds. The resultant drugs are amongst the highest affinity ligands for the 5-HT_{2A} receptor discovered to date.[112,123]

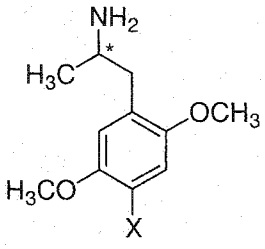

DOX

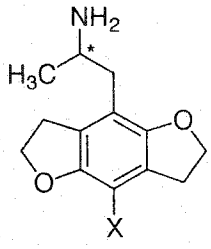

2

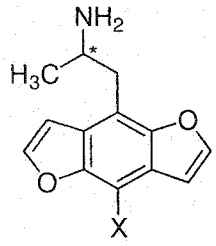

3

Based on the previous work, a radioligand was designed that incorporates the potent tetrahydrobenzo[1,2-*b*;4,5-*b'*]difuran nucleus of **2**. The novel compound **4** contains four tritium atoms in the structure and should maintain the high affinity at the 5-HT_{2A} receptor that has been observed in the non-radiolabeled, parent compounds **2**. It is anticipated that radioligand **4** will be employed for future radioligand competition binding assays in our lab and elsewhere. The synthesis of compound **4** was designed to avoid complications associated with the stereocenter of the 2-aminopropyl compounds by utilizing the 2-aminoethyl derivative instead. As mentioned in the Introduction, the presence of an α-methyl group on the 2-aminoalkyl side chain of arylalkylamines prolongs the in vivo actions of the drug but does not increase 5-HT_{2A} receptor binding affinity. Thus, the absence of the α-methyl group on this radioligand should be of little consequence for receptor binding assays.

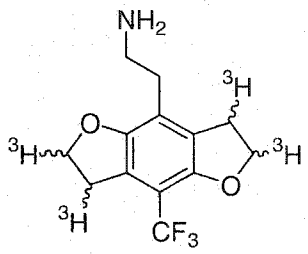

4

A compound series that incorporates a positionally modified tetrahydrobenzo[1,2-*b*;5,4-*b*']difuran scaffold was also designed based on previous data. Shulgin, et al. reported that 2,6-dimethoxy-4-methylamphetamine (**5**), an arylalkylamine in which the 5-methoxy group has been transposed to the 6-position, retained many of the in vivo qualitative characteristics of typical hallucinogenic arylalkylamines.[166] This finding was of interest because it had been believed previously that the presence of the 5-alkoxy substituent of this class of compounds was required to impart hallucinogenic activity because a 5-methoxy appendage is ubiquitous to the family of potent arylalkylamines.

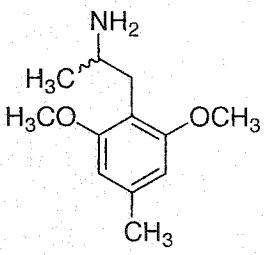

5

To investigate the atypical arylalkylamine substitution pattern reflected in **5**, a short series of conformationally-restricted analogues was designed that reflected the 2,6-dioxygenated arrangement. Compound **6** was designed to constrain the alkoxy substituents into a region of space that is defined by the plane of the phenyl ring. Further,

the effect of aromatization of this new substitution pattern was investigated by the synthesis of analogue **7**. The fully aromatic compound **7** was designed to study the effects on 5-HT_{2A} receptor binding affinity of increased aromatic surface area of the benzo[1,2-*b*;5,4-*b'*]difuran nucleus.

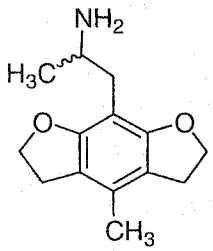

6

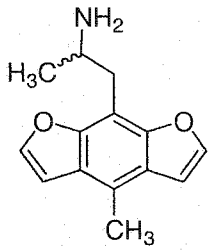

7

Tetrahydronaphthofurans

Previous efforts by this laboratory to produce conformationally-restricted analogues of arylalkylamines in which the 2-aminoalkyl side chain is constrained by incorporation into a tethered ring system have been concentrated on a series of tetrahydronaphthofurans that were designed and synthesized by Monte, et al.[116] The compounds of this series were considered to be "hybrid" structures between the hallucinogenic arylalkylamine and ergoline families. It had been hypothesized since the late 1950's that the A ring of LSD corresponds to the phenyl ring of the arylalkylamines and that the 5-oxygen of arylalkylamines serves as a bioisostere of the indole N-1-nitrogen of LSD. Thus, tetrahydronaphthofuran series **8** was hypothesized to imitate the A, B, and C rings of LSD.

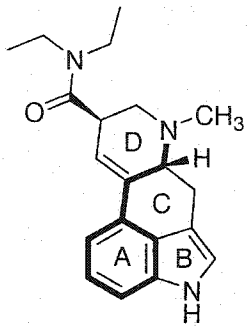

LSD

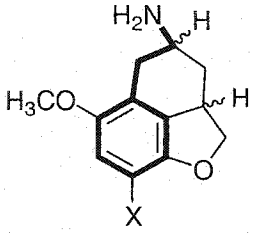

8; X = H, Br

The majority of the compounds in series **8**, however, exhibited rather low affinity for the 5-HT_{2A} receptor and none of the compounds in the series produced hallucinogen-like effects in animal models. One compound, however, the brominated *syn* analogue of series **8**, did exhibit high affinity for the receptor but lacked the behavioral effects of LSD in animal models.[116] These results suggested that the proposed structural alignment between the arylalkylamines and ergolines was imperfect. Alternatively, the high binding affinity but lack of hallucinogenic activity of the *syn* brominated analogue of series **8** may indicate that this drug simply may not possess the ability to activate the receptor. The information gained from the study of this series of compounds led to changes in our understanding of the relationship between the arylalkylamine and ergoline drug classes. A new series of tetrahydronaphthofurans, compounds **9** – **14**, based on a molecular scaffold similar to series **8**, was designed to alter the spatial orientation of the basic amine of the ligand. The compounds in the new drug series were also designed to incorporate the known optimal configuration of the 2- and 5-alkoxy substituents of arylalkylamines.

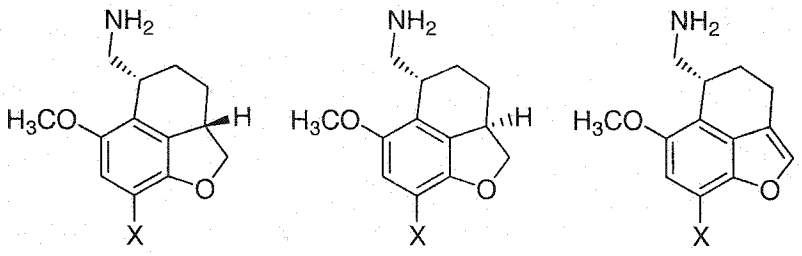

9; X = H
12; X = Br

10; X = H
13; X = Br

11; X = H
14; X = Br

The alkoxy group of compounds **9** - **14** that corresponds to the 5-methoxy group of typical arylalkylamines is incorporated into an appended dihydrofuran ring, thereby constraining the substituent into the plane defined by the phenyl ring. The substituent corresponding to the 2-methoxy group, although not tethered to the phenyl ring, is sterically constrained to an orientation that is also near the plane of the phenyl ring. The close proximity of the aminomethyl group effectively prohibits full rotation about the aryl-oxygen bond of the 6-methoxy group, thereby maintaining this substituent in an orientation that is near optimal.

Compounds **9** - **14** also localize the basic amine moiety to a region of space that is out of the plane defined by the phenyl ring. The peri-interaction between the aminomethyl and the adjacent methoxy forces the aminomethyl group out of plane. Conformational restriction of the alkylamine was designed to test the hypothesis that the 2-aminoalkyl side chain of arylalkylamines adopts an anti-periplanar conformation upon binding to the 5-HT_{2A} receptor agonist binding site (See Figure 12 for schematic diagram of anti-periplanar and other rotameric configurations). Molecular modeling of compounds **12**, **13**, and **14** and the compound that exhibited the highest 5-HT_{2A} receptor affinity of series **8**, the *syn* brominated analogue, (Figure 13) demonstrates that compounds **12, 13**, and **14** adopt an energetically favored conformation that closely

resembles an anti-periplanar conformation. The three compounds **12**, **13**, and **14** all position the basic amine out of the plane of the phenyl ring (1.52 Å, 1.06 Å, and 1.41 Å from the plane for **12**, **13**, and **14** respectively). The *syn* brominated analogue of series **8**, however, appears quite different; Figure 13 demonstrates that the amine of this compound lies closer to the plane of the phenyl ring than the other compounds (0.86 Å from the plane for *syn* brominated **8**). While *syn* brominated **8** mimics an anti-periplanar conformation, the basic amine is locked into a position closer to the plane of the phenyl ring than the compounds of the new series. The hypothesis that the amine must lie in an anti-periplanar conformation and out of the plane of the phenyl ring is based, in part, on solution NMR studies of amphetamine. It has been demonstrated that the alkylamine moiety of the 2-aminopropyl group of amphetamine adopts an out-of-plane, anti-periplanar orientation under simulated physiological conditions and, thus, it seems plausible that this energetically favored conformation may be the physiologically active one.[117]

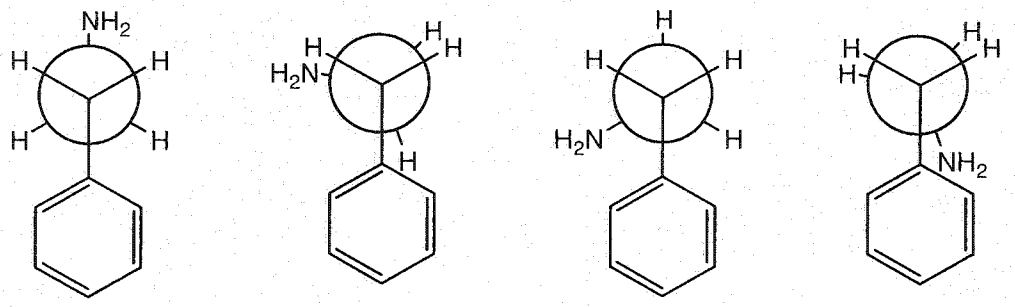

anti-periplanar, anti, or trans | anticlinal | synclinal or gauche | synperiplanar

Figure 12. Fischer projections of the rotational conformations of typical phenethylamines.

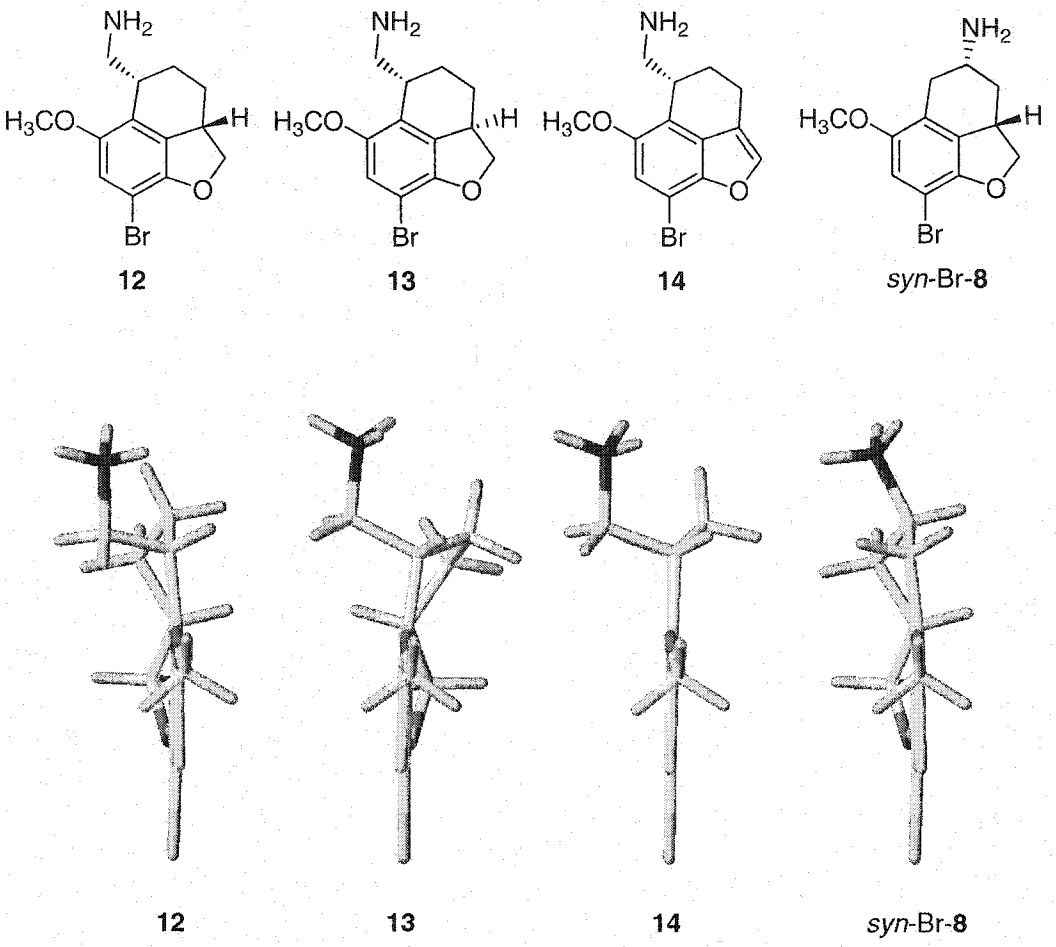

Figure 13. Illustration of out-of-plane, anti-periplanar conformation for compounds **12**, **13**, and **14** compared to in-plane, anti-periplanar naphthofuran *syn*-Br-**8**.

In addition to investigation of the optimal 2-aminoalkyl conformation, compounds **9** - **14** were designed to probe the effect of aromatization of the dihydrofuran ring. As mentioned previously, compounds that incorporate a benzodifuran molecular scaffold were found to be highly potent in both binding affinity and efficacy at the 5-HT_{2A} receptor. It was therefore predicted that aromatization of the dihydrofuran ring would increase the affinity and efficacy of these compounds at the 5-HT_{2A} receptor. Finally, compounds **9** - **14** were designed either to exclude or incorporate an aromatic bromide at the 8-position that corresponds to the *para*- or 4-position of typical arylalkylamines to

test the hypothesis that this substituent was also required to convey high 5-HT_{2A} receptor affinity and efficacy to this class of compounds.

Molecular Modeling and *De Novo* Drug Design

Publication of the atomic coordinates of bovine rhodopsin, a prototypical GPCR, has enabled development of a 5-HT_{2A} receptor model. Initially, a typical bovine rhodopsin-based homology model of the human 5-HT_{2A} receptor was proposed; however, it soon became apparent that the information derived from the crystal structure alone would not suffice for our drug design purposes. Although the published structure was a great step forward for GPCR modeling and research, the structure was the inactive form of the opsin protein. Consequently, a 5-HT_{2A} receptor structure based solely on this *inactive* GPCR template would have resulted in a model of the *inactive* form of the target receptor. Docking of agonist compounds to this inactive state is confounded by the fact that agonist drugs for the 5-HT_{2A} receptor are believed to favorably bind only the "high affinity" state of the receptor. This state occurs when the receptor is coupled to an intracellular G-protein. The inactive bovine rhodopsin structure is believed to resemble more closely the "low affinity" state; thus, homology models based on this structure would not appropriately dock agonist molecules. Therefore, rather than employing this structure directly as the foundation for the 5-HT_{2A} receptor model, computer-generation, or *in silico*-generation, of an activated form of the bovine rhodopsin protein was undertaken and used for homology model development and ligand docking studies. A

schematic diagram of the molecular modeling methodology that was proposed is shown in Figure 14.

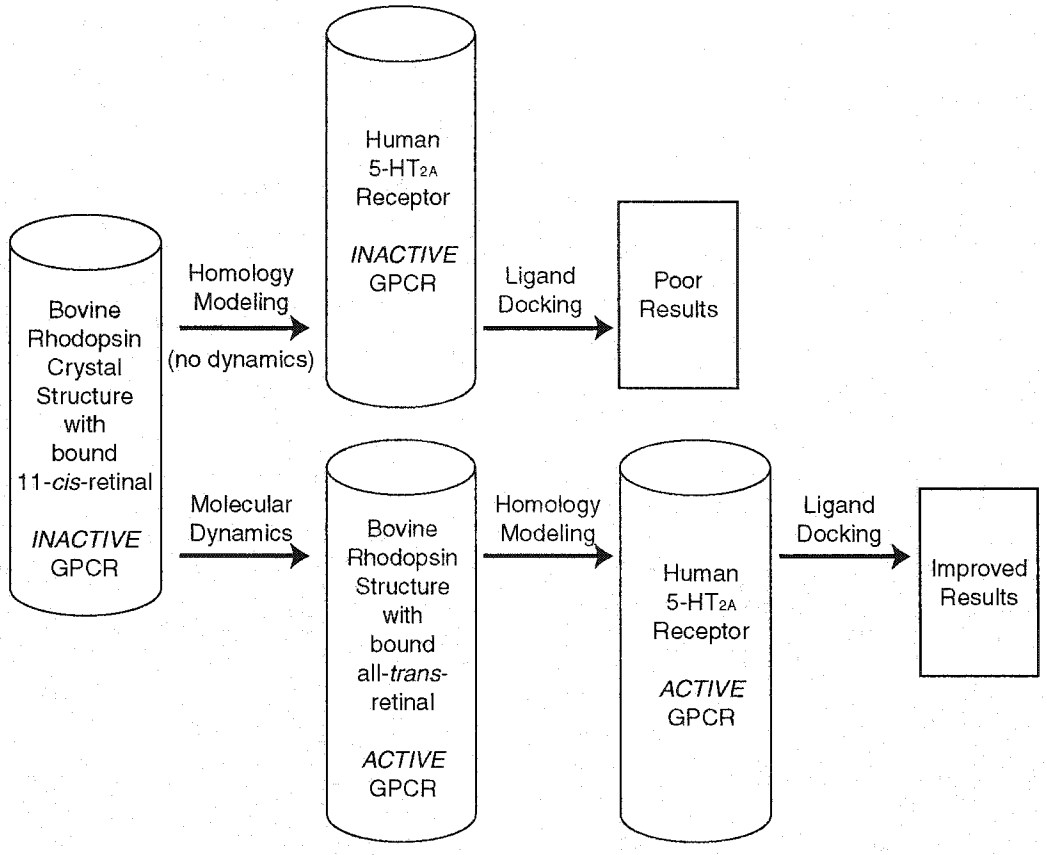

Figure 14. Molecular modeling sequence.

In Silico Activation of Bovine Rhodopsin

The crystal structure of bovine rhodopsin contains a retinal chromophore, derived from vitamin A, covalently linked to $K_{7.43(296)}$. The chromophore requires interactions with proximal rhodopsin residues to maintain a bound state.[155] In the inactive, or dark state of this receptor, the chromophore exists as the "inverse agonist" 11-*cis*-retinal (**15**).[155] Upon absorption of a single photon, isomerization of the 11,12-olefinic bond

converts the chromophore into the "agonist" all-*trans*-retinal (**16**). Subsequent protein relaxation to accommodate the isomerization-induced potential energy increase renders the protein transiently active. It is the active form of the rhodopsin structure that activates the intracellular G-protein, transducin, thereby facilitating nucleotide exchange, thus triggering a signaling cascade that is ultimately necessary for vision.[155,167] The isomerized retinal (**16**) maintains fewer stabilizing interactions in this isomeric form and is subsequently hydrolyzed from $K_{7.43(296)}$ and dissociates from the protein.

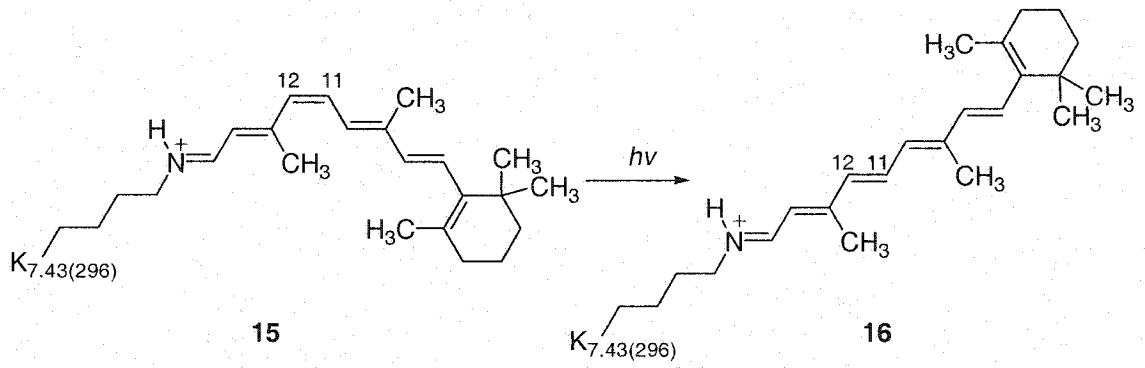

15 16

Figure 15. Light induced isomerization of 11-*cis*-retinal (**15**) to all-*trans*-retinal (**16**).

Utilizing molecular dynamics, simulation of the biophysical process of receptor activation was proposed. The mechanism by which the bovine rhodopsin protein is transformed from an inactive to an active state has been the subject of direct experiments of both the wild type protein and site-directed mutant proteins using various forms of spectroscopy.[168-174] Collectively, these studies suggest that following the *cis-trans* photochemical isomerization of the bound 11-*cis*-retinal chromophore, TM3 and TM6 undergo rearrangement, likely rigid body motion, relative to one another (Figure 16). Thus, by utilizing a molecular dynamics scheme that artificially favors rigid body motion,

we hypothesized that a satisfactory model of *active* bovine rhodopsin could be generated beginning with the *inactive* published structure. This method was expected to offer a superior structural basis for the development of a homology-based model of the human 5-HT_{2A} receptor.

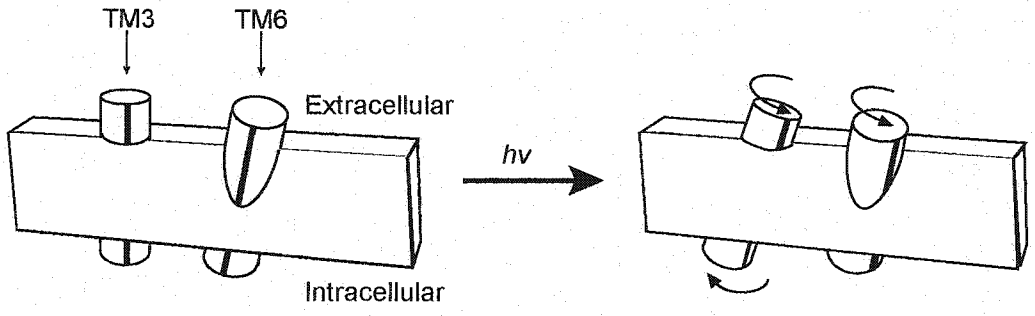

Adapted from Gether, et al.[175]

Figure 16. Schematic diagram of bovine rhodopsin activation events.

Homology Modeling of the Serotonin-2A Receptor

Utilization of an *in silico* activated bovine rhodopsin template, in conjunction with multiple sequence alignments of monoamine GPCRs, a survey of the body of GPCR mutagenesis research, and detailed structural investigation of the bovine rhodopsin crystal structure, was expected to produce an improved 5-HT_{2A} receptor model relative to what has been previously available. The resultant model was to be challenged by examining its ability to explain pharmacological data for known 5-HT_{2A} receptor agonists. This testing would be accomplished through computational docking of agonist drugs using an unbiased ligand docking routine. Finally, it was envisioned that the receptor would be employed as a design tool for novel ligands in which new ideas for

functional moieties on proposed compounds could be targeted to specific regions of the agonist binding site.

Conformational Restriction of Mescaline

Docking of mescaline to the 5-HT_{2A} receptor model resulted in a counterintuitive binding orientation and prompted the design and synthesis of a conformationally-restricted analogue (**17**) that mimicked the proposed binding orientation. This compound, a substituted indanyl-system into which the structure of mescaline is embedded, was designed to restrict the motion of the 2-aminoethyl side chain in favor of an orientation similar to that found for the docked parent compound, mescaline. It was expected that this *de novo* designed drug would bind to the 5-HT_{2A} receptor with higher affinity than the parent compound primarily because the new drug would not encounter the entropic penalty that mescaline suffers due to the flexible 2-aminoethyl side chain.

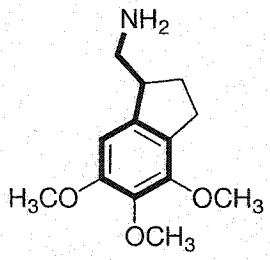

17

RESULTS

Synthesis

Benzodifurans

A Radiolabeled Analogue of 2,5-Dimethoxy-4-X-Arylalkylamines

Potential radioligand **4** was designed specifically as a potent, high specific-activity tool for the 5-HT_{2A} receptor. The synthesis of the non-radiolabeled version of **4** (Figure 17) commenced with N-protection of **18** (generated according to literature precedent)[121] as the trifluoroacetamide to afford **19**.[123] Trifluoroacetamide **19** was then treated with copper iodide and tetramethylammonium trifluoroacetate to replace the aryl bromide with a trifluoromethyl group to afford **20**, followed by oxidation of the tetrahydrobenzo[1,2-*b*;4,5-*b'*]difuran nucleus of **20** using DDQ to afford benzodifuran **21**.[112,176,177] The protecting group of **21** was then removed by base hydrolysis, product **22** converted to the hydrochloride salt, and then catalytically hydrogenated to afford non-isotopically labeled ("cold") **4**. Although the radiolabeling (tritiation) step has not been completed at the time of this writing, it is envisioned that facile incorporation of four atoms of tritium per molecule of **4** will supplant the final hydrogenation step to

produce the target radioligand **4**.[178] This reaction will be carried out in the near future by radiochemists at a laboratory contracted by the National Institute of Mental Health.

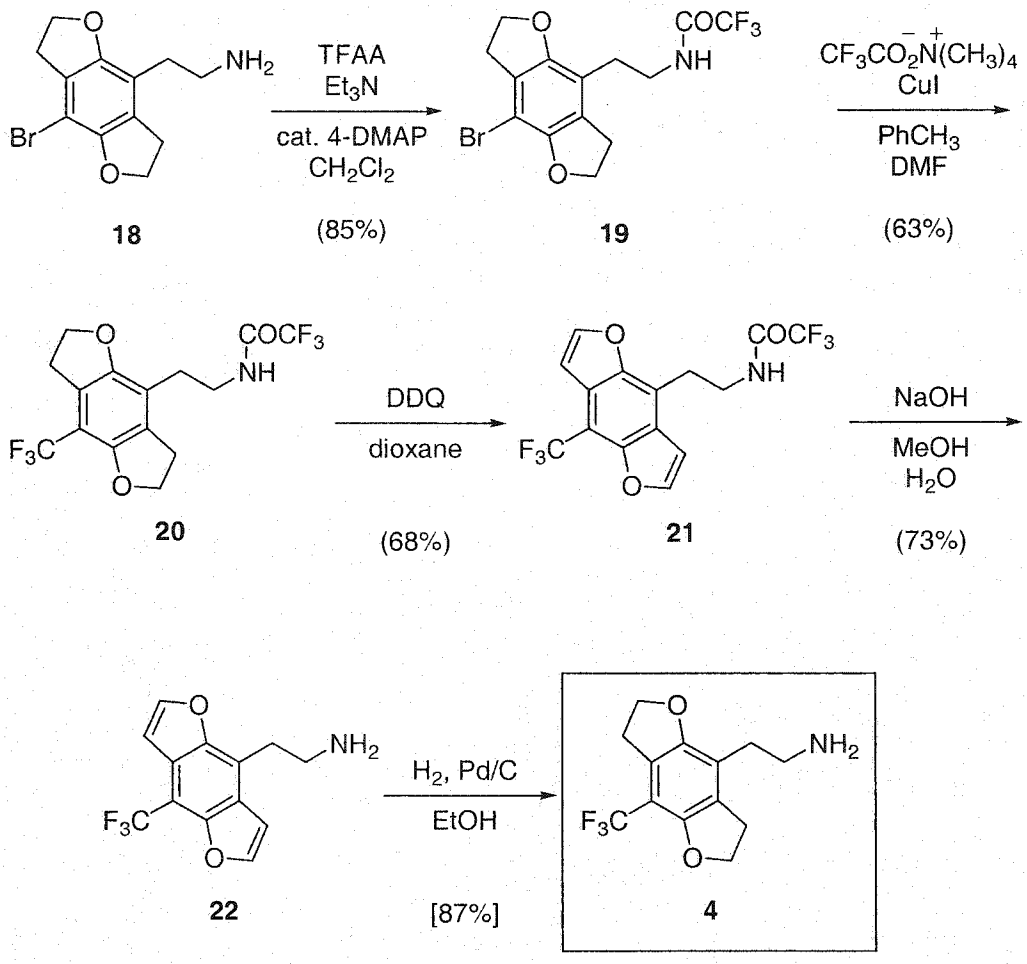

Figure 17. Synthesis of "cold" **4**.

Analogues of 2,6-Dimethoxy-4-Methylamphetamine

The synthesis of (±)-**6** and (±)-**7** (Figure 18) commenced with dialkylation of commercially available orcinol (**23**) utilizing reaction with excess 1-bromo-2-chloro-ethane and potassium carbonate in acetone at reflux.[179] Under these conditions non-

hydrated orcinol was superior to orcinol monohydrate as an alkylation substrate – yields of desired product **24** were 75% and 35%, respectively. Aromatic dibromination was accomplished using bromine in acetic acid and product **25** was subjected to Grignard conditions to effect ring closure and afford the substituted tetrahydro-benzo[1,2-*b*;5,4-*b'*]difuran **26**. This tricyclic material was then regioselectively lithiated at the single, non-substituted aromatic position and the resulting anion quenched with DMF to afford **27**.[180] Substituted benzaldehyde **27** was treated with nitroethane utilizing piperidinium acetate to catalyze the Knoevenagel condensation and afford nitroalkene **28**. A sample of this nitroalkene was then reduced to the alkylamine to afford (±)-**6** using sodium aluminum hydride. Another sample of nitroalkene **28** was treated with DDQ in dioxane at reflux to afford the fully aromatized nitroalkene **29**. This nitroalkene was then similarly reduced with sodium aluminum hydride to the alkylamine to afford product (±)-**7**.

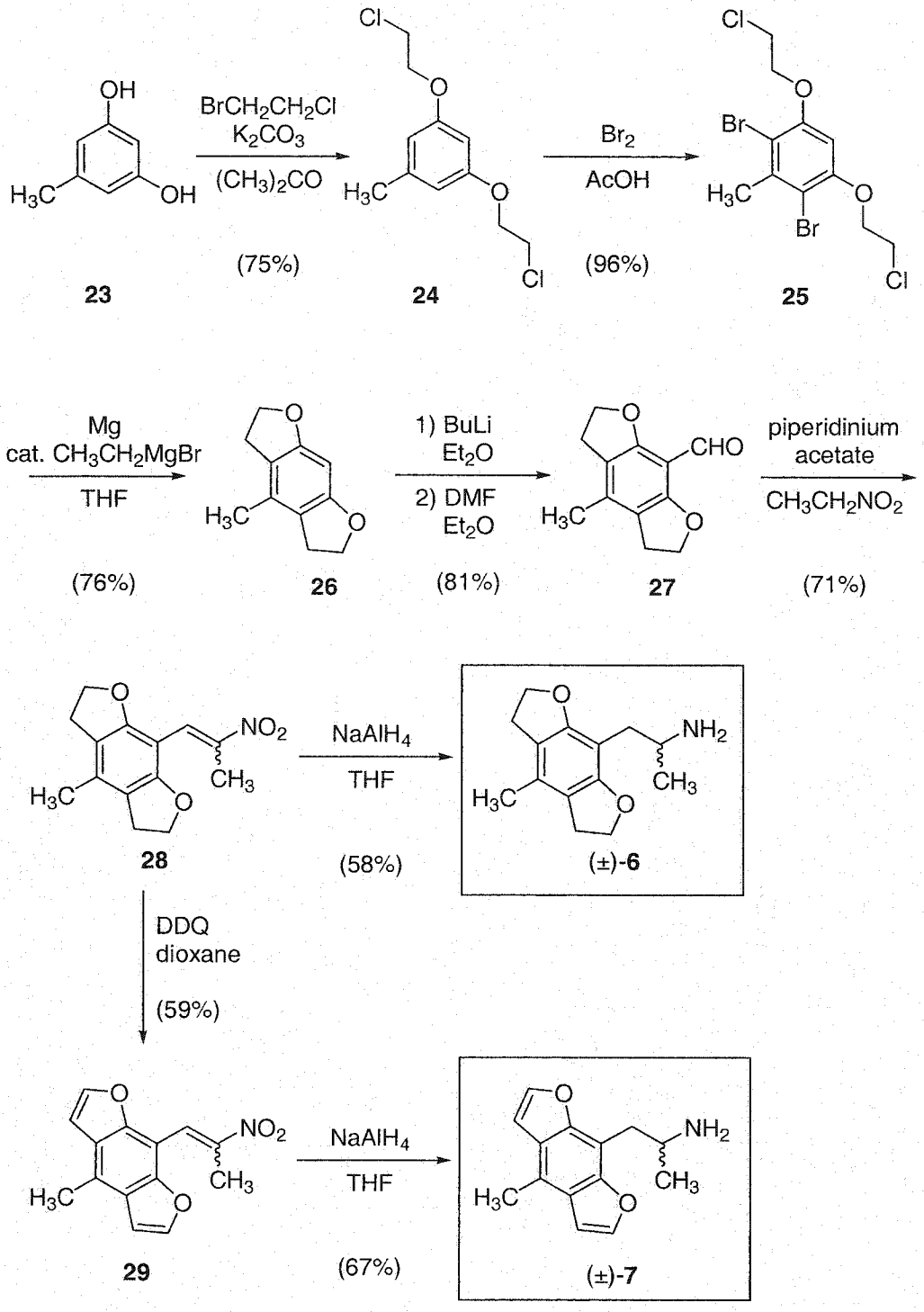

Figure 18. Synthesis of target compounds (±)-**6** and (±)-**7**.

Tetrahydronaphthofurans

Analysis of the target naphthofurans revealed that the six racemic compounds of the proposed series could be derived from a single intermediate, (±)-**9**, also one of the target compounds. The non-aromatized compounds of this naphthofuran series contain two stereocenters and thus, two pairs of enantiomers, the *syn*- and *anti*-racemates. A divergent synthetic scheme was designed to generate separately each enantiomeric pair. Various combinations of bromination, N-protection/deprotection, aromatization, and reduction of (±)-**9** were envisioned to generate the remainder of the series from this divergent intermediate.

Retrosynthetic analysis of (±)-**9** revealed the straightforward disconnection scheme depicted in Figure 19. A carbon-carbon bond forming reaction would be utilized to functionalize ketone (±)-**30** and install the aminomethyl group of the product. It was envisioned that ketone (±)-**30** could be derived from an intramolecular Friedel-Crafts acylation of a substituted propionic acid. The required acid could be obtained from homologation of a substituted acetic acid that is derived from the corresponding methyl ester (±)-**31**. This substituted ester (±)-**31** could be generated by radical cyclization of a γ-aryloxycrotonate derived from O-alkylation of substituted phenol **32** with crotonate **33**.

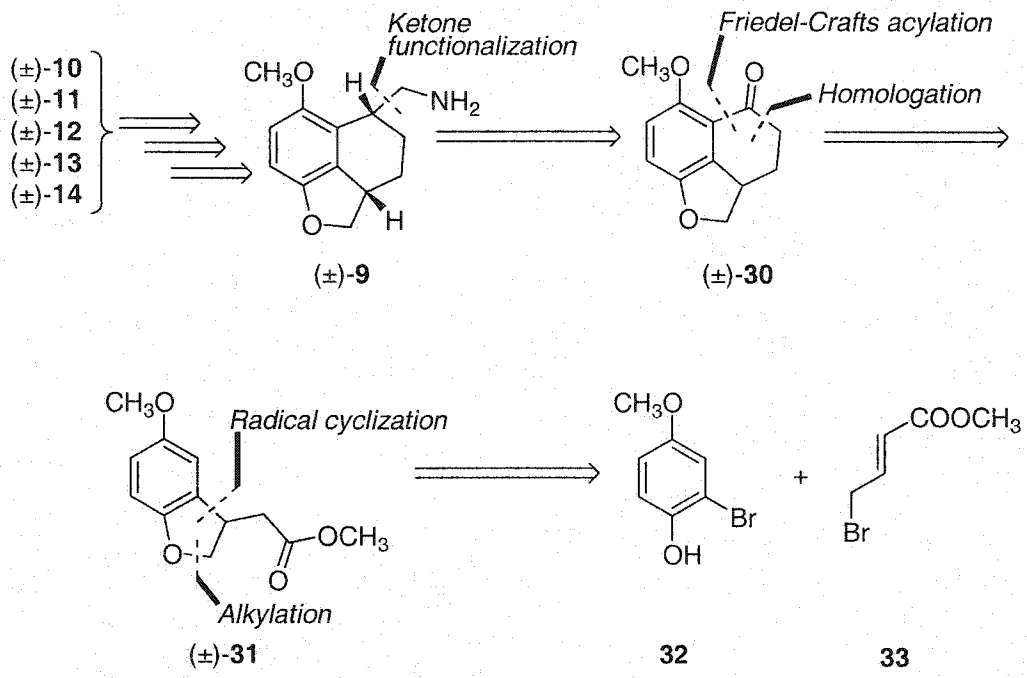

Figure 19. Retrosynthetic analysis of target compounds (±)-**9** - (±)-**14**.

Synthesis of compounds (±)-**9** - (±)-**14** (Figure 20) commenced with the regioselective bromination of 4-methoxyphenol (**34**) to afford **32** utilizing a method by Curran, et al.[181] Substituted phenol **32** was subsequently O-alkylated using Finkelstein conditions with methyl 4-bromocrotonate (**33**) to yield **35**. Routine base-catalyzed O-alkylation at room temperature afforded exclusively the olefin isomerized product **36** (Figure 21), however, rather than the desired allylic ether **35**. Similar isomerization of γ-aryloxycrotonates has been observed and investigated by others.[182] Utilization of exactly one equivalent of potassium carbonate and 0 °C reaction temperature resolved these difficulties. The methyl ester **35** was then subjected to radical reaction conditions to effect ring closure and afford benzofuran (±)-**31**. Limitations imposed by the high dilution requirements of typical radical reactions were overcome by employing a reaction

design that maintained a low concentration of tributyltin hydride, thus resulting in fewer side reactions. Benzofuran (±)-**31** was then subjected to base hydrolysis to afford substituted acetic acid (±)-**37**.[116] Utilizing chemistry originally developed by Monte, et al., (±)-**37** was converted to the acyl chloride with oxalyl chloride and subsequently to diazoketone (±)-**38** by reaction with diazomethane.[116] Diazoketone (±)-**38** was then subjected to Wolff rearrangement by treatment with silver benzoate and triethylamine in methanol to afford the homologated methyl ester (±)-**39**.[183] Ester (±)-**39** was subsequently hydrolyzed with base to afford propionic acid (±)-**40**.

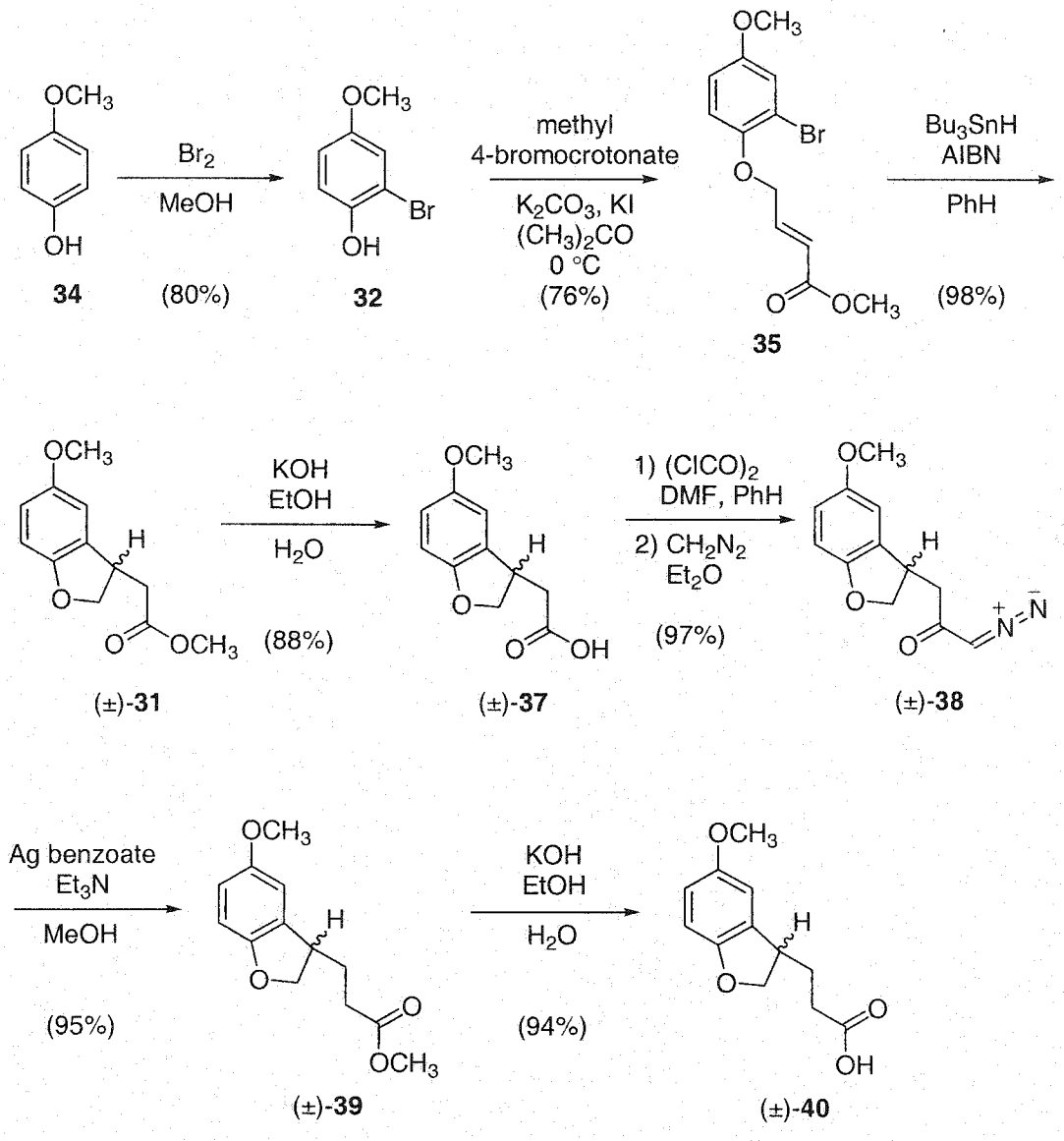

Figure 20. Synthesis of propionic acid (±)-**40**.

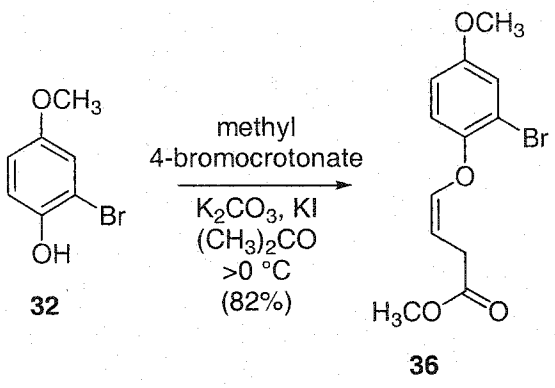

Figure 21. Isomerization difficulties with O-alkylation reaction temperature > 0 °C.

An alternative synthetic scheme (Figure 22) was also employed to generate a larger quantity of propionic acid (±)-**40**. This alternate route involved reduction of methyl ester (±)-**31** to alcohol (±)-**41** using sodium aluminum hydride, followed by protection of the alcohol to afford tosylate (±)-**42**.[184] The tosylate group was then displaced by reaction with potassium cyanide in ethanol to afford (±)-**43**, followed by base hydrolysis of the nitrile to generate homologated acid (±)-**40**.

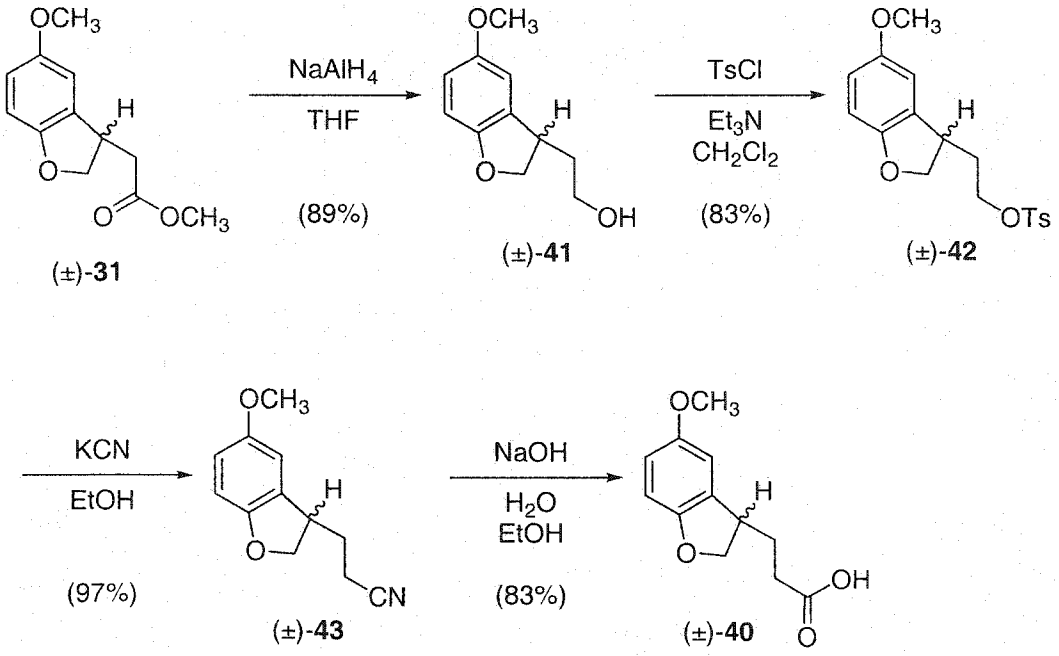

Figure 22. Alternative synthesis of propionic acid (±)-**40**.

Propionic acid (±)-**40** was then converted to the acyl chloride and subjected to Friedel-Crafts conditions to effect ring closure and afford tricyclic ketone (±)-**30** (Figure 23).[185,186] The ketone moiety of (±)-**30** was functionalized utilizing reaction with trimethylsilyl cyanide and zinc iodide in dichloromethane.[187,188] The adduct that was formed by this reaction could not be purified and was directly reduced with sodium aluminum hydride to afford amino alcohol (±)-**44**. Alcohol (±)-**44** was then dehydrated using acidic conditions to yield substituted aminomethyl styrene (±)-**45**. Subsequently, catalytic reduction of (±)-**45** to afford exclusively *syn* product (±)-**9** was accomplished. It was anticipated that reduction of styrene (±)-**45** would result in a mixture of *syn* and *anti* products (±)-**9** and (±)-**10** that would be amenable to separation by chromatography. Interestingly, however, ^{1}H NMR examination of the product of this reaction indicated the

absence of the *anti*-epimer. X-ray analysis of hydrochloride salt crystals of compound (±)-**9** confirmed the *syn*-geometry of the product (Figure 24).

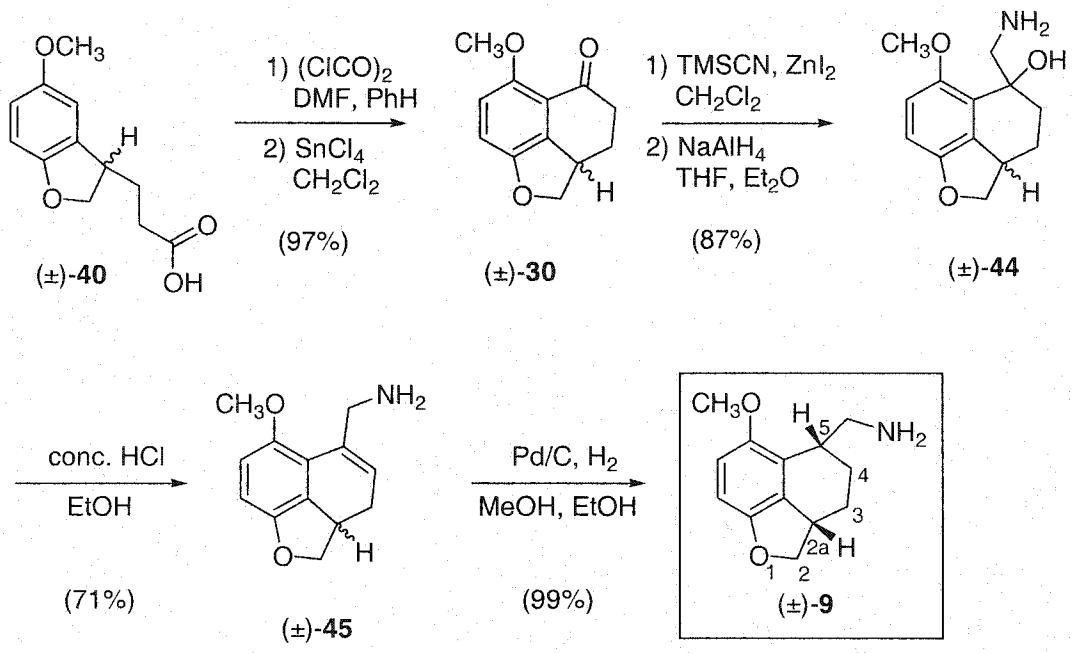

Figure 23. Synthesis of divergent product (±)-**9**.

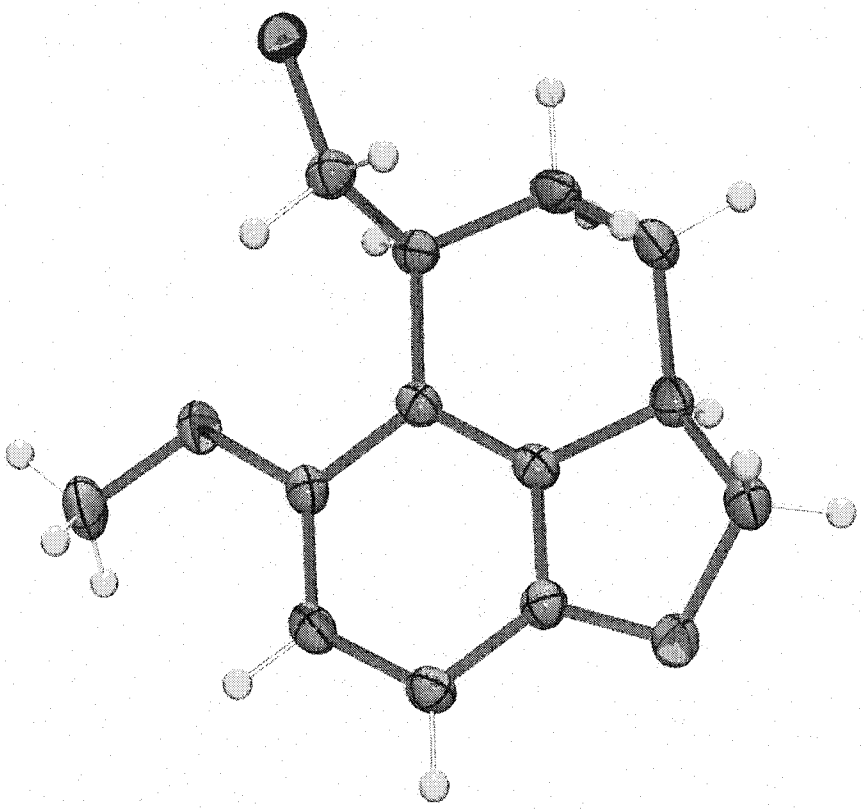

Figure 24. X-ray crystal structure of (±)-**9**.

It is hypothesized that the selectivity observed in the catalytic reduction of (±)-**45** arose from steric-induced facial selectivity. Styrene (±)-**45** appears slightly concave when viewed in the plane of the styrene olefin bond and thus, hydrogen addition to the β–face (concave side) would be somewhat more difficult than addition to the less hindered α–face (convex side) of (±)-**45**. Also, the axial protons of C-2 and C-3 are both oriented in a direction that would sterically obstruct approach from the β–face as shown in Figure 25. The figure depicts a molecular model of styrene (±)-**45** and demonstrates the slight curvature of the structure and the axial proton of C-3. The occurrence of facial

selectivity in compounds that have structures similar to styrene (±)-**45** has been observed and reported in the literature (Figure 26). For example, epoxidation of compound **46** was found to occur in a 99:1 ratio in favor of oxygen addition to the less hindered α-face.[189] Also, reduction of ketone **47** resulted in hydride addition exclusively to the less hindered α-face of the molecule.[190]

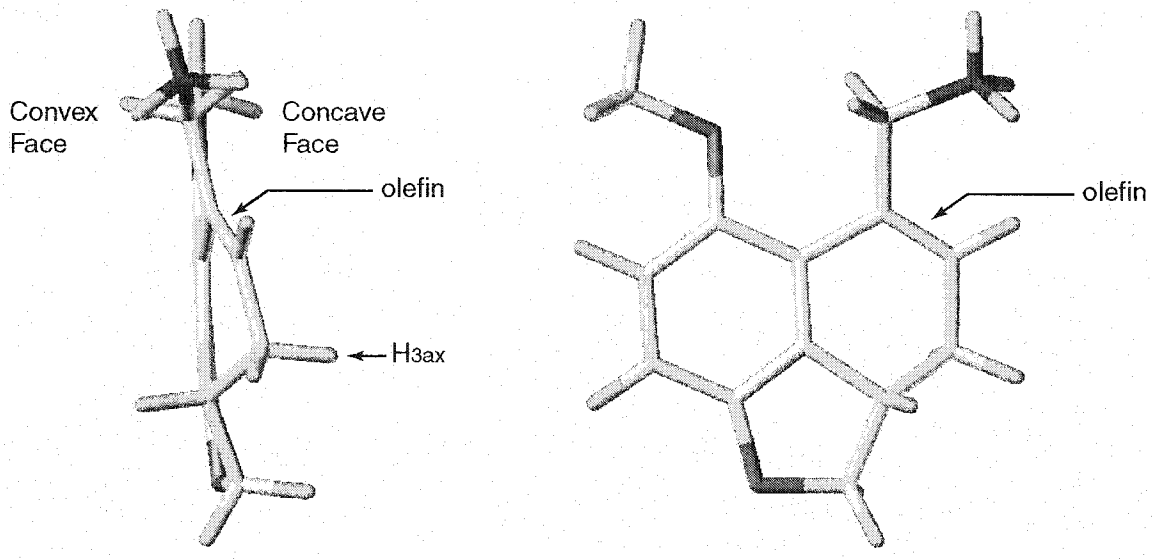

Figure 25. Orthographic view of styrene (±)-**45** suggests that the concave face is hindered to catalyst-mediated hydrogen addition.

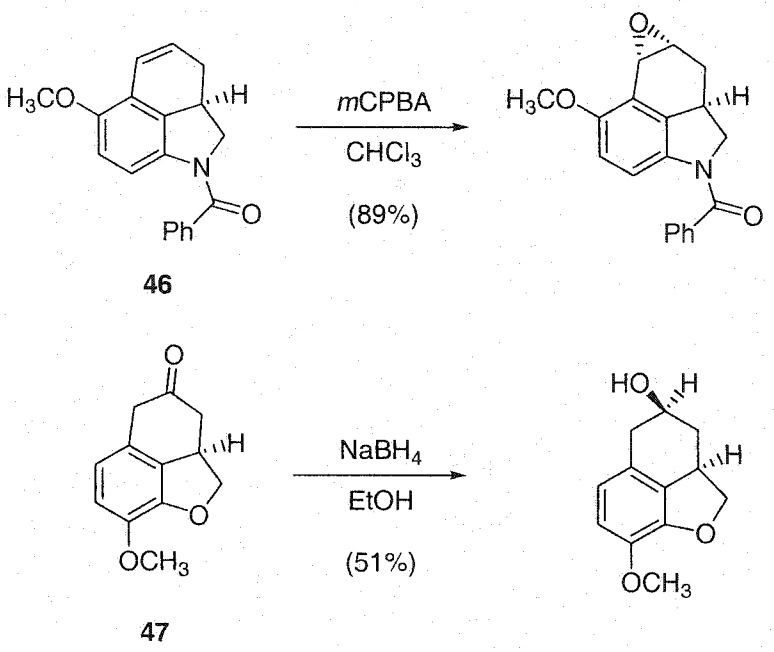

Figure 26. Facial selectivity observed with molecular scaffolds similar to styrene (±)-**45**.

Synthesis of the remaining target compounds of the naphthofuran series began with aromatic bromination of (±)-**9** to afford the *syn* brominated product (±)-**12** (Figure 27). Next, a sample of (±)-**12** was N-protected to afford (±)-**48**. Selective oxidation of the dihydrofuran ring of (±)-**48** was accomplished utilizing reaction with exactly one equivalent of DDQ in dioxane to afford (±)-**49**. Base hydrolysis was then employed to remove the N-protecting group and afford the product (±)-**14**.

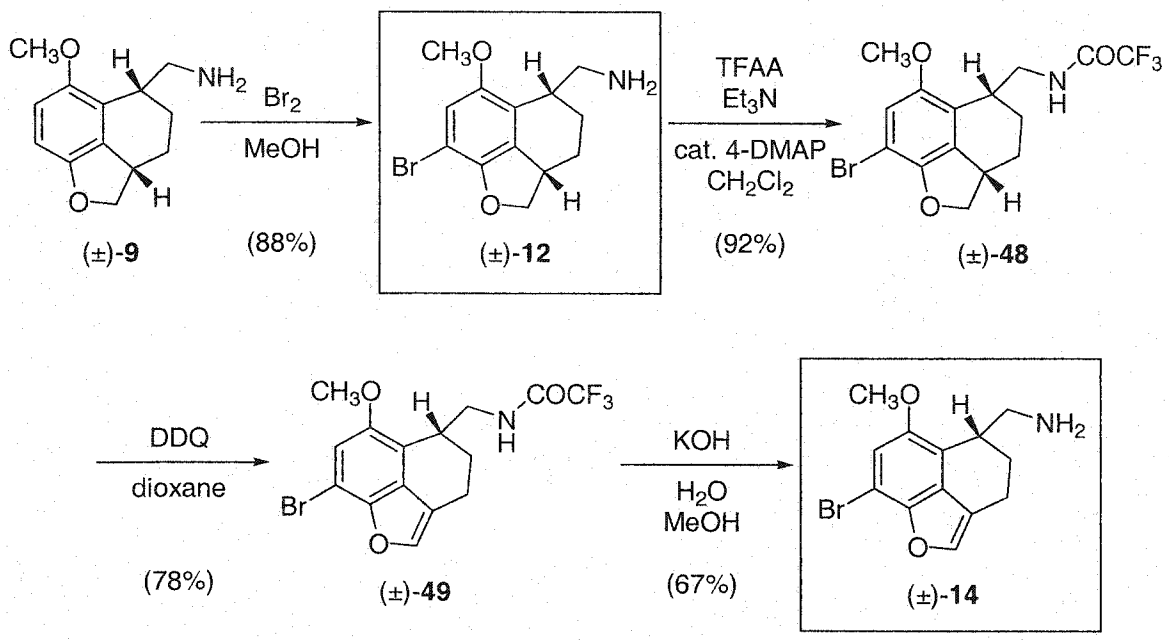

Figure 27. Synthesis of target compounds (±)-**12** and (±)-**14**.

Finally, a portion of (±)-**9** was N-protected as the trifluoroacetamide to afford (±)-**50** (Figure 28). Trifluoroacetamide (±)-**50** was subsequently oxidized utilizing reaction with one equivalent of DDQ to afford (±)-**51**. The N-protecting group of (±)-**51** was then removed by base hydrolysis to afford product (±)-**11**. A further review of literature pertaining to facially selective hydrogenation suggested that the two target *anti*-products, (±)-**10** and (±)-**13**, of the current series might be obtained by utilizing conditions that favor catalyst coordination with the primary amine of the substrate.[191-193] It was anticipated that metal-mediated reduction in a non-polar solvent would enable the basic amine moiety of (±)-**11** to interact electronically with the metal catalyst and thus, hydrogen delivery from the metal would occur on the same face as the amino group resulting in the *anti* product (±)-**10**.[193] Indeed, catalytic hydrogenation of primary amine (±)-**11** in hexane proceeded as anticipated and ^{1}H NMR studies of the crude product

indicated that the reduction had produced an approximately 97:3 ratio of *anti*/*syn* isomers. The ^{1}H NMR spectra of (±)-**9** and (±)-**10** are different in the region of the spectrum that corresponds to aliphatic protons. The benzylic protons (of C-2a and C-5) of (±)-**9** appear in the spectrum as two distinct groups of peaks at approximately 2.9 ppm and 3.2 ppm whereas the corresponding protons of (±)-**10** are found as a multiplet at approximately 3.4 ppm. There are also significant splitting pattern and frequency differences for the methylene protons (of C-3 and C-4) of the two products. A sample of (±)-**10** was then brominated using elemental bromine in methanol to afford *anti* product (±)-**13**. The *anti*-geometry of compounds (±)-**10** and (±)-**13** was ultimately confirmed by X-ray analysis of a crystal of the tosylate salt of (±)-**13** (Figure 29).

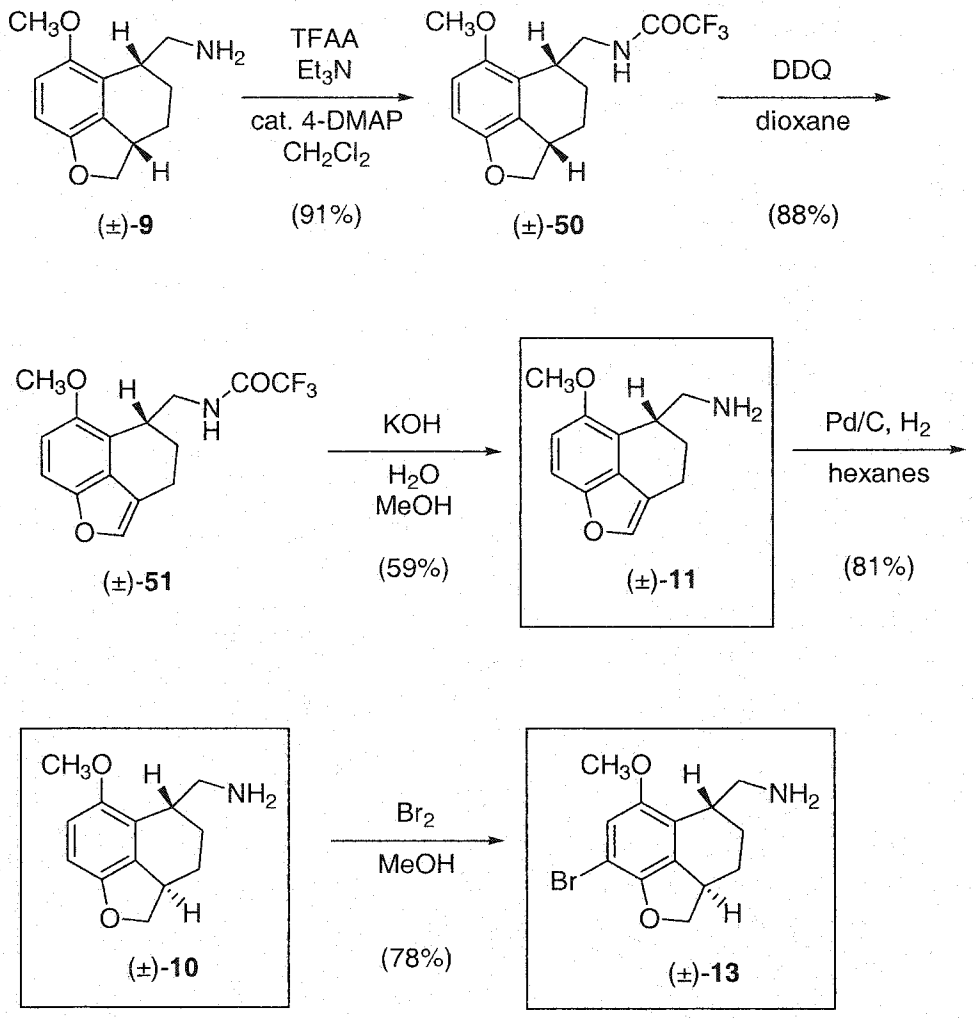

Figure 28. Synthesis of target compounds (±)-**11**, (±)-**10**, and (±)-**13**.

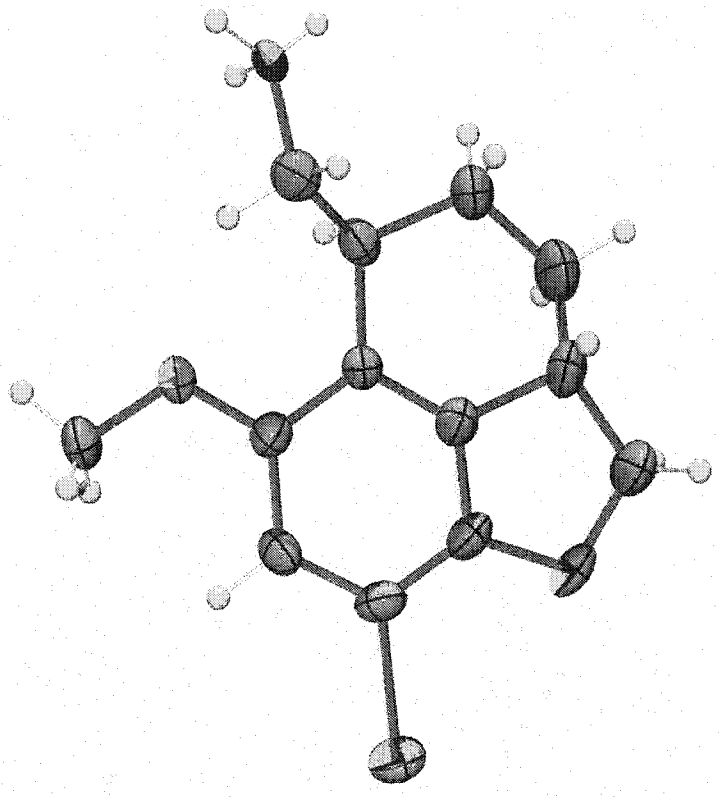

Figure 29. X-ray crystal structure of (±)-**13**.

Pharmacology

The pharmacological results presented in this section were carried out by much appreciated collaborators mentioned in the Acknowledgements section. The details of the methods used to derive the following data will not be presented in full, however, a general description of the experiments as well as references to experimental methodology are supplied. A full account of the work presented here will be published in the primary literature in short order.

The target compounds that were synthesized were subjected to a battery of in vitro experiments to test for potential hallucinogenic activity. All compounds were tested to measure binding affinity at the 5-HT_{2A} receptor and, in some cases, affinity at the 5-HT_{2C} and 5-HT_{1A} receptors. Most compounds were assayed for their ability to activate the 5-HT_{2A} receptor by quantification of IP_3 accumulation, a product of the phospholipase C signaling pathway. Finally, one of the target compounds was examined for its ability to substitute for a training drug in an animal model of hallucinogenesis. At the time of this writing, some pharmacological testing is not complete, however, the results that are now available are discussed below.

Radioligand Competition Binding Studies

The 5-HT_{2A} receptor is believed to be the primary site of action for hallucinogenic drugs, thus, the target compounds were tested for their ability to displace a radiolabeled ligand from preparations of cloned 5-HT_{2A}, 5-HT_{2C}, and 5-HT_{1A} receptors. The precise methodology that has been employed to conduct these radioligand competition binding studies has been described elsewhere.[112] The results of radioligand competition experiments for the target compounds are given in Table 2. Included at the bottom of the table for comparison are the K_i values for several selected reference compounds. Several of the compounds represented in Table 2 were subjected to further examination in other assay systems including receptor efficacy and/or drug discrimination paradigms.

Table 2. Results of radioligand competition binding studies at cloned receptors.

Compound	K_i, nM (SEM)		
	5-HT_{2A} (±)-[^{125}I]-DOI	5-HT_{2C} (±)-[^{125}I]-DOI	5-HT_{1A} [^{3}H]8-OH-DPAT
4	1.8 (0.3) [a]	3.2 (0.5) [a]	125 (34) [a]
(±)-**5**	49 (6.3)	50 (12)	nd
(±)-**6**	6.3 (1.3)	7.5 (0.6)	nd
(±)-**7**	1.8 (0.8)	0.9 (0.1)	nd
(±)-*syn*-Br-**8**	16 (1.5)	4.0 (0.2)	960 (48)
(±)-**9**	700 (130)	59 (0.6)	3000 (460)
(±)-**10**	310 (34)	34 (4.7)	1000 (336)
(±)-**11**	200 (9.2)	11 (1.2)	860 (170)
(±)-**12**	8.7 (0.2)	2.8 (0.2)	520 (67)
(±)-**13**	9.3 (0.2)	4.9 (0.6)	550 (81)
(±)-**14**	2.6 (0.2)	1.1 (0.2)	105 (6)
(±)-**17**	2041 (121) [b]	1567 (139) [c]	nd
DOM	19 (2.0) [d]	nd	nd
DOB	2.2 (0.3) [e]	2.8 (0.7) [e]	nd
psilocin	25 (4.7)	nd	nd
mescaline	6000 (1500) [b]	6200 (800) [c]	3000 (140)
LSD	3.5 (0.62)	5.5 (0.31)	1.1 (0.01)

nd = not determined

[a] data supplied by B. Roth at Case Western Reserve University. [b] [^{3}H]ketanserin as radioligand. [c] [^{3}H]mesulergine as radioligand. [d] data from Nichols, et al.[194] [e] data from Chambers, et al.[112]

Inositol Triphosphate Accumulation Studies

As a measure of 5-HT_{2A} receptor functional activity, a number of the target compounds were analyzed for their ability to stimulate IP_3 accumulation in NIH-3T3 cells stably expressing the 5-HT_{2A} receptor. Accumulation of IP_3 was determined using a modified version of a previously published protocol.[195] The results from these studies are shown below in Table 3. For comparison, data for selected reference compounds are included at the bottom of the table.

Table 3. Results of the IP_3 accumulation studies at cloned rat 5-HT_{2A} receptors.

Compound	EC_{50} at 5-HT_{2A}, nM (SEM)	percent maximal 5-HT stimulation (SEM)
(±)-*syn*-Br-**8**	2090 (125)	63 (3.0)
(±)-**11**	>10000	10 @ 10 μM
(±)-**12**	1100 (283)	49 (8.0)
(±)-**13**	340 (65)	37 (8.0)
(±)-**14**	120 (14)	33 (2.0)
(±)-**17**	3300 (570)	90 (4.8)
DOB	72 (3.6)	79 (6.0)
psilocin	2300 (290)	46 (2.4)
mescaline	2600 (360)	92 (6.3)
LSD	9.8 (3.7)	22 (2.6)

Drug Discrimination Studies

As a measure of hallucinogenic activity, one of the compounds that was synthesized, (±)-**17**, was examined for its effects in rats that were trained to distinguish a

training drug from saline. A two-lever drug discrimination paradigm was employed as a screen for hallucinogenic activity. Briefly, rats were trained to discriminate the effects of saline injection from the effects of either ip injection of LSD (186 nmol/kg) for study of 5-HT_{2A} receptor-mediated effects (hallucinogen-like) or ip injection of LY293284 (75 nmol/kg) for study of 5-HT_{1A} receptor-mediated effects. The response of the animal to the test drug was quantified by counting the number of presses of the appropriate drug lever. Potencies of test drugs were measured using ED_{50} values for those drugs that substituted completely for the training drug, LSD or LY293284. Drugs that did not substitute completely for the training drug were scored as producing either "partial substitution" (PS) or "no substitution" (NS) in which case the percentage of rats responding at a given dosage level is indicated in Table 4. At least 59% of the tested rats must have selected the drug lever for a score of PS to be assigned and 80% of those tested must have selected the drug lever for a score of full substitution. The precise methodology has been described in detail elsewhere.[196-199] The target compounds that were tested in the drug discrimination assay are presented along with their ED_{50} values and 95% confidence intervals (CI). For comparison, drug discrimination data for selected reference compounds are included at the bottom of the table.

Table 4. Results of the drug discrimination studies in LSD- or LY293284-trained rats.

Compound	LSD-trained		LY293284-trained	
	ED_{50} (μmol/kg)	95% CI	ED_{50} (μmol/kg)	95% CI
(±)-**5**	6.04	(3.66 – 9.95)	nd	nd
(±)-**17**	6.61	(3.8 – 11.5)	19.28	(10.43 – 35.63)
8-OH-DPAT	66.7% @ 0.88	PS	0.099	(0.056 – 0.174)
DOB	1.12	(0.86 – 1.46)	nd	nd
psilocin	1.01	(0.69 – 1.46)	nd	nd
mescaline	33.5	(20.9 – 53.5)	nd	nd
LSD	0.037	(0.023 – 0.058)	nd	nd

nd = not determined

Molecular Modeling

In Silico Activation of Bovine Rhodopsin

The bovine rhodopsin protein for which the crystal structure is available is the *inactive* form of the protein – with the "inverse agonist" 11-*cis*-retinal (**15**) isomer bound.[124,155] Our research objective is to understand the binding orientations of compounds that behave as human 5-HT_{2A} receptor *agonists*. Thus, a more appropriate structure for ligand docking studies would be one founded on an *active* state GPCR template. At the present time no such structure is available. Therefore, *in silico*

generation of an active state GPCR template based on the rhodopsin crystal structure was accomplished using weighted mass molecular dynamics – a molecular dynamics simulation protocol that favors rigid body motion of macromolecular structures over high frequency atomic motion thereby synthetically activating the rhodopsin structure in a time efficient manner.[200] The resulting active GPCR template was then used as the structural core for a 5-HT_{2A} receptor homology model. The structure that emerged from the molecular dynamics activation was then mutated to the human 5-HT_{2A} receptor sequence and subsequently used in ligand docking studies.

To create a model of the activated bovine rhodopsin protein, *in silico* isomerization of the bound chromophore was performed followed by relaxation of the resulting high energy protein structure. The process of structural relaxation was quantified by inter-atomic distance measurement of amino acid residues that correspond to double cysteine mutants in a study by Farrens, et al.[174] In brief, the Farrens experiments consisted of a series of double cysteine mutants of rhodopsin ($V_{3.54(139)}$ and each of $K_{6.31(248)}$, $E_{6.32(249)}$, $V_{6.33(250)}$, $T_{6.34(251)}$, and $R_{6.35(252)}$) that were electron spin labeled (Figure 30). To quantify tertiary structural changes, the double cysteine, electron spin labeled proteins were examined in either the absence or presence of light to ascertain changes of inter-spin distance that occur during the receptor activation process. Their experiments indicated that, following exposure to light, TM6 tilted and rotated relative to TM3 (Figure 31).

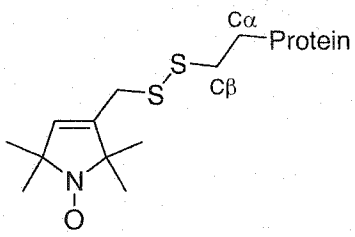

Figure 30. Electron spin label used in Farrens, et al.[174] study of rhodopsin activation.

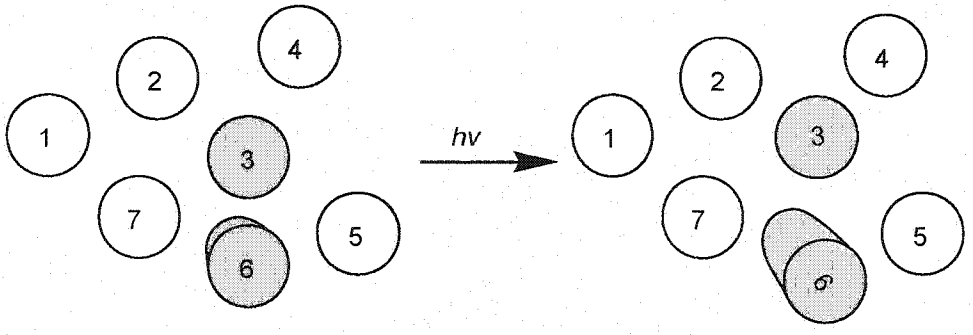

View is from intracellular face of helical bundle, Adapted from Farrens, et al.[174]

Figure 31. Representation of proposed rigid body motion between TM3 and TM6.

In our analysis of *in silico* activation of the native bovine rhodopsin protein, we noted that the majority of protein rigid body motion in the model system did indeed occur in TM3 and TM6 relative to one another. Inter-atomic measurements of specific atom pairs, atoms that correspond to the beta-carbon (Cβ) of the double cysteine mutants discussed above, indicated that motion in the isomerized model system correlated with the data observed in the Farrens, et al.[174] study (Table 5). Further, the *in silico* rigid body motion of the TM α-helices was observed to cause a disruption of inter-helical hydrogen bonds between $E_{3.49(134)}$ and $E_{6.30(247)}$ as well as $R_{3.50(135)}$ and $E_{6.30(247)}$, members of the conserved $E/D_{3.49}$-$R_{3.50}$-$Y/F_{3.51}$ sequence and conserved $E_{6.30}$, known to be important for

GPCR activation.[41,153] During the *in silico* activation process, this group of residues was observed to migrate apart – an indication that the end point structure from molecular dynamics simulation represents an active form of bovine rhodopsin. Figure 32 depicts a schematic diagram of the initial crystal structure and the end point structure. The figure graphically depicts the changes in tertiary structure that were observed during the *in silico* simulation of bovine rhodopsin activation.

Table 5. Weighted masses molecular dynamics results. Inter-atomic measured and inter-spin[174] measured distances.

Measured amino acid pair	Change in inter-atomic distance from initial structure; Cβ of first residue to Cβ of second, Å[a]					Change in inter-spin distance from initial structure; Å [b]
	Dynamics simulation time					
	0 ps	250 ps	500 ps	750 ps	1000 ps	
$V_{3.54(139)}$ - $K_{6.31(248)}$	0.0	2.50	1.54	1.71	2.44	+11 (1)
$V_{3.54(139)}$ - $E_{6.32(249)}$	0.0	0.65	0.39	0.46	1.06	0 (2.5)
$V_{3.54(139)}$ - $V_{6.33(250)}$	0.0	2.40	0.71	-0.47	0.06	-4.5 (2.5)
$V_{3.54(139)}$ - $T_{6.34(251)}$	0.0	0.37	-0.07	1.11	1.48	+11 (1)
$V_{3.54(139)}$ - $R_{6.35(252)}$	0.0	-2.49	-0.84	1.35	1.56	+6.5 (2.5)

a. Change in RMS distance compared to t = 0 ps structure from the Cβ of residue 139 to Cβ of the residue listed. *b*. Estimated values from Farrens, et al.[174] double cysteine mutant inter-spin labeling studies. Spin label movements found in the Farrens, et al. study are of greater magnitude than the dynamics simulation possibly because the inter-spin measured distances occur further from the protein backbone than the current measure of inter-atomic Cβ distances.

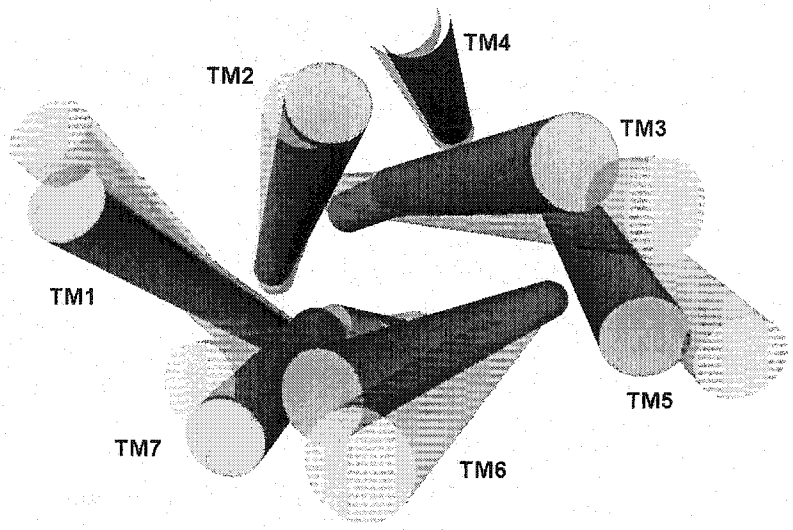

Crystal structure shown as transparent cylinders, *in silico* activated structure as dark grey. View is from intracellular face of helical bundle.

Figure 32: Schematic representation of bovine rhodopsin *in silico* activation results.

We believe that, as a first approximation, the end-point of the *in silico* activation experiment does explain the observed data from rhodopsin activation studies, however, no assumption is, or should be, made about the activation pathway or intermediate stages of the model system and a relationship to the biophysical process that occurs naturally. The specific path of molecular motion during rhodopsin activation and intermediates thereof is currently being investigated by other researchers.[155,172-174,201]

Control experiments were also performed for the *in silico* activation studies to be certain that the observed rigid body motion of TM3 and TM6 had its origin in the 11-*cis*-

to all-*trans*-retinal isomerization and was not simply an artifact of the computer simulation. To investigate the effects of molecular dynamics simulation alone on the initial system, the original crystal structure, less chromophore isomerization, was subjected to identical manipulation and molecular dynamics simulation. The results of this experiment indicated that macromolecular motion was induced by chromophore isomerization because only small structural fluctuations were observed during this control experiment. To investigate the reversibility of the isomerization-induced macromolecular motion, the final activated rhodopsin structure was modified by reversion of the all-*trans*-retinal (**16**) ligand back to the 11-*cis*-retinal isomer (**15**). This complex was then subjected to a similar weighted mass molecular dynamics regime and the results of this experiment indicated that TM3 and TM6 did migrate toward their initial placements in the crystal structure. Although the structure did not converge completely with the initial crystal structure (1.22 Å RMSD), it more closely resembled the product of the previous control experiment (0.83 Å RMSD), the end-point of the protein containing **15** that was subjected to parallel manipulation and dynamics. These experiments were used to show that the rigid body motion observed during *in silico* rhodopsin activation was not simply a software artifact, but was instead induced by isomerization of the chromophore.

Homology Modeling of the Serotonin-2A Receptor

The *in silico* activated bovine rhodopsin structure was used directly for development of the human 5-HT_{2A} homology receptor model. Rather than simply aligning the primary sequences of bovine rhodopsin and the human 5-HT_{2A} receptor, the amino acid sequences of bovine rhodopsin and a number of 5-HT, dopamine, and

histamine receptors were aligned using currently available software (Appendix A). The use of multiple sequences in the alignment served to verify the correct alignment of key GPCR motifs such as the conserved $E/D_{3.49}$-$R_{3.50}$-$Y/F_{3.51}$ sequence at the base of TM3 as well as the residues involved in ionic interaction between $D_{2.50}$-$N_{7.51}$ in TM2 and TM7. The result of multiple sequence alignment indicated that there was relatively low sequence identity between the bovine rhodopsin sequence and any of the monoamine receptors (Appendix B), however, there was sufficient homology and chemical similarity located in the alignment of the TM regions to model the target receptor.

The resultant human 5-HT_{2A} receptor model was used to generate initial placements for molecules that are representative of several compound classes known to activate the 5-HT_{2A} receptor. Hallucinogenic drugs including certain ergolines, tryptamines, and arylalkylamines were employed in the ligand docking routine to test the receptor and investigate its ability to explain previously generated in vitro data. Ligand docking was accomplished by utilizing software programmed to randomly orient the small molecule in the receptor, flex and rotate unrestricted moieties on the ligand, minimize the contacts and energy with the receptor, and then score the resulting orientation. This process was repeated (typically 10^4 iterations per molecule) and the results were ranked and analyzed. The software that was employed does not, however, make allowances for flexibility in the receptor and thus, the receptor/ligand complexes that were ranked highest were further refined using an additional software package. The resulting binding orientations were scrutinized by visual and computational inspection. Typically, top ranked binding orientations that were chosen to be further refined converged to a single, final binding orientation.

The unbiased fashion in which the docking algorithm operated served to test the receptor model without undue human influence. Thus, binding orientations that were generated in these experiments reflect no human manipulation other than programming the location, typically within a 24 Å diameter sphere, of the putative binding site. Most ligand docking that has been performed on previous 5-HT_{2A} receptor models has relied on manual placement of small molecules into putative binding regions. This previously utilized method, while informative at times, is clearly biased by the programmer and thus, viable and novel binding orientations may be overlooked or discarded. Many of the binding orientations that were found during the present study explain specific inferences that have developed from the body of in vitro data pertaining to the 5-HT_{2A} receptor. A detailed description of representative binding orientations for different drug classes will be described in the Discussion section of this discourse.

De Novo Drug Design

Docking of mescaline to the receptor model indicated a novel binding mode in which the side chain adopted a gauche orientation. We hypothesized that an increase in binding affinity for the 5-HT_{2A} receptor might be attained by conformational restriction of the core mescaline structure into an indan ring system. This compound, (±)-**17**, was synthesized in a straightforward fashion beginning with indanone **52** supplied by a collaborator, Stewart Frescas. Indanone **52** was synthesized by condensation of benzaldehyde **53** with malonic acid to afford cinnamic acid **54**. The double bond of **54** was then catalytically reduced to afford the propionic acid **55**. Acid **55** was then cyclized to indanone **52** utilizing Friedel-Crafts reaction conditions. Similar to compound (±)-**30**

of the previously discussed series, the ketone moiety of **52** was functionalized utilizing reaction with trimethylsilyl cyanide and directly reduced to aminoalcohol (±)-**56**. Dehydration of (±)-**56** afforded styrene **57** and subsequent catalytic reduction of the olefin yielded the final compound (±)-**17**.

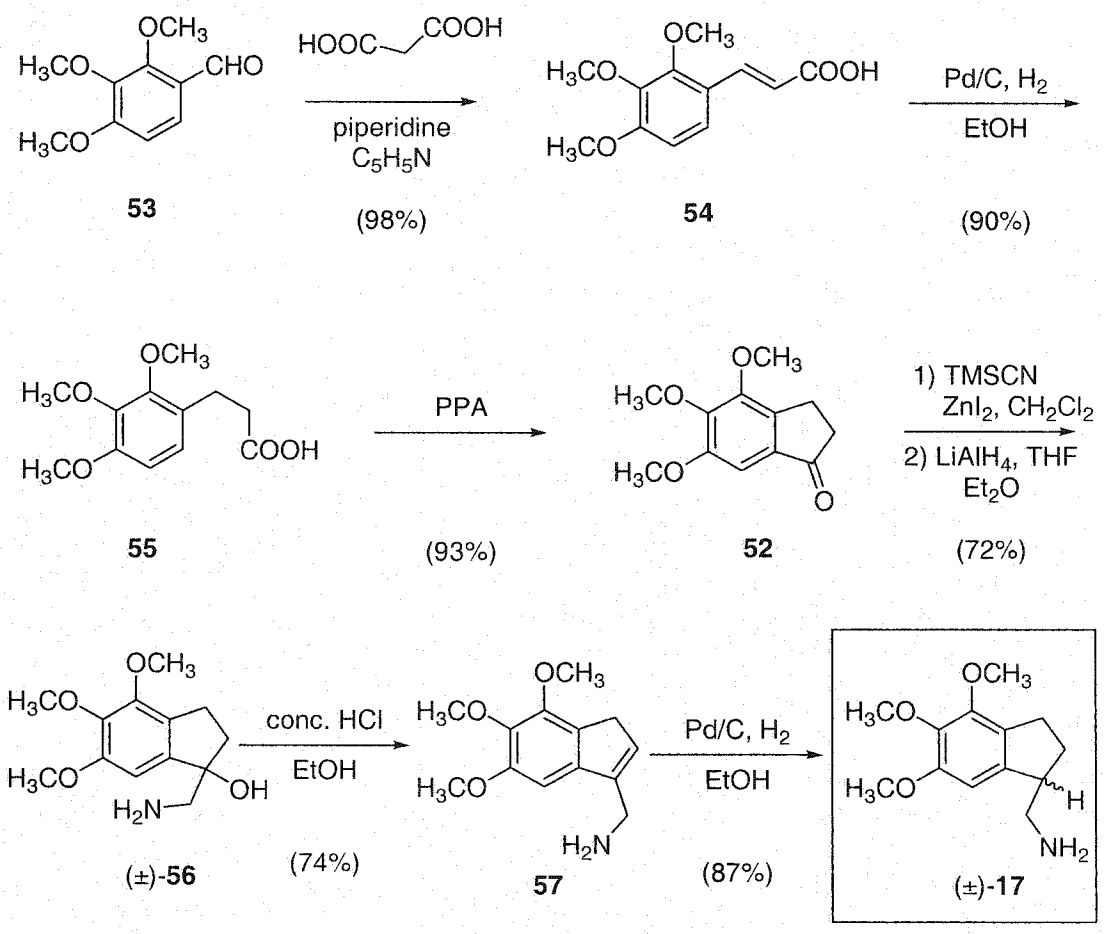

Figure 33. Synthesis of conformationally-restricted mescaline analogue (±)-**17**.

DISCUSSION

Conformationally-Restricted Arylalkylamines

Benzodifurans

Compound **4**, produced as a non-radiolabeled form of a novel radioligand, was pharmacologically tested by utilizing high throughput screening by collaborators at Case Western Reserve University. The results from this screening indicate that compound **4** has high affinity for both the 5-HT_{2A} and 5-HT_{2C} receptor isoforms (Table 2). These data had been qualitatively predicted based on the results of a previously tested series of compounds.[112] The high affinity that ligand **4** exhibits for both the 5-HT_{2A} and 5-HT_{2C} receptors suggests that the radiolabeled form of this compound will be a useful pharmacological tool for future in vitro competition binding assays.

Next, relocation of the 5-alkoxy substituent of typical arylalkylamines to the 6-position, as in 2,6-dimethoxy-4-methylamphetamine ((±)-**5**), resulted in deleterious effects on 5-HT_{2A} receptor binding affinity. Compound (±)-**5** had an approximately three-fold lower affinity for the 5-HT_{2A} receptor compared to the parent compound, DOM (DOX, where X = CH_3). The conformationally-restricted analogues of (±)-**5**, compound (±)-**6** based on the 2,3,5,6-tetrahydrobenzo[1,2-*b*;5,4-*b'*]difuran nucleus and

compound (±)-**7** based on the aromatic benzo[1,2-*b*;5,4-*b'*]difuran nucleus, possessed an approximate seven-fold and 27-fold increase in affinity, respectively, compared to non-rigid, positional isomer (±)-**5**.

Diminished 5-HT_{2A} receptor affinity for (±)-**5** compared to DOM is likely the result of the altered position of the methoxy group. It could be that the 5-methoxy group of DOM interacts optimally with the binding site, thus helping to explain the high potency for the structures of typical arylalkylamines. Translocation of the important 5-methoxy group to the 6-position diminishes the positive contribution of this common ligand/receptor interaction and results in lower binding affinity.

To explain their increased affinity, conformationally-restricted analogues (±)-**6** and (±)-**7**, however, must be able to form reinforcing interactions with the receptor that the non-rigid counterpart (±)-**5** cannot. Previously studied compounds based on the tetrahydrobenzo[1,2-*b*;4,5-*b'*]difuran heterocycle, structurally similar to the conformationally-restricted analogues (±)-**6** and (±)-**7**, demonstrated that arylmethoxy group rigidification resulted in a binding affinity increase of up to 40-fold relative to the corresponding non-rigid compounds.[112,121-123] Thus, conformationally-restricted analogues (±)-**6** and (±)-**7** were correctly predicted to display enhanced affinity for the 5-HT_{2A} receptor. Rigidification of the alkoxy substituents of the new rigid compounds into the plane of the phenyl ring presumably decreased the entropic barrier to binding and thereby enhanced affinity for the 5-HT_{2A} receptor. This conformational restriction, we hypothesize, enables the rigid compounds to form tighter hydrogen bonds with amino acids in the agonist binding site by constraining the bulky alkoxy substituents into a conformation that decreases steric repulsion. This restriction may also direct the lone

pairs of electrons of the oxygen atoms toward a hydrogen bond acceptor of the protein. Alternatively, the increased hydrophobicity of the added methylene groups may enhance the ability of compound (±)-**6** to partition into the hydrophobic binding site. The current studies also have indicated that aromatization of the dihydrofuran rings ((±)-**7**) increased binding affinity 27-fold relative to the corresponding non-rigid compound (±)-**5**, an effect also observed in the series of compounds tested previously.[112,121-123] Presumably this increase in affinity for the receptor occurred from enhanced partitioning of the drug into the hydrophobic agonist binding site or from improved π-π-type or T-type edge-face interactions with aromatic residues of the agonist binding site.

Tetrahydronaphthofurans

Compounds (±)-**9** - (±)-**14** were assayed for their ability to bind to the 5-HT_{2A} receptor and to activate the phospholipase C pathway by quantifying IP_3 accumulation. The receptor affinity results (Table 2) indicate that the three compounds that contain an aromatic bromide, (±)-**12**, (±)-**13**, and (±)-**14**, exhibit appreciable affinity for the receptor. The analogues that lack an aromatic bromide, (±)-**9**, (±)-**10**, and (±)-**11**, however, were found to have significantly lower affinity for the 5-HT_{2A} receptor. Direct comparison of brominated and non-brominated counterparts (e.g. (±)-**12** vs. (±)-**9**, (±)-**13** vs. (±)-**10**, and (±)-**14** vs. (±)-**11**) demonstrates that the presence of a bromine atom on the phenyl ring results in 33- to 81-fold increase in binding affinity for members of this drug series. A general requirement for potent hallucinogenic arylalkylamines is that the substituent at the *para*-position, the 8-position of the currently discussed series, be a bulky,

hydrophobic group.[60,202,203] Thus, the disparity in binding affinity between brominated and non-brominated compounds in this series was not surprising.

The benzofuran-containing compounds (±)-**11** and (±)-**14** were found to exhibit significantly higher affinity for the 5-HT_{2A} receptor than the corresponding non-aromatized counterparts. Aromatization of the dihydrofuran ring of compounds in the current series resulted in a 1.5- to 3.5-fold increase in binding affinity for the 5-HT_{2A} receptor. Again, this result was predicted because previously synthesized compounds have shown that extension of the core aromatic system to the dihydrofuran rings of compounds containing the tetrahydrobenzo[1,2-*b*;4,5-*b'*]difuran nucleus has the effect of enhancing binding affinity and efficacy at this receptor.[112,121-123] Although it is not clear how exactly this effect is brought about, it may be that oxidation of the dihydrofuran ring increases the aromatic surface area of the drug, thereby aiding in partitioning and enhancing hydrophobic interactions within the agonist binding site.

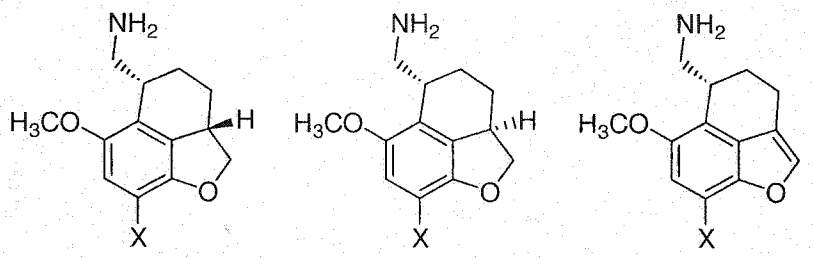

(±)-**9**; X = H
(±)-**12**; X = Br

(±)-**10**; X = H
(±)-**13**; X = Br

(±)-**11**; X = H
(±)-**14**; X = Br

Finally, comparison of 5-HT_{2A} receptor binding affinity of the *syn* and *anti* compounds, (±)-**9**, (±)-**10**, (±)-**12**, and (±)-**13**, shows that there is little difference in affinity between the pair of *syn* compounds and the pair of *anti* compounds. The results indicate no appreciable difference between the brominated compounds, *syn* product

(±)-**12** compared to *anti* product (±)-**13**, and only an approximate 2-fold difference between the non-brominated compounds, *syn* product (±)-**9** compared to *anti* product (±)-**10**, in favor of *anti* product (±)-**10**. The pharmacological similarity that is represented by the receptor binding results of these compounds may be explained by the observation that the *syn* and *anti* compounds offer little difference in their respective three-dimensional molecular structure. Figure 34 depicts *syn* product (±)-**12** and *anti* product (±)-**13** aligned by key structural features of arylalkylamines (bromine, nitrogen, and oxygen atoms). Comparison of these two ligands illustrates the apparently minor difference between them. Thus, the difference with respect to binding to the agonist site of the 5-HT_{2A} receptor could also be construed as being very minor and may explain their similar pharmacology. Assuming there is space enough for a slight shift in binding orientation, it appears that both compounds may be accommodated within the binding site. The aromatic compound (±)-**14** is likewise very similar in molecular shape to *syn* and *anti* products (±)-**12** and (±)-**13**. This observation suggests that the increase in affinity that results from aromatization of the dihydrofuran ring must be largely of an electronic or hydrophobic nature.

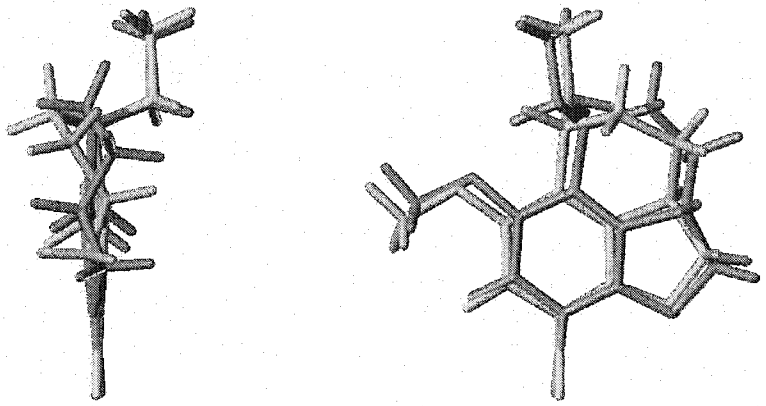

12 shown in red, **13** in green.
RMSD aligned by nitrogen, oxygen, and bromine atoms, orthographic view.

Figure 34. Structural comparison of **12** and **13**.

Compounds (±)-**11**, (±)-**12**, (±)-**13**, and (±)-**14** of the present series were tested for their ability to activate the phospholipase C pathway by quantifying IP_3 accumulation. These data (Table 3) indicate that the compounds tested are not potent agonists in this pathway. The most efficacious compound, (±)-**14**, while exhibiting a sub-micromolar EC_{50}, was found to be only a weak partial agonist. The brominated compounds of the present series, (±)-**12**, (±)-**13**, and (±)-**14**, however, displayed at least 2-fold increased potency compared to the previously synthesized *syn* brominated (±)-**8**. Recently, the aromatic brominated compound (±)-**14** has been found to be relatively potent for activation of a different signaling pathway, one where LSD has, in our laboratory, recently been found to be extremely potent. It is unknown which of these pathways may be the signaling pathway that correlates best with hallucinogenesis.

Molecular Modeling and *De Novo* Drug Design

The ability of the 5-HT_{2A} receptor model to explain empirical data has survived tests of known compounds and has been used to identify distinct binding modes for ergolines, tryptamines, and arylalkylamines that are compatible with the known SAR of these structural classes.

Ergoline binding to the human 5-HT_{2A} receptor

Docking of LSD, a partial agonist, to the 5-HT_{2A} receptor model resulted in the drug bound to the receptor in an orientation that presented the protonated amine of the ligand to $D_{3.32(155)}$, a residue conserved across the family of monoamine GPCRs, forming a strong ionic bond.[205] Inspection of the binding orientation also revealed that the N-1-hydrogen of the ligand formed a hydrogen bond with the hydroxyl and backbone carbonyl group of $S_{5.46(242)}$. The importance of the N-1-hydrogen/$S_{5.46(242)}$ hydroxyl interaction for ergolines has been suggested by others based on mutational evidence, species-specific receptor binding data, and data derived from ligand N-1-alkylation, as discussed in the Introduction section of this work.[145,160,206,207] Further, it was observed that the amide carbonyl oxygen of LSD accepts a hydrogen bond from the amide group of $N_{6.55(343)}$, a residue at the extracellular side of TM6. To the best of our knowledge, this interaction has not been previously identified by mutational or SAR studies. We hypothesize that the hydrogen bond between the amide carbonyl oxygen substituent of LSD and $N_{6.55(343)}$ may be directly involved in 5-HT_{2A} receptor *antagonism*. This hydrogen bond between the ergoline and receptor may dampen the full range of motion of TM6, thereby preventing normal activation of the receptor that typically occurs with a

drug that is a full agonist. That members of the ergoline class of drugs are invariably partial agonists or antagonists and *not* full agonists at the 5-HT_{2A} receptor may be explained by this hypothesis.

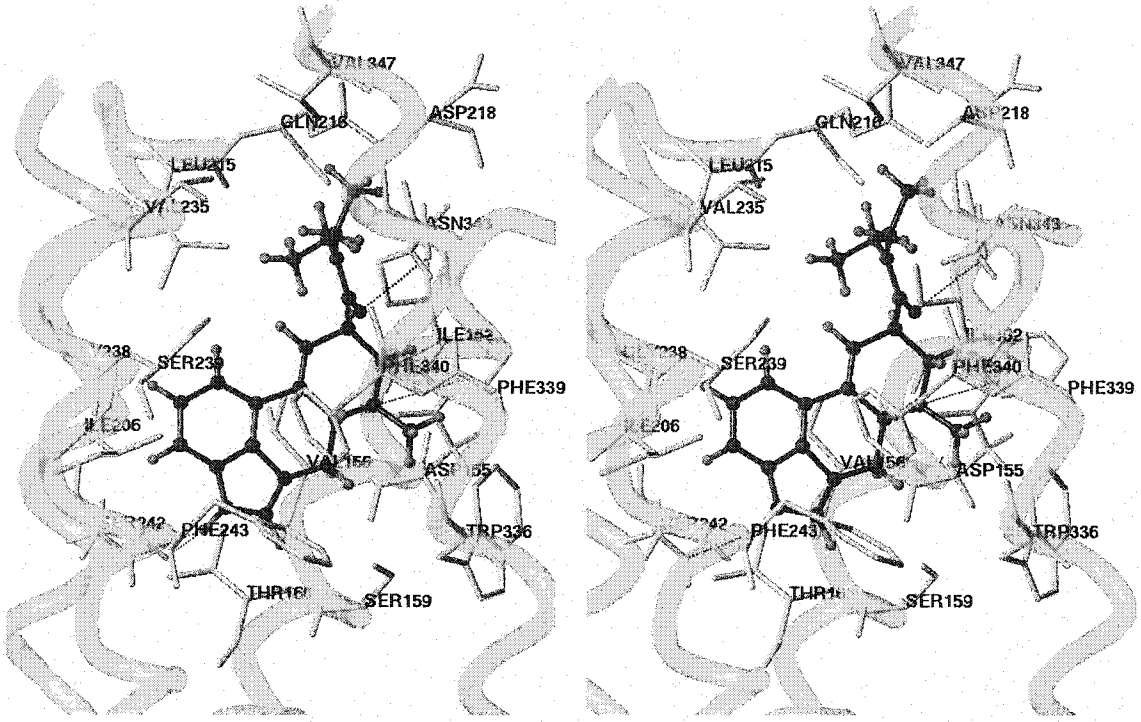

Hydrogen bonds are shown as dashed lines.

Figure 35: Stereo view (cross-eyed) of LSD docked to the 5-HT_{2A} receptor model.

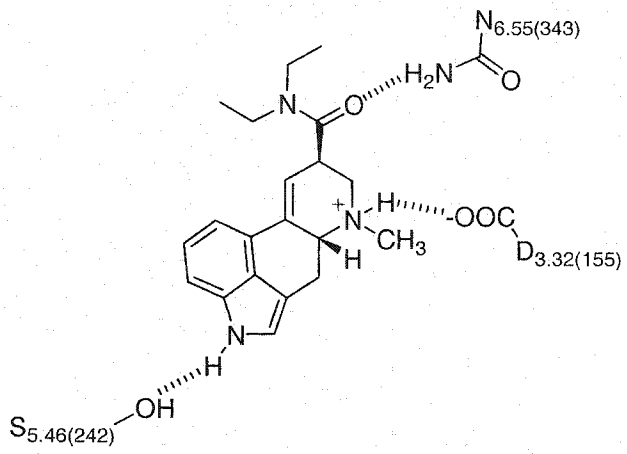

Figure 36. Schematic representation of LSD in the 5-HT_{2A} receptor model.

Tryptamine binding to the human 5-HT_{2A} receptor

Investigation of the binding orientation of 5-HT, the endogenous ligand for this receptor, resulted in ambiguous results. The relatively high degree of conformational flexibility of the ligand led to multiple potential docking orientations. Thus, conformationally-restricted analogues of known drugs were employed and have proven valuable for these modeling studies by locking ligand structures into a rigid conformation – ideally one that is biologically active. Compound rigidity simplifies ligand docking by limiting the number of rotameric forms of the drug and thus, reducing the computational time and calculations necessary to complete the docking phase of studies. To limit the uncertainty of the tryptamine orientation in the binding site, we employed the conformationally-restricted analogue (*R*)-(+)-3-(*N*-methylpyrrolidin-2-ylmethyl)-5-methoxyindole (**58**).

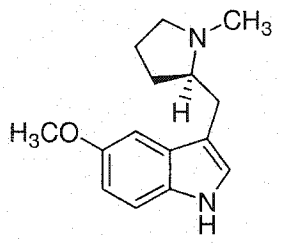

58

Compound **58** was chosen because it has been fully characterized in vitro and the more active enantiomer is known.[208] The results of docking **58** into the 5-HT_{2A} receptor model were unambiguous. The docked orientation, followed by minimization, produced only one favorable binding orientation. The docked orientation (Figure 37) indicates that the protonated amine of **58** interacts with $D_{3.32(155)}$ in the same manner as LSD. The 5-methoxy group of **58** was found to be involved with hydrogen bonds from the hydroxyl groups of both $S_{3.36(159)}$ and $T_{3.37(160)}$ and, finally, the indole N-1-hydrogen was found to interact with the hydroxyl of $S_{5.43(239)}$. This binding mode demonstrates that the orientation of the indole nucleus of **58** differs in orientation from the indole nucleus embedded in the ergoline (LSD) structure.

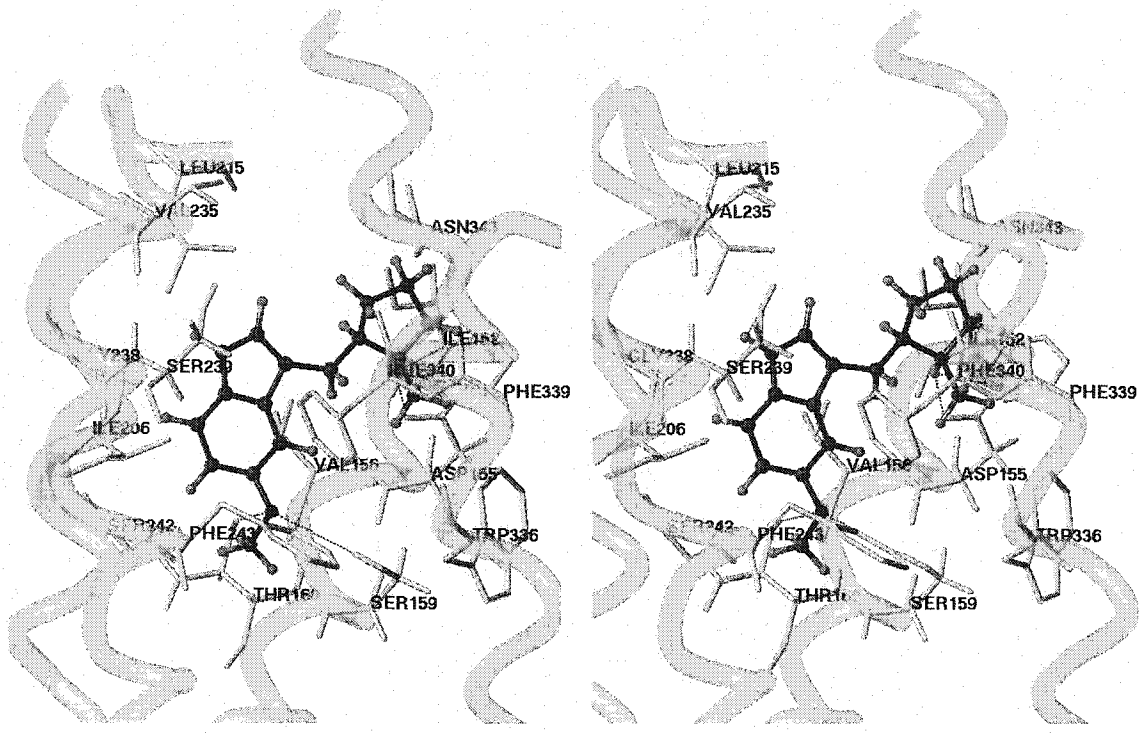

Hydrogen bonds are shown as dashed lines.

Figure 37. Stereo view (cross-eyed) of (*R*)-(+)-3-(*N*-methylpyrrolidin-2-ylmethyl)-5-methoxyindole (**58**) docked to the 5-HT_{2A} receptor model.

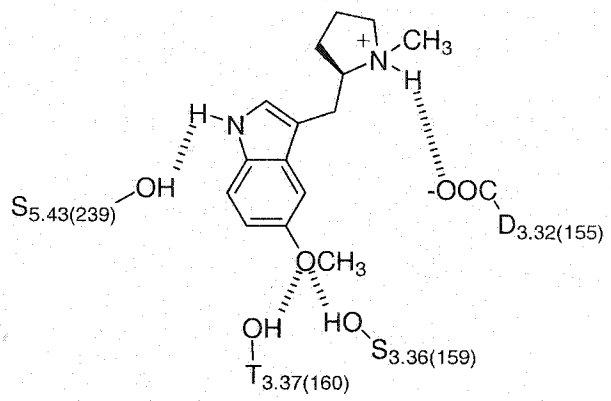

Figure 38. Schematic representation of **58** in the 5-HT_{2A} receptor model.

Members of the tryptamine class of hallucinogenic drugs that have a 4-hydroxy substituent (i.e. psilocin) are also active at the 5-HT_{2A} receptor. The presence of an acidic moiety suggests that there is flexibility in the requirements for hydrogen bond directionality or donor/acceptor role reversals between the ligand and receptor to account for the similar pharmacology of both the 4-hydroxy and 5-methoxytryptamines. During the docking experiments of selected tryptamines, the role of $S_{3.36(159)}$ was of particular interest. Almaula, et al.[140] have shown that mutation of this residue to alanine or cysteine has no effect on the binding affinity of LSD and only a minor deleterious effect on the affinity of bufotenine (the N,N-dimethyl analogue of 5-HT). Conversely, these 5-HT_{2A} receptor point mutations led to marked reduction in the affinity of 5-HT. The authors therefore suggested that $S_{3.36(159)}$ may form an additional hydrogen bond to the protonated amino group of 5-HT which cannot occur if the amino group is N-alkylated due to steric effects, such as in bufotenine. The docking results obtained from the present 5-HT_{2A} molecular model provide an attractive alternate explanation – a binding orientation in which the 5-oxygen moiety of the indole nucleus in compound **58** accepts a hydrogen bond from $S_{3.36(159)}$. Mutation of this residue to alanine would therefore be expected to deleteriously affect affinity of 5-HT for the receptor.

Other studies of site-directed mutants and species-specific binding data, however, do not fit a single binding orientation model for the tryptamine drug class. Instead, it appears that there may be at least two distinct orientations for tryptamine ligands to bind and activate the 5-HT_{2A} receptor. Studies have shown that some N-1-alkyl substituted tryptamines exhibit species selectivity, parallel to the effect demonstrated by the N-1-alkyl substituted ergolines.[145,206,207] These findings suggest a direct interaction of the

N-1-substituent of both compound classes, tryptamines and ergolines, with $S_{5.46(242)}$ – the lone amino acid difference in the putative binding domain of the human and rat 5-HT_{2A} homologues – an alanine in the 5-HT_{2A} rat homologue. Support for an ergoline-like binding orientation for some tryptamines comes from a study by Shih, et al.[209] in which it was observed that psilocin binds with 15-fold higher affinity to the human 5-HT_{2A} receptor compared to the rat 5-HT_{2A} receptor. This species-dependent difference in binding affinity for psilocin indicates that some part of the ligand must interact with $S_{5.46(242)}$. This same study, however, reported that bufotenine binds with comparable affinity to both species homologues, suggesting a binding orientation for this compound in which the importance of $S_{5.46(242)}$ is diminished.

Indeed, the 5-HT_{2A} receptor computer model has indicated that psilocin may adopt a binding orientation that resembles either the embedded tryptamine moiety of the ergoline compound class in which the N-1-hydrogen of psilocin interacts directly with $S_{5.46(242)}$ or an orientation like that found for **58**. It seems plausible that tryptamines may bind in either of the two modes demonstrated by the distinct orientations of psilocin in Figures 39 and 40 and that minor structural variations in the ligand may lead to changes in the docking orientation. The observation that multiple, divergent binding modes were found for the native ligand, 5-HT, during the docking phase also supports a dual binding mode hypothesis for the tryptamine family.

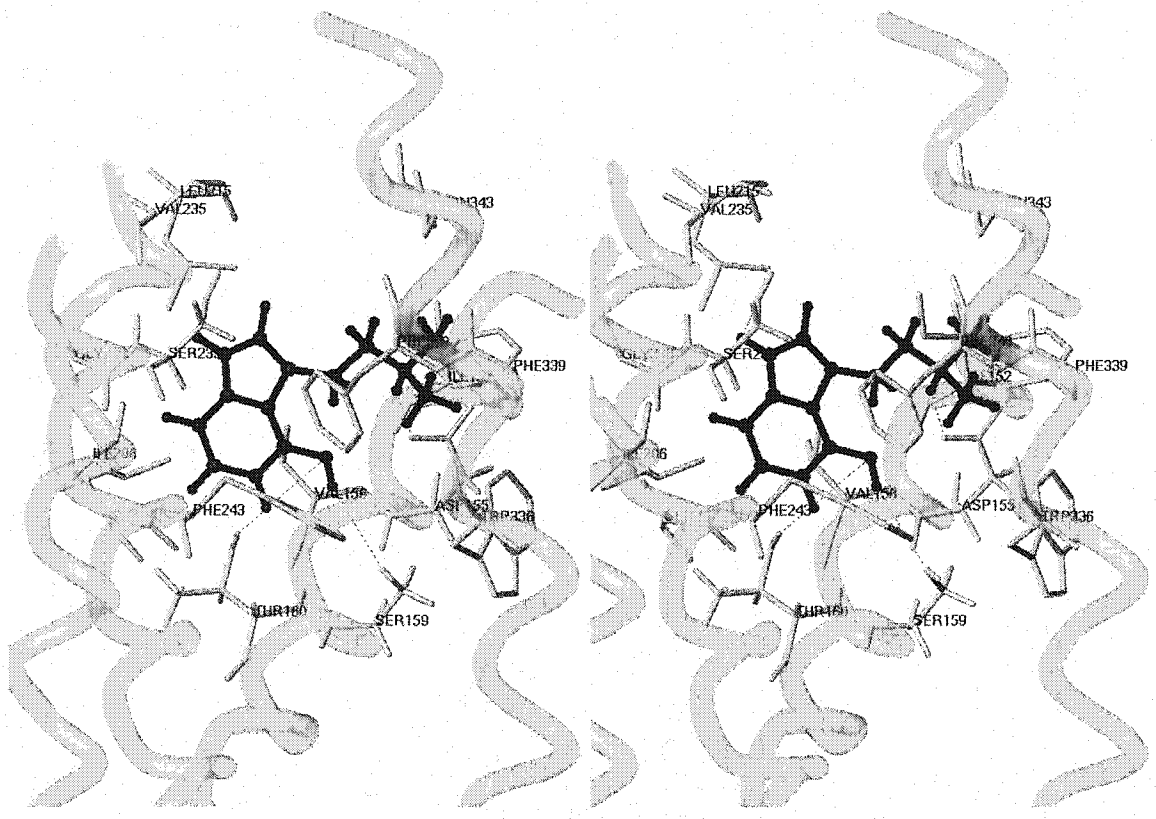

Hydrogen bonds are shown as dashed lines.

Figure 39. Stereo view (cross-eyed) of psilocin docked to the 5-HT_{2A} receptor model in an orientation like that of **58**.

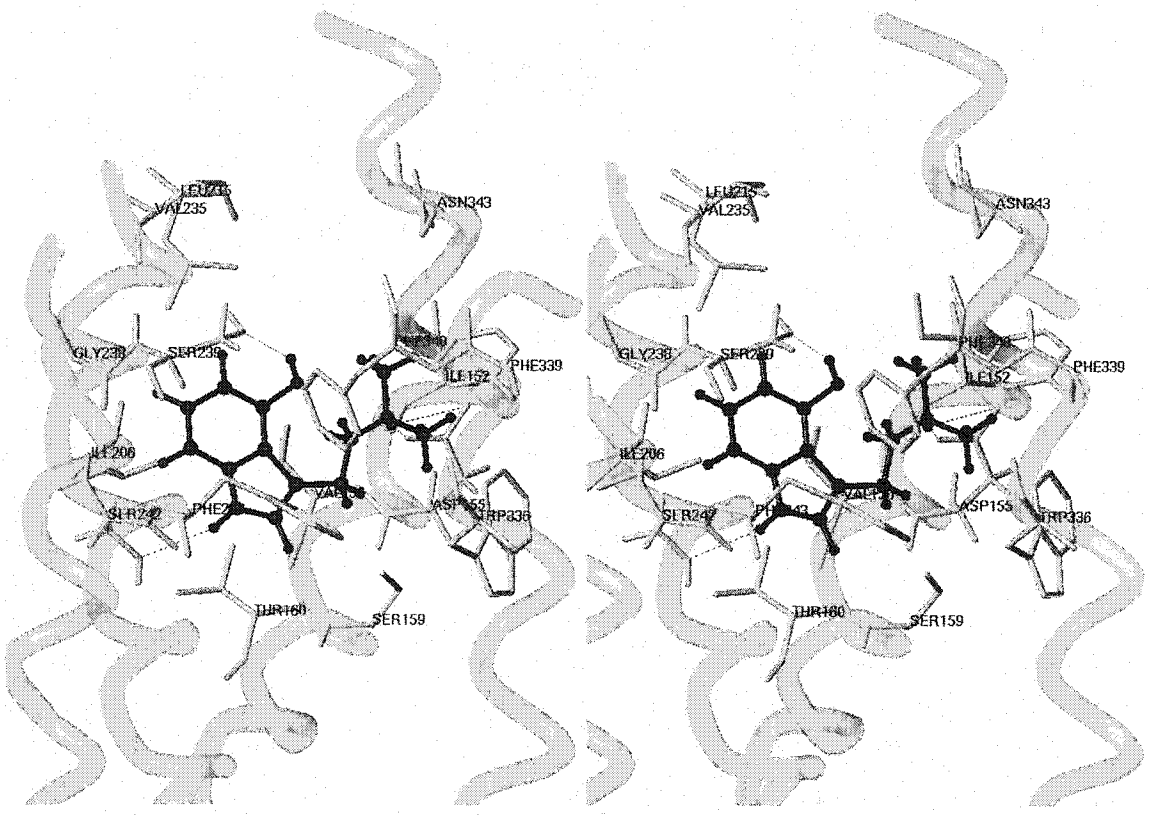

Hydrogen bonds are shown as dashed lines.

Figure 40. Stereo view (cross-eyed) of psilocin docked to the 5-HT_{2A} receptor model in an orientation like that of LSD.

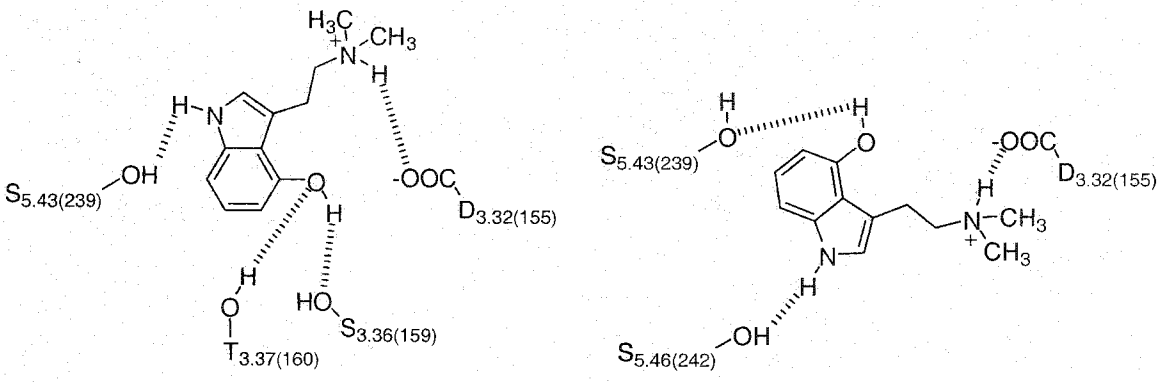

Figure 41. Schematic representation of possible psilocin orientations in the 5-HT_{2A} receptor model.

Arylalkylamine binding to the human 5-HT_{2A} receptor

Following the success of limiting the number of possible binding orientations by utilizing a conformationally-restricted tryptamine analogue, a semi-rigid arylalkylamine analogue was tested in the 5-HT_{2A} receptor model. (1*R*,2*S*)-2-(2,5-dimethoxy-4-methylphenyl)cyclopropylamine (**59**), the enantiomer of this drug known to possess the higher affinity for the receptor, was docked into our receptor model.[210] The resulting binding orientation of **59** indicated that the protonated amine of the ligand forms an ionic bond with $D_{3.32(155)}$ as was observed with the ergoline and tryptamine class binding. Further, the 2-methoxy group of **59** was found to interact with the hydroxyl groups of $S_{3.36(159)}$ and $T_{3.37(160)}$, one helical turn down TM3 from $D_{3.32(155)}$, and the 5-methoxy group was observed to interact with the hydroxyl of $S_{5.43(239)}$. The *para*-substituent, in this case a methyl group, known to be important for agonist efficacy, was found projecting into a hydrophobic pore lined by $I_{4.56(206)}$, $L_{4.65(215)}$ and $G_{5.42(238)}$.[202,211] The nature of the interactions between the *para*-substituent of hallucinogenic arylalkylamines and the 5-HT_{2A} receptor have long been speculated upon, however, it may now be surmised from this binding model that the interaction is both of a steric as well as a hydrophobic nature and that the presence of a hydrophobic, bulky substituent at this position positively affects binding affinity of this drug class.

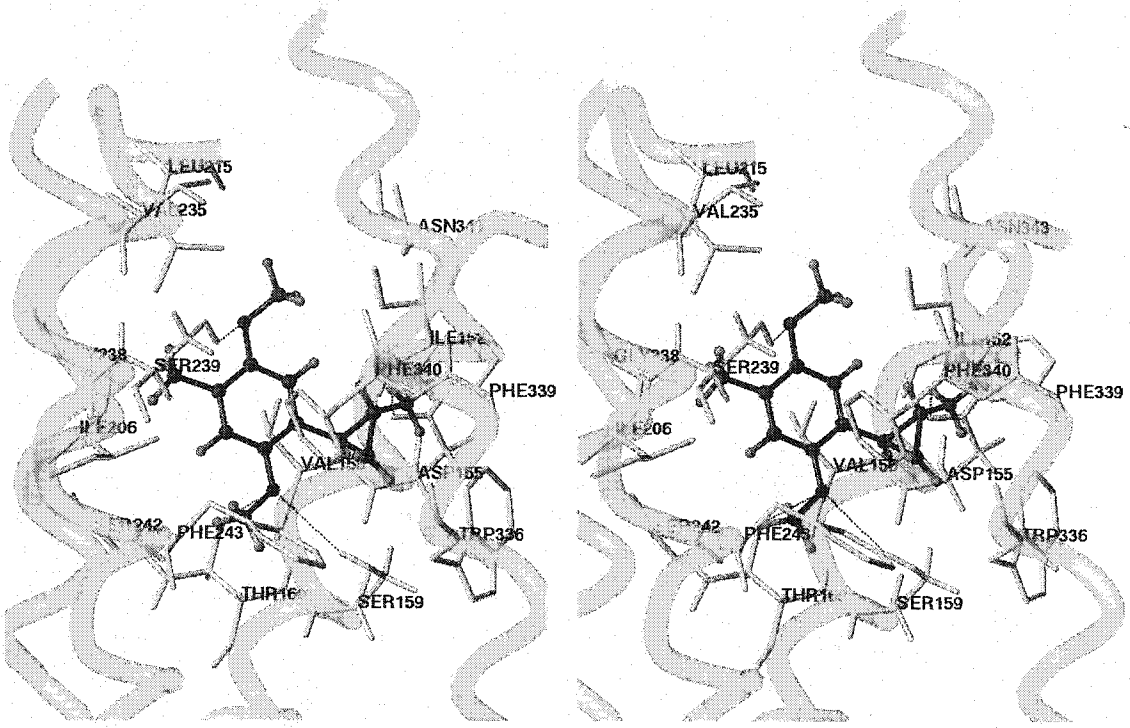

Hydrogen bonds are shown as dashed lines.

Figure 42. Stereo view (cross-eyed) of (1*R*,2*S*)-2-(2,5-dimethoxy-4-methylphenyl)-cyclopropylamine (**59**) docked to the 5-HT_{2A} receptor model.

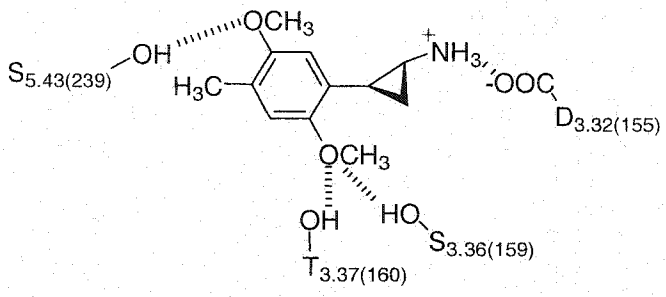

Figure 43. Schematic representation of **59** in the 5-HT_{2A} receptor model.

The basis for stereospecific biological activity of the 1*R*,2*S*-enantiomer of **59**, when compared with its 1*S*,2*R*-antipode, is not immediately evident from the binding model, but possibly resides in the inability of the less active enantiomer to adopt a similar

binding orientation. This is due principally to the non-bonded interaction between H-1 of the cyclopropane ring and H-6 of the aromatic ring. In the structurally simpler hallucinogenic arylpropylamines, a non-bonded interaction between the α-methyl group and H-6 in the less active *S*-enantiomer would similarly disfavor a conformation that could be superimposed on the ligand in Figure 42, offering a possible explanation for the lower affinity of the *S*-isomer compared to its *R*-antipode in the hallucinogenic arylalkylamines.[111,112]

Docking studies of other members of the arylalkylamine class of drugs indicated an interesting binding orientation for mescaline when docked to the 5-HT_{2A} receptor model. The docked conformer of mescaline (Figure 44) indicated that the drug adopts a gauche orientation upon binding. This conformation is somewhat higher in energy than the anti-conformation and was not predicted. However, although somewhat surprising, the docking results appeared reasonable because the protonated amine of the ligand formed an ionic interaction with $D_{3.32(155)}$ and each of the three methoxy groups of the ligand formed hydrogen bonds with receptor residues known to be important for agonist binding to the 5-HT_{2A} receptor. The methoxy groups of mescaline were found to interact with the hydroxyl groups of $S_{3.36(159)}$ and $T_{3.37(160)}$, one helical turn down TM3 from $D_{3.32(155)}$, and the hydroxyl of $S_{5.43(239)}$. Furthermore, inactivity of mescaline analogues with tethered methoxy groups had earlier led us to predict that the 3- and 5-methoxy groups might be twisted out of plane.[199] Indeed, such conformations were observed in these docking experiments. Comparison of the docked orientation of mescaline to the DOX analogues indicated that the phenyl ring of mescaline is rotated approximately 30° in the plane and about the centroid of the ring.

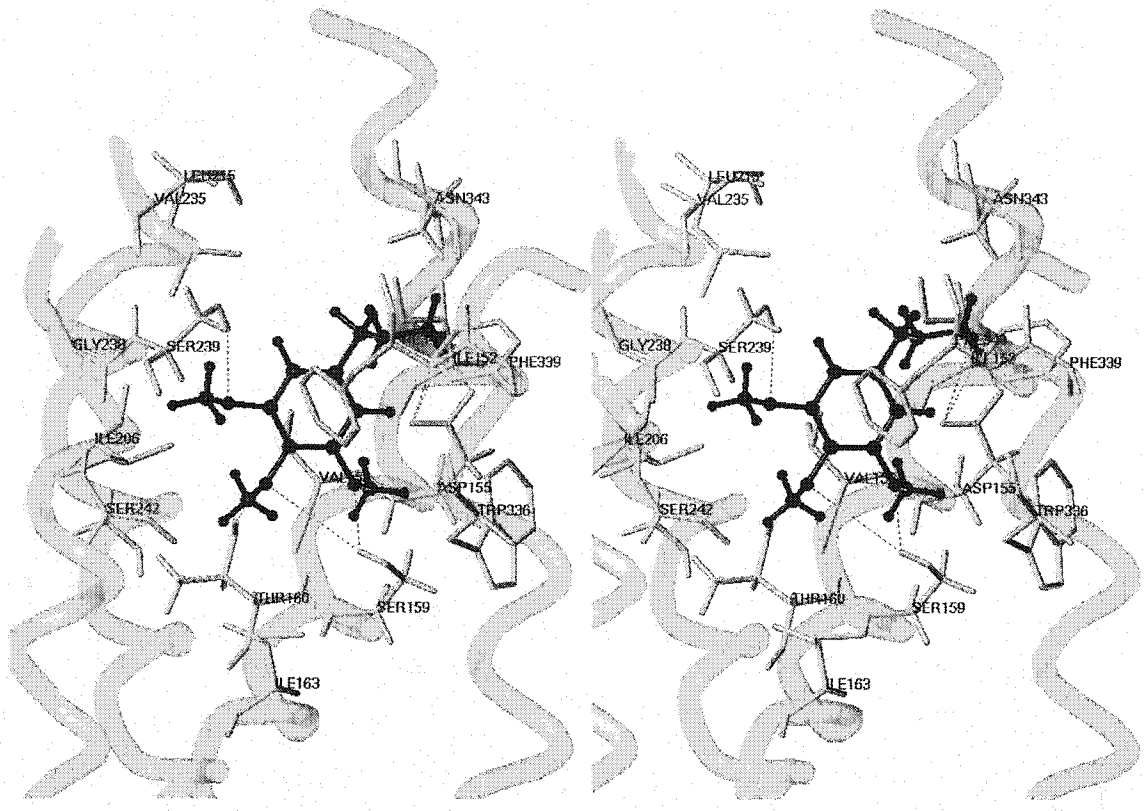

Hydrogen bonds are shown as dashed lines.

Figure 44. Stereo view (cross-eyed) of mescaline docked to the 5-HT_{2A} receptor model.

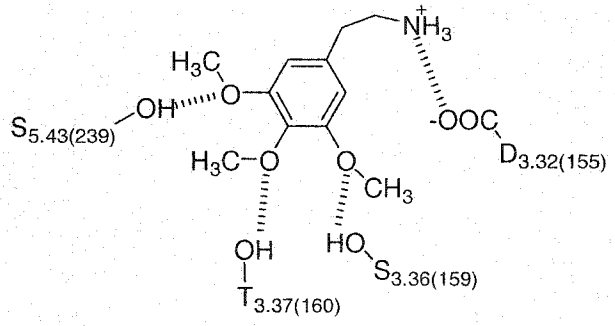

Figure 45. Schematic representation of mescaline in the 5-HT_{2A} receptor model.

Conformational Restriction of Mescaline

Pharmacological tests of the de novo designed, conformationally-restricted analogue of mescaline, (±)-**17**, were conducted and the results were compared directly with mescaline as a control (Table 2 – 4). The pharmacological data confirmed the model-derived prediction of higher binding affinity for the new compound. When compared to the parent compound, mescaline, compound (±)-**17** bound to the 5-HT_{2A} receptor with 3-fold higher affinity and exhibited approximately equal efficacy at the receptor. Interestingly, (±)-**17** shows 55-fold selectivity for the 5-HT_{1A} receptor. In vivo tests of this compound were also performed and those results indicated that this drug fully substitutes for LSD in animal models of hallucinogenesis. The predicted binding orientation for the enantiomers is shown below in Figures 46 and 47. Comparison to the parent compound, mescaline, showed that the enantiomers of **17** form cognate interactions with the putative agonist binding site. It can be predicted that the *S*-enantiomer allows binding in an orientation most similar to mescaline itself. Thus far, however, it is not been possible to resolve the enatiomers of (±)-**17** to test this prediction.

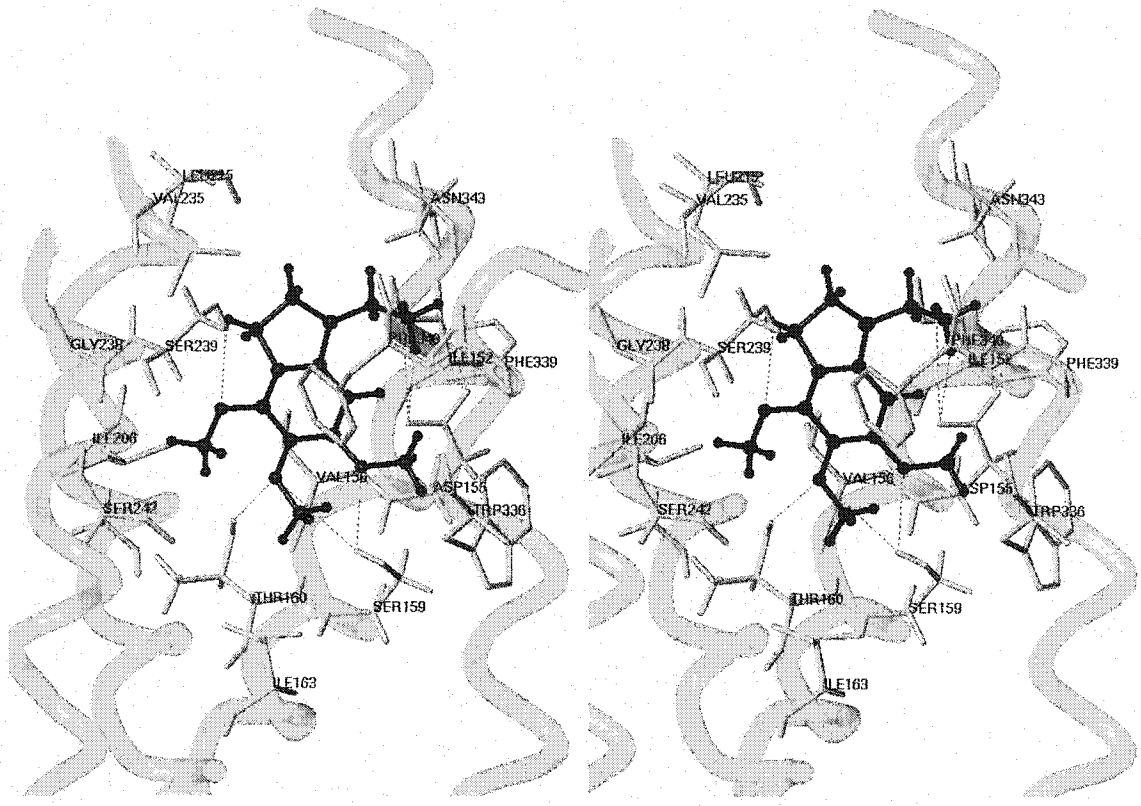

Hydrogen bonds are shown as dashed lines.

Figure 46. Stereo view (cross-eyed) of *R*-enantiomer of **17** docked to the 5-HT_{2A} receptor model.

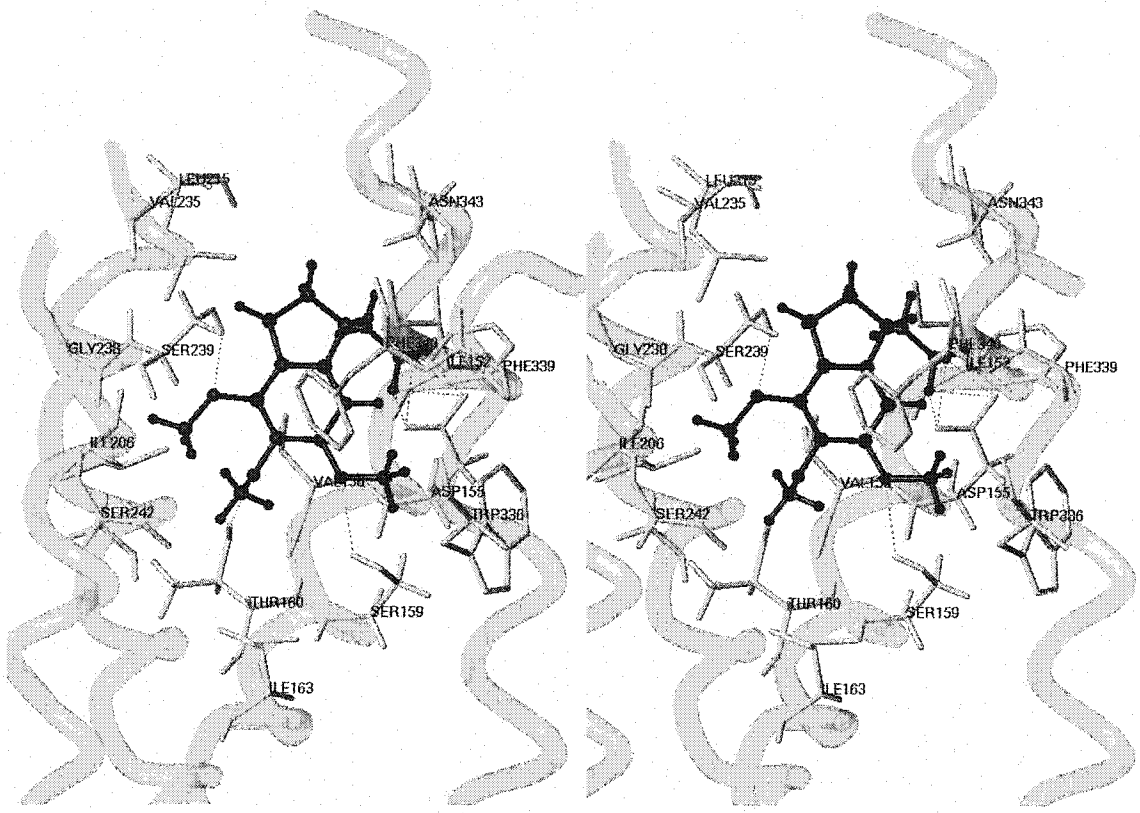

Hydrogen bonds are shown as dashed lines.

Figure 47. Stereo view (cross-eyed) of *S*-enantiomer of **17** docked to the 5-HT_{2A} receptor model.

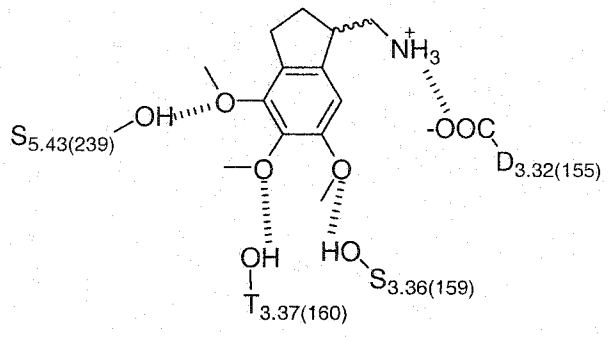

Figure 48. Schematic representation of (±)-**17** in the 5-HT_{2A} receptor model.

CONCLUSIONS

In summary, the ten target compounds, all conformationally-restricted analogues of drugs known to bind and activate the 5-HT_{2A} receptor, were synthesized and pharmacologically evaluated. Each of the target compounds was designed to test specific hypotheses and to serve as novel pharmacological probes of receptor function. The target compounds and the majority of the chemical intermediates have not been described previously in the literature, thus, several novel synthetic routes and techniques were devised to produce these new 5-HT_{2A} receptor probes.

During the course of the synthesis of target compounds **9** - **14**, facial selectivity was observed during the reduction of aminomethyl styrene **45**. Although unexpected at the time, similar structural selectivity could be synthetically useful for the production of compounds that have a molecular architecture not unlike **45**. Also, the synthetic route that was designed to produce the two *anti* compounds of the naphthofuran series, **10** and **13**, again rendered facial selectivity crucial. The reduction of benzofuran **11** demonstrated the synthetic utility of facial selectivity and could be envisioned to be useful for other compounds that contain a functional group that could coordinate with a metal catalyst.

Although the compounds of the naphthofuran series **9** - **14** were found to have limited efficacy at the 5-HT_{2A} receptor, some of the compounds do display relatively high

affinity. Further, interpretation and comparison of the receptor affinity and efficacy data for compounds **9** – **14** with the data from compound *syn*-Br-**8** suggests that the new series of naphthofurans more closely resemble the active conformation of non-restricted arylalkylamines, such as the DOX compounds, than the previous series of naphthofurans, **8**. Compounds **9** – **14** may lack the properties of a 5-HT_{2A} receptor full agonist for a number of reasons. The added bulk of the ethano bridge used to conformationally-restrict the 2-aminoalkyl group may either have introduced deleterious steric interactions with the receptor or may excessively limit the flexibility of the drug. That some of the compounds in this series possess very high affinity but low efficacy may support the latter explanation. Presumably, the strongest interaction is between the charged amine of the ligand and the conserved aspartate in TM3 of the receptor. Thus, it seems logical that this interaction acts as an "anchor" for the ligand, resulting in attractions and repulsions with amino acid residues of the TM segments ultimately resulting in receptor activation. Possibly, compounds of series **9** – **14** could either inhibit full motion of the TM segments because of the added bulk or may not be able to form extensive hydrogen bond interactions because the rigid nature of the molecule does not allow constructive interaction between, for instance, the O(1) of the ligand (corresponds to O(5) of DOX analogues) and $S_{5.43(239)}$. Alternatively, the reason that the compounds of the current naphthofuran series do not extensively activate the receptor may reside in the finding that the side chain orientation of the docked binding orientation for the cyclopropyl-containing arylalkylamine **59** indicated in Figure 42 is not accessible to the compounds of the current series.

The design and synthesis of the conformationally-restricted mescaline analogue, **17**, was made possible by the synergism of molecular modeling and organic synthesis. The method that was used to design this compound may serve as a model for future chemical discoveries by which observations made from ligand docking experiments offer ideas about novel binding orientations. The drug conformations and interactions with the protein may then dictate the design of novel structures that could benefit from additional hydrogen bond interactions or enhanced hydrophobic and steric interactions.

Construction of the homology-model of the human 5-HT_{2A} receptor has offered this research laboratory a novel tool for the design of new chemical probes for the receptor. The computer model, while useful for explaining much of the empirical data derived from receptor binding assays, requires improvement if it is to be useful for predictive purposes. Future research concerning details of the 5-HT_{2A} receptor can be facilitated by a unification of research efforts between molecular modeling, molecular biology, pharmacology, and medicinal chemistry. Each avenue of research has the ability to contribute significant advances toward a better understanding of receptor structure and function and thus, the results that are generated may be incorporated directly into the receptor model. An iterative procedure involving molecular modeling, conformationally-restricted analogue synthesis, and pharmacology experiments in which a model of the 5-HT_{2A} receptor is incrementally improved appears, for now, to be the most efficacious way to study the agonist binding site in detail.

EXPERIMENTAL

General Procedures

Chemistry

All reagents were commercially available and were used without further purification unless otherwise indicated. Dry THF and diethyl ether were obtained by distillation from benzophenone-sodium under nitrogen immediately before use. Melting points were determined using a Thomas-Hoover apparatus and are uncorrected. ^{1}H NMR spectra were recorded using either a 500 MHz Varian DRX-5000s or a 300 MHz Bruker ARX-300 NMR spectrometer. Chemical shifts are reported in δ values ppm relative to an internal reference (0.03%, v/v) of tetramethylsilane (TMS) in $CDCl_3$, except where noted. Abbreviations used to report NMR peaks are as follows: bs = broad singlet, d = doublet, dd = doublet of doublets, dq = doublet of quartets, dt = doublet of triplets, m = multiplet, q = quartet, s = singlet, t = triplet, td = triplet of doublets. Chemical ionization mass spectra (CIMS), using isobutane as the carrier gas, were obtained with a Finnigan 4000 spectrometer. Elemental analyses were performed by the Purdue University Microanalysis Laboratory and are within ±0.4% of the calculated values unless otherwise noted. Optical rotations were measured on a Perkin-Elmer 241 polarimeter at the sodium

D line (λ = 589 nm). Thin-layer chromatography was performed using J.T. Baker-flex silica gel IB2-F, plastic-backed sheets with fluorescent indicator, visualizing with UV light at 254 nm and eluting with 4:1 hexanes-ethyl acetate unless otherwise noted. Column chromatography was carried out using silica gel 60, 230-400 mesh (J.T. Baker). All reactions were carried out under an inert atmosphere of argon unless otherwise indicated.

Pharmacology

Cells stably transfected to express either the rat 5-HT_{2A}, rat 5-HT_{2C}, or human 5-HT_{1A} receptor[212] were maintained in minimum essential medium, containing 10% dialyzed fetal bovine serum (Gibco BRL) and supplemented with L-glutamine, Pen/Strep, and Geneticin. The cells were cultured at 37 °C in a H_2O saturated atmosphere of 95% air and 5% CO_2. For radioligand binding assays, cells were split into 100 mm^2 culture dishes when they reached 90% confluency. Upon reaching 100% confluency in the culture dishes, the cells were washed with sterile filtered phosphate-buffered solution and left to incubate in serum-free Opti-MEM for five hours. After incubation, the cells were harvested by centrifugation (15000g, 20 min) and placed immediately in a freezer at -80 °C until the assay was performed. For IP_3 accumulation experiments the cells were seeded into 24 well plates and assays were performed when 70% confluency was achieved.

Radioreceptor Competition Assays

For saturation assays, 0.125 to 6 nM [^{3}H]DOB or [^{125}I]DOI were used for the 5-HT_{2A} and 5-HT_{2C} receptors and 0.25 to 10 nM [^{3}H]8-OH-DPAT for the 5-HT_{1A} receptor. The total volume of the assay was 250 μL. Nonspecific binding was defined in the presence of 10 μM cinanserin (rat 5-HT_{2A} receptor expressing cells), 10 μM mianserin (rat 5-HT_{2C} receptor expressing cells), or 10 μM 5-HT (human 5-HT_{1A} receptor expressing cells). Competition binding experiments were carried out in a total volume of 500 μL with either 1.0 nM [^{3}H]DOB, 0.20 nM [^{125}I]DOI, or 2.0 nM [^{3}H]8-OH-DPAT. Previously harvested cells were resuspended and added to each well containing assay buffer (50 mM Tris, 0.5 mM EDTA, 10 mM $MgCl_2$; pH = 7.4), radioligand, and test compound (or in the case of the saturation assays, cinanserin, mianserin, or 5-HT). Incubation was carried out at 25 °C for 60 min and terminated by rapid filtration using a pre-chilled Packard 96-well harvester with GF/B Uni-filters that had been pre-incubated for 30 min in 0.3% polyethylenimine. The filters were rinsed using chilled wash buffer (10 mM Tris, 154 mM NaCl) and left to dry overnight. The following day, Microscint-O was added and radioactivity was determined using a TopCount (Packard) scintillation counter. GraphPad Prism (GraphPad Software, San Diego, CA) was used to analyze the saturation and competition binding curves.

Inositol Triphosphate Accumulation Studies in Cells Expressing the 5-HT_{2A} Receptor

Accumulation of inositol phosphates was determined using a modified version of a previously published protocol.[195] Briefly, cells expressing the rat 5-HT_{2A} receptor were

labeled for 18-20 h in CRML medium containing 1.0 μCi/mL [^{3}H]*myo*-inositol. After pre-treating the cells with 10 μM pargyline/10 mM LiCl for 15 min, the cells were exposed to a test drug for 30 min at 37 °C, under an atmosphere of 95% O_2 and 5% CO_2. The assay was terminated by aspirating the medium and adding 10 mM formic acid. Following incubation for 16 h at 4 °C, the [^{3}H]inositol phosphates were separated from the cellular debris on Dowex-1 ion-exchange columns and eluted with 1.0 M ammonium formate and 0.10 M formic acid. The vials were counted for tritium using a TriCarb scintillation counter (Packard Instrument Corp.).

Synthesis

Benzodifurans

***N*-Trifluoroacetyl-1-(8-bromo-2,3,6,7-tetrahydrobenzo[1,2-*b*;4,5-*b'*]difuran-4-yl)-2-aminoethane (19).** The hydrobromide salt of previously synthesized **18** (1.43 g, 3.92 mmol) was suspended in a stirred mixture of CH_2Cl_2 (40 mL) and 4-*N*,*N*-dimethyl-aminopyridine (0.04 g, 0.3 mmol). Triethylamine (1.91 mL, 13.8 mmol) was added and the mixture was cooled to 0 °C. Trifluoroacetic anhydride (1.33 mL, 9.41 mmol) was then added dropwise and the mixture was allowed to warm to RT and stirred overnight. The reaction mixture was diluted with CH_2Cl_2 (40 mL) and washed with 1 N HCl (40 mL), sat. $NaHCO_3$ (40 mL), and brine (20 mL). The organic fractions were then dried ($MgSO_4$), filtered, and evaporated, to leave a white solid: (1.3 g, 85%); mp 196 – 197 °C;

^{1}H NMR (500 MHz, $CDCl_3$) δ 2.72 (t, 2 H, ArC*H*$_2$CH$_2$N, *J* = 6.0 Hz), 3.18 (t, 4 H, ArC*H*$_2$CH$_2$O, *J* = 8.4 Hz), 3.53 (q, 2 H, ArCH$_2$C*H*$_2$N, *J* = 6.0 Hz), 4.58 (t, 2 H, ArOC*H*$_2$, *J* = 9.0 Hz), 4.63 (t, 2 H, ArOC*H*$_2$, *J* = 9.6 Hz), 7.14 (bs, 1 H, N*H*); CIMS *m/z* 380 (M + H); Anal. ($C_{14}H_{13}BrF_3NO_3$) C, H, N.

***N*-Trifluoroacetyl-1-(8-trifluoromethyl-2,3,6,7-tetrahydrobenzo[1,2-*b*;4,5-*b'*]difuran-4-yl)-2-aminoethane (20).** Toluene (50 mL) was added to a flask fitted with a Dean-Stark trap and containing tetramethylammonium trifluoroacetate (2.5 g, 13.2 mmol), copper iodide (2.8 g, 14.7 mmol), and **19** (1.0 g, 2.6 mmol).[177] This mixture was heated at reflux for 4 h to azeotrope residual H_2O present in the starting materials. Anhydrous DMF (17 mL, 210 mmol) was added slowly with concomitant removal of toluene to bring the reaction temperature to 145 °C for 4 h. The reaction was cooled to RT, diluted with H_2O (100 mL), and extracted with CH_2Cl_2 (4 × 50 mL). The organic layers were combined, dried ($MgSO_4$), filtered, and evaporated to leave a white solid that was subjected to column chromatography (4:1 hexanes-EtOAc as eluent) to afford the title compound as white crystals: (0.60 g, 63%); mp 170-171 °C; ^{1}H NMR (500 MHz, $CDCl_3$) δ 2.81 (t, 2 H, ArC*H*$_2$CH$_2$N, *J* = 6.5 Hz), 3.10 (t, 2 H, ArC*H*$_2$CH$_2$O, *J* = 8.7 Hz), 3.32 (t, 2 H, ArC*H*$_2$CH$_2$O, *J* = 8.0 Hz), 3.52 (q, 2 H, ArCH$_2$C*H*$_2$N, *J* = 6.5 Hz), 4.57 (t, 2 H, ArOC*H*$_2$, *J* = 8.9 Hz), 4.66 (t, 2 H, ArOC*H*$_2$, *J* = 8.7 Hz), 7.20 (bs, 1 H, N*H*); CIMS *m/z* 370 (M + H); Anal. ($C_{15}H_{13}F_6NO_3$) C, H, N.

***N*-Trifluoroacetyl-1-(8-trifluoromethylbenzo[1,2-*b*;4,5-*b'*]difuran-4-yl)-2-aminoethane (21).** A solution of DDQ (0.74 g, 3.3 mmol) in dioxane (12 mL) was slowly added to a solution of protected amine **20** (0.30 g, 0.81 mmol) in dioxane (15 mL).[176] The solution was heated at reflux for 24 h, at which time TLC indicated reaction

completion. The reaction was then cooled to RT and the precipitate that formed was removed by vacuum filtration. The filter cake was washed thoroughly with CH_2Cl_2 and then the solvents were removed by rotary evaporation. The brown oil that remained was subjected to column chromatography (4:1 hexanes-EtOAc as eluent) to afford a white solid product: (0.20 g, 68%); mp 150-151 °C; ^{1}H NMR (500 MHz, $CDCl_3$) δ 3.49 (t, 2 H, ArC*H*$_2$CH$_2$N, *J* = 6.7 Hz), 3.77 (q, 2 H, ArCH$_2$C*H*$_2$N, *J* = 6.4 Hz), 6.48 (bs, 1 H, N*H*), 6.93 (d, 1 H, Ar*H*, *J* = 2.1 Hz), 7.06 (m, 1 H, Ar*H*), 7.75 (d, 1 H, Ar*H*, *J* = 2.0 Hz), 7.77 (d, 1 H, Ar*H*, *J* = 2.0 Hz); CIMS *m/z* 366 (M + H); Anal. ($C_{15}H_9F_6NO_3$) C, H, N.

1-(8-Trifluoromethylbenzo[1,2-*b*;4,5-*b'*]difuran-4-yl)-2-aminoethane hydrochloride (22). The protected amine **21** (0.15 g, 0.4 mmol) was dissolved in MeOH (20 mL) and cooled to 0 °C. Aqueous 5 N NaOH (10 mL) was added to this solution and the mixture was allowed to stir overnight and was then diluted with Et_2O (50 mL). The phases were separated and the aqueous layer was extracted with Et_2O (3 × 50 mL). The organic layers were combined, dried ($MgSO_4$), filtered, and evaporated to yield a tan oil. This oil was dissolved in anhydrous Et_2O (25 mL) and filtered through glass wool. A slight excess of ethanolic 1 N HCl was added dropwise to the solution with vigorous stirring. The flask was then placed in a freezer overnight and the precipitate was collected by vacuum filtration. The resulting solid was recrystallized from *i*-PrOH to afford white, fluffy crystals: (0.09 g, 73%); mp 271-273 °C (dec.); ^{1}H NMR (500 MHz, D_2O) δ 3.40 (t, 2 H, ArC*H*$_2$CH$_2$N, *J* = 6.8 Hz), 3.46 (t, 2 H, ArCH$_2$C*H*$_2$N, *J* = 7.3 Hz), 7.07 (d, 1 H, Ar*H*, *J* = 1.7 Hz), 7.10 (m, 1 H, Ar*H*), 7.85 (d, 1 H, Ar*H*, *J* = 1.7 Hz), 7.89 (d, 1 H, Ar*H*, *J* = 1.7 Hz); CIMS *m/z* 270 (M + H); Anal. ($C_{13}H_{11}ClF_3NO_2$) C, H, N.

1-(2,3,6,7-Tetrahydro-8-trifluoromethyl-2,3,6,7-tetrahydrobenzo[1,2-*b*;4,5-*b*']difuran-4-yl)-2-aminoethane hydrochloride (4). A sample of **22** (0.05 g, 0.16 mmol) was dissolved in absolute EtOH (50 mL) and added to a Parr flask that contained Pd/C (10%, 0.05 g) and absolute EtOH (5 mL). The flask was placed on a Parr-shaker apparatus and shaken for 24 h at 50 psi H_2. TLC monitoring of reaction progress indicated completion at 24 h. The reaction mixture was vacuum filtered through Celite and the solvent removed by rotary evaporation. The resulting white solid was recrystallized from EtOH: (0.04 g, 87%); mp 271-273 °C (dec.); ^{1}H NMR (500 MHz, D_2O) δ 2.75 (t, 2 H, ArCH_2CH$_2$N, J = 7.2 Hz), 2.98 (t, 2 H, ArCH$_2$CH_2N, J = 7.2 Hz), 3.32 (t, 2 H, ArCH_2CH$_2$O, J = 8.3 Hz), 3.38 (t, 2 H, ArCH_2CH$_2$O, J = 8.5 Hz), 4.62 (t, 2 H, ArOCH_2, J = 8.6 Hz), 4.66 (t, 2 H, ArOCH_2, J = 8.7 Hz); CIMS *m/z* 274 (M + H); Anal. ($C_{13}H_{15}ClF_3NO_2$) C, H, N.

3,5-Bis(2-chloroethoxy)toluene (24). To a mechanically stirred solution of orcinol (**23**) (5.0 g, 40 mmol) in acetone (25 mL) was added K_2CO_3 (22.3 g, 161 mmol) and 1-bromo-2-chloroethane (33 mL, 400 mmol). The reaction mixture was heated at reflux for 48 h, cooled to RT, then diluted with Et_2O (100 mL), and filtered through Celite. The filter cake was washed thoroughly with CH_2Cl_2 and acetone and the filtrate was then evaporated to leave a residue that was subsequently taken up in Et_2O (250 mL) and washed with aqueous 2N NaOH (5 × 25 mL). The organic layer was then dried ($MgSO_4$), filtered, and evaporated to leave a solid that was recrystallized from EtOH to afford the desired product as tan crystals: (7.4 g, 75%); mp 111-112 °C; ^{1}H NMR (300 MHz, $CDCl_3$) δ 2.28 (s, 3 H, ArCH_3), 3.77 (t, 4 H, ArOCH_2, J = 6.0 Hz), 4.18 (t, 4 H,

$ArOCH_2CH_2$, J = 6.0 Hz), 6.30 (m, 1 H, Ar*H*, J = 1.0 Hz), 6.37 (m, 2 H, Ar*H*, J = 1.0 Hz); CIMS *m/z* 249 (M + H); Anal. ($C_{11}H_{14}Cl_2O_2$) C, H.

2,6-Dibromo-3,5-bis(2-chloroethoxy)toluene (25). Dialkylated compound **24** (3.6 g, 14 mmol) was dissolved in AcOH (300 mL) in an aluminum foil covered flask and then cooled to 15 °C. Next, a solution of bromine (4.6 g, 29 mmol) in AcOH (50 mL) was added dropwise over 1.5 h and the reaction was allowed to warm to RT and stirred overnight. The reaction mixture was then added to H_2O (1200 mL) and cooled to 0 °C. The precipitate that formed was vacuum filtered and the filter cake washed thoroughly with cold H_2O. The white solid that resulted was collected and recrystallized from EtOH to afford white crystals: (5.6 g, 96%); mp 125 °C; ^{1}H NMR (300 MHz, $CDCl_3$) δ 2.59 (s, 3 H, $ArCH_3$), 3.79 (t, 4 H, $ArOCH_2$, J = 6.0 Hz), 4.23 (t, 4 H, $ArOCH_2CH_2$, J = 6.0 Hz), 6.41 (s, 1 H, Ar*H*); CIMS *m/z* 405 (M + H), 407, 409; Anal. ($C_{11}H_{12}Br_2Cl_2O_2$) C, H.

4-Methyl-2,3,5,6-tetrahydrobenzo[1,2-*b*;5,4-*b*']difuran (26). To a room temperature suspension of magnesium (Aldrich, -50 mesh, 99+%; 2.33 g, 96.0 mmol) in anhydrous THF (34 mL) was added ethyl magnesium bromide (2.13 mL, 3.0 M in Et_2O). The internal reaction temperature increased and then an anhydrous THF solution (84 mL) of **25** (13 g, 32.0 mmol) was added dropwise such that the internal reaction temperature did not exceed 35 °C. After stirring at RT for 8 h, the reaction was diluted with Et_2O (100 mL) and quenched by slow addition of cold aqueous 1 N HCl (200 mL). Upon cessation of gas evolution, the phases were separated and the aqueous layer was extracted with Et_2O (5 × 75 mL), the organic layers combined, dried ($MgSO_4$), filtered, and evaporated to leave a tan solid that was recrystallized from EtOH to afford white crystals: (4.3 g, 76%); mp 108-109 °C; ^{1}H NMR (300 MHz, $CDCl_3$) δ 2.06 (s, 3 H, $ArCH_3$), 2.95 (t, 4 H,

ArCH_2, J = 8.3 Hz), 4.47 (t, 4 H, ArOCH_2, J = 8.5 Hz), 6.08 (s, 1 H, ArH); MS (CI) m/z 177 (M + H); Anal. ($C_{11}H_{12}O_2$) C, H.

8-Formyl-4-methyl-2,3,5,6-tetrahydrobenzo[1,2-*b*;5,4-*b*']difuran (27). To a stirred solution of **26** (1.5 g, 8.5 mmol) in anhydrous Et_2O (15 mL) at -78 °C was added *n*-BuLi (3.75 mL, 2.5 M in hexanes) dropwise. The reaction was allowed to warm to 0 °C over 4 h and then quenched by the slow addition of an anhydrous Et_2O (7 mL) solution of anhydrous DMF (1.65 mL, 21 mmol). The reaction mixture was allowed to warm to RT and stirred overnight and was then quenched by the addition of H_2O (100 mL). The reaction mixture was extracted with CH_2Cl_2 (3 × 50 mL) and the organic layers were combined, dried ($MgSO_4$), filtered, and evaporated to leave a yellow solid that was recrystallized from Et_2O to give off-white, needle-like crystals: (1.4 g, 81%); mp 190-191 °C; ^{1}H NMR (300 MHz, $CDCl_3$) δ 2.09 (s, 3 H, ArCH_3), 2.97 (t, 4 H, ArCH_2, J = 8.6 Hz), 4.67 (t, 4 H, ArOCH_2, J = 8.9 Hz), 7.23 (s, 1 H, ArH), 10.09 (s, 1 H, ArCHO); MS (CI) m/z 205 (M + H); Anal. ($C_{12}H_{12}O_3$) C, H.

4-Methyl-8-(2-nitropropenyl)-2,3,5,6-tetrahydrobenzo[1,2-*b*;5,4-*b*']difuran (28). To a solution of aldehyde **27** (1.0 g, 4.9 mmol) in nitroethane (14.0 mL) was added piperidinium acetate (0.71 g, 4.9 mmol). The reaction mixture was heated at reflux for 1 h and was then diluted with CH_2Cl_2 (100 mL) and washed with H_2O (2 × 50 mL). The organic layer was then washed with brine (30 mL), dried ($MgSO_4$), filtered, and evaporated to leave a yellow solid that was recrystallized from *i*-PrOH to afford bright yellow crystals: (0.9 g, 71%); mp 144-145 °C; ^{1}H NMR (300 MHz, $CDCl_3$) δ 2.09 (s, 3 H, ArCH_3), 2.16 (s, 3 H, ArCHCCH_3), 3.00 (t, 4 H, ArCH_2, J = 9.0 Hz), 4.59 (t, 4 H,

ArOCH_2, J = 9.3 Hz), 7.86 (s, 1 H, ArC*H*); MS (CI) *m/z* 262 (M + H); Anal. ($C_{14}H_{15}NO_4$) C, H, N.

(±)-4-Methyl-8-(2-aminopropyl)-2,3,5,6-tetrahydrobenzo[1,2-*b*;5,4-*b'*]difuran hydrochloride ((±)-6). To a suspension of sodium aluminum hydride (0.16 g, 2.9 mmol) in anhydrous THF (20 mL) was added dropwise an anhydrous THF (7 mL) solution of nitropropene **28** (0.30 g, 1.2 mmol). The reaction mixture was heated at reflux for 4 h and then cooled to RT. Very cautiously, H_2O (1 mL) dissolved in THF (10 mL) was added to the reaction mixture, followed by 5 N KOH (5 mL). The resulting suspension was filtered through Celite and the filter cake was washed well with warm THF and Et_2O and the solvents were evaporated to leave a residue that was dissolved in Et_2O (8 mL). The solution was filtered through a plug of glass wool and acidified with anhydrous, ethanolic 1 N HCl until moist pH paper indicated the solution was neutral. The flask was then placed in a freezer overnight and was vacuum filtered to isolate the white solid. The solid was recrystallized from *i*-PrOH to afford white, needle-like crystals: (0.18 g, 58%); mp 262-263 °C; ^{1}H NMR (500 MHz, D_2O) δ 1.10 (d, 3 H, $ArCH_2CHCH_3$, J = 6.5 Hz), 1.99 (s, 3 H, $ArCH_3$), 2.63 (d, 2 H, $ArCH_2CH$, J = 6.5 Hz), 2.94 (t, 4 H, $ArCH_2CH_2$, J = 8.4 Hz), 3.45 (m, 1 H, $ArCH_2CH$, J = 6.5 Hz), 4.45 (t, 4 H, $ArOCH_2$, J = 8.8 Hz); MS (CI) *m/z* 234 (M + H); Anal. ($C_{14}H_{20}ClNO_2$) C, H, N.

4-Methyl-8-(2-nitropropenyl)-benzo[1,2-*b*;5,4-*b'*]difuran (29). Nitropropene **28** (0.60 g, 2.3 mmol) was dissolved in dioxane (25 mL) and to this solution was slowly added a dioxane (35 mL) solution of DDQ (2.1 g, 9.2 mmol). The reaction mixture was heated at reflux for 16 h and was then allowed to cool to RT and diluted with CH_2Cl_2 (100 mL), at which time a precipitate formed. The precipitate was removed by vacuum filtration

through a short pad of silica, and the filter cake was washed thoroughly with CH_2Cl_2. The filtrate was evaporated and the resulting residue was purified by column chromatography (eluent 4:1 hexanes/EtOAc) to afford a yellow solid: (0.35 g, 59%); mp 187-188 °C; ^{1}H NMR (300 MHz, $CDCl_3$) δ 2.52 (s, 3 H, ArCHCC*H*$_3$), 2.66 (s, 3 H, ArC*H*$_3$), 6.85 (s, 2 H, ArOCHC*H*), 7.07 (s, 1 H, ArC*H*CNO$_2$), 7.62 (s, 2 H, ArOC*H*); MS (CI) *m/z* 258 (M + H); Anal. ($C_{14}H_{11}NO_4$) C, H, N.

(±)-4-Methyl-8-(2-aminopropyl)-benzo[1,2-*b*;5,4-*b'*]difuran ((±)-7). An anhydrous THF (3.5 mL) solution of the nitropropene **29** (0.1 g, 0.39 mmol) was added dropwise to a suspension of sodium aluminum hydride (0.05 g, 0.9 mmol) in anhydrous THF (7 mL). The reaction was heated at reflux for 4 h and then cooled to RT. Very cautiously, H_2O (0.2 mL) dissolved in THF (2 mL) was added dropwise to the reaction mixture, followed by 5 N KOH (1 mL). The resulting suspension was filtered through Celite and the filter cake was washed well with warm THF and Et_2O and the solvents were evaporated to leave a residue that was dissolved in Et_2O (5 mL). This solution was then filtered through a short plug of glass wool and evaporated to leave a tan oil (the hydrochloride salt of this compound could not be made sufficiently pure due to stability problems, thus, it was pharmacologically tested as the primary amine): (0.06 g, 67%); ^{1}H NMR (300 MHz, $CDCl_3$) δ 1.13 (d, 3 H, ArCH$_2$CHC*H*$_3$, *J* = 6.5 Hz), 2.45 (bs, 2H, N*H*$_2$), 2.63 (s, 3 H, ArC*H*$_3$), 3.25 (d, 2 H, ArC*H*$_2$CH, *J* = 6.8 Hz), 3.59 (m, 1 H, ArCH$_2$C*H*, *J* = 6.5 Hz), 6.82 (s, 2 H, ArOCHC*H*), 7.62 (s, 2 H, ArOC*H*); MS (CI) *m/z* 230 (M + H); Anal. ($C_{14}H_{15}NO_2$) C, H, N.

Tetrahydronaphthofurans

2-Bromo-4-methoxyphenol (32).[181] Bromine (91.4 mL, 1.78 mol) was added dropwise to a stirred solution of 4-methoxyphenol (**34**) (200 g, 1.61 mol) in MeOH (840 mL) at 0 °C. The mixture was allowed to warm to RT and stirred overnight. The solvent was removed by rotary evaporation and the residue was purified by vacuum distillation (130 °C @ 25 mm Hg) to afford a clear liquid: (262 g, 80%); ^{1}H NMR (300 MHz, $CDCl_3$) δ 3.72 (s, 3 H, OC*H*$_3$), 5.18 (bs, 1 H, O*H*), 6.78 (dd, 1 H, Ar*H*, *J* = 8.9, 3.0 Hz), 6.92 (d, 1 H, Ar*H*, *J* = 8.9 Hz), 7.00 (d, 1 H, Ar*H*, *J* = 3.0 Hz); MS (CI) *m/z* 203 (M + H).

Methyl 4-(2-bromo-4-methoxyphenoxy)-but-2-enoate (35). To a mechanically stirred solution of **32** (193 g, 950 mmol) in anhydrous acetone (1.0 L) was added potassium carbonate (131 g, 950 mmol) and potassium iodide (159 g, 958 mmol). This mixture was mechanically stirred and cooled to 0 °C followed by dropwise addition over 2 h of methyl 4-bromocrotonate (170 g, 951 mmol) in anhydrous acetone (1.5 L). The reaction was allowed to warm to RT and was stirred for 18 h. Et_2O (500 mL) was added and the mixture was then vacuum filtered. The filter cake was washed well with acetone (500 mL) and the filtrate was evaporated. The resulting residue was dissolved in Et_2O (700 mL) and washed with cold, aqueous 2 N NaOH (2 × 200 mL). The organic layer was washed with brine (200 mL), dried ($MgSO_4$), filtered, and evaporated to leave a light yellow oil that solidified upon cooling. This solid was recrystallized from Et_2O to afford large, tan crystals: (229 g, 76%); mp 48-49 °C; ^{1}H NMR (300 MHz, $CDCl_3$) δ 3.73 (s, 3 H, ArOC*H*$_3$), 3.74 (s, 3 H, CO_2C*H*$_3$), 4.66 (q, 2 H, ArOC*H*$_2$, *J* = 2.1 Hz), 6.27 (dt, 1 H,

$ArOCH_2CHCH$, J = 15.6, 2.1 Hz), 6.77 (m, 2 H, Ar*H*), 7.02 (dt, 1 H, $ArOCH_2CHCH$, J = 15.9, 3.6 Hz), 7.09 (m, 1 H, Ar*H*); MS (CI) *m/z* 301 (M + H), Anal. ($C_{12}H_{13}BrO_4$) C, H.

(±)-Methyl 2-(2,3-dihydro-5-methoxybenzofuran-3-yl)acetate ((±)-31). To a stirred solution of compound **35** (32.8 g, 109 mmol) in dry benzene (1140 mL) at reflux was added portionwise AIBN (1.6 g, 10 mmol). To this mixture was added Bu_3SnH (32.3 mL, 120 mmol) dissolved in dry benzene (420 mL) dropwise over a period of 1.5 h. The reaction was maintained at reflux for an additional 1 h and was then cooled to RT. The solvent was removed by rotary evaporation and the resulting residue was dissolved in Et_2O (1.0 L) and an aqueous solution of potassium fluoride (150 mL, 60%) was added. This mixture was stirred vigorously overnight and the precipitate that formed was removed by vacuum filtration and the filter cake washed well with Et_2O (500 mL). The filtrate was evaporated, subjected to flash chromatography (4:1 hexanes/EtOAc), and fractions containing the product pooled and solvents removed by rotary evaporation to leave a clear oil: (24 g, 98%); ^{1}H NMR (500 MHz, $CDCl_3$) δ 2.54 (dd, 1 H, $CH_2CO_2CH_3$, J = 16.8, 9.0 Hz), 2.74 (dd, 1 H, $CH_2CO_2CH_3$, J = 16.8, 5.7 Hz), 3.68 (s, 3 H, CO_2CH_3), 3.71 (s, 3 H, $ArOCH_3$), 3.80 (m, 1 H, ArC*H*, J = 2.7 Hz), 4.18 (dd, 1 H, $ArOCH_2$, J = 9.0 Hz), 4.68 (t, 1 H, $ArOCH_2$, J = 9.0 Hz), 6.68 (m, 3 H, Ar*H*); MS (CI) *m/z* 223 (M + H); Anal. ($C_{12}H_{14}O_4$) C, H.

(±)-(2,3-Dihydro-5-methoxybenzofuran-3-yl)acetic acid ((±)-37). A solution of H_2O (100 mL), EtOH (50 mL), and KOH (20.0 g, 357 mmol) was added to a solution of the methyl ester (±)-**31** (11.9 g, 53.6 mmol) in EtOH (100 mL). This mixture was heated at reflux for 1 h and then cooled to RT. The solvents were removed by rotary evaporation and the resulting residue was dissolved in H_2O (50 mL) and acidified with cold, conc.

HCl. This solution was then extracted with CH_2Cl_2 (4 × 40 mL) and the organic layers were pooled and washed with brine, dried ($MgSO_4$), filtered, and evaporated to leave a white solid. The product was recrystallized from EtOAc to yield white, granular crystals: (9.8 g, 88%); mp 110-112 °C; ^{1}H NMR (300 MHz, DMSO-d_6) δ 2.54 (dd, 1 H, CH_2CO_2H, J = 14.0, 9.5 Hz), 2.82 (dd, 1 H, CH_2CO_2H, J = 14.3, 5.6 Hz), 3.72 (s, 3 H, $ArOCH_3$), 3.75 (m, 1 H, ArC*H*, J = 6.5 Hz), 4.17 (dd, 1 H, $ArOCH_2$, J = 8.8, 7.1 Hz), 4.69 (t, 1 H, $ArOCH_2$, J = 8.9 Hz), 6.67 (s, 2 H, Ar*H*), 6.91 (s, 1 H, Ar*H*), 12.40 (bs, 1 H, CO_2H); MS (CI) *m/z* 209 (M + H); Anal. ($C_{11}H_{12}O_4$) C, H.

(±)-1-Diazo-3-(2,3-dihydro-5-methoxybenzofuran-3-yl)propan-2-one ((±)-38).[116] To a solution of acid (±)-**37** (5.0 g, 24.0 mmol) in dry benzene (40 mL) was added DMF (2 drops) followed by the dropwise addition of oxalyl chloride (2.72 mL, 31.2 mmol). After stirring for 3 h, the solvent and excess oxalyl chloride were removed by rotary evaporation. Meanwhile, an Et_2O solution of CH_2N_2 cooled in an ice-salt bath was generated using an Aldrich Diazald Kit and a Diazald (16.47 g, 76.9 mmol) solution in Et_2O (105 mL) dripped into a 60° C solution of KOH (5.25 g, 94 mmol) in Carbitol (32 mL) and H_2O (11 mL). The solid acyl chloride of (±)-**37** was dissolved in anhydrous Et_2O (55 mL) and added dropwise to the CH_2N_2 solution. After stirring at 0 °C for 1.5 h, a precipitate had formed and the excess CH_2N_2 was removed by attaching the apparatus to a H_2O aspirator. After most of the solvent had been removed, the remaining volatiles were removed by rotary evaporation to leave the diazoketone as a yellow solid: (5.4 g, 97%). An analytical sample of the diazoketone was recrystallized from Et_2O. mp 70 – 72 °C (lit.[116] mp 73 – 74 °C); ^{1}H NMR (300 MHz, $CDCl_3$) δ 2.74 (m, 2 H, CH_2COCHN_2), 3.74 (s, 3 H, $ArOCH_3$), 3.90 (m, 1 H, ArC*H*), 4.19 (dd, 1 H, $ArOCH_2$, J =

9.1, 6.0 Hz), 4.70 (t, 1 H, ArOCH_2, J = 9.0 Hz), 5.25 (s, 1 H, CH_2COCHN_2), 6.73 (m, 3 H, ArH); MS (CI) m/z 233 (M + H).

(±)-Methyl 3-(2,3-dihydro-5-methoxybenzofuran-3-yl)propionate ((±)-39). To a stirred solution of diazoketone (±)-**38** (5.4 g, 23.3 mmol) in anhydrous MeOH (100 mL) was added very slowly a solution of silver benzoate (0.4 g, 1.7 mmol) in anhydrous Et_3N (4.0 mL). This reaction was allowed to stir overnight and was then diluted with Et_2O (100 mL) and vacuum filtered to remove the solids. The filter cake was washed well with Et_2O and the filtrate was concentrated. The residue was dissolved in CH_2Cl_2 (200 mL), washed with aqueous 0.5 M NaOH (2 × 40 mL), brine (20 mL), dried ($MgSO_4$), filtered, and evaporated to leave a tan oil: (5.2 g, 95%); ^{1}H NMR (500 MHz, $CDCl_3$) δ 1.93 (m, 1 H, ArCHCH_2CH$_2$), 2.08 (m, 1 H, ArCHCH_2CH$_2$), 2.38 (m, 2 H, ArCHCH$_2$CH_2), 3.42 (m, 1 H, ArCH), 3.67 (s, 3 H, CO_2CH_3), 3.77 (s, 3 H, ArOCH_3), 4.19 (dd, 1 H, ArCHCH_2O, J = 8.8, 5.8 Hz), 4.59 (t, 1 H, ArCHCH_2O, J = 8.8 Hz), 6.68 (m, 2 H, ArH), 6.75 (s, 1 H, ArH); MS (CI) m/z 237 (M + H); Anal. ($C_{13}H_{16}O_4$) C, H.

(±)-3-(2,3-Dihydro-5-methoxybenzofuran-3-yl)propionic acid ((±)-40). Methyl ester (±)-**39** (5.2 g, 22.0 mmol) was dissolved in EtOH (80 mL) and then a solution of KOH (5.0 g, 89.0 mmol) in H_2O (25 mL) and EtOH (13 mL) was added and the mixture was stirred overnight. The EtOH was removed by rotary evaporation and the resulting mixture was diluted with H_2O (50 mL) and acidified with cold, conc. HCl. The resulting suspension was extracted with CH_2Cl_2 (4 × 40 mL) and the organic layers were pooled, washed with brine (50 mL), dried ($MgSO_4$), filtered, and evaporated to leave a white, amorphous solid. This solid was recrystallized from Et_2O to afford white crystals: (4.6 g, 94%); mp 100-101 °C; ^{1}H NMR (500 MHz, $CDCl_3$) δ 1.77 (m, 1 H, ArCHCH_2CH$_2$), 2.00

(m, 1 H, ArCHCH_2CH$_2$), 2.34 (m, 2 H, ArCHCH$_2$CH_2), 3.48 (m, 1 H, ArC*H*), 3.73 (s, 3 H, ArOCH_3), 4.22 (dd, 1 H, ArCHCH_2O, J = 8.7, 6.0 Hz), 4.59 (t, 1 H, ArCHCH_2O, J = 9.5 Hz), 6.72 (m, 2 H, Ar*H*), 6.91 (s, 1 H, Ar*H*), 12.21 (bs, 1 H, CO_2H); MS (CI) *m/z* 223 (M + H); Anal. ($C_{12}H_{14}O_4$) C, H.

Alternate route to propionic acid (±)-40. (±)-2-(5-Methoxy-2,3-dihydrobenzofuran-3-yl)ethanol ((±)-41). To a stirred suspension of lithium aluminum hydride (32 g, 840 mmol) in anhydrous Et_2O (500 mL) was added dropwise an anhydrous Et_2O (450 mL) solution of methyl ester (±)-**31** (45.5 g, 205 mmol). The reaction was stirred at RT overnight and quenched by the careful dropwise addition of a solution of H_2O (25 mL) in THF (250 mL) followed by 5 N KOH (20 mL). The solids were removed by vacuum filtration through a pad of Celite and the filter cake was washed well with warm THF (500 mL). The solvents were then removed by rotary evaporation to leave a clear oil that was homogeneous by TLC analysis: (39 g, 89%). An analytical sample was purified by column chromatography (1:1 hexanes/EtOAc as eluent); ^{1}H NMR (500 MHz, $CDCl_3$) δ 1.61 (bs, 1 H, CH$_2$O*H*), 1.84 (m, 1 H, ArCHCH_2CH$_2$), 2.04 (m, 1 H, ArCHCH_2CH$_2$), 3.56 (m, 1 H, ArC*H*), 3.75 (t, 2 H, ArCHCH$_2$CH_2, J = 4.2 Hz), 3.76 (s, 3 H, ArOCH_3), 4.25 (dd, 1 H, ArCHCH_2O, J = 8.9, 6.5 Hz), 4.65 (t, 1 H, ArCHCH_2O, J = 8.9 Hz), 6.68 (m, 2 H, Ar*H*), 6.77 (m, 1 H, Ar*H*); MS (CI) *m/z* 195 (M + H), 177 (M + H - H_2O); Anal. ($C_{11}H_{14}O_3$) C, H.

Continuation of Alternate Route. (±)-2-(5-Methoxy-2,3-dihydrobenzofuran-3-yl)ethyl *p*-toluenesulfonate ((±)-42). A solution of Et_3N (170 mL, 1.22 mol) in CH_2Cl_2 (400 mL) was added dropwise to a 0 °C solution of alcohol (±)-**41** (78.6 g, 405 mmol) and *p*-toluenesulfonyl chloride (163 g, 855 mmol) in CH_2Cl_2 (1300 mL). After stirring

for 1 h, the reaction was allowed to warm to RT and stirred an additional 2 h. The reaction was then quenched by the addition of saturated Na_2CO_3 (500 mL). The layers were separated and the aqueous phase was extracted with CH_2Cl_2 (3 × 350 mL). The organic phases were pooled and washed with saturated Na_2CO_3 (200 mL), dried ($MgSO_4$), filtered, and evaporated to leave a white solid that was recrystallized from EtOAc to afford white crystals. (117 g, 83%); mp 88-89 °C; ^{1}H NMR (500 MHz, $CDCl_3$) δ 1.96 (m, 1 H, ArCHCH_2CH$_2$), 2.08 (m, 1 H, ArCHCH_2CH$_2$), 2.46 (s, 3 H, ArCH_3), 3.50 (m, 1 H, ArC*H*), 3.75 (s, 3 H, ArOCH_3), 4.12 (m, 3 H, ArCHCH$_2$CH_2, ArCHCH_2O), 4.52 (t, 1 H, ArCHCH_2O, J = 9.0 Hz), 6.67 (m, 3 H, Ar*H*), 7.36 (d, 2 H, Ar*H*, J = 9.0 Hz), 7.81 (d, 2 H, ArH, J = 6.0 Hz); MS (CI) *m/z* 349 (M + H); Anal. ($C_{18}H_{20}O_5S$) C, H.

Continuation of Alternate Route. (±)-3-(5-Methoxy-2,3-dihydrobenzofuran-3-yl)propionitrile ((±)-43). Potassium cyanide (16.0 g, 246 mmol) was added to a solution of tosylate (±)-**42** (58.8 g, 169 mmol) in absolute EtOH (1.0 L). The mixture was heated at reflux for 9 h and then cooled to RT. The solids were removed by vacuum filtration and the filter cake was washed well with EtOH. The filtrate volume was reduced under vacuum to about 400 mL and was then diluted with Et_2O (500 mL). This solution was then washed with H_2O (500 mL), brine (200 mL), dried ($MgSO_4$), filtered, and evaporated to leave a tan oil that was homogeneous by TLC: (33 g, 97%). An analytical sample was purified by column chromatography (4:1 hexanes/EtOAc). ^{1}H NMR (500 MHz, $CDCl_3$) δ 1.98 (m, 1 H, ArCHCH_2CH$_2$), 2.07 (m, 1 H, ArCHCH_2CH$_2$), 2.41 (m, 2 H, ArCHCH$_2$CH_2), 3.55 (m, 1 H, ArC*H*), 3.77 (s, 3 H, ArOCH_3), 4.25 (m, 1 H, ArCHCH_2O), 4.63 (dt, 1 H, ArCHCH_2O, J = 8.9, 2.6 Hz), 6.72 (m, 3 H, Ar*H*); MS (CI) *m/z* 204 (M + H); Anal. ($C_{12}H_{13}NO_2$) C, H, N.

Continuation of Alternate Route. (±)-3-(5-Methoxy-2,3-dihydrobenzofuran-3-yl)propionic acid ((±)-40). Nitrile (±)-**43** (36.5 g, 180 mmol) was dissolved in EtOH (1.0 L) and then 2 N NaOH (500 mL) was added. The reaction was heated at reflux overnight and then cooled to RT. The EtOH was removed by rotary evaporation and the resulting suspension was cooled and acidified by dropwise addition of 2 N HCl. The mixture was extracted with CH_2Cl_2 (4 × 400 mL). The organic layers were pooled and washed with brine (300 mL), dried (Na_2SO_4), filtered, and evaporated to leave a white solid. Recrystallization from EtOAc gave off-white needles: (33 g, 83%); NMR spectra and melting point were identical to that reported above.

(±)-6-Methoxy-2,2a,3,4-tetrahydronaphtho[1,8-*bc*]furan-5-one ((±)-30). Propionic acid (±)-**40** (33 g, 150 mmol) was dissolved in dry benzene (850 mL) and then DMF (4 mL) was added. Oxalyl chloride (26 mL, 298 mmol) was added to the mixture dropwise and the reaction was allowed to stir at RT for 4 h. The solvent and excess oxalyl chloride were removed by rotary evaporation and the residue was dissolved in CH_2Cl_2 (460 mL). The reaction flask was submerged in an ice bath and then $SnCl_4$ (22 mL, 188 mmol) was added dropwise. The ice bath was removed and the reaction was allowed to stir for 1 h and then poured onto ice (300 g). The layers were separated and the aqueous phase was extracted with CH_2Cl_2 (3 × 250 mL). The organic layers were then pooled and washed with brine (200 mL), dried ($MgSO_4$), filtered, and evaporated to leave a tan solid that was recrystallized from EtOAc: (29.7 g, 97%); mp 105-106 °C; ^{1}H NMR (500 MHz, $CDCl_3$) δ 1.89 (dq, 1 H, ArCHCH_2CH$_2$, J = 7.0, 2.0 Hz), 2.31 (m, 1 H, ArCHCH_2CH$_2$), 2.57 (m, 1 H, ArCHCH$_2$CH_2), 2.76 (m, 1 H, ArCHCH$_2$CH_2), 3.68 (m, 1 H, ArCH), 3.88 (s, 3 H, ArOCH_3), 4.10 (dd, 1 H, ArCHCH_2O, J = 6.4, 4.5 Hz), 4.84 (t, 1 H, ArCHCH_2O, J = 8.5

Hz), 6.69 (d, 1 H, Ar*H*, *J* = 3.6 Hz), 6.93 (d, 1 H, Ar*H*, *J* = 3.6 Hz); MS (CI) *m/z* 205 (M + H); Anal. ($C_{12}H_{12}O_3$) C, H.

(±)-5-Aminomethyl-6-methoxy-2a,3,4,5-tetrahydro-2H-naphtho[1,8-*bc*]furan-5-ol hydrochloride ((±)-44). Zinc iodide (0.4 g, 1.3 mmol) was added to a solution of ketone (±)-**30** (10 g, 49 mmol) in CH_2Cl_2 (500 mL). TMSCN (7.2 mL, 54 mmol) was then added and the reaction was heated at reflux for 14 h. Comparison of the IR spectrum of the reaction mixture to the IR spectrum of the starting material (±)-**30** indicated the absence of the C=O peak at 1681 cm^{-1} and the appearance of a new peak at 2361 cm^{-1} (CN). The reaction was then concentrated by rotary evaporation and the residue was dissolved in anhydrous THF (200 mL) and added dropwise to a suspension of lithium aluminum hydride (2.8 g, 74 mmol) in anhydrous Et_2O (100 mL). The reaction mixture was stirred overnight and then quenched by the careful addition of H_2O (10 mL) dissolved in THF (100 mL). The resulting suspension was then filtered and the filter cake washed well with warm THF (500 mL). The filtrate was then diluted with Et_2O (300 mL) and washed with H_2O (2 × 200 mL), dried (Na_2SO_4), filtered, and evaporated to leave a tan solid. This solid was dissolved in anhydrous Et_2O (200 mL) and acidified with anhydrous 1 N HCl in EtOH. The solvents were then removed by rotary evaporation and the resulting white solid was recrystallized from EtOH to afford white crystals: (11.5 g, 87%); mp 191-193 °C (dec.); ^{1}H NMR (500 MHz, DMSO-d_6) δ 1.56 (q, 1 H, ArCHCH_2CH$_2$, *J* = 12.4 Hz), 1.78 (t, 1 H, ArCHCH_2CH$_2$, *J* = 13.2 Hz), 1.96 (m, 1 H, ArCHCH$_2$CH_2, *J* = 5.2 Hz), 2.31 (d, 1 H, ArCHCH$_2$CH_2, *J* = 13.0 Hz), 2.86 (d, 1 H, CH_2N, *J* = 12.9 Hz), 3.24 (d, 1 H, CH_2N, *J* = 13.1 Hz), 3.26 (m, 1 H, ArC*H*, not visible in DMSO spectrum, present in D_2O spectrum), 3.73 (s, 3 H, ArOCH_3), 3.86 (dd, 1 H,

ArCHCH_2O, J = 12.1, 4.3 Hz), 4.67 (t, 1 H, ArCHCH_2O, 8.3 Hz), 6.68 (dd, 2 H, ArH, 9.1, 8.5 Hz), 7.89 (bs, 2 H, CH_2NH_2); MS (CI) m/z 236 (M + H), 218 (M + H – H_2O).

(±)-(6-Methoxy-2a,3-dihydro-2H-naphtho[1,8-*bc*]furan-5-yl)aminomethane hydrochloride ((±)-45). Conc. HCl (40 mL) was added to a solution of the hydrochloride salt of aminoalcohol (±)-**44** (18 g, 67 mmol) in absolute EtOH (500 mL). The solution was heated at reflux for 6 h, at which time the reaction mixture had taken on a green color. The solution was concentrated to dryness and the resulting white solid was recrystallized from EtOH to afford white crystals: (12 g, 71%); mp 255-257 °C (dec.); ^{1}H NMR (500 MHz, D_2O) δ 1.98 (t, 1 H, ArCHCH_2CH, J = 12.3 Hz), 2.48 (dt, 1 H, ArCHCH_2CH, J = 16.5, 7.5 Hz), 3.44 (m, 1 H, ArCHCH$_2$O), 3.69 (s, 3 H, ArOCH_3), 3.75 (d, 1 H, CH_2N, J = 13.2 Hz), 4.04 (d, 1 H, CH_2N, J = 13.0 Hz), 4.06 (m, 1 H, ArCHCH_2O), 4.77 (t, 1 H, ArCHCH_2O, J = 8.7 Hz), 6.04 (d, 1 H, ArCCHCH$_2$, J = 4.2 Hz), 6.62 (d, 1 H, ArH, J = 5.7 Hz), 6.70 (d, 1 H, ArH, J = 9.0 Hz); MS (CI) m/z 218 (M + H), 201 (M + H – NH_3); Anal. ($C_{13}H_{16}ClNO_2$) C, H, N.

(±)-*syn*-(6-Methoxy-2a,3,4,5-tetrahydro-2H-naphtho[1,8-*bc*]furan-5-yl)aminomethane hydrochloride ((±)-9). The hydrochloride salt of aminostyrene (±)-**45** (7.0 g, 28 mmol) was dissolved in a mixture of MeOH (175 mL) and EtOH (50 mL) and added to a Parr hydrogenation flask containing 10% Pd/C (0.70 g) and EtOH (10 mL). The flask was placed on a hydrogenation apparatus, pressurized to 60 psi H_2, and shaken for 24 h. The reaction mixture was vacuum filtered through a pad of Celite and the filter cake was washed well with MeOH. The solvents were removed by rotary evaporation and the resulting white solid was recrystallized from EtOH: (7.0 g, 99%); mp 262-263 °C; ^{1}H NMR (500 MHz, D_2O) δ 1.34 (q, 1 H, ArCHC(3)H_2CH$_2$, J = 12.3 Hz), 1.87

(dt, 1 H, ArCHC(3)H_2CH$_2$, J =11.7, 5.5 Hz), 2.00 (t, 2 H, ArCHCH$_2$C(4)H_2, J = 14.6 Hz), 2.90 (dd, 1 H, ArCHCH$_2$N, J = 12.6, 4.2 Hz), 3.17 (dd, 1 H, CH_2N, J = 12.6, 4.8 Hz), 3.22 (m, 2 H, CH_2N, ArCHCH$_2$O), 3.75 (s, 3 H, ArOCH_3), 3.91 (dd, 1 H, ArCHCH_2O, 12.8, 8.2 Hz), 4.71 (t, 1 H, ArCHCH_2O, J = 8.2 Hz, not visible in D_2O spectrum, present in DMSO spectrum), 6.64 (d, 1 H, ArH, J = 8.5 Hz), 6.70 (d, 1 H, ArH, J = 8.5 Hz); MS (CI) m/z 220 (M + H), 203 (M + H - NH_3); Anal. ($C_{13}H_{18}ClNO_2$) C, H, N.

(±)-*syn*-(8-Bromo-6-methoxy-2a,3,4,5-tetrahydro-2H-naphtho[1,8-*bc*]furan-5-yl)-aminomethane hydrochloride ((±)-12). Bromine (0.78 g, 0.005 mmol, 0.2 N MeOH solution) was added dropwise to a solution of (±)-**9** (1.28 g, 0.005 mmol) in MeOH (150 mL) at 0 °C. The yellow solution turned clear upon warming to RT. Et_2O (200 mL) was added and the precipitate that formed was collected by vacuum filtration. This solid was stirred in conc. NH_4OH solution (300 mL) and extracted with CH_2Cl_2 (4 × 100 mL). The organic phases were pooled and dried (Na_2SO_4), filtered, and evaporated to leave a clear oil. The resulting oil was dissolved in anhydrous Et_2O, filtered through a small plug of glass wool, and acidified with 1 N ethanolic HCl. The precipitate was collected by vacuum filtration and then recrystallized from *i*-PrOH to yield needle-like crystals: (1.5 g, 88%); mp 258-260 °C (dec.); ^{1}H NMR (500 MHz, D_2O) δ 1.38 (q, 1 H, ArCHC(3)H_2CH$_2$, J = 12.2 Hz), 1.84 (m, 1 H, ArCHC(3)H_2CH$_2$), 2.04 (m, 2 H, ArCHCH$_2$C(4)H_2,), 2.92 (dt, 1 H, ArCHCH$_2$N, J = 10.2, 3.6 Hz), 3.18 (d, 2 H, CH_2N, J = 8.8 Hz), 3.32 (m, 1 H, ArCHCH$_2$O), 3.78 (s, 3 H, ArOCH_3), 4.01 (dd, 1 H, ArCHCH_2O, J = 12.7, 8.7 Hz), 4.84 (t, 1 H, ArCHCH_2O, J = 8.3 Hz), 6.89 (s, 1 H, ArH); MS (CI) m/z 298 (M + H), 300; Anal. ($C_{13}H_{17}BrClNO_2$) C, H, N.

(±)-*syn*-*N*-Trifluoroacetyl-1-(8-bromo-6-methoxy-2a,3,4,5-tetrahydro-2H-naphtho-[1,8-*bc*]furan-5-yl)aminomethane ((±)-48). To a stirred suspension of the hydrobromide salt of (±)-**12** (1.3 g, 3.6 mmol) and 4-dimethylaminopyridine (0.04 g, 0.3 mmol) in CH_2Cl_2 (40 mL) was added Et_3N (16.0 mL, 12.0 mmol) and the mixture was cooled to 0 °C. Trifluoroacetic anhydride (2.5 mL, 17 mmol) was then added to the reaction dropwise. The mixture was then allowed to warm to RT and stirred for 8 h. The mixture was diluted with CH_2Cl_2 (50 mL) and washed with 2N HCl (50 mL), saturated $NaHCO_3$ (50 mL), and brine (50 mL). The organic phase was then dried ($MgSO_4$), filtered, and evaporated to leave a white solid that was recrystallized from Et_2O: (1.2 g, 92%); mp 197-198 °C; ^{1}H NMR (500 MHz, $CDCl_3$) δ 1.55 (q, 1 H, ArCHC(3)H_2CH$_2$, J = 11.4 Hz), 1.86 (dt, 1 H, ArCHC(3)H_2CH$_2$, J = 13.1, 5.8 Hz), 2.02 (d, 2 H, ArCHCH$_2$C(4)H_2, J = 11.6 Hz), 3.16 (q, 1 H, ArCHCH$_2$N, J = 6.3 Hz), 3.38 (m, 1 H, ArCHCH_2N), 3.42 (m, 1 H, ArCHCH_2N), 3.53 (p, 1 H, ArCHCH$_2$O, J = 6.7 Hz), 3.81 (s, 3 H, ArOCH$_3$), 4.06 (dd, 1 H, ArCHCH_2O, J = 13.0, 8.3 Hz), 4.81 (t, 1 H, ArCHCH_2O, J = 8.2 Hz), 6.72 (s, 1 H, ArH), 7.26 (bs, 1 H, NHCOCF$_3$); MS (CI) *m/z* 394 (M + H), 396; Anal. ($C_{15}H_{15}BrF_3NO_3$) C, H, N.

(±)-*N*-Trifluoroacetyl-1-(8-bromo-6-methoxy-4,5-dihydro-3H-naphtho[1,8-*bc*]furan-5-yl)aminomethane ((±)-49). A solution of DDQ (1.73 g, 7.6 mmol) in dioxane (250 mL) was added slowly to a solution of (±)-**48** (3.0 g, 7.6 mmol) in dioxane (100 mL). The reaction was allowed to stir at RT for 8 h and was then diluted with CH_2Cl_2 (100 mL) and filtered through a short pad of silica gel. The silica gel was washed well with CH_2Cl_2 and the solvent was then removed by rotary evaporation. The black solid that resulted was subjected to column chromatography (1:1 hexanes/EtOAc as eluent)

resulting in an off-white, solid product that was recrystallized from Et_2O to afford white, fluffy crystals: (2.3 g, 78%); mp 172-174 °C; ^{1}H NMR (500 MHz, $CDCl_3$) δ 1.92 (m, 1 H, ArCCH$_2$C*H*$_2$), 2.13 (dt, 1 H, ArCCH$_2$C*H*$_2$, *J* = 6.2 Hz), 2.72 (m, 1 H, ArCC*H*$_2$CH$_2$), 2.85 (dt, 1 H, ArCC*H*$_2$CH$_2$, *J* = 13.9, 2.2 Hz), 3.34 (td, 1 H, ArCHC*H*$_2$N, *J* = 13.6, 3.1 Hz), 3.49 (m, 1 H, ArCHC*H*$_2$N), 3.64 (dt, 1 H, ArC*H*, *J* = 12.3, 3.5 Hz), 3.91 (s, 3 H, ArOC*H*$_3$), 7.03 (s, 1 H, Ar*H*), 7.40 (s, 1 H, Ar*H*), 7.62 (bs, 1 H, N*H*COCF$_3$); MS (CI) *m/z* 392 (M + H); Anal. ($C_{15}H_{13}BrF_3NO_3$) C, H, N.

(±)-(8-Bromo-6-methoxy-4,5-dihydro-3H-naphtho[1,8-*bc*]furan-5-yl)aminomethane hydrochloride ((±)-14). A solution of (±)-**49** (1.1 g, 2.8 mmol) in MeOH (150 mL) was cooled to 0 °C and then 5 N KOH solution (25 mL) was added slowly. The reaction was allowed to warm to RT. stirred overnight, and then the MeOH was removed by rotary evaporation. The residue was diluted with H_2O (25 mL) and extracted with Et_2O (4 × 100 mL), dried (Na_2SO_4), filtered, and evaporated to afford a clear oil. This oil was dissolved in Et_2O (100 mL), filtered through a plug of glass wool, and neutralized by the slow addition of 1 N ethanolic HCl. The solvents were removed by rotary evaporation and the resulting white residue was recrystallized from MeOH to afford the title compound: (0.6 g, 67%); mp 222-223 °C; ^{1}H NMR (500 MHz, CD_3OD) δ 1.82 (m, 1 H, ArCCH$_2$C*H*$_2$), 2.19 (dt, 1 H, ArCCH$_2$C*H*$_2$, *J* = 11.6, 2.7 Hz), 2.72 (t, 1 H, ArCC*H*$_2$CH$_2$, *J* = 13.4 Hz), 2.75 (m, 1 H, ArCC*H*$_2$CH$_2$), 3.04 (dd, 1 H, ArCHC*H*$_2$N, *J* = 13.1, 6.4 Hz), 3.10 (dd, 1 H, ArCHC*H*$_2$N, *J* = 12.9, 6.4 Hz), 3.45 (m, 1 H, ArC*H*CH$_2$N), 3.83 (s, 3 H, ArOC*H*$_3$), 7.07 (s, 1 H, Ar*H*), 7.48 (s, 1 H, Ar*H*); MS (CI) *m/z* 296 (M + H); Anal. ($C_{13}H_{15}BrClNO_2$) C, H, N.

(±)-*syn*-*N*-Trifluoroacetyl-(6-methoxy-2a,3,4,5-tetrahydro-2H-naphtho[1,8-*bc*]furan-5-yl)aminomethane ((±)-50). To a stirred suspension of the hydrochloride salt of (±)-**9** (3.1 g, 12.1 mmol) and 4-dimethylaminopyridine (0.12 g, 0.98 mmol) in CH_2Cl_2 (150 mL) was added Et_3N (6.0 mL, 43.0 mmol) and the mixture was cooled to 0 °C. Trifluoroacetic anhydride (4.13 mL, 29.0 mmol) was then added to the reaction dropwise. The reaction was then allowed to warm to RT and stirred for 8 h. The mixture was diluted with CH_2Cl_2 (200 mL) and washed with 2N HCl (100 mL), saturated $NaHCO_3$ (100 mL), and brine (100 mL). The organic phase was then dried ($MgSO_4$), filtered, and evaporated to leave a white solid that was recrystallized from Et_2O: (3.5 g, 91%); mp 181-183 °C; ^{1}H NMR (500 MHz, $CDCl_3$) δ 1.51 (q, 1 H, ArCHC(3)H_2CH$_2$, J = 13.0 Hz), 1.88 (dt, 1 H, ArCHC(3)H_2CH$_2$, J = 9.6, 5.7 Hz), 2.01 (m, 2 H, ArCHCH$_2$C(4)H_2), 3.23 (p, 1 H, ArC*H*CH$_2$N, J = 7.0 Hz), 3.28 (m, 1 H, ArC*H*CH$_2$O), 3.40 (m, 1 H, ArCHCH_2N), 3.57 (p, 1 H, ArCHCH_2N, J = 6.3 Hz), 3.82 (s, 3 H, ArOCH_3), 3.96 (dd, 1 H, ArCHCH_2O, J = 12.9, 8.2 Hz), 4.72 (t, 1 H, ArCHCH_2O, J = 8.1 Hz), 6.62 (s, 2 H, Ar*H*), 7.64 (bs, 1 H, N*H*COCF$_3$); MS (CI) *m/z* 316 (M + H); Anal. ($C_{15}H_{16}F_3NO_3$) C, H, N.

(±)-*N*-Trifluoroacetyl-(6-methoxy-4,5-dihydro-3H-naphtho[1,8-*bc*]furan-5-yl)aminomethane ((±)-51). A solution of DDQ (2.16 g, 9.5 mmol) in dioxane (330 mL) was added slowly to a solution of (±)-**50** (3.0 g, 9.5 mmol) in dioxane (125 mL). The reaction was allowed to stir at RT for 8 h and was then diluted with CH_2Cl_2 (100 mL) and filtered through a short pad of silica gel. The silica gel was washed well with CH_2Cl_2 and the solvent was removed by rotary evaporation. The dark solid that resulted was subjected to column chromatography (1:1 hexanes/EtOAc as eluent) resulting in a off-white, solid

product that was recrystallized from Et_2O to afford white, fluffy crystals: (2.6 g, 88%); mp 141-142 °C; ^{1}H NMR (500 MHz, $CDCl_3$) δ 1.95 (m, 1 H, ArCCH$_2$C*H*$_2$), 2.13 (dt, 1 H, ArCCH$_2$C*H*$_2$, *J* = 13.9, 2.2 Hz), 2.73 (t, 1 H, ArCC*H*$_2$, *J* = 13.6 Hz), 2.85 (d, 1 H, ArCC*H*$_2$, *J* = 16.2 Hz), 3.37 (dt, 1 H, ArCHC*H*$_2$N, *J* = 12.3, 3.5 Hz), 3.52 (m, 1 H, ArC*H*CH$_2$N), 3.68 (m, 1 H, ArCHC*H*$_2$N), 3.92 (s, 3 H, ArOC*H*$_3$), 6.88 (d, 1 H, Ar*H*, *J* = 8.8 Hz), 7.28 (d, 1 H, Ar*H*, *J* = 8.8 Hz), 7.35 (s, 1 H, Ar*H*), 7.83 (bs, 1 H, N*H*COCF$_3$); MS (CI) *m/z* 314 (M + H); Anal. ($C_{15}H_{14}F_3NO_3$) C, H, N.

(±)-(6-Methoxy-4,5-dihydro-3H-naphtho[1,8-*bc*]furan-5-yl)aminomethane hemioxalate ((±)-11). A solution of (±)-**51** (1.7 g, 5.4 mmol) in MeOH (250 mL) was cooled to 0 °C and then 5 N KOH solution (30 mL) was added slowly. The reaction mixture was allowed to warm to RT and stirred overnight and then the MeOH was removed by rotary evaporation. The residue was diluted with H_2O (25 mL) and extracted with Et_2O (4 × 100 mL), dried (Na_2SO_4), filtered, and evaporated to afford a clear oil. This oil was dissolved in Et_2O (100 mL), filtered through a plug of glass wool, and neutralized by the slow addition of oxalic acid (54 mL, 0.1 M in MeOH). The solvents were removed and the resulting white residue was recrystallized from MeOH to afford the hemioxalate salt: (0.9 g, 59%); mp 243 °C; ^{1}H NMR (500 MHz, CD_3OD) δ 1.82 (m, 1 H, ArCCH$_2$C*H*$_2$), 2.17 (dt, 1 H, ArCCH$_2$C*H*$_2$, *J* = 11.9, 2.8 Hz), 2.69 (t, 1 H, ArCC*H*$_2$, *J* = 13.6 Hz), 2.78 (dt, 1 H, ArCC*H*$_2$, *J* = 12.0, 3.1 Hz), 3.03 (m, 2 H, ArCHC*H*$_2$N, *J* = 13.0, 6.4 Hz), 3.46 (m, 1 H, ArC*H*CH$_2$), 3.81 (s, 3 H, ArOC*H*$_3$), 6.88 (d, 1 H, Ar*H*, *J* = 8.7 Hz), 7.19 (d, 1 H, Ar*H*, *J* = 8.7 Hz), 7.35 (s, 1 H, Ar*H*); MS (CI) *m/z* 218 (M + H); Anal. ($C_{15}H_{17}NO_6$) C, H, N.

(±)-*anti*-(6-Methoxy-2a,3,4,5-tetrahydro-2H-naphtho[1,8-*bc*]furan-5-yl)amino-methane hydrochloride ((±)-10). The primary amine of (±)-**11** (0.17 g, 0.83 mmol) was dissolved in hexane (200 mL) and added to a Parr flask containing 10% Pd/C (0.10 g) and hexane (5 mL). The flask was then pressurized and shaken at 65 psi H_2 for 24 h. The solution was filtered through Celite, the filter cake washed well with EtOH, and the solvents removed by rotary evaporation to leave a clear oil. This oil was dissolved in anhydrous Et_2O (100 mL) and filtered through a small plug of glass wool. The solution was then acidified with ethanolic 1 N HCl and the precipitate that formed was collected by vacuum filtration and then recrystallized from *i*-PrOH to afford needle-like crystals: (0.14 g, 81%); mp 185-186 °C; ^{1}H NMR (500 MHz, D_2O) δ 1.22 (q, 1 H, ArCHC(3)H_2CH$_2$, J = 11.2 Hz), 1.52 (q, 1 H, ArCHC(3)H_2CH$_2$, J = 9.7 Hz), 2.18 (dd, 1 H, ArCHCH$_2$C(4)H_2, J = 12.5, 3.3 Hz), 2.30 (d, 1 H, ArCHCH$_2$C(4)H_2, J = 12.2 Hz), 3.30 (dd, 2 H, CH_2N, J = 12.4, 7.6 Hz), 3.34 (m, 1 H, ArCHCH$_2$O), 3.38 (m, 1 H, ArCHCH$_2$N), 3.78 (s, 3 H, ArOCH_3), 3.97 (t, 1 H, ArCHCH_2O, J = 10.4 Hz), 4.84 (t, 1 H, ArCHCH_2O, J = 8.4 Hz), 6.71 (d, 1 H, ArH, J = 8.3 Hz), 6.77 (d, 1 H, ArH, J = 8.5 Hz); MS (CI) *m/z* 220 (M + H), 203 (M + H - NH_3); Anal. ($C_{13}H_{18}ClNO_2$) C, H, N.

(±)-*anti*-(8-Bromo-6-methoxy-2a,3,4,5-tetrahydro-2H-naphtho[1,8-*bc*]furan-5-yl)-aminomethane hydrochloride ((±)-13). Bromine (0.16 g, 0.001 mmol, 0.2 N MeOH solution) was added dropwise to a solution of the hydrochloride salt of (±)-**10** (0.26 g, 0.001 mmol) in MeOH (25 mL) at 0 °C. The reaction mixture was allowed to stir and warm to RT overnight. Et_2O (75 mL) was added and the precipitate that formed was collected by vacuum filtration. This solid was stirred in conc. NH_4OH solution (100 mL) and extracted with Et_2O (4 × 100 mL). The organic phases were pooled and dried

(Na_2SO_4), filtered, and evaporated to leave a clear oil. This oil was dissolved in anhydrous Et_2O, filtered through a small plug of glass wool, and acidified with 1 N ethanolic HCl. The precipitate was collected by vacuum filtration and then recrystallized from *i*-PrOH to yield needle-like crystals: (0.26 g, 78%); mp 231-232 °C; ^{1}H NMR (500 MHz, CD_3OD) δ 1.25 (1 H, q, ArCHC(3)H_2CH$_2$, J = 12.1 Hz), 1.53 (1 H, m, ArCHC(3)H_2CH$_2$), 2.18 (1 H, dd, ArCHCH$_2$C(4)H_2, J = 12.3, 3.8 Hz), 2.25 (1 H, m, ArCHCH$_2$C(4)H_2), 3.16 (1 H, m, CH_2N), 3.37 (1 H, m, CH_2N), 3.43 (1 H, m, ArCHCH$_2$N), 3.76 (3 H, s, ArOCH_3), 3.96 (1 H, t, ArCHCH_2O, J = 8.8 Hz), 4.75 (1 H, t, ArCHCH_2O, J = 7.9 Hz), 6.80 (1 H, s, ArH); MS (CI) *m/z* 298 (M + H); Anal. ($C_{13}H_{17}BrClNO_2$) C, H, N.

1-Substituted Indan

(±)-1-Aminomethyl-2,3-dihydro-4,5,6-trimethoxy-inden-1-ol hydrochloride ((±)-56). Zinc iodide (0.4 g, 1.3 mmol) was added to a solution of ketone (±)-**52** (10 g, 45 mmol) in CH_2Cl_2 (600 mL). TMSCN (6.6 mL, 50 mmol) was then added and the reaction was heated at reflux for 5 h. The clear solution turned red after approximately 0.5 h of heating. The reaction was then concentrated and the resulting residue was dissolved in anhydrous THF (400 mL) and added dropwise to a suspension of lithium aluminum hydride (2.5 g, 66 mmol) in anhydrous Et_2O (400 mL). The reaction mixture was stirred overnight and then quenched by the careful addition of H_2O (20 mL) dissolved in THF (200 mL). The resulting suspension was then filtered and the filter cake washed well with warm THF (500 mL). The filtrate was then diluted with Et_2O (300 mL) and washed

with H_2O (2 × 200 mL), dried (Na_2SO_4), filtered, and evaporated to leave a tan solid. This solid was dissolved in anhydrous Et_2O (200 mL) and acidified with anhydrous 1 N HCl in EtOH. The solvents were then removed by rotary evaporation and the resulting white solid was used directly in the next reaction: (9.4 g, 72%); mp 143-144 °C (dec.); ^{1}H NMR (500 MHz, DMSO-d_6) δ 1.55 (m, 1 H, $ArCH_2CH_2$, J = 3.0 Hz), 2.20 (m, 1 H, $ArCH_2CH_2$, J = 3.2 Hz), 2.62 (m, 1 H, $ArCH_2$, J = 5.1 Hz), 2.68 (dt, 1 H, $ArCH_2$, J = 5.0, 3.0 Hz), 3.02 (d, 2 H, CH_2N, J = 6.3 Hz), 3.61 (s, 3 H, $ArOCH_3$), 3.71 (s, 3 H, $ArOCH_3$), 3.73 (s, 3 H, $ArOCH_3$), (s, 1 H, ArH); MS (CI) *m/z* 254 (M + H), 236 (M + H – H_2O).

(4,5,6-Trimethoxy-3H-inden-1-yl)aminomethane hydrochloride (57). Conc. HCl (20 mL) was added to a solution of the hydrochloride salt of aminoalcohol (±)-**56** (9.0 g, 31 mmol) in absolute EtOH (1.0 L). The solution was heated at reflux overnight and then concentrated to dryness and the resulting white solid was recrystallized from EtOAc/EtOH to afford white crystals: (6.2 g, 74%); mp 223-225 °C; ^{1}H NMR (500 MHz, D_2O) δ 3.52 (s, 2 H, $ArCH_2$), 3.79 (s, 3 H, $ArOCH_3$), 3.87 (s, 3 H, $ArOCH_3$), 3.97 (s, 3 H, $ArOCH_3$), 4.13 (s, 2 H, CH_2N), 6.60 (s, 1 H, ArH), 6.89 (s, 1 H, ArCCH); MS (CI) *m/z* 236 (M + H), 218 (M + H – NH_3); Anal. ($C_{13}H_{18}ClNO_3$) C, H, N.

(±)-(2,3-Dihydro-4,5,6-trimethoxy-1H-inden-1-yl)aminomethane hydrochloride ((±)-17). The hydrochloride salt of aminostyrene **57** (5.5 g, 20 mmol) was dissolved in a mixture of EtOH (200 mL) and MeOH (50 mL) and added to a Parr hydrogenation flask containing 10% Pd/C (0.55 g) and EtOH (10 mL). This was placed on a hydrogenation apparatus, pressurized to 45 psi H_2, and shaken for 24 h. The reaction mixture was vacuum filtered through a pad of Celite and the filter cake was washed well with EtOH. The solvents were removed by rotary evaporation and the resulting white solid was

recrystallized from EtOH: (4.8 g, 87%); mp 245 °C; ^{1}H NMR (500 MHz, DMSO-d_6) δ 1.82 (m, 1 H, ArCH$_2$C*H*$_2$, *J* = 3.3 Hz), 2.34 (m, 1 H, ArCH$_2$C*H*$_2$, *J* = 3.2 Hz), 2.85 (m, 1 H, ArC*H*$_2$, *J* = 3.1 Hz), 2.97 (dt, 2 H, C*H*$_2$N, *J* = 5.0, 3.0 Hz), 3.20 (m, 1 H, ArC*H*$_2$)3.36 (m, 1 H, ArC*H*, *J* = 6.3 Hz), 3.72 (s, 3 H, ArOC*H*$_3$), 3.80 (s, 3 H, ArOC*H*$_3$), 3.84 (s, 3 H, ArOC*H*$_3$), 6.65 (s, 1 H, Ar*H*); MS (CI) *m/z* 238 (M + H), 221 (M + H - NH$_3$); Anal. ($C_{13}H_{20}ClNO_2$) C, H, N.

Molecular Modeling

Weighted Masses Molecular Dynamics

In brief, the crystal structure of bovine rhodopsin[124] (PDB code 1F88) was modified by deletion of the metal atoms, H_2O, etc. to leave one partially complete molecule of rhodopsin with bound 11-*cis*-retinal (**15**) remaining. The N- and C-termini, intra- and extracellular loops were deleted (with the exception of the extracellular loop between TM4 and TM5 because of the TM interactions) using Quanta. Specifically, $W_{1.30(35)}$-$K_{1.61(66)}$, $T_{2.37(70)}$-$H_{2.67(100)}$, $T_{3.23(108)}$-$C_{3.55(140)}$, $E_{4.39(150)}$-$V_{5.62(227)}$, $A_{6.29(246)}$-$H_{6.61(278)}$, and $I_{7.33(286)}$-$C_{7.69(322)}$ remained after the original PDB file was truncated. The coordinates of the helices were then used as input by a parallelized version of CHARMM (version c28a3)[213] on an IBM SP system. Neutral caps were applied to the end groups. N-termini were capped with acetyl groups and C-termini were capped with *N*-methylamino groups. Any hydrogen atoms that were missing were added using the HBUILD facility of CHARMM and the model was then saved (referred to as

cis-rhodopsin). The covalently linked chromophore was then *in silico* isomerized from 11-*cis*-retinal (**15**) to all-*trans*-retinal (**16**) by modification of torsion angles to situate the ionone ring of the chromophore in the vicinity of $T_{3.33(118)}$, $C_{4.56(167)}$, $A_{4.57(168)}$, $P_{4.60(171)}$, $S_{4.65(176)}$, $Y_{4.67(178)}$, $I_{4.69(189)}$ and $F_{5.38(203)}$ and the file was then saved (*trans*-rhodopsin). From this point forward, both *cis*-rhodopsin and *trans*-rhodopsin were treated identically in all operations (*cis*-rhodopsin as a control experiment). Bond lengths, angles and improper dihedral angles were artificially weighted using constraints on the internal coordinate system of 500, 5000, and 5000, respectively (Appendix E).[200] A distance dielectric constant, timestep of 0.001, and non-bonded update every 5 steps was used during all molecular dynamics simulations. To relax the initial structures using CHARMM, 100 steps of steepest descent minimization were performed followed by dynamics using the Verlet leap-frog algorithm for 10 ps of heating to 300 K, 10 ps of equilibrium, and 1200 ps of production time. The final 100 ps of dynamics were averaged and the resulting structure was minimized using the Adopted Basis Newton-Raphson minimization protocol for 1000 steps. The final structure of *trans*-rhodopsin was then used as the structural template for homology modeling.

Homology Modeling

A sequence alignment (Figure 49 and Appendix A) of bovine rhodopsin, the human 5-HT_{2A} receptor, and other monoamine GPCRs was generated using ClustalW[214] with the PAM250 scoring matrix, a gap penalty of 12 and an extension penalty of 4. A homology model of the human 5-HT_{2A} receptor was then generated using Modeler 4.0[215] on an SGI Octane machine. The output structure was relaxed with 50 steps of steepest

descent minimization using CHARMM and the resulting structure was then used as input for docking.

```
TM1 rh      35 WQFSMLAAYMFLLIMLGFPINFLTLYVTVQHK      66
    h5h2a   72 QEKNWSALLTAVVIILTIAGNILVIMAVSLEK     103
               ------A------I-L----N-L--------K

TM2 rh      70 TPLNYILLNLAVADLFMVFGGFTTTLYTSLH      100
    h5h2a  107 NATNYFLMSLAIADMLLGFLVMPVSMLTILY      137
               ---NY-L--LA-AD----F--------T-L-

TM3 rh     108 TGCNLEGFFATLGGEIALWSLVVLAIERYVVVC     140
    h5h2a  146 KLCAVWIYLDVLFSTASIMHLCAISLDRYVAIQ     178
               --C--------L--------L------RYV---

TM4 rh     150 ENH.AIMGVAFTWVMALACAAPPLVGWSRYI       179
    h5h2a  188 SRTKAFLKIIAVWTISVGISMPIPVFGLQDD       218
               ----A-------W--------P--V------

TM5 rh     202 SFVIYMFVVHFIIPLIVIFFCYGQLV            227
    h5h2a  234 .FVLIGSFVSFFIPLTIMVITYFLTI            258
               -FV-----V-F-IPL------Y----

TM6 rh     246 AEKEVTRMVIIMVIAFLICWLPYAGVAFYIFTH     278
    h5h2a  317 NEQKACKVLGIVFFLFVVMWCPFFITNIMAVIC     349
               -E--------I----F---W-P-----------

TM7 rh     286 IFMTIPAFFAKTSAVYNPVIYIMMNKQFRNCMVTTLC 322
    h5h2a  360 ALLNVFVWIGYLSSAVNPLVYTLFNKTYRSAFSRYIQ 396
               ------------S---NP--Y---NK--R--------
```

Only putative TM segments shown.
Top = bovine rhodopsin, middle = human 5-HT_{2A} receptor, bottom = consensus.

Figure 49: Sequence alignment of bovine rhodopsin and human 5-HT_{2A} receptor.

Docking

All hydrogens and lone pairs of electrons were added to the human 5-HT_{2A} receptor model and Kollman All-Atom charges were calculated using the Biopolymer package of Sybyl 6.6.[216,217] Ligand molecules were generated using Spartan,[218] the basic amine of the ligands was protonated, and a formal +1 charge was applied. Semi-empirical geometry optimization was utilized to generate initial ligand conformations. The ligands were then imported into Sybyl and Gasteiger charges were computed and files saved. Residues within a 12 Å radius of $D_{3.32(155)}$ were used for the generation of a molecular surface[219] and spheres[217] and then property grids were calculated using the appropriate bundled software. DOCK[217] was then used to generate preliminary placements for the ligand molecules. Ligand orientations were chosen based on clustered matches generated by DOCK and were then optimized using a local minimization with the Tripos force field of Sybyl. Almost invariably, a sample of top-ranking clusters converged on the final low energy structures that were shown in the Discussion section of the current discourse.

LIST OF REFERENCES

LIST OF REFERENCES

1. Sanders-Bush, E.; Mayer, S. 5-Hydroxytryptamine (Serotonin) Receptor Agonists and Antagonists. In *The Pharmacological Basis of Therapeutics;* Hardman, J. G., Limbird, L., Molinoff, P. B., Ruddon, R. W., Gilman, A. G., Eds.; McGraw-Hill: New York, **1996**, pp. 249-263.

2. Peroutka, S. J.; Howell, T. A. The Molecular Evolution of G Protein-Coupled Receptors: Focus on 5-Hydroxytryptamine Receptors. *Neuropharmacology* **1994**, *33*, 319-324.

3. Erspamer, V. Occurrence of Indolealkylamines in Nature. In *5-Hydroxy-tryptamine and Related Indolealkylamines.;* Erspamer, V., Eds.; Springer-Verlag: Berlin, **1966**, pp. 132-181.

4. Rapport, M. M.; Green, A. A.; Page, I. H. Crystalline Serotonin. *Science* **1948**, *108*, 329-331.

5. Page, I. H. The Discovery of Serotonin. *Perspect. Biol. Med.* **1976**, *20*, 1-8.

6. Wooley, D. W.; Shaw, E. A Biochemical and Pharmacological Suggestion About Certain Mental Disorders. *Proc. Natl. Acad. Sci. U. S. A.* **1954**, *40*, 228-231.

7. Brodie, B. B.; Shore, P. A. A Concept for a Role of Serotonin and Norepinephrine as Chemical Mediators in the Brain. *Ann. N. Y. Acad. Sci.* **1957**, *66*, 631-642.

8. Udenfriend, S. Biochemistry of Serotonin and Other Indoleamines. *Vitam. Horm.* **1959**, *17*, 133-151.

9. Luby, E. D.; Cohen, B. D.; Rosenbaum, F.; Domino, E. F. Study of a New Schizophreniomimetic Drug Sernyl. *AMA Arch. Neurol. Psychiatry* **1959**, *81*, 363-369.

10. Luby, E. D.; Gottlieb, J. S.; Cohen, B. D.; Rosenbaum, F.; Domino, E. F. Model Psychosis and Schizophrenia. *Am. J. Psychiatry* **1962**, *119*, 61-65.

11. Hollister, L. E. Drug-Induced Psychoses and Schizophrenic Reactions, a Critical Comparison. *Ann. N. Y. Acad. Sci.* **1962**, *96*, 80-88.

12. Matz, R.; Rick, W.; Thompson, H.; Gershon, S. Clozapine--A Potential Antipsychotic Agent without Extrapyramidal Manifestations. *Curr. Ther. Res. Clin. Exp.* **1974**, *16*, 687-695.

13. Reynolds, G. P.; Garrett, N. J.; Rupniak, N.; Jenner, P.; Marsden, C. D. Chronic Clozapine Treatment of Rats Down-Regulates Cortical 5-HT_2 Receptors. *Eur. J. Pharmacol.* **1983**, *89*, 325-326.

14. Fink, H.; Morgenstern, R.; Oelssner, W. Clozapine--A Serotonin Antagonist? *Pharmacol. Biochem. Behav.* **1984**, *20*, 513-517.

15. Roth, B. L.; Tandra, S.; Burgess, L. H.; Sibley, D. R.; Meltzer, H. Y. D_4 Dopamine Receptor Binding Affinity Does Not Distinguish Between Typical and Atypical Antipsychotic Drugs. *Psychopharmacology (Berl)* **1995**, *120*, 365-368.

16. Glennon, R. A. Central Serotonin Receptors as Targets for Drug Research. *J. Med. Chem.* **1987**, *30*, 1-12.

17. Fuller, R. W. The Pharmacology and Therapeutic Potential of Serotonin Receptor Agonists and Antagonists. In *Advances in Drug Research;* Testa, D., Eds.; Academic Press Ltd.: London, **1988**, pp. 349-380.

18. Sjoerdsma, A.; Palfreyman, M. G. History of Serotonin and Serotonin Disorders. In *The Neuropharmacology of Serotonin.;* Whitaker-Azmitia, P. M., Peroutka, S. J., Eds.; Annals of the NY Academy of Sciences: New York, **1990**, pp. 1-8.

19. Mikuni, M.; Meltzer, H. Y. Reduction of Serotonin-2 Receptors in Rat Cerebral Cortex after Subchronic Administration of Imipramine, Chlorpromazine, and the Combination Thereof. *Life Sci.* **1984**, *34*, 87-92.

20. Peroutka, S. J.; Snyder, S. H. Long-Term Antidepressant Treatment Decreases Spiroperidol-Labeled Serotonin Receptor Binding. *Science* **1980**, *210*, 88-90.

21. Peroutka, S. J.; Snyder, S. H. Regulation of $Serotonin_2$ (5-HT_2) Receptors Labeled with [3H]Spiroperidol by Chronic Treatment with the Antidepressant Amitriptyline. *J. Pharmacol. Exp. Ther.* **1980**, *215*, 582-587.

22. Blier, P.; De Montigny, C. Effect of Chronic Tricylic Antidepressant Treatment on the Serotoninergic Autoreceptor: A Microiontophoretic Study in the Rat. *Naunyn Schmiedebergs Arch. Pharmacol.* **1980**, *314*, 123-128.

23. Chaput, Y.; De Montigny, C.; Blier, P. Effects of a Selective 5-HT Reuptake Blocker, Citalopram, on the Sensitivity of 5-HT Autoreceptors: Electrophysiological Studies in the Rat Brain. *Naunyn Schmiedebergs Arch. Pharmacol.* **1986**, *333*, 342-348.

24. Mizuta, T.; Segawa, T. Chronic Effects of Imipramine and Lithium on Postsynaptic 5-HT_{1A} and 5-HT_{1B} Sites and on Presynaptic 5-HT_3 Sites in Rat Brain. *Jpn. J. Pharmacol.* **1988**, *47*, 107-113.

25. Robinson, D. S.; Alms, D. R.; Shrotriya, R. C.; Messina, M.; Wickramaratne, P. Serotonergic Anxiolytics and Treatment of Depression. *Psychopathology* **1989**, *22 Suppl 1*, 27-36.

26. Barbaccia, M. L.; Brunello, N.; Chuang, D. M.; Costa, E. On the Mode of Action of Imipramine: Relationship between Serotonergic Axon Terminal Function and Down-Regulation of Beta-Adrenergic Receptors. *Neuropharmacology* **1983**, *22*, 373-383.

27. Mackenzie, E. T.; Edvinsson, L.; Scatton, B. Functional Bases for a Central Serotonergic Involvement in Classic Migraine: A Speculative View. *Cephalalgia* **1985**, *5*, 69-78.

28. Bradley, P. B.; Engel, G.; Feniuk, W.; Fozard, J. R.; Humphrey, P. P.; Middlemiss, D. N.; Mylecharane, E. J.; Richardson, B. P.; Saxena, P. R. Proposals for the Classification and Nomenclature of Functional Receptors for 5-Hydroxytryptamine. *Neuropharmacology* **1986**, *25*, 563-576.

29. Roth, B. L.; Meltzer, H. Y. The Role of Serotonin in Schizophrenia. In *Psychopharmacology: The Fourth Generation of Progress;* Bloom, F. E., Kupfer, D. J., Eds.; Raven Press: New York, **1994**, pp. 1215-1227.

30. Abraham, H. D.; Aldridge, A. M.; Gogia, P. The Psychopharmacology of Hallucinogens. *Neuropsychopharmacology* **1996**, *14*, 285-298.

31. Vollenweider, F. X.; Geyer, M. A. A Systems Model of Altered Consciousness: Integrating Natural and Drug-Induced Psychoses. *Brain Res. Bull.* **2001**, *56*, 495-507.

32. Descarries, L.; Audet, M. A.; Doucet, G.; Garcia, S.; Oleskevich, S.; Seguela, P.; Soghomonian, J. J.; Watkins, K. C. Morphology of Central Serotonin Neurons. Brief Review of Quantified Aspects of Their Distribution and Ultrastructural Relationships. *Ann. N. Y. Acad. Sci.* **1990**, *600*, 81-92.

33. Nieforth, K. A.; Gianutsos, G. Central Nervous System Stimulants. In *Principles of Medicinal Chemistry*. Foye, W. O., Lemke, T. L., Williams, D. A., Eds.; Williams and Witkins: Baltimore, **1995**, pp 270-304.

34. Aghajanian, G. K.; Foote, W. E.; Sheard, M. H. Lysergic Acid Diethylamide: Sensitive Neuronal Units in the Midbrain Raphe. *Science* **1968**, *161*, 706-708.

35. Glennon, R. A.; Titeler, M.; McKenney, J. D. Evidence for 5-HT_2 Involvement in the Mechanism of Action of Hallucinogenic Agents. *Life Sci.* **1984**, *35*, 2505-2511.

36. Titeler, M.; Lyon, R. A.; Glennon, R. A. Radioligand Binding Evidence Implicates the Brain 5-HT_2 Receptor as a Site of Action for LSD and Phenylisopropylamine Hallucinogens. *Psychopharmacology (Berl)* **1988**, *94*, 213-216.

37. Aghajanian, G. K.; Karek, G. J. Serotonin-Glutamate Interactions: A New Target for Antipsychotic Drugs. *Neuropsychopharmacol.* **1999**, *21*, S122-S1333.

38. McKenna, T. Food of the Gods: The Search for the Original Tree of Knowledge. Bantam Books, New York, **1992**.

39. O'Brien, C. P. Drug Addiction and Drug Abuse. In *The Pharmacological Basis of Therapeutics;* Hardman, J. G., Limbird, L. E., Molinoff, P. B., Ruddon, R. W., Gilman, A. G., Eds.; McGraw-Hill, New York, **1996**, pp. 573-577.

40. Glennon, R. A. Do Classical Hallucinogens Act as 5-HT_2 Agonists or Antagonists? *Neuropsychopharmacology* **1990**, *3*, 509-517.

41. Roth, B. L.; Willins, D. L.; Kristiansen, K.; Kroeze, W. K. 5-Hydroxytryptamine$_2$-Family Receptors (5-Hydroxytryptamine$_{2A}$, 5-Hydroxytryptamine$_{2B}$, 5-Hydroxytryptamine$_{2C}$): Where Structure Meets Function. *Pharmacol. Ther.* **1998**, *79*, 231-257.

42. Ciprian-Ollivier, J.; Cetkovich-Bakmas, M. G. Altered Consciousness States and Endogenous Psychoses: A Common Molecular Pathway? *Schizophr. Res.* **1997**, *28*, 257-265.

43. O'Reilly, P. O.; Reich, G. Lysergic Acid and the Alcoholic. *Dis Nerv Syst* **1962**, *23*, 331-334.

44. Savage, C. Alcoholism and Transcendence. *J. Nerv. Ment. Dis.* **1962**, *135*, 429-435.

45. Abuzzahab, F. S., Sr.; Anderson, B. J. A Review of LSD Treatment in Alcoholism. *Int. Pharmacopsychiatry* **1971**, *6*, 223-235.

46. Abramson, H. A. The Use of LSD as an Adjuvant to Psychotherapy: Fact and Fiction. In *LSD - A Total Study;* Sankar, D. V. S., Eds.; PJD Publications Ltd.: Westbury, NY, **1975**, pp. 687-700.

47. LSD Infofax. http://www.nida.nih.gov/infofax/lsd.html (accessed March, 2002).

48. Fanchamps; A. Some Compounds with Hallucinogenic Activity. In *Ergot Alkaloids and Related Compounds;* Berde, B., Schild, E., Eds.; Springer-Verlag: Berlin, **1978**, pp. 567-583.

49. Abraham, H. D.; Aldridge, A. M. Adverse Consequences of Lysergic Acid Diethylamide. *Addiction* **1993**, *88*, 1327-1334.

50. Browning, L. S. Lysergic Acid Diethylamide: Mutagenic Effects in *Drosophila*. *Science* **1968**, *161*, 1022-1023.

51. Warkany, J.; Takacs, E. Lysergic Acid Diethylamide (LSD): No Teratogenicity in Rats. *Science* **1968**, *159*, 731-732.

52. Van Went, G. F. Mutagenicity Testing of 3 Hallucinogens: LSD, Psilocybin and Delta 9-THC, Using the Micronucleus Test. *Experientia* **1978**, *34*, 324-325.

53. Furst, P. T. Peyote Among the Huichol Indians of Mexico. In *Flesh of the Gods: The Ritual Use of Hallucinogens;* Furst, P. T., Eds.; Praeger Publishers: New York, **1972**, pp. 180-181.

54. Schultes, R. E.; Hofmann, A. Plants of the Gods: Origins of Hallucinogen Use. McGraw-Hill, New York, **1979**.

55. Schultes, R. E. The Beta-Carboline Hallucinogens of South America. *J. Psychoactive Drugs* **1982**, *14*, 205-220.

56. Wasson, R. G. Seeking the Magic Mushroom. *Life*, May 13, **1957**, pp 100-109.

57. Hofmann, A.; Heim, R.; Brack, A.; Kobel, H. [Psilocybin, a Psychotropic Substance from the Mexican Mushroom Psilocybe Mexicana Heim.]. *Experientia* **1958**, *14*, 107-109.

58. Leonard, H. L.; Rapoport, J. L. Relief of Obsessive-Compulsive Symptoms by LSD and Psilocin. *Am. J. Psychiatry* **1987**, *144*, 1239-1240.

59. Lyttle, T.; Goldstein, D.; Gartz, J. Bufo Toads and Bufotenine: Fact and Fiction Surrounding an Alleged Psychedelic. *J. Psychoactive Drugs* **1996**, *28*, 267-290.

60. Shulgin, A. T.; Sargent, T.; Naranjo, C. Structure--Activity Relationships of One-Ring Psychotomimetics. *Nature* **1969**, *221*, 537-541.

61. Shulgin, A. T.; Shulgin, A. Pihkal: A Chemical Love Story. Transform Press, Berkeley, **1991**.

62. Urbina, M. El Peyote y El Ololiuqui. *Anales Museo Nac. Mexico* **1903**, *7*, 25-48.

63. Shawcross, W. E. Recreational Use of Ergoline Alkaloids from *Argyreia Nervosa. J. Psychoactive Drugs* **1983**, *15*, 251-259.

64. Müller-Schweinitzer, E.; Weidmann, H. In *Ergot Alkaloids and Related Compounds;* Berde, B., Schild, H. O., Eds.; Springer-Verlag: New York, **1978**, pp. 87-196.

65. Hofmann, A. The Chemistry of LSD and its Modifications. In *LSD - A Total Study;* Sankar, D. V. S., Eds.; PJD Publications Ltd.: Westbury, NY, **1975**, pp. 107-139.

66. Gudermann, T.; Nurnberg, B.; Schultz, G. Receptors and G Proteins as Primary Components of Transmembrane Signal Transduction. Part 1. G-Protein-Coupled Receptors: Structure and Function. *J. Mol. Med.* **1995**, *73*, 51-63.

67. Ostrowski, J.; Kjelsberg, M. A.; Caron, M. G.; Lefkowitz, R. J. Mutagenesis of the Beta 2-Adrenergic Receptor: How Structure Elucidates Function. *Annu. Rev. Pharmacol. Toxicol.* **1992**, *32*, 167-183.

68. Fong, T. M. Mechanistic Hypotheses for the Activation of G-Protein-Coupled Receptors. *Cell Signal.* **1996**, *8*, 217-224.

69. Roth, B. L.; Choudhary, M. S.; Khan, N.; Uluer, A. Z. High-Affinity Agonist Binding is Not Sufficient for Agonist Efficacy at 5-Hydroxytryptamine$_{2A}$ Receptors: Evidence in Favor of a Modified Ternary Complex Model. *J. Pharmacol. Exp. Ther.* **1997**, *280*, 576-583.

70. Hoyer, D.; Clarke, D. E.; Fozard, J. R.; Hartig, P. R.; Martin, G. R.; Mylecharane, E. J.; Saxena, P. R.; Humphrey, P. P. International Union of Pharmacology Classification of Receptors for 5-Hydroxytryptamine (Serotonin). *Pharmacol. Rev.* **1994**, *46*, 157-203.

71. Palacios, J. M.; Waeber, C.; Hoyer, D.; Mengod, G. Distribution of Serotonin Receptors. *Ann. N. Y. Acad. Sci.* **1990**, *600*, 36-52.

72. Andrade, R.; Malenka, R. C.; Nicoll, R. A. A G Protein Couples Serotonin and GABAB Receptors to the Same Channels in Hippocampus. *Science* **1986**, *234*, 1261-1265.

73. Aghajanian, G. K.; Sprouse, J. S.; Rasmussen, K. Physiology of the Midbrain Serotonin System. In *Psychopharmacology: The Third Generation of Progess;* Meltzer, H., Eds.; Raven Press: New York, **1987**, pp. 141-149.

74. Leysen, J. E.; Niemegeers, C. J.; Tollenaere, J. P.; Laduron, P. M. Serotonergic Component of Neuroleptic Receptors. *Nature* **1978**, *272*, 168-171.

75. Peroutka, S. J.; Snyder, S. H. Multiple Serotonin Receptors: Differential Binding of [3H]5-Hydroxytryptamine, [3H]Lysergic Acid Diethylamide And [3H]Spiroperidol. *Mol. Pharmacol.* **1979**, *16*, 687-699.

76. Rhee, S. G.; Choi, K. D. Multiple Forms of Phospholipase C Isozymes and Their Activation Mechanisms. *Adv. Second Messenger Phosphoprotein Res.* **1992**, *26*, 35-61.

77. Helton, L. A.; Thor, K. B.; Baez, M. 5-Hydroxytryptamine$_{2A}$, 5-Hydroxy-tryptamine$_{2B}$, and 5-Hydroxytryptamine$_{2C}$ Receptor mRNA Expression in the Spinal Cord of Rat, Cat, Monkey and Human. *Neuroreport* **1994**, *5*, 2617-2620.

78. Ullmer, C.; Schmuck, K.; Kalkman, H. O.; Lubbert, H. Expression of Serotonin Receptor mRNAs in Blood Vessels. *FEBS Lett.* **1995**, *370*, 215-221.

79. Wainscott, D. B.; Lucaites, V. L.; Kursar, J. D.; Baez, M.; Nelson, D. L. Pharmacologic Characterization of the Human 5-Hydroxytryptamine$_{2B}$ Receptor: Evidence for Species Differences. *J. Pharmacol. Exp. Ther.* **1996**, *276* , 720-727.

80. Choi, D. S.; Maroteaux, L. Immunohistochemical Localisation of the Serotonin 5-HT$_{2B}$ Receptor in Mouse Gut, Cardiovascular System, and Brain. *FEBS Lett.* **1996**, *391*, 45-51.

81. Choi, D. S.; Ward, S. J.; Messaddeq, N.; Launay, J. M.; Maroteaux, L. 5-HT$_{2B}$ Receptor-Mediated Serotonin Morphogenetic Functions in Mouse Cranial Neural Crest and Myocardiac Cells. *Development* **1997**, *124*, 1745-1755.

82. Pazos, A.; Hoyer, D.; Palacios, J. M. The Binding of Serotonergic Ligands to the Porcine Choroid Plexus: Characterization of a New Type of Serotonin Recognition Site. *Eur. J. Pharmacol.* **1984**, *106*, 539-546.

83. Pazos, A.; Probst, A.; Palacios, J. M. Serotonin Receptors in the Human Brain--IV. Autoradiographic Mapping of Serotonin-2 Receptors. *Neuroscience* **1987**, *21*, 123-139.

84. Molineaux, S. M.; Jessell, T. M.; Axel, R.; Julius, D. 5-HT$_{1C}$ Receptor is a Prominent Serotonin Receptor Subtype in the Central Nervous System. *Proc. Natl. Acad. Sci. U. S. A* **1989**, *86*, 6793-6797.

85. Julius, D.; Livelli, T. J.; Jessell, T. M.; Axel, R. Ectopic Expression of the Serotonin-1C Receptor and the Triggering of Malignant Transformation. *Science* **1989**, *244*, 1057-1062.

86. Pazos, A.; Cortes, R.; Palacios, J. M. Quantitative Autoradiographic Mapping of Serotonin Receptors in the Rat Brain. II. Serotonin-2 Receptors. *Brain Res.* **1985**, *346*, 231-249.

87. Pazos, A.; Probst, A.; Palacios, J. M. Serotonin Receptors in the Human Brain--III. Autoradiographic Mapping of Serotonin-1 Receptors. *Neuroscience* **1987**, *21*, 97-122.

88. Roth, B. L.; Chuang, D. M. Multiple Mechanisms of Serotonergic Signal Transduction. *Life Sci.* **1987**, *41*, 1051-1064.

89. Willins, D. L.; Deutch, A. Y.; Roth, B. L. Serotonin 5-HT_{2A} Receptors are Expressed on Pyramidal Cells and Interneurons in the Rat Cortex. *Synapse* **1997**, *27*, 79-82.

90. Cohen, M. L.; Fuller, R. W.; Wiley, K. S. Evidence for 5-HT_2 Receptors Mediating Contraction in Vascular Smooth Muscle. *J. Pharmacol. Exp. Ther.* **1981**, *218*, 421-425.

91. Roth, B. L.; Nakaki, T.; Chuang, D. M.; Costa, E. Aortic Recognition Sites for Serotonin (5HT) are Coupled to Phospholipase C and Modulate Phosphatidylinositol Turnover. *Neuropharmacology* **1984**, *23*, 1223-1225.

92. De Chaffoy, D. C.; Leysen, J. E.; De Clerck, F.; Van Belle, H.; Janssen, P. A. Evidence that Phospholipid Turnover is the Signal Transducing System Coupled to Serotonin-S2 Receptor Sites. *J. Biol. Chem.* **1985**, *260*, 7603-7608.

93. Roth, B. L.; Nakaki, T.; Chuang, D. M.; Costa, E. 5-Hydroxytryptamine$_2$ Receptors Coupled to Phospholipase C in Rat Aorta: Modulation of Phosphoinositide Turnover by Phorbol Ester. *J. Pharmacol. Exp. Ther.* **1986**, *238*, 480-485.

94. Wilcox, B. D.; Rydelek-Fitzgerald, L.; Jeffrey, J. J. Regulation of Collagenase Gene Expression by Serotonin and Progesterone in Rat Uterine Smooth Muscle Cells. *J. Biol. Chem.* **1992**, *267*, 20752-20757.

95. Berridge, M. J.; Downes, C. P.; Hanley, M. R. Lithium Amplifies Agonist-Dependent Phosphatidylinositol Responses in Brain and Salivary Glands. *Biochem. J.* **1982**, *206*, 587-595.

96. Conn, P. J.; Sanders-Bush, E. Selective 5HT-2 Antagonists Inhibit Serotonin Stimulated Phosphatidylinositol Metabolism in Cerebral Cortex. *Neuropharmacology* **1984**, *23*, 993-996.

97. Vaidya, V. A.; Marek, G. J.; Aghajanian, G. K.; Duman, R. S. 5-HT_{2A} Receptor-Mediated Regulation of Brain-Derived Neurotrophic Factor mRNA in the Hippocampus and the Neocortex. *J. Neurosci.* **1997**, *17*, 2785-2795.

98. Nakaki, T.; Roth, B. L.; Chuang, D. M.; Costa, E. Phasic and Tonic Components in 5-HT_2 Receptor-Mediated Rat Aorta Contraction: Participation of Ca++ Channels and Phospholipase C. *J. Pharmacol. Exp. Ther.* **1985**, *234*, 442-446.

99. Roth, B. L. Role of Phosphoinositide Hydrolysis and Protein Kinase C Activation on $5HT_2$ Receptor Function in Smooth Muscle. In *Serotonin: From Cell Biology to Pharmacology and Therapeutics;* Paoletti, R., Vanhoutte, P. M., Brunello, N., Maggi, F. M., Eds.; Kluwer Academic Press: Dordrecht, **1990**, pp. 33-38.

100. Nichols, D. E. Studies of the Relationship Between Molecular Structure and Hallucinogenic Activity. *Pharmacol. Biochem. Behav.* **1986**, *24*, 335-340.

101. Nichols, D. E.; Oberlender, R.; McKenna, D. J. Stereochemical Aspects of Hallucinogenesis. In *Biochemistry and Physiology of Substance Abuse;* Watson, R., Eds.; CRC Press: Boca Raton, **1991**, pp. 1-39.

102. Perrine, D. M. Psychedelics: LSD to XTC. In *The Chemistry of Mind-Altering Drugs;* The American Chemical Society: Washington, D.C., **1996**, pp. 255-332.

103. Benington, F.; Morin, R. D.; Clark, L. C. Mescaline Analogs. I. 2,4,6-Trialkoxy-β-Phenethylamines. *J. Org. Chem.* **1954**, *19*, 11-16.

104. Patel, A. R. Mescaline and Related Compounds. *Fortschr. Arzneimittelforsch.* **1968**, *11*, 11-47.

105. Aldous, F. A.; Barrass, B. C.; Brewster, K.; Buxton, D. A.; Green, D. M.; Pinder, R. M.; Rich, P.; Skeels, M.; Tutt, K. J. Structure-Activity Relationships in Psychotomimetic Phenylalkylamines. *J. Med. Chem.* **1974**, *17*, 1100-1111.

106. Shulgin, A. T. Psychotomimetic Drugs: Structure-Activity Relationships. In *Handbook of Psychopharmacology;* Iversen, L. L., Iversen, S. D., Snyder, S. H., Eds.; Plenum Press: New York, **1978**, pp. 243-333.

107. Nichols, D. E.; Glennon, R. A. Medicinal Chemistry and Structure-Activity Relationships of Hallucinogens. In *Hallucinogens: Neurochemical, Behavorial, and Clinical Perspectives;* Jacobs, B. L., Eds.; Raven Press: New York, **1984**, pp. 95-142.

108. Nichols, D. E.; Frescas, S.; Marona-Lewicka, D.; Huang, X.; Roth, B. L.; Gudelsky, G. A.; Nash, J. F. 1-(2,5-Dimethoxy-4-(trifluoromethyl)phenyl)-2-aminopropane: A Potent Serotonin $5\text{-}HT_{2A/2C}$ Agonist. *J. Med. Chem.* **1994**, *37*, 4346-4351.

109. Standridge, R. T.; Howell, H. G.; Gylys, J. A.; Partyka, R. A.; Shulgin, A. T. Phenylakylamines with Potential Psychotherapeutic Utility. 1. 2-Amino-1-(2,5-dimethoxy-4-methylphenyl)butane. *J. Med. Chem.* **1976**, *19*, 1400-1404.

110. Barfknecht, C. F.; Nichols, D. E. Correlation of Psychotomimetic Activity of Phenethylamines and Amphetamines with 1-Octanol-Water Partition Coefficients. *J. Med. Chem.* **1975**, *18*, 208-210.

111. Johnson, M. P.; Hofman, A. J.; Nichols, D. E.; Mathis, C. A. Binding to the Serotonin 5-HT_2 Receptor by the Enantiomers of ^{125}I-DOI. *Neuropharmacology* **1987**, *26*, 1803-1806.

112. Chambers, J. J.; Kurrasch-Orbaugh, D. M.; Parker, M. A.; Nichols, D. E. Enantiospecific Synthesis and Pharmacological Evaluation of a Series of Super-Potent, Conformationally Restricted 5-$HT_{(2A/2C)}$ Receptor Agonists. *J. Med. Chem.* **2001**, *44*, 1003-1010.

113. Nichols, D. E.; Barfknecht, C. F.; Rusterholz, D. B.; Benington, F.; Morin, R. D. Asymmetric Synthesis of Psychotomimetic Phenylisopropylamines. *J. Med. Chem.* **1973**, *16*, 480-483.

114. Glennon, R. A.; Young, R.; Benington, F.; Morin, R. D. Behavioral and Serotonin Receptor Properties of 4-Substituted Derivatives of the Hallucinogen 1-(2,5-Dimethoxyphenyl)-2-aminopropane. *J. Med. Chem.* **1982**, *25*, 1163-1168.

115. Lemaire, D.; Jacob, P., III; Shulgin, A. T. Ring-Substituted Beta-Methoxyphenethylamines: A New Class of Psychotomimetic Agents Active in Man. *J. Pharm. Pharmacol.* **1985**, *37*, 575-577.

116. Monte, A. P.; Marona-Lewicka, D.; Lewis, M. M.; Mailman, R. B.; Wainscott, D. B.; Nelson, D. L.; Nichols, D. E. Substituted Naphthofurans as Hallucinogenic Phenethylamine-Ergoline Hybrid Molecules with Unexpected Muscarinic Antagonist Activity. *J. Med. Chem.* **1998**, *41*, 2134-2145.

117. Makriyannis, A.; Knittel, J. Conformational-Analysis of Amphetamine in Solution Based on Unambiguous Assignment of the Diastereotopic Benzylic Protons in the H-1-NMR Spectra. *Tetrahedron Lett.* **1981**, *22*, 4631-4634.

118. Seggel, M. R.; Yousif, M. Y.; Lyon, R. A.; Titeler, M.; Roth, B. L.; Suba, E. A.; Glennon, R. A. A Structure-Affinity Study of the Binding of 4-Substituted Analogues of 1-(2,5-Dimethoxyphenyl)-2-aminopropane at 5-HT_2 Serotonin Receptors. *J. Med. Chem.* **1990**, *33*, 1032-1036.

119. Oberlender, R. A.; Kothari, P. J.; Nichols, D. E.; Zabik, J. E. Substituent Branching in Phenethylamine-type Hallucinogens: A Comparison of 1-[2,5-Dimethoxy-4-(2-butyl)phenyl]-2-aminopropane and 1-[2,5-Dimethoxy-4-(2-methylpropyl)phenyl]-2-aminopropane. *J. Med. Chem.* **1984**, *27*, 788-792.

120. Shulgin, A. T.; Dyer, D. C. Psychotomimetic Phenylisopropylamines. 5. 4-Alkyl-2,5-dimethoxyphenylisopropylamines. *J. Med. Chem.* **1975**, *18*, 1201-1204.

121. Monte, A. P.; Marona-Lewicka, D.; Parker, M. A.; Wainscott, D. B.; Nelson, D. L.; Nichols, D. E. Dihydrobenzofuran Analogues of Hallucinogens. 3. Models of 4-Substituted (2,5-Dimethoxyphenyl)alkylamine Derivatives with Rigidified Methoxy Groups. *J. Med. Chem.* **1996**, *39*, 2953-2961.

122. Parker, M. Studies of Perceptiotropic Phenethylamines: Determinants of Affinity for the 5-HT_{2A} Receptor. Ph.D., Purdue University, West Lafayette, Indiana USA, **1998**.

123. Parker, M. A.; Marona-Lewicka, D.; Lucaites, V. L.; Nelson, D. L.; Nichols, D. E. A Novel (Benzodifuranyl)aminoalkane with Extremely Potent Activity at the 5-HT_{2A} Receptor. *J. Med. Chem.* **1998**, *41*, 5148-5149.

124. Palczewski, K.; Kumasaka, T.; Hori, T.; Behnke, C. A.; Motoshima, H.; Fox, B. A.; Le, T. I.; Teller, D. C.; Okada, T.; Stenkamp, R. E.; Yamamoto, M.; Miyano, M. Crystal Structure of Rhodopsin: A G Protein-Coupled Receptor *Science* **2000**, *289*, 739-745.

125. Dohlman, H. G.; Caron, M. G.; Lefkowitz, R. J. A Family of Receptors Coupled to Guanine Nucleotide Regulatory Proteins. *Biochemistry* **1987**, *26*, 2657-2664.

126. Baldwin, J. M. Structure and Function of Receptors Coupled to G Proteins. *Curr. Opin. Cell Biol.* **1994**, *6*, 180-190.

127. Ballesteros, J. A.; Shi, L.; Javitch, J. A. Structural Mimicry in G Protein-Coupled Receptors: Implications of the High-Resolution Structure of Rhodopsin for Structure-Function Analysis of Rhodopsin-Like Receptors. *Mol. Pharmacol.* **2001**, *60*, 1-19.

128. Gershengorn, M. C.; Osman, R. Minireview: Insights into G Protein-Coupled Receptor Function using Molecular Models. *Endocrinology* **2001**, *142*, 2-10.

129. Shih, J. C.; Gallaher, T.; Wang, C. D.; Chen, K. Site-Directed Mutagenesis of Serotonin 5-HT_2 Receptors. *J. Chem. Neuroanat.* **1992**, *5*, 281-282.

130. Ballesteros, J. A.; Weinstein, H. Integrated Methods for the Construction of Three-Dimensional Models and Computational Probing of Structure-Function Relations in G Protein-Coupled Receptor. *Methods Neurosci.* **1995**, *25*, 366-428.

131. Hibert, M. F.; Trumpp-Kallmeyer, S.; Bruinvels, A.; Hoflack, J. Three-Dimensional Models of Neurotransmitter G-Binding Protein-Coupled Receptors. *Mol. Pharmacol.* **1991**, *40*, 8-15.

132. Westkaemper, R. B.; Glennon, R. A. Approaches to Molecular Modeling Studies and Specific Application to Serotonin Ligands and Receptors. *Pharmacol. Biochem. Behav.* **1991**, *40*, 1019-1031.

133. Edvardsen, O.; Sylte, I.; Dahl, S. G. Molecular Dynamics of Serotonin and Ritanserin Interacting with the 5-HT_2 Receptor. *Brain Res. Mol. Brain Res.* **1992**, *14*, 166-178.

134. Trumpp-Kallmeyer, S.; Hoflack, J.; Bruinvels, A.; Hibert, M. Modeling of G-Protein-Coupled Receptors: Application to Dopamine, Adrenaline, Serotonin, Acetylcholine, and Mammalian Opsin Receptors. *J. Med. Chem.* **1992**, *35*, 3448-3462.

135. Wang, C. D.; Gallaher, T. K.; Shih, J. C. Site-Directed Mutagenesis of the Serotonin 5-Hydroxytrypamine$_2$ Receptor: Identification of Amino Acids Necessary for Ligand Binding and Receptor Activation. *Mol. Pharmacol.* **1993**, *43*, 931-940.

136. Kristiansen, K.; Edvardsen, O.; Dahl, S. Molecular Modeling of Ketanserin and Its Interactions with the 5-HT_2 Receptor. *Med. Chem. Res.* **1993**, *3*, 370-385.

137. Westkaemper, R.; Glennon, R. Molecular Graphics Models of Members of the 5-HT_2 Subfamily: 5-HT_{2A}, 5-HT_{2B} and 5-HT_{2C} Receptors. *Med. Chem. Res.* **1993**, *3*, 317-335.

138. Choudhary, M. S.; Sachs, N.; Uluer, A.; Glennon, R. A.; Westkaemper, R. B.; Roth, B. L. Differential Ergoline and Ergopeptine Binding to 5-Hydroxytryptamine$_{2A}$ Receptors: Ergolines Require an Aromatic Residue at Position 340 for High Affinity Binding. *Mol. Pharmacol.* **1995**, *47*, 450-457.

139. Weinstein, H.; Zhang, D. Receptor Models and Ligand-Induced Responses: New Insights for Structure-Activity Relations. In *QSAR and Molecular Modelling: Concepts;* Sanz, F., Giraldo, J., Manaut, F., Eds.; Prous Science Publishers: Barcelona, **1995**, pp. 497-507.

140. Almaula, N.; Ebersole, B. J.; Zhang, D.; Weinstein, H.; Sealfon, S. C. Mapping the Binding Site Pocket of the Serotonin 5-Hydroxytryptamine$_{2A}$ Receptor. Ser3.36(159) Provides a Second Interaction Site for the Protonated Amine of Serotonin but not of Lysergic Acid Diethylamide or Bufotenin. *J. Biol. Chem.* **1996**, *271*, 14672-14675.

141. Pazos, A.; Hoyer, D.; Palacios, J. M. Mesulergine, A Selective Serotonin-2 Ligand in the Rat Cortex, does not Label these Receptors in Porcine and Human Cortex: Evidence for Species Differences in Brain Serotonin-2 Receptors. *Eur. J. Pharmacol.* **1984**, *106*, 531-538.

142. Pritchett, D. B.; Bach, A. W.; Wozny, M.; Taleb, O.; Dal Toso, R.; Shih, J. C.; Seeburg, P. H. Structure and Functional Expression of Cloned Rat Serotonin 5HT-2 Receptor. *EMBO J.* **1988**, *7*, 4135-4140.

143. Saltzman, A. G.; Morse, B.; Whitman, M. M.; Ivanshchenko, Y.; Jaye, M.; Felder, S. Cloning of the Human Serotonin 5-HT_2 and 5-HT_{1C} Receptor Subtypes. *Biochem. Biophys. Res. Commun.* **1991**, *181*, 1469-1478.

144. Kao, H. T.; Adham, N.; Olsen, M. A.; Weinshank, R. L.; Branchek, T. A.; Hartig, P. R. Site-Directed Mutagenesis of a Single Residue Changes the Binding Properties of the Serotonin 5-HT_2 Receptor from a Human to a Rat Pharmacology. *FEBS Lett.* **1992**, *307*, 324-328.

145. Johnson, M. P.; Loncharich, R. J.; Baez, M.; Nelson, D. L. Species Variations in Transmembrane Region V of the 5-Hydroxytryptamine Type 2A Receptor Alter the Structure-Activity Relationship of Certain Ergolines and Tryptamines. *Mol. Pharmacol.* **1994**, *45*, 277-286.

146. Choudhary, M. S.; Craigo, S.; Roth, B. L. A Single Point Mutation (Phe340→Leu340) of a Conserved Phenylalanine Abolishes 4-[125I]Iodo-(2,5-dimethoxy)phenylisopropylamine and [3H]Mesulergine but not [3H]Ketanserin Binding to 5-Hydroxytryptamine$_2$ Receptors. *Mol. Pharmacol.* **1993**, *43*, 755-761.

147. Moereels, H.; Janssen, P. Molecular Modeling of G-Protein Coupled Receptors: Going Step by Step. *Med. Chem. Res.* **1993**, *3*, 335-343.

148. Zhang, D.; Weinstein, H. Signal Transduction by a 5-HT_2 Receptor: A Mechanistic Hypothesis from Molecular Dynamics Simulations of the Three-Dimensional Model of the Receptor Complexed To Ligands. *J. Med. Chem.* **1993**, *36*, 934-938.

149. Holtje, H. D.; Jendretzki, U. K. Construction of a Detailed Serotoninergic 5-HT_{2A} Receptor Model. *Arch. Pharm. (Weinheim)* **1995**, *328*, 577-584.

150. Roth, B. L.; Shoham, M.; Choudhary, M. S.; Khan, N. Identification of Conserved Aromatic Residues Essential for Agonist Binding and Second Messenger Production at 5-Hydroxytryptamine$_{2A}$ Receptors. *Mol. Pharmacol.* **1997**, *52*, 259-266.

151. Hartig, P.; Kao, H. T.; Macchi, M.; Adham, N.; Zgombick, J.; Weinshank, R.; Branchek, T. The Molecular Biology of Serotonin Receptors. An Overview. *Neuropsychopharmacology* **1990**, *3*, 335-347.

152. Hargrave, P. A.; McDowell, J. H. Rhodopsin and Phototransduction: A Model System for G Protein-Linked Receptors. *FASEB J.* **1992**, *6*, 2323-2331.

153. Shapiro, D. A.; Kristiansen, K.; Weiner, D. M.; Kroeze, W. K.; Roth, B. L. Evidence for a Model of Agonist-Induced Activation of 5-HT_{2A} Serotonin Receptors which Involves the Disruption of a Strong Ionic Interaction Between Helices 3 and 6. *J. Biol. Chem.* **2002**, *277*, 11441-11449.

154. Cohen, G. B.; Yang, T.; Robinson, P. R.; Oprian, D. D. Constitutive Activation of Opsin: Influence of Charge at Position 134 and Size at Position 296. *Biochemistry* **1993**, *32*, 6111-6115.

155. Okada, T.; Ernst, O. P.; Palczewski, K.; Hofmann, K. P. Activation of Rhodopsin: New Insights from Structural and Biochemical Studies. *Trends Biochem. Sci.* **2001**, *26*, 318-324.

156. Sealfon, S. C.; Chi, L.; Ebersole, B. J.; Rodic, V.; Zhang, D.; Ballesteros, J. A.; Weinstein, H. Related Contribution of Specific Helix 2 and 7 Residues to Conformational Activation of the Serotonin 5-HT_{2A} Receptor. *J. Biol. Chem.* **1995**, *270*, 16683-16688.

157. Chung, F. Z.; Wang, C. D.; Potter, P. C.; Venter, J. C.; Fraser, C. M. Site-Directed Mutagenesis and Continuous Expression of Human Beta- Adrenergic Receptors. Identification of a Conserved Aspartate Residue Involved in Agonist Binding and Receptor Activation. *J. Biol. Chem.* **1988**, *263*, 4052-4055.

158. Fraser, C. M.; Wang, C. D.; Robinson, D. A.; Gocayne, J. D.; Venter, J. C. Site-Directed Mutagenesis of M1 Muscarinic Acetylcholine Receptors: Conserved Aspartic Acids Play Important Roles in Receptor Function. *Mol. Pharmacol.* **1989**, *36*, 840-847.

159. Wang, C. D.; Buck, M. A.; Fraser, C. M. Site-Directed Mutagenesis of Alpha 2A-Adrenergic Receptors: Identification of Amino Acids Involved in Ligand Binding and Receptor Activation by Agonists. *Mol. Pharmacol.* **1991**, *40*, 168-179.

160. Almaula, N.; Ebersole, B. J.; Ballesteros, J. A.; Weinstein, H.; Sealfon, S. C. Contribution of A Helix 5 Locus to Selectivity of Hallucinogenic and Nonhallucinogenic Ligands for the Human 5-Hydroxytryptamine$_{2A}$ and 5-Hydroxytryptamine$_{2C}$ Receptors: Direct and Indirect Effects on Ligand Affinity Mediated by the Same Locus. *Mol. Pharmacol.* **1996**, *50*, 34-42.

161. Vauquelin, G.; Bottari, S.; Kanarek, L.; Strosberg, A. D. Evidence for Essential Disulfide Bonds in Beta1-Adrenergic Receptors of Turkey Erythrocyte Membranes. Inactivation by Dithiothreitol. *J. Biol. Chem.* **1979**, *254*, 4462-4469.

162. Moxham, C. P.; Ross, E. M.; George, S. T.; Malbon, C. C. Beta-Adrenergic Receptors Display Intramolecular Disulfide Bridges In Situ: Analysis by Immunoblotting and Functional Reconstitution. *Mol. Pharmacol.* **1988**, *33*, 486-492.

163. Henderson, R.; Baldwin, J. M.; Ceska, T. A.; Zemlin, F.; Beckmann, E.; Downing, K. H. Model for the Structure of Bacteriorhodopsin Based on High-Resolution Electron Cryo-Microscopy. *J. Mol. Biol.* **1990**, *213*, 899-929.

164. Henderson, R.; Schertler, G. F. The Structure of Bacteriorhodopsin and its Relevance to the Visual Opsins and Other Seven-Helix G-Protein Coupled Receptors. *Philos. Trans. R. Soc. Lond B Biol. Sci.* **1990**, *326*, 379-389.

165. Schertler, G. F.; Hargrave, P. A. Projection Structure of Frog Rhodopsin in Two Crystal Forms. *Proc. Natl. Acad. Sci. U. S. A* **1995**, *92*, 11578-11582.

166. Shulgin, A. T., Substituted α-Methyl-β-Phenylethylamines as Central Nervous System Stimulants. Br. Patent GB 1,147,379, **1969**.

167. Sakmar, T. P. Rhodopsin: A Prototypical G Protein-Coupled Receptor. *Prog. Nucleic Acid Res. Mol. Biol.* **1998**, *59*, 1-34.

168. Rothschild, K. J.; Cantore, W. A.; Marrero, H. Fourier Transform Infrared Difference Spectra of Intermediates in Rhodopsin Bleaching. *Science* **1983**, *219*, 1333-1335.

169. Farahbakhsh, Z. T.; Hideg, K.; Hubbell, W. L. Photoactivated Conformational Changes in Rhodopsin: A Time-Resolved Spin Label Study. *Science* **1993**, *262*, 1416-1419.

170. Resek, J. F.; Farahbakhsh, Z. T.; Hubbell, W. L.; Khorana, H. G. Formation of the Meta II Photointermediate is Accompanied by Conformational Changes in the Cytoplasmic Surface of Rhodopsin. *Biochemistry* **1993**, *32*, 12025-12032.

171. Salamon, Z.; Wang, Y.; Brown, M. F.; Macleod, H. A.; Tollin, G. Conformational Changes in Rhodopsin Probed by Surface Plasmon Resonance Spectroscopy. *Biochemistry* **1994**, *33*, 13706-13711.

172. Garcia-Quintana, D.; Francesch, A.; Garriga, P.; De Lera, A. R.; Padros, E.; Manyosa, J. Fourier Transform Infrared Spectroscopy Indicates a Major Conformational Rearrangement in the Activation of Rhodopsin. *Biophys. J.* **1995**, *69*, 1077-1082.

173. Lin, S. W.; Sakmar, T. P. Specific Tryptophan UV-Absorbance Changes are Probes of the Transition of Rhodopsin to its Active State. *Biochemistry* **1996**, *35*, 11149-11159.

174. Farrens, D. L.; Altenbach, C.; Yang, K.; Hubbell, W. L.; Khorana, H. G. Requirement of Rigid-Body Motion of Transmembrane Helices for Light Activation of Rhodopsin. *Science* **1996**, *274*, 768-770.

175. Gether, U.; Kobilka, B. K. G Protein-Coupled Receptors. II. Mechanism of Agonist Activation. *J. Biol. Chem.* **1998**, *273*, 17979-17982.

176. Moron, J.; Bisagni, E. Synthesis of 4-Methylfuro[3',2':5,6]benzo-furo[3,2-C]pyridine. *J. Heterocycl. Chem.* **1986**, *23*, 1637-1639.

177. Carr, G. E.; Chambers, R. D.; Holmes, T. F.; Parker, D. G. Sodium Perfluoroalkane Carboxylates as Sources of Perfluoroalkyl Groups. *J. Chem. Soc., Perkin Trans. I.* **1988**, *38*, 921-926.

178. Chao, Q.; Deng, L.; Shih, H.; Leoni, L. M.; Genini, D.; Carson, D. A.; Cottam, H. B. Substituted Isoquinolines and Quinazolines as Potential Antiinflammatory Agents. Synthesis and Biological Evaluation of Inhibitors of Tumor Necrosis Factor Alpha. *J. Med. Chem.* **1999**, *42*, 3860-3873.

179. Walsh, D. A.; Franzyshen, S. K.; Yanni, J. M. Synthesis and Antiallergy Activity of 4-(Diarylhydroxymethyl)-1-[3-(aryloxy)propyl]piperidines and Structurally Related Compounds. *J. Med. Chem.* **1989**, *32*, 105-118.

180. Pocci, M.; Bertini, V.; Demunno, A.; Alfei, S.; Alfei, S. Unexpected Behavior of the Methoxymethoxy Group in the Metalation/Formylation Reactions of 3-Methoxymethoxyanisole. *Tetrahedron Lett.* **2001**, *42*, 1351-1354.

181. Curran, D. P.; Xu, J. *O*-Bromo-*P*-Methoxyphenyl Ethers. Protecting/Radical Translocating (PRT) Groups that Generate Radicals from C-H Bonds β to Oxygen Atoms. *J. Am. Chem. Soc.* **1996**, *118*, 3142-3147.

182. Sunitha, K.; Balabubramanian, K. K. A Reinvestigation of the Claisen Rearrangement of Methyl γ-Aryloxycrotonates. A Convenient Synthesis of 3-Ethylidenebenzofuran-2(3H)-ones. *Tetrahedron* **1987**, *43*, 3269-3278.

183. Abraham, D. J.; Kennedy, P. E.; Mehanna, A. S.; Patwa, D. C.; Williams, F. L. Design, Synthesis, and Testing of Potential Antisickling Agents. 4. Structure-Activity Relationships of Benzyloxy and Phenoxy Acids. *J. Med. Chem.* **1984**, *27*, 967-978.

184. Barnett, C. J.; Wilson, T. M.; Wendel, S. R.; Winningham, M. J.; Deeter, J. B. Asymmetric Synthesis of Lometrexol ((6*R*)-5,10-Dideaza-5,6,7,8-tetrahydrofolic Acid). *J. Org. Chem.* **1994**, *59*, 7038-7045.

185. Horaguchi, S.; Mamoru, H.; Suzuki, T. Furan Derivatives. IV. On the Effects of Substituents in the Synthesis of 4,5-Dihydro-3H-naphtho[1,8-*Bc*]furans. *Bull. Chem. Soc. Jpn.* **1982**, *55*, 865-869.

186. Flaugh, M. E.; Mullen, D. L.; Fuller, R. W.; Mason, N. R. 6-Substituted 1,3,4,5-Tetrahydrobenz[cd]indol-4-amines: Potent Serotonin Agonists. *J. Med. Chem.* **1988**, *31*, 1746-1753.

187. Groutas, W. C.; Felkner, D. Synthetic Applications of Cyanotrimethylsilane, Iodotrimethylsilane, Azidotrimethylsilane, and Methylthiotrimethylsilane. *Synthesis* **1980**, *11*, 861-868.

188. Debernardis, J. F.; Kyncl, J. J.; Basha, F. Z.; Arendsen, D. L.; Martin, Y. C.; Winn, M.; Kerkman, D. J. Conformationally Defined Adrenergic Agents. 2. Catechol Imidazoline Derivatives: Biological Effects at Alpha 1 and Alpha 2 Adrenergic Receptors. *J. Med. Chem.* **1986**, *29*, 463-467.

189. Leanna, M. R.; Martinelli, M. J.; Varie, D. L.; Kress, T. J. Diasteroselectivity in Ergoline Synthesis: A Face Selective Epoxidation. *Tetrahedron Lett.* **1989**, *30*, 3935-3938.

190. Haefliger, W. V.; Klöppner, E. Stereospezifische Synthese Einer Neuen Morphin-Teilstruktur. *Helv. Chim. Acta* **1982**, *65*, 1837-1852.

191. Thompson, H. W. Stereochemical Control of Reductions. The Directive Effect of Carbomethoxy vs. Hydroxymethyl Groups in Catalytic Hydrogenation. *J. Org. Chem.* **1971**, *36*, 2577-2581.

192. Thompson, H. W.; McPherson, E.; Lences, B. L. Stereochemical Control of Reductions. 5. Effects of Electron Density and Solvent on Group Haptophilicity. *J. Org. Chem.* **1976**, *41*, 2903-2906.

193. Ranade, V. S.; Consiglio, G.; Prins, R. Functional-Group-Directed Diastereoselective Hydrogenation of Aromatic Compounds. *J. Org. Chem.* **2000**, *65*, 1132-1138.

194. Nichols, D. E.; Snyder, S. E.; Oberlender, R.; Johnson, M. P.; Huang, X. M. 2,3-Dihydrobenzofuran Analogues of Hallucinogenic Phenethylamines. *J. Med. Chem.* **1991**, *34*, 276-281.

195. Berg, K. A.; Clarke, W. P.; Sailstad, C.; Saltzman, A.; Maayani, S. Signal Transduction Differences between 5-Hydroxytryptamine Type 2A And Type 2C Receptor Systems. *Mol. Pharmacol.* **1994**, *46*, 477-484.

196. Colpaert, F. C.; Niemegeers, C. J.; Janssen, P. A. A Drug Discrimination Analysis of Lysergic Acid Diethylamide (LSD): In Vivo Agonist and Antagonist Effects of Purported 5-Hydroxytryptamine Antagonists and of Pirenperone, A LSD-Antagonist. *J. Pharmacol. Exp. Ther.* **1982**, *221*, 206-214.

197. Appel, J. B.; Cunningham, K. A. The Use of Drug Discrimination Procedures to Characterize Hallucinogenic Drug Actions. *Psychopharmacol. Bull.* **1986**, *22*, 959-967.

198. Oberlender, R.; Nichols, D. E. Drug Discrimination Studies with MDMA and Amphetamine. *Psychopharmacology (Berl)* **1988**, *95*, 71-76.

199. Monte, A. P.; Waldman, S. R.; Marona-Lewicka, D.; Wainscott, D.B.; Nelson, D. L.; Sanders-Bush, E.; Nichols, D. E. Dihydrobenzofuran Analogues of Hallucinogens. 4. Mescaline Derivatives. *J. Med. Chem.* **1997**, *40*, 2997-3008.

200. Elamrani, S.; Berry, M. B.; Phillips, G. N., Jr.; McCammon, J. A. Study of Global Motions in Proteins by Weighted Masses Molecular Dynamics: Adenylate Kinase as a Test Case. *Proteins* **1996**, *25*, 79-88.

201. Borhan, B.; Souto, M. L.; Imai, H.; Shichida, Y.; Nakanishi, K. Movement of Retinal Along the Visual Transduction Path. *Science* **2000**, *288*, 2209-2212.

202. Nichols, D. E. Potential Psychotomimetics: Bromomethoxyamphetamines and Structural Congeners of Lysergic Acid. Ph.D., University of Iowa, Iowa City, Iowa USA, **1973**.

203. Oberlender, R.; Ramachandran, P. V.; Johnson, M. P.; Huang, X. M.; Nichols, D. E. Effect of a Chiral 4-Alkyl Substituent in Hallucinogenic Amphetamines. *J. Med. Chem.* **1995**, *38*, 3593-3601.

204. Tsuda, M.; Touhara, H.; Nakanishi, K.; Kitaura, K.; Morokuma, K. Calometric and Molecular Orbital Studies of Hydrogen Bonding between Hydrogen Flouride and Cyclic Ethers. *J. Am. Chem. Soc.* **1978**, *100*, 7189-7196.

205. Ho, B. Y.; Karschin, A.; Branchek, T.; Davidson, N.; Lester, H. A. The Role of Conserved Aspartate and Serine Residues in Ligand Binding and in Function of the 5-HT_{1A} Receptor: A Site-Directed Mutation Study. *FEBS Lett.* **1992**, *312*, 259-262.

206. Nelson, D. L.; Lucaites, V. L.; Audia, J. E.; Nissen, J. S.; Wainscott, D. B. Species Differences in the Pharmacology of the 5-Hydroxytryptamine$_2$ Receptor: Structurally Specific Differentiation by Ergolines and Tryptamines. *J. Pharmacol. Exp. Ther.* **1993**, *265*, 1272-1279.

207. Johnson, M. P.; Audia, J. E.; Nissen, J. S.; Nelson, D. L. N(1)-Substituted Ergolines and Tryptamines Show Species Differences for the Agonist-Labeled 5-HT_2 Receptor. *Eur. J. Pharmacol.* **1993**, *239*, 111-118.

208. Gerasimov, M.; Marona-Lewicka, D.; Kurrasch-Orbaugh, D. M.; Qandil, A. M.; Nichols, D. E. Further Studies on Oxygenated Tryptamines with LSD-Like Activity Incorporating a Chiral Pyrrolidine Moiety into the Side Chain. *J. Med. Chem.* **1999**, *42*, 4257-4263.

209. Shih, J. C.; Chen, K.; Gallaher, T. K. Structure and Function of Serotonin 5-HT_2 Receptors. *NIDA Res. Monogr* **1994**, *146*, 284-297.

210. Nichols, D. E.; Woodard, R.; Hathaway, B. A.; Lowy, M. T.; Yom, K. W. Resolution and Absolute Configuration of Trans-2-(2,5-Dimethoxy-4-methylphenyl)cyclopropylamine, A Potent Hallucinogen Analogue. *J. Med. Chem.* **1979**, *22*, 458-460.

211. Domelsmith, L. N.; Eaton, T. A.; Houk, K. N.; Anderson, G. M., III; Glennon, R. A.; Shulgin, A. T.; Castagnoli, N., Jr.; Kollman, P. A. Photoelectron Spectra of Psychotropic Drugs. 6. Relationships between the Physical Properties and Pharmacological Actions of Amphetamine Analogues. *J. Med. Chem.* **1981**, *24*, 1414-1421.

212. Julius, D.; Huang, K. N.; Livelli, T. J.; Axel, R.; Jessell, T. M. The $5HT_2$ Receptor Defines a Family of Structurally Distinct but Functionally Conserved Serotonin Receptors. *Proc. Natl. Acad. Sci. U. S. A.* **1990**, *87*, 928-932.

213. Brooks, B. R.; Bruccoleri.R.E.; Olafson, B. D.; States, D. J.; Swaminathan, S.; Karplus, M., CHARMM: A Program for Macromolecular Energy, Minimization, and Dynamics Calculations. *J.Comp.Chem.* **1983,** *4*, 187-217.

214. Higgins, D. G.; Thompson, J. D.; Gibson, T. J. Using CLUSTAL for Multiple Sequence Alignments. *Methods Enzymol.* **1996**, *266*, 383-402.

215. Sali, A.; Blundell, T. L. Comparative Protein Modeling By Satisfaction of Spatial Restraints. *J. Mol. Biol.* **1993**, *234*, 779-815.

216. *Sybyl*, 6.6; Tripos Inc.: 1699 South Hanley Rd., St. Louis, Missouri, 63144, USA, **2001**.

217. Kuntz, I. D.; Blaney, J. M.; Oatley, S. J.; Langridge, R.; Ferrin, T. E. A Geometric Approach to Macromolecule-Ligand Interactions. *J. Mol. Biol.* **1982**, *161*, 269-288.

218. *Spartan*, 5.0; Wavefunction, Inc.: 18401 Von Karman Ave., Ste. 370, Irvine, California, 92612, USA, **2001**.

219. Richards, F. M. Areas, Volumes, Packing and Protein Structure. *Annu. Rev. Biophys. Bioeng.* **1977**, *6*, 151-176.

220. McArdle, P. C. *ABSEN* - A PC Computer Program for Listing Systematic Absences and Space-Group Determination. *J. Appl. Cryst.* **1996**, *29*, 306.

221. Otwinowski, Z.; Minor, W. Processing of X-Ray Diffraction Data Collected in Oscillation Mode. *Methods Enzymol.* **1997**, *276*, 307-326.

222. *SHELXL97*; A Program for Crystal Structure Refinement; Sheldrick, G. M.; Univ. of Gottingen, Germany **1997**.

223. Altomare, A.; Burla, M. C.; Camalli, M.; Cascarano, C.; Giacovazzo, A.; Guagliardi, A. G. G.; Moliterni, G.; Polidori, G.; Spagna, R. Sir97: A New Tool for Crystal Structure Determination and Refinement. *J. Appl. Cryst.* **1999**, *32*, 115-119.

224. International Tables for Crystallography. Kluwer Academic Publishers, Utrecht, The Netherlands, **1992**.

225. Flack, H. D. On Enantiomorph-Polarity Estimation. *Acta Cryst.* **1983**, *A39*, 876-881.

226. *ORTEPII*; Johnson, C. K.; Oak Ridge National Laboratory, Tennessee, USA., **1976**.

227. *PLUTON*; A Molecular Graphics Program; Spek, A. L.; Univ. of Ultrecht, The Netherlands, **1991**.

APPENDICES

Appendix A – Multiple Sequence Alignment

Generated using ClustalW[214] with the PAM250 scoring matrix, a gap penalty of 12 and an extension penalty of 4.

```
        Bovine Rhodopsin          WQFSMLAAYMFLLIMLGFPINFLTLYVTVQHK
        Human 5-HT1A              -YQVITSLLLGTLIFCAVLGNACVVAAIALER
        Human 5-HT1B              -WKVLLVMLLALITLATTLSNAFVIATVYRTR
        Human 5-HT1D              -LKISLAVVLSVITLATVLSNAFVLTTILLTR
        Human 5-HT1E              -EKMLICMTLVVITTLTTLLNLAVIMAIGTTK
        Human 5-HT1F              -SKILVSLTLSGLALMTTTINSLVIAAIIVTR
        Human 5-HT2A              QEKNWSALLTAVVIILTIAGNILVIMAVSLEK
        Rat   5-HT2A              QEKNWSALLTTVVIILTIAGNILVIMAVSLEK
        Human 5-HT2B              -KLHWAALLILMVIIPTIGGNTLVILAVSLEK
        Human 5-HT2C              -VQNWPALSIVIIIIMTIGGNILVIMAVSMEK
        Rat   5-HT2C              -VQNWPALSIVVIIIMTIGGNILVIMAVSMEK
TM1     Human 5-HT5A              ---VLILTLLGFLVAATFAWNLLVLATILRVR
        Human 5-HT6               ----WVAAALCVVIALTAAANSLLIALICTQP
        Human 5-HT7               VEKVVIGSILTLITLLTIAGNCLVVISVCFVK
        Human D1                  ---ILTACFLSLLILSTLLGNTLVCAAVIRFR
        Human D2                  -NYYATLL--TLLIAVIVFGNVLVCMAVSREK
        Human D3                  -AYYALSY--CALILAIVFGNGLVCMAVLKER
        Human D4                  -QGAAALVGGVLLIGAVLAGNSLVCVSVATER
        Human D5                  -SQVVTACLLTLLIIWTLLGNVLVCAAIVRSR
        Human H1                  -QLMPLVVVLSTICLVTVGLNLLVLYAVRSER
        Human H2                  ---ITITVVLAVLILITVAGNVVVCLAVGLNR
        Human H3                  ---AVLAALMALLIVATVLGNALVMLAFVADS
        Human H4                  ---VTLAFFMSLVAFAIMLGNALVILAFVVDK

        Bovine Rhodopsin          TPLNYILLNLAVADLFMVFGGFTTTLYTSLH
        Human 5-HT1A              NVANYLIGSLAVTDLMVSVLVLPMAALYQVL
        Human 5-HT1B              TPANYLIASLAVTDLLVSILVMPISTMYTVT
        Human 5-HT1D              TPANYLIGSLATTDLLVSILVMPISIAYTIT
        Human 5-HT1E              QPANYLICSLAVTDLLVAVLVMPLSIIYIVM
        Human 5-HT1F              HPANYLICSLAVTDFLVAVLVMPFSIVYIVR
        Human 5-HT2A              NATNYFLMSLAIADMLLGFLVMPVSMLTILY
        Rat   5-HT2A              NATNYFLMSLAIADMLLGFLVMPVSMLTILY
        Human 5-HT2B              YATNYFLMSLAVADLLVGLFVMPIALLTIMF
        Human 5-HT2C              NATNYFLMSLAIADMLVGLLVMPLSLLAILY
        Rat   5-HT2C              NATNYFLMSLAIADMLVGLLVMPLSLLAILY
TM2     Human 5-HT5A              RVPHNLVASMAVSDVLVAALVMPLSLVHELS
        Human 5-HT6               NTSNFFLVSLFTSDLMVGLVVMPPAMLNALY
        Human 5-HT7               QPSNYLIVSLALADLSVAVAVMPFVSVTDLI
        Human D1                  KVTNFFVISLAVSDLLVAVLVMPWKAVAEIA
        Human D2                  TTTNYLIVSLAVADLLVATLVMPWVVYLEVV
        Human D3                  TTTNYLVVSLAVADLLVATLVMPWVVYLEVT
        Human D4                  TPTNSFIVSLAAADLLLALLVLPLFVYSEVQ
        Human D5                  NMTNVFIVSLAVSDLFVALLVMPWKAVAEVA
        Human H1                  TVGNLYIVSLSVADLIVGAVVMPMNILYLLM
        Human H2                  NLTNCFIVSLAITDLLLGLLVLPFSAIYQLS
        Human H3                  TQNNFFLLNLAISDFLVGAFCIPLYVPYVLT
        Human H4                  HRSSYFFLNLAISDFFVGVISIPLYIPHTLF
```

	Bovine Rhodopsin	TGCNLEGFFATLGGEIALWSLVVLAIERYVVVC
	Human 5-HT_{1A}	VTCDLFIALDVLCCTSSILHLCAIALDRYWAIT
	Human 5-HT_{1B}	VVCDFWLSSDITCCTASILHLCVIALDRYWAIT
	Human 5-HT_{1D}	ILCDIWLSSDITCCTASILHLCVIALDRYWAIT
	Human 5-HT_{1E}	FLCEVWLSVDMTCCTCSILHLCVIALDRYWAIT
	Human 5-HT_{1F}	VVCDIWLSVDITCCTCSILHLSAIALDRYRAIT
	Human 5-HT_{2A}	KLCAVWIYLDVLFSTASIMHLCAISLDRYVAIQ
	Rat 5-HT_{2A}	KLCAIWIYLDVLFSTASIMHLCAISLDRYVAIQ
	Human 5-HT_{2B}	VLCPAWLFLDVLFSTASIMHLCAISVDRYIAIK
	Human 5-HT_{2C}	YLCPVWISLDVLFSTASIMHLCAISLDRYVAIR
	Rat 5-HT_{2C}	YLCPVWISLDVLFSTASIMHLCAISLDRYVAIR
TM3	Human 5-HT_{5A}	RLCQLWIACDVLCCTASIWNVTAIALDRYWSIT
	Human 5-HT_{6}	GLCLLWTAFDVMCCSASILNLCLISLDRYLLIL
	Human 5-HT_{7}	FFCNVFIAMDVMCCTASIMTLCVISIDRYLGIT
	Human D_1	SFCNIWVAFDIMCSTASILNLCVISVDRYWAIS
	Human D_2	IHCDIFVTLDVMMCTASILNLCAISIDRYTAVA
	Human D_3	ICCDVFVTLDVMMCTASILNLCAISIDRYTAVV
	Human D_4	RLCDALMAMDVMLCTASIFNLCAISVDRFVAVA
	Human D_5	AFCDVWVAFDIMCSTASILNLCVISVDRYWAIS
	Human H_1	PLCLFWLSMDYVASTASIFSVFILCIDRYRSVQ
	Human H_2	VFCNIYTSLDVMLCTASILNLFMISLDRYCAVM
	Human H_3	GLCKLWLVVDYLLCTSSAFNIVLISYDRFLSVT
	Human H_4	EICVFWLTTDYLLCTASVYNIVLISYDRYLSVS

	Bovine Rhodopsin	ENH-AIMGVAFTWVMALACAAPP-LVGWSRY
	Human 5-HT_{1A}	TPRRAAALISLTWLIGFLISIPP-MLGWRTP
	Human 5-HT_{1B}	TPKRAAVMIALVWVFSISISLPP-FF-WRQA
	Human 5-HT_{1D}	TAGHAATMIAIVWAISICISIPP-LF-WRQA
	Human 5-HT_{1E}	TAKRAALMILTVWTISIFISMPP-LF-WRSH
	Human 5-HT_{1F}	TPKHAGIMITIVWIISVFISMPP-LF-WRHQ
	Human 5-HT_{2A}	SRTKAFLKIIAVWTISVGISMPIPVFGLQDD
	Rat 5-HT_{2A}	SRTKAFLKIIAVWTISVGISMPIPVFGLQDD
	Human 5-HT_{2B}	SRATAFIKITVVWLISIGIAIPVPIKGIETD
	Human 5-HT_{2C}	SRTKAIMKIAIVWAISIGVSVPIPVIGLRDE
	Rat 5-HT_{2C}	SRTKAIMKIAIVWAISIGVSVPIPVIGLRDE
TM4	Human 5-HT_{5A}	RKCVSNVMIALTWALSAVISLAPLLFGWGET
	Human 5-HT_{6}	TPLRALALVLGAWSLAALASFLPLLLGWHEL
	Human 5-HT_{7}	NGKCMAKMILSVWLLSASITLPP-LFGWAQN
	Human D_1	TPKAAFILISVAWTLSVLISFIPVQLSWHKA
	Human D_2	SKRRVTVMISIVWVLSFTISCPL-LFGLNN-
	Human D_3	SCRRVALMITAVWVLAFAVSCPL-LFGFNTT
	Human D_4	GSRRQLLLIGATWLLSAAVAAPV-LCGLNDV
	Human D_5	TQRMALVMVGLAWTLSILISFIPVQLNWHRD
	Human H_1	TKTRASATILGAWFLSFLWVIPI-LG-WNHF
	Human H_2	TPVRVAISLVLIWVISITLSFLSIHLGWNSR
	Human H_3	DTRRAVRKMLLVWVLAFLLYGPAILSWEYLS
	Human H_4	GVLKIVTLMVVVWVLAFLVNGPMILVSESWK

	Bovine Rhodopsin	SFVIYMFVVHFIIPLIVIFFCYGQLV
	Human 5-HT_{1A}	-YTIYSTFGAFYIPLLLMLVLYGRIF
	Human 5-HT_{1B}	-YTVYSTVGAFYFPTLLLIALYGRIY
	Human 5-HT_{1D}	-YTIYSTCGAFYIPSVLLIILYGRIY
	Human 5-HT_{1E}	-YTIYSTLGAFYIPLTLILILYYRIY
	Human 5-HT_{1F}	-STIYSTFGAFYIPLALILILYYKIY
	Human 5-HT_{2A}	NFVLIGSFVSFFIPLTIMVITYFLTI
	Rat 5-HT_{2A}	NFVLIGSFVAFFIPLTIMVITYFLTI
	Human 5-HT_{2B}	DFMLFGSLAAFFTPLAIMIVTYFLTI
	Human 5-HT_{2C}	NFVLIGSFVAFFIPLTIMVITYCLTI
	Rat 5-HT_{2C}	NFVLIGSFVAFFIPLTIMVITYFLTI
TM5	Human 5-HT_{5A}	-YAVFSTVGAFYLPLCVVLFVYWKIY
	Human 5-HT_{6}	-FVLVASGLTFFLPSGAICFTYCRIL
	Human 5-HT_{7}	-YTIYSTAVAFYIPMSVMLFMYYQIY
	Human D_1	-YAISSSVISFYIPVAIMIVTYTRIY
	Human D_2	-FVVYSSIVSFYVPFIVTLLVYIKIY
	Human D_3	-FVIYSSVVSFYLPFGVTVLVYARIY
	Human D_4	-YVVYSSVCSFFLPCPLMLLLYWATF
	Human D_5	-YAISSSLISFYIPVAIMIVTYTRIY
	Human H_1	WFKVMTAIINFYLPTLLMLWFYAKIY
	Human H_2	-YGLVDGLVTFYLPLLIMCITYYRIF
	Human H_3	YFLITASTLEFFTPFLSVTFFNLSIY
	Human H_4	YILAITSFLEFVIPVILVAYFNMNIY

	Bovine Rhodopsin	A-EKEVTR---MVIIMVIAFLICWLPYAGVAFYIFTH
	Human 5-HT_{1A}	ARERKTVK---TLGIIMGTFILCWLPFFIVALVLP-F
	Human 5-HT_{1B}	ARERKATK---TLGIILGAFIVCWLPFFIISLVMP-I
	Human 5-HT_{1D}	ARERKATK---ILGIILGAFIICWLPFFVVSLVLP-I
	Human 5-HT_{1E}	TRERKAAR---ILGLILGAFILSWLPFFIKELIVG-L
	Human 5-HT_{1F}	TRERKAAT---TLGLILGAFVICWLPFFVKELVVN-V
	Human 5-HT_{2A}	SNEQKACK---VLGIVFFLFVVMWCPFFITNIMAV-I
	Rat 5-HT_{2A}	SNEQKACK---VLGIVFFLFVVMWCPFFITNIMAV-I
	Human 5-HT_{2B}	SNEQRASK---VLGIVFFLFLLMWCPFFITNITLV-L
	Human 5-HT_{2C}	NNERKASK---VLGIVFFVFLIMWCPFFITNILSV-L
	Rat 5-HT_{2C}	NNEKKASK---VLGIVFFVFLIMWCPFFITNILSV-L
TM6	Human 5-HT_{5A}	K-EQRAAL---MVGILIGVFVLCWIPFFLTELISP-L
	Human 5-HT_{6}	KHSRKALKASLTLGILLGMFFVTWLPFFVANIVQA-V
	Human 5-HT_{7}	KREQKAAT---TLGIIVGAFTVCWLPFFLLSTARPFI
	Human D_1	KRETKVLK---TLSVIMGVFVCCWLPFFILNCILP-F
	Human D_2	QKEKKATQ---MLAIVLGVFIICWLPFFITHILNI-H
	Human D_3	LREKKATQ---MVAIVLGAFIVCWLPFFLTHVLNT-H
	Human D_4	GRERKAMR---VLPVVVGAFLLCWTPFFVVHITQA-L
	Human D_5	KKETKVLK---TLSVIMGVFVCCWLPFFILNCMVP-F
	Human H_1	NRERKAAK---QLGFIMAAFILCWIPYFIFFMVIA-F
	Human H_2	IREHKATV---TLAAVMGAFIICWFPYFTAFVYRG-L
	Human H_3	SRDRKVAK---SLAVIVSIFGLCWAPYTLLMIIRAAC
	Human H_4	LRARRLAK---SLAILLGVFAVCWAPYSLFTIVLSFY

	Bovine Rhodopsin	IFMT-IPAFFAKTSAVYNPVIYIMMNKQFRNCMVTTLC
	Human 5-HT_{1A}	LLGA-IINWLGYSNSLLNPVIYAYFNKDFQNAFKKIIK
	Human 5-HT_{1B}	AIFD-FFTWLGYLNSLINPIIYTMSNEDFKQAFHKLIR
	Human 5-HT_{1D}	ALFD-FFTWLGYLNSLINPIIYTVFNEEFRQAFQKIVP
	Human 5-HT_{1E}	EVAD-FLTWLGYVNSLINPLLYTSFNEDFKLAFKKLIR
	Human 5-HT_{1F}	EMSN-FLAWLGYLNSLINPLIYTIFNEDFKKAFQKLVR
	Human 5-HT_{2A}	ALLN-VFVWIGYLSSAVNPLVYTLFNKTYRSAFSRYIQ
	Rat 5-HT_{2A}	ALLN-VFVWIGYLSSAVNPLVYTLFNKTYRSAFSRYIQ
	Human 5-HT_{2B}	MLLE-IFVWIGYVSSGVNPLVYTLFNKTFRDAFGRYIT
	Human 5-HT_{2C}	KLLN-VFVWIGYVCSGINPLVYTLFNKIYRRAFSNYLR
	Rat 5-HT_{2C}	KLLN-VFVWIGYVCSGINPLVYTLFNKIYRRAFSKYLR
TM7	Human 5-HT_{5A}	IWKS-IFLWLGYSNSFFNPLIYTAFNKNYNSAFKNFFS
	Human 5-HT_{6}	GLFD-VLTWLGYCNSTMNPIIYPLFMRDFKRALGRFLP
	Human 5-HT_{7}	LWVERTFLWLGYANSLINPFIYAFFNRDLRTTYRSLLQ
	Human D_1	NTFD-VFVWFGWANSSLNPIIY-AFNADFRKAFSTLLG
	Human D_2	VLYS-AFTWLGYVNSAVNPIIYTTFNIEFRKAFLKILH
	Human D_3	ELYS-ATTWLGYVNSALNPVIYTTFNIEFRKAFLKILS
	Human D_4	RLVS-AVTWLGYVNSALNPVIYTVFNAEFRNVFRKALR
	Human D_5	TTFD-VFVWFGWANSSLNPVIY-AFNADFQKVFAQLLG
	Human H_1	HLHM-FTIWLGYINSTLNPLIYPLCNENFKKTFKRILH
	Human H_2	VLEA-IVLWLGYANSALNPILYAALNRDFRTGYQQLF-
	Human H_3	DYWYETSFWLLWANSAVNPVLYPLCHHSFRRAFTKLLC
	Human H_4	SVWYRIAFWLQWFNSFVNPLLYPLCHKRFQKAFLKIFC

Appendix B – Percent Similarity Chart

Table 6. Percent similarity, ClustalW (PAM250 scoring matrix).[214]

	1 Bovine rhodopsin	2 Human 5-HT$_{1A}$	3 Human 5-HT$_{1B}$	4 Human 5-HT$_{1D}$	5 Human 5-HT$_{1E}$	6 Human 5-HT$_{1F}$	7 Human 5-HT$_{2A}$	8 Rat 5-HT$_{2A}$	9 Human 5-HT$_{2B}$	10 Human 5-HT$_{2C}$	11 Rat 5-HT$_{2C}$	12 Human 5-HT$_{5A}$	13 Human 5-HT$_{6}$	14 Human 5-HT$_{7}$	15 Human D$_1$	16 Human D$_2$	17 Human D$_3$	18 Human D$_4$	19 Human D$_5$	20 Human H$_1$	21 Human H$_2$	22 Human H$_3$	23 Human H$_4$
1		16	18	16	15	14	15	14	15	16	16	18	17	20	14	18	18	17	16	16	15	18	17
2			37	39	39	37	23	23	23	23	24	31	22	29	30	28	30	27	30	26	31	24	22
3				59	45	46	24	24	23	25	25	33	26	30	30	29	28	23	28	28	27	25	20
4					46	45	25	26	25	27	28	31	27	33	31	32	31	26	30	31	29	23	21
5						55	30	30	25	29	29	31	26	33	28	29	28	26	28	30	27	20	22
6							27	27	24	28	28	31	25	33	33	32	30	25	30	29	29	18	21
7								91	39	46	48	24	23	21	20	24	26	22	20	17	24	17	20
8									39	48	48	24	23	21	20	25	25	22	20	17	25	17	19
9										38	40	22	22	18	24	24	23	22	20	18	24	16	18
10											89	26	23	21	19	25	26	22	20	19	25	18	18
11												25	23	21	20	25	26	22	19	19	25	17	19
12													26	31	28	31	26	28	25	25	22	22	20
13														24	27	22	25	23	23	21	30	20	18
14															26	26	27	21	24	19	30	18	17
15																25	26	20	54	18	32	19	19
16																	52	33	25	24	29	21	22
17																		37	27	27	27	24	22
18																			22	20	26	25	17
19																				17	30	20	19
20																					27	23	22
21																						21	19
22																							40
23																							

Numbering of Y-axis is identical to X-axis.

Appendix C – X-Ray Structure Data

X-ray crystallography of (±)-*syn*-(6-methoxy-2a,3,4,5-tetrahydro-2H-naphtho-[1,8-*bc*]furan-5-yl)aminomethane hydrochloride ((±)-9). A colorless plate of $C_{13}H_{18}ClNO_2$ having approximate dimensions of 0.47 × 0.45 × 0.30 mm was mounted on a glass fiber in a random orientation. Preliminary examination and data collection were performed with Mo K_α radiation (λ = 0.71073 Å) on a Nonius KappaCCD. Cell constants and an orientation matrix for data collection were obtained from least-squares refinement, using the setting angles of 8730 reflections in the range $5 < \theta < 27°$. The triclinic cell parameters and calculated volume are: a = 31.227(0), b = 5.477(0), c = 7.618(1) Å, V = 1302.9(3) Å^3. For Z = 4 and F.W. = 255.75 the calculated density is 1.30 g/cm^3. The refined mosaicity from DENZO/SCALEPACK was 0.41° indicating good crystal quality. The space group was determined by the program ABSEN.[220] From the systematic presences of:

$$h\,01\ h = 2n$$

$$0kl\ k + 1 = 2n$$

and from least-squares refinement, the space group was determined to be $Pna2_1$(#33). The data were collected at a temperature of 150 ± 1 K. Data were collected to a maximum 2θ of 55.0°.

A total of 8730 reflections were collected, of which 2906 were unique. Lorentz and polarization corrections were applied to the data. The linear absorption coefficient is 2.8/cm for Mo K_α radiation. An empirical absorption correction using SCALEPACK[221]

was applied. Transmission coefficients ranged from 0.771 to 0.919 with an average value of 0.883. A secondary extension correction was applied.[222] The final coefficient, refined in least-squares, was 0.0560000 (in absolute units). Intensities of equivalent reflections were averaged. The agreement factor for the averaging was 4.5% based on intensity.

The structure was solved by direct methods using SIR97.[223] The remaining atoms were located in succeeding difference Fourier syntheses. Hydrogen atoms were included in the refinement but restrained to ride on the atom to which they are bonded. The structure was refined in full-matrix least-squares where the function minimized was $\Sigma w(|Fo|^2-|Fc|^2)^2$ and the weight w is defined as $1/[\sigma^2(Fo^2)+(0.0423P)^2+0.3126P]$ where $P = (Fo^2+2Fc^2)/3$.

Scattering factors were taken from the "International Tables for Crystallography."[224] 2718 reflections were used in the refinements. However, only reflections with $F_o^2>2\sigma(F_o^2)$ were used in calculating R. The final cycle of refinement included 168 variable parameters and converged (largest parameter shift was 0.00 times its esd) with unweighted and weighted agreement factors of:

$R1 = \Sigma|Fo-Fc|/\Sigma Fo = 0.035$

$R2 = SQRT(\Sigma w(Fo^2-Fc^2)^2/\Sigma w(Fo^2)^2) = 0.083$

The standard deviation of an observation of unit weight was 1.06. The highest peak in the final difference Fourier had a height of 0.25 e/A^3. The minimum negative peak had a height of -0.40 e/A^3. The factor for the determination of the absolute structure[225] refined to 0.37.

Refinement was performed on a AlphaServer 2100 using SHELXL97.[222] Crystallographic drawings were done using programs ORTEP[226] and PLUTON.[227]

X-ray crystallography of (±)-*anti*-(8-bromo-6-methoxy-2a,3,4,5-tetrahydro-2H-naphtho[1,8-*bc*]furan-5-yl)aminomethane *p*-toluenesulfonate ((±)-13). A colorless needle of $C_{20}H_{24}BrNO_5S$ having approximate dimensions of 0.43 × 0.15 × 0.06 mm was mounted on a glass fiber in a random orientation. Preliminary examination and data collection were performed with Mo K_α radiation (λ = 0.71073 Å) on a Nonius KappaCCD. Cell constants and an orientation matrix for data collection were obtained from least-squares refinement, using the setting angles of 25045 reflections in the range $2 < \theta < 24°$. The triclinic cell parameters and calculated volume are: a = 12.3325(4), b = 14.9439(6), c = 18.3514(10) Å, α = 89.551(2), β = 74.271(2), γ = 72.695(3)°, V = 3098.3(3) Å^3. For Z = 6 and F.W. = 470.39 the calculated density is 1.51 g/cm^3. The refined mosaicity from DENZO/SCALEPACK was 0.79° indicating moderate crystal quality. The space group was determined by the program ABSEN.[220] There were no systematic absences; the space group was determined to be P1(#2). The data were collected at a temperature of 150 ± 1 K. Data were collected to a maximum 2θ of 49.5°.

A total of 25045 reflections were collected, of which 10481 were unique. Lorentz and polarization corrections were applied to the data. The linear absorption coefficient is 21.0/cm for Mo K_α radiation. An empirical absorption correction using SCALEPACK[221] was applied. Transmission coefficients ranged from 0.528 to 0.876 with an average value of 0.740. Intensities of equivalent reflections were averaged. The agreement factor for the averaging was 8.7% based on intensity.

The structure was solved by direct methods using SIR97.[223] The remaining atoms were located in succeeding difference Fourier syntheses. Hydrogen atoms were included in the refinement but restrained to ride on the atom to which they are bonded. The

structure was refined in full-matrix least-squares where the function minimized was $\Sigma w(|Fo|^2-|Fc|^2)^2$ and the weight w is defined as $1/[\sigma^2(Fo^2)+(0.0473P)^2+0.0000P]$ where $P=(Fo^2+2Fc^2)/3$.

Scattering factors were taken from the "International Tables for Crystallography."[224] 10474 reflections were used in the refinements. However, only reflections with $F_o^2>2\sigma(F_o^2)$ were used in calculating R. The final cycle of refinement included 798 variable parameters and converged (largest parameter shift was 0.00 times its esd) with unweighted and weighted agreement factors of:

$R1 = \Sigma|Fo-Fc|/\Sigma Fo = 0.058$

$R2 = SQRT(\Sigma w(Fo^2-Fc^2)^2/\Sigma w(Fo^2)^2) = 0.114$

The standard deviation of an observation of unit weight was 1.03. The highest peak in the final difference Fourier had a height of 0.45 e/A^3. The minimum negative peak had a height of -0.93 e/A^3.

Refinement was performed on a AlphaServer 2100 using SHELXL97.[222] Crystallographic drawings were done using programs ORTEP[226] and PLUTON.[227]

Appendix D – Analytical Data

Table 7. Elemental Analysis Data.

Cpd.	Formula	Calc. %C	Calc. %H	Calc. %N	Found %C	Found %H	Found %N	Delta %C	Delta %H	Delta %N
4	$C_{13}H_{15}ClF_3NO_2$	50.41	4.88	4.52	50.16	4.68	4.59	0.25	0.20	0.07
(±)-**6**	$C_{14}H_{20}ClNO_2$	62.33	7.47	5.19	62.15	7.48	5.26	0.18	0.01	0.07
(±)-**7**	$C_{14}H_{15}NO_2$	73.34	6.59	6.11	73.65	6.43	6.19	0.31	0.16	0.08
(±)-**9**	$C_{13}H_{18}ClNO_2$	61.05	7.09	5.48	60.85	6.97	5.44	0.20	0.12	0.04
(±)-**10**	$C_{13}H_{18}ClNO_2$	61.05	7.09	5.48	60.90	6.90	5.70	0.15	0.19	0.22
(±)-**11**	$C_{15}H_{17}NO_6$	58.63	5.58	4.56	58.28	5.82	4.37	0.35	0.24	0.19
(±)-**12**	$C_{13}H_{17}BrClNO_2$	46.66	5.12	4.19	46.87	5.11	4.13	0.21	0.01	0.06
(±)-**13**	$C_{13}H_{17}BrClNO_2$	46.66	5.12	4.19	46.84	5.29	4.18	0.18	0.17	0.01
(±)-**14**	$C_{13}H_{15}BrClNO_2$	46.94	4.55	4.21	47.00	4.58	4.15	0.06	0.03	0.06
(±)-**17**	$C_{13}H_{20}ClNO_3$	57.04	7.36	5.12	56.77	7.30	5.27	0.27	0.06	0.15
19	$C_{14}H_{13}BrF_3NO_3$	44.23	3.45	3.68	44.09	3.42	3.51	0.14	0.03	0.17
20	$C_{15}H_{13}F_6NO_3$	48.79	3.55	3.79	48.75	3.69	3.72	0.04	0.14	0.07
21	$C_{15}H_9F_6NO_3$	49.33	2.48	3.84	49.26	2.54	3.69	0.07	0.06	0.15
22	$C_{13}H_{11}ClF_3NO_2$	51.07	3.63	4.58	50.67	3.61	4.66	0.40	0.02	0.08
24	$C_{11}H_{14}Cl_2O_2$	53.03	5.66		52.65	5.40		0.38	0.26	
25	$C_{11}H_{12}Br_2Cl_2O_2$	32.47	2.97		32.63	2.82		0.16	0.15	
26	$C_{11}H_{12}O_2$	74.98	6.86		74.90	6.53		0.08	0.33	
27	$C_{12}H_{12}O_3$	70.57	5.92		70.24	5.93		0.33	0.01	
28	$C_{14}H_{15}NO_4$	64.36	5.79	5.36	64.01	5.99	5.53	0.35	0.20	0.17
29	$C_{14}H_{11}NO_4$	65.37	4.31	5.44	65.30	4.40	5.16	0.07	0.09	0.28
(±)-**30**	$C_{12}H_{12}O_3$	70.57	5.92		70.42	5.98		0.15	0.06	
(±)-**31**	$C_{12}H_{14}O_4$	64.85	6.35		64.78	6.49		0.07	0.14	
35	$C_{12}H_{13}BrO_4$	47.86	4.35		47.90	4.26		0.04	0.09	
(±)-**37**	$C_{11}H_{12}O_4$	63.45	5.81		63.05	5.74		0.40	0.07	
(±)-**39**	$C_{13}H_{16}O_4$	66.09	6.83		66.13	6.92		0.04	0.09	
(±)-**40**	$C_{12}H_{14}O_4$	64.85	6.35		64.89	6.37		0.04	0.02	
(±)-**41**	$C_{11}H_{14}O_3$	68.02	7.27		67.69	7.15		0.33	0.12	
(±)-**42**	$C_{18}H_{20}O_5S$	62.05	5.79		62.08	5.91		0.03	0.12	
(±)-**43**	$C_{12}H_{13}NO_2$	70.92	6.45	6.89	70.82	6.48	6.82	0.10	0.03	0.07
(±)-**45**	$C_{13}H_{16}ClNO_2$	61.54	6.36	5.52	61.54	6.39	5.53	0.00	0.03	0.01
(±)-**48**	$C_{15}H_{15}BrF_3NO_3$	45.70	3.84	3.55	45.52	3.80	3.41	0.18	0.04	0.14
(±)-**49**	$C_{15}H_{13}BrF_3NO_3$	45.94	3.34	3.57	45.92	3.40	3.42	0.02	0.06	0.15
(±)-**50**	$C_{15}H_{16}F_3NO_3$	57.14	5.12	4.44	57.07	4.99	4.39	0.07	0.13	0.05
(±)-**51**	$C_{15}H_{14}F_3NO_3$	57.51	4.50	4.47	57.31	4.38	4.37	0.20	0.12	0.10
57	$C_{13}H_{18}ClNO_3$	57.46	6.68	5.15	57.21	6.58	5.25	0.25	0.10	0.10

Appendix E – Typical Input Files Employed for Molecular Modeling

Sample CHARMM input file for weighted masses molecular dynamics.

```
* Generate PSF and CHARMM coordinate set for trans-bovine-rhodopsin
*

bomlev -5
wrnlev 0
prnlev 5

open read file unit 21 name "$CHM_DATA/AMINOH.BIN"
read RTF file unit 21
close unit 21

open read file unit 21 name "$CHM_DATA/PARM.BIN"
read PARA file unit 21
close unit 21

open read unit 77 card name cis.rtf
read rtf card unit 77 append
close unit 77

open read formatted unit 27 name cis.psf
read psf card unit 27

open read formatted unit 27 name cis-min-none.pdb
read coor pdb  unit 27

nbond cutnb 15.0 cton 11.0 ctof 14.0 swit vswi -
rdie eps 1.0

energy

cons ic bond 500 angle 5000 impr 5000
mini sd 100 nprint 10

open unit 12 write form name dihe-heat.res
open unit 14 write unformatted name dihe-heat.cor
open unit 15 write form name dihe-heat.ene

dyna leap verlet strt -
iseed 1938 -
nstep 10000 timestep 0.001 -
nprint 50 iprfrq 200 -
firstt 200.0 finalt 300.0 teminc 30.0 -
iasors 1 iasvel 1 -
inbfrq 5 ihtfrq 100 ntrfrq 100 -
iunwrite 12 iuncrd 14 nsavcrd 100 kunit 15

open write formatted unit 28 name dihe-heat.pdb
write coor pdb unit 28
* energy minimized coords for cis
*

stop
```

Sample SPHGEN input file for sphere generation of binding site.

```
rec.ms
R
X
0.0
4.0
1.4
rec.sph
```

Sample DOCK input file for ligand docking.

```
flexible_ligand                 yes
orient_ligand                   yes
score_ligand                    yes
minimize_ligand                 yes
multiple_ligands                no
random_seed                     0
anchor_search                   no
torsion_drive                   yes
clash_overlap                   0.5
conformation_cutoff_factor      5
match_receptor_sites            yes
random_search                   no
ligand_centers                  no
automated_matching              yes
maximum_orientations            10000
write_configurations            yes
write_configuration_total       100
intramolecular_score            yes
intermolecular_score            yes
gridded_score                   yes
grid_version                    4
bump_filter                     yes
bump_maximum                    5
contact_score                   yes
contact_cutoff_distance         4.5
contact_clash_overlap           0.75
contact_clash_penalty           50
chemical_score                  yes
energy_score                    yes
energy_cutoff_distance          10
distance_dielectric             yes
dielectric_factor               4
attractive_exponent             6
repulsive_exponent              12
atom_model                      a
vdw_scale                       1
electrostatic_scale             1
ligand_atom_file                1r2s_mesc_t.mol2
receptor_site_file              rec.sph
score_grid_prefix               grid
vdw_definition_file             ~/dock/parameter/vdw.defn
```

```
chemical_definition_file        ~/dock/parameter/chem.defn
chemical_score_file             ~/dock/parameter/chem_score.tbl
flex_definition_file            ~/dock/parameter/flex.defn
flex_drive_file                 ~/dock/parameter/flex_drive.tbl
ligand_contact_file             1r2s_mesc_t_cnt.mol2
ligand_chemical_file            1r2s_mesc_t_chm.mol2
ligand_energy_file              1r2s_mesc_t_nrg.mol2
torsion_minimize                yes
contact_minimize                yes
chemical_minimize               yes
energy_minimize                 yes
initial_translation             1
initial_rotation                0.1
initial_torsion                 10
maximum_iterations              100
contact_convergence             0.01
chemical_convergence            0.01
energy_convergence              0.01
maximum_cycles                  1
```

Appendix F – Docking Results of *R*-Enantiomer of Compound **14**

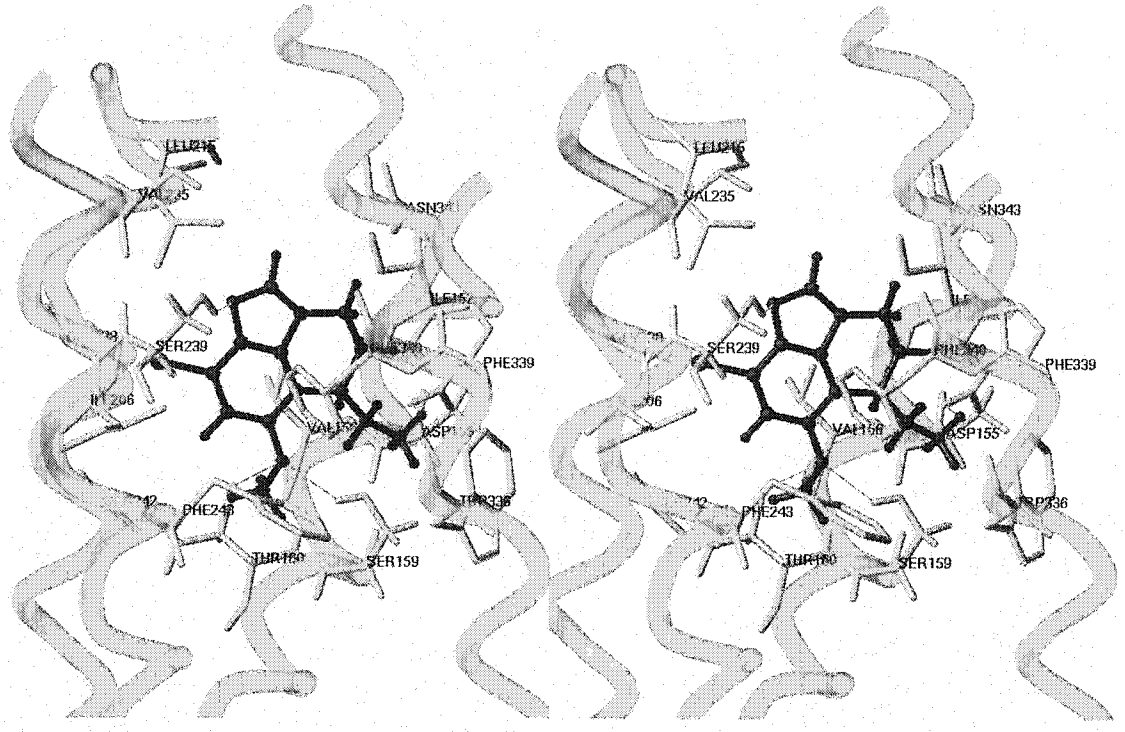

Hydrogen bonds are shown as dashed lines.

Figure 50. Stereo view (cross-eyed) of *R*-enantiomer of **14** docked to the 5-HT_{2A} receptor model.

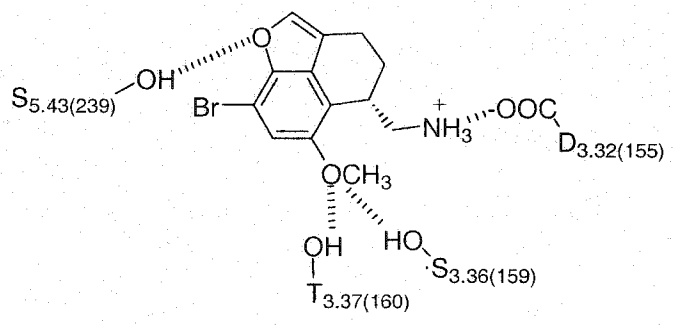

Figure 51. Schematic representation of *R*-enantiomer of **14** in the 5-HT_{2A} receptor model.

VITA

VITA

James Joseph Chambers was born on March 12, 1975 in Syosset, NY to John and Eleanor Chambers. Living on Long Island, he enjoyed everything that involved the ocean – fishing, boating, swimming, etc. Subsequent to graduation from Hicksville High School, he spent four snowy but very rewarding years at SUNY Buffalo where he embarked on his formal training as a medicinal chemist under the tutelage of Dr. Wayne K. Anderson. He received a *rare* B.S. in Medicinal Chemistry (1997) and then began an intelectually stimulating and rewarding graduate career at Purdue University, working with Dr. David E. Nichols on the development of conformationally-restricted arylalkylamines and a computer model of the serotonin-2A receptor. It was during his stay at Purdue that the author met his wife and best friend, Rebecca. Together, along with their dog, Zazu, they enjoy very much traveling, backpacking and exploring the remaining wilderness of Indiana, Michigan and the surrounding states. The next stop for the author, his wife, dog, and new cat, Neko, is the San Francisco Bay area where James and Rebecca have accepted post-doctoral positions at UCSF and UC Berkeley, respectively. The author looks forward very much to further development of his scientific knowledge and to the day when he may pursue his own research interests.

PUBLICATION

J. Med. Chem. **2001**, *44*, 1003−1010

Enantiospecific Synthesis and Pharmacological Evaluation of a Series of Super-Potent, Conformationally Restricted 5-$HT_{2A/2C}$ Receptor Agonists

James J. Chambers, Deborah M. Kurrasch-Orbaugh, Matthew A. Parker, and David E. Nichols*

Department of Medicinal Chemistry and Molecular Pharmacology, School of Pharmacy and Pharmacal Sciences, Purdue University, West Lafayette, Indiana 47907

Received November 17, 2000

The affinity of ligands for either the 5-HT_{2A} or 5-HT_{2C} agonist binding site was enhanced by modification of the 2,5-oxygen substituents that are found in typical hallucinogenic amphetamines such as **4b** (DOB). Restriction of the conformationally flexible 2,5-dimethoxy substituents into fused dihydrofuran rings generally resulted in increased potency relative to the parent 2,5-dimethoxy compounds. The pure enantiomers of these arylalkylamines were obtained by enantiospecific synthesis that involved acylation of the heterocyclic nucleus **7** with *N*-trifluoroacetyl-protected D- or L-alanyl chloride, followed by ketone reduction and *N*-deprotection. The enantiomers demonstrated modest stereoselectivity at the two receptors. Several general trends within these classes of new compounds were observed during their pharmacological investigation. For most pairs of optical isomers tested, the *R*-enantiomers of the compounds containing heterocycle **7** bound with only slightly higher affinity than their *S*-antipodes at the 5-HT_{2A} and 5-HT_{2C} receptors. Likewise, functional studies indicated that the *R*-enantiomers generally displayed increased potency compared to the *S*-enantiomers. Aromatization of the dihydrofuran rings of these arylalkylamines further increased affinity and potency. Only a few compounds were full agonists with most of them possessing intrinsic activities in the range of 60−80%. These compounds with a fully aromatic linear tricyclic nucleus are some of the highest-affinity ligands for the 5-HT_{2A} receptor reported to date.

Introduction

Over the past four decades, a vast base of information has been gathered about the physiological role of the neurotransmitter serotonin (5-HT, 5-hydroxytryptamine, **1**). Serotonin is known to be important in physiological systems ranging from hemodynamics and intestinal motility to normal cognition and perceptual processes. Receptors for this endogenous compound have been shown to exist almost ubiquitously throughout the body and especially in the gut and both central and peripheral nervous systems. Molecular biology techniques have led to the discovery of numerous different receptor subtypes for 5-HT, with the possibility of a different physiological role for each.[1] The 5-HT receptor subtype of most interest to our laboratory is the 5-HT_{2A} isoform. Agonist activation of this receptor is believed to be responsible for induction of the unique alterations in consciousness produced by substances such as LSD (*d*-lysergic acid *N,N*-diethylamide, **2**) and psilocin (4-hydroxy-*N,N*-dimethyltryptamine, **3**).[2]

The molecular determinants for agonist binding to the 5-HT_{2A} receptor have been of great interest to our laboratory in order that we might gain a better understanding of the physiological role of serotonin at this site. One of the factors complicating this research is that structurally diverse classes of compounds retain the ability to bind to and activate this receptor. Chemical classes such as the ergolines (LSD, **2**), tryptamines (psilocin, **3**), and amphetamines (DOB, 4-bromo-2,5-dimethoxyamphetamine, **4b**) represent a cross-section of compounds that cause hallucinogenesis in humans by putative activation of this receptor. The chemical diversity of these compounds, coupled with the difficulty of melding them into a common pharmacophore, has led to much speculation about the functional topography of the 5-HT_{2A} receptor.

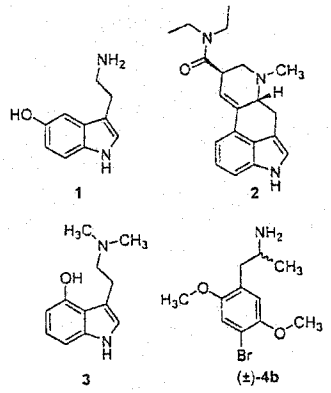

Although it is reasonably well-established that activation of the 5-HT_{2A} receptor by an exogenous ligand leads to hallucinogenesis, agonists that exhibit high affinity for this receptor invariably also bind to the 5-HT_{2C} receptor.[1] This finding has raised questions regarding the involvement of the 5-HT_{2C} receptor in hallucinogenesis.[3] The 5-HT_{2A} and 5-HT_{2C} receptors share a relatively high overall sequence homology and, more importantly, are 80% homologous within the transmembrane regions in which the agonist binding

* Address correspondence to: Dr. David E. Nichols, Dept. of Medicinal Chemistry and Molecular Pharmacology, RHPH Pharmacy Bldg., Rm. 506C, Purdue University, West Lafayette, IN 47907-1333. Phone: (765) 494-1461. Fax: (765) 494-1414. E-mail: drdave@pharmacy.purdue.edu.

10.1021/jm000491y CCC: $20.00
Published on Web 01/26/2001

site is thought to reside.[4] Thus, it is believed that these two receptors must also share structural features within the agonist binding site. A truly selective agonist would be an invaluable tool for investigating the differences in neuropharmacology between these chemically quite similar receptors.

Recent findings suggest that enough structural variance may exist between the agonist binding sites of the 5-HT_{2A} and 5-HT_{2C} receptors to confer moderate chemical selectivity. Additionally, animal behavioral models of hallucinogenic activity have supported in vitro data showing differential activity for the enantiomers of both amphetamine and LSD analogues.[5,6] We chose to explore further the importance of stereochemical selectivity in this receptor family through the synthesis and pharmacological evaluation of enantiomerically pure novel arylalkylamines.

We have recently reported the synthesis and preliminary pharmacological analysis of several semirigid analogues of DOB (±-**4b**) and related amphetamines.[7-9] As a continuation of our studies of these extremely potent 5-$HT_{2A/2C}$ receptor agonists, we present here the enantiospecific synthesis and pharmacological evaluation of a series of semirigid compounds. These compounds incorporate either a tetrahydrobenzo[1,2-*b*;4,5-*b'*]difuran heterocycle in place of the phenyl ring of amphetamines, as in the **5** series, or the fully aromatic benzo[1,2-*b*;4,5-*b'*]difuran counterpart, as in the **6** series. Specifically, the tricyclic nucleus was substituted at the 4- and 8-positions to generate arylalkylamine analogues of 2,5-dimethoxyamphetamine (2,5-DMA, **4a**), DOB (**4b**), and 2,5-dimethoxy-4-trifluoromethylamphetamine (DOTFM, **4c**). The chiral side chain was derived from the enantiomers of alanine. Both the *R*- and *S*-enantiomers of the six arylalkylamine structures were synthesized and evaluated pharmacologically.

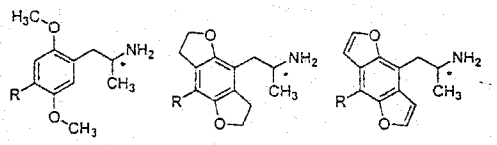

4 **5** **6**

Chemistry

An important intermediate in the synthetic scheme employed to produce these compounds is the heterocyclic nucleus tetrahydrobenzo[1,2-*b*;4,5-*b'*]difuran (**7**).[10] Although our previously reported synthesis of this compound required only three steps and gave a useful yield,[11] the straightforward improvements reported here (Scheme 1) provided **7** in 63% overall yield beginning with commercially available 1,4-bis(2-hydroxyethoxy)-benzene (**8**).

To effect the Friedel–Crafts acylation of **7**, our synthetic pathway (Scheme 2) required the acid chloride of optically pure D- or L-alanine (**11**). (Only the *R*-enantiomers are shown in the scheme.) Protection of the amino group of (*R* or *S*)-**11** to afford trifluoroacetamide (*R* or *S*)-**12** was accomplished following a previously reported procedure.[12] This very hygroscopic solid was then converted to the acid chloride using oxalyl chloride to afford (*R* or *S*)-**13**, which was then used without purification in the subsequent aromatic acylation. This

Scheme 1[a]

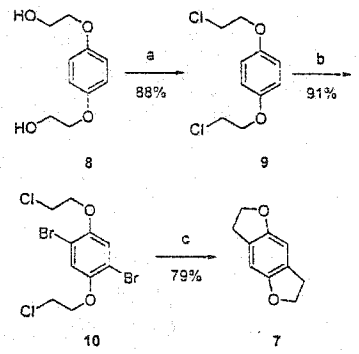

[a] (a) $SOCl_2$, C_5H_5N, CH_2Cl_2; (b) Br_2, $ZnCl_2$, AcOH; (c) Mg, EtMgBr, THF.

route afforded the optically pure ketone (*R* or *S*)-**14**, which was then reduced with triethylsilane in trifluoroacetic acid to afford the protected arylalkylamine (*R* or *S*)-**15**.[13]

The *N*-protected arylalkylamine (*R* or *S*)-**15** was hydrolyzed in base and then acidified to afford the hydrochloride salt of the unsubstituted product (*R* or *S*)-**5a**. The aromatic counterpart of this "non-*para*-substituted" amphetamine analogue was synthesized by oxidation of (*R* or *S*)-**15** with 2,3-dichloro-5,6-dicyano-1,4-benzoquinone (DDQ) to produce the aromatized amide (*R* or *S*)-**16**.[14] Subsequently, alkaline hydrolysis and acidification was used to obtain the hydrochloride salt of (*R* or *S*)-**6a**.

To complete the synthesis of the remaining compounds in this series, the amide (*R* or *S*)-**15** from above was brominated to afford the protected arylalkylamine (*R* or *S*)-**17**[11] followed by hydrolysis and conversion to the hydrochloride salt of (*R* or *S*)-**5b**. Compound (*R* or *S*)-**17** was likewise oxidized to the fully aromatic compound (*R* or *S*)-**18** using DDQ and then hydrolyzed and acidified to afford (*R* or *S*)-**6b** as the hydrochloride salt.

Brominated amide (*R* or *S*)-**17** was utilized to produce the final compounds (*R* or *S*)-**5c** and (*R* or *S*)-**6c**. The aromatic bromine of (*R* or *S*)-**17** was replaced by a trifluoromethyl substituent by reaction with copper iodide and tetramethylammonium trifluoroacetate[15] to afford (*R* or *S*)-**19**, which was hydrolyzed and acidified to obtain the hydrochloride salt of (*R* or *S*)-**5c**. Finally, oxidation of (*R* or *S*)-**19** followed by hydrolysis and acidification of the product afforded the hydrochloride salt of (*R* or *S*)-**6c**. The Mosher amides[16] of (*R*)- and (*S*)-**6c** were analyzed by HPLC to ascertain that no racemization had occurred during any of the synthetic steps; indeed this was found to be the case, with enantiomeric purities of both compounds in excess of 99%. In addition, it was noted that treatment of the tetrahydro compound (*R* or *S*)-**5b** with elemental bromine could under certain conditions lead to some oxidation to give small amounts of aromatized side products. In view of the high pharmacological activity that was found for (*R* or *S*)-**6b**, HPLC analysis of the *N*-trifluoroacetyl derivatives of (*R*)- and (*S*)-**5b** was used to verify that they contained no significant amounts of such oxidation products, which after hydrolysis might have contaminated (*R* or *S*)-**5b** and confounded the pharmacological results.

Scheme 2[a]

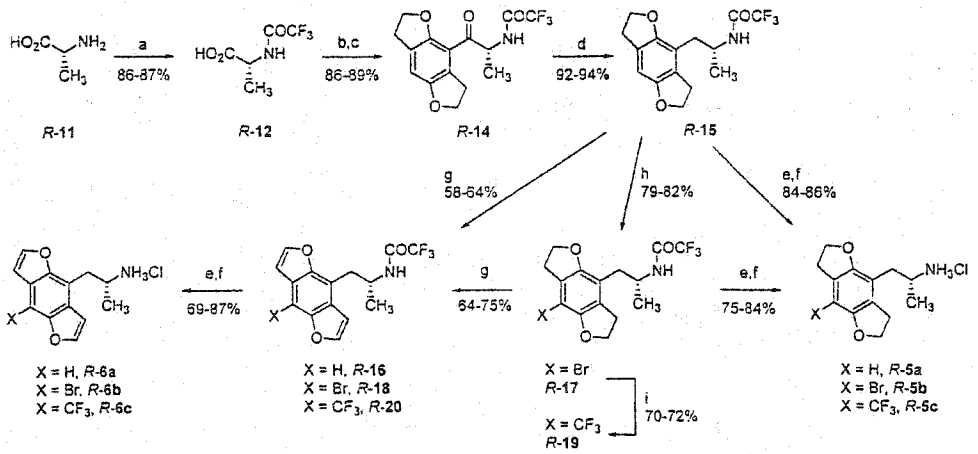

[a] (a) Et_3N, CF_3CO_2Et, MeOH; (b) $(COCl)_2$, CH_2Cl_2, C_5H_5N; (c) $AlCl_3$, 7, CH_2Cl_2; (d) Et_3SiH, CF_3CO_2H; (e) NaOH, MeOH, H_2O; (f) HCl, EtOH (anhyd); (g) DDQ, dioxane; (h) Br_2, AcOH; (i) $CF_3CO_2N(CH_3)_4$, CuI, $PhCH_3$, DMF.

Table 1. Results of the Radioligand Competition Binding Studies of Nonrigid (series 4) and Rigid (series 5 and 6) Compounds at Cloned Rat 5-HT_{2A} and 5-HT_{2C} Receptors

		K_i, nM (SEM)	
compd	X	at 5-HT_{2A}, [^{3}H]DOB	at 5-HT_{2C}, [^{125}I]DOI
(*R*)-**4a** (2,5-DMA)	H	2340 (326)	520 (34)
(±)-**4b** (DOB)	Br	2.2 (0.33)	2.8 (0.68)
(±)-**4c** (DOTFM)	CF_3	2.2 (0.26)	3.78 (1.12)
(*R*)-**5a**	H	54.4 (5.40)	8.2 (2.4)
(*S*)-**5a**	H	227 (24.5)	119 (31.8)
(*R*)-**5b**	Br	1.2 (0.26)	0.26 (0.025)
(*S*)-**5b**	Br	2.6 (0.33)	1.1 (0.20)
(*R*)-**5c**	CF_3	0.70 (0.090)	1.9 (0.32)
(*S*)-**5c**	CF_3	2.0 (0.17)	1.6 (0.19)
(*R*)-**6a**	H	1.5 (0.090)	0.79 (0.24)
(*S*)-**6a**	H	37.9 (5.40)	6.0 (0.17)
(*R*)-**6b**	Br	0.31 (0.042)	0.11 (0.014)
(*S*)-**6b**	Br	0.68 (0.083)	0.25 (0.046)
(*R*)-**6c**	CF_3	0.29 (0.030)	0.40 (0.13)
(*S*)-**6c**	CF_3	0.32 (0.030)	0.69 (0.098)

Table 2. Results of the Phosphoinositide Hydrolysis Studies of Nonrigid (series 4) and Rigid (series 5 and 6) Compounds at Cloned Rat 5-HT_{2A} Receptors

compd	X	EC_{50} at 5-HT_{2A}, nM (SEM)	percent maximal 5-HT stimulation (SEM)
(*R*)-**4a** (2,5-DMA)	H	>10000	16 (3.1) @ 100 μM
(±)-**4b** (DOB)	Br	72 (3.6)	79 (6.0)
(±)-**4c** (DOTFM)	CF_3	68.4 (12.6)	86 (3.5)
(*R*)-**5a**	H	5650 (376)	99 (0.7)
(*S*)-**5a**	H	2360 (210)	62 (3.1)
(*R*)-**5b**	Br	8.38 (1.86)	80 (7.8)
(*S*)-**5b**	Br	35 (1.0)	76 (5.0)
(*R*)-**5c**	CF_3	28 (6.7)	69 (3.9)
(*S*)-**5c**	CF_3	30 (6.2)	60 (1.2)
(*R*)-**6a**	H	590 (20)	76 (3.2)
(*S*)-**6a**	H	650 (68)	68 (2.3)
(*R*)-**6b**	Br	2.7 (0.55)	93 (9.9)
(*S*)-**6b**	Br	19 (1.6)	79 (1.5)
(*R*)-**6c**	CF_3	3.8 (0.53)	60 (3.9)
(*S*)-**6c**	CF_3	12 (1.4)	52 (6.0)

Pharmacology

Radioligand binding assays and phosphoinositide hydrolysis were employed to pharmacologically characterize this class of 5-$HT_{2A/2C}$ receptor agonists. As indicated in Table 1, the 5-HT_{2A} and 5-HT_{2C} receptor competition binding data were generated using [^{3}H]-DOB and [^{125}I]DOI, respectively. As a measure of functional activity, compounds were analyzed for their ability to stimulate phosphoinositide hydrolysis in NIH-3T3 cells expressing the 5-HT_{2A} receptor. The results of those assays are shown in Table 2.

Results and Discussion

The pharmacological data generated by the testing of these enantiomerically pure, rigid analogues have led to some new ideas about the interactions of the 5-HT_{2A} receptor binding site with agonist ligands. Perhaps the most interesting finding in Table 1 is that affinity for both of the 5-HT_2 receptor isoforms is generally increased in the rigidified tetrahydrobenzo[1,2-*b*;4,5-*b*']-difuran compounds (series 5) compared to their corresponding 2,5-dimethoxyamphetamine analogues (series 4). A similar potency trend is observed in the phosphoinositide hydrolysis data (Table 2). One reasonable explanation for this phenomenon is that the tethered alkyl ether groups of the two rigid series are acting as conformationally restricted mimics of the methoxy substituents in the analogous amphetamine analogues (series 4). In this view, the conformationally restricted compounds have higher affinity because they do not incur the entropic penalty experienced when the compounds with freely rotating methoxy groups bind. Another possible explanation for the increase in binding affinity for the benzo[1,2-*b*;4,5-*b*']difuran analogues is that the alkylamine side chain of these analogues is likely to exist in an anti-periplanar conformation (in a plane perpendicular to that of the aromatic system). Solution NMR studies of amphetamine analogues indicate that the alkylamine side chain resides in this out-of-plane orientation under simulated physiological conditions.[17] If the out-of-plane rotamer is the biologically active conformation, then these rigid analogues may also derive increased affinity through the enhancement of energetic accessibility to the anti-periplanar conformation.

An additional trend that can be observed in Tables 1 and 2 is that the benzo[1,2-*b*;4,5-*b*']difuran-containing compounds (series **6**) bind with higher affinity and exhibit increased potency relative to the corresponding tetrahydrobenzo[1,2-*b*;4,5-*b*']difurans (series **5**), indicating that the compounds in series **6** possess more favorable interactions with the agonist binding site. This may be due to the increased hydrophobicity of the extended tricyclic aromatic nucleus in **6a**–**c** relative to the tetrahydro congeners **5a**–**c** and a resulting greater tendency to partition into the hydrophobic receptor binding site. It is also possible that the extended aromaticity of the benzo[1,2-*b*;4,5-*b*']difurans (series **6**) may result in enhanced affinity by increasing the effective aromatic surface area on the ligand available for favorable π-stacking interactions with the agonist binding site, while still maintaining some (albeit weaker) hydrogen-bond acceptor properties of the furan oxygen atoms. It is interesting to note that although potency is generally increased for the aromatic compounds **6a**–**c** relative to the tetrahydro compounds **5a**–**c**, the intrinsic activity of these compounds remains largely unchanged.

The data in Tables 1 and 2 indicate that (with the exception of the 5-HT_{2C} data for (*R*)- and (*S*)-**5c**) the *R*-enantiomer binds with higher affinity and exhibits greater potency than the corresponding *S*-antipode. However, the data also indicate that the degree of enantioselectivity exhibited by the pairs of enantiomers in the two rigid series is relatively modest, *except for the compounds lacking a substituent para to the side chain, i.e., 5a and 6a*. It might be inferred that a hydrophobic substituent at that location induces a conformational change in the ligand-binding domain such that the region in the vicinity of the α-methyl group is dramatically altered. It is known that the effect of appending a hydrophobic substituent to the 4-position of amphetamine analogues is to increase hallucinogenic activity, presumably by increasing affinity and/or efficacy at the 5-HT_{2A} receptor.[18] This effect is dramatically demonstrated in this new series of arylalkylamine analogues in progressing from (*R* or *S*)-**5a** to the brominated arylalkylamine (*R*- or *S*)-**5b**. Only affinity is increased slightly when comparing (*R* or *S*)-**5b** to the trifluoromethylated arylalkylamine (*R* or *S*)-**5c**.

Nevertheless, it must be noted that the nonsubstituted (*R*)-**6a** has rather remarkable affinity, being about comparable to the most potent amphetamine derivatives such as **4c**, although its functional potency is still rather low (EC_{50} ca. 600 nM). Therefore, the fully aromatic system must compensate in some way for the lack of this substituent, even though its absence is clearly relevant to the high degree of stereoselectivity observed in **6a** versus **6b**. These will be interesting effects to study when a satisfactory three-dimensional model of the 5-HT_{2A} receptor is ultimately developed.

In summary, tethering the 2,5-dimethoxy substituents of hallucinogenic amphetamines in the form of tetrahydrofuran or furan rings has led to the most potent 5-$HT_{2A/2C}$ receptor ligands yet reported. Our anticipation that receptor isoform selectivity might arise in these series has not been borne out, but these compounds will be useful tools in further exploring the role of these receptors in behavior and cognition.

Experimental Section

Chemistry. All reagents were commercially available and were used without further purification unless otherwise indicated. Dry THF and diethyl ether were obtained by distillation from benzophenone-sodium under nitrogen immediately before use. Melting points were determined using a Thomas-Hoover apparatus and are uncorrected. ^{1}H NMR spectra were recorded using a 300-MHz Bruker ARX-300 NMR spectrometer. Chemical shifts are reported in δ values ppm relative to an internal reference (0.03%, v/v) of tetramethylsilane (TMS) in $CDCl_3$, except where noted. Chemical ionization mass spectra (CIMS) using isobutane as the carrier gas were obtained with a Finnigan 4000 spectrometer. Elemental analyses were performed by the Purdue University Microanalysis Laboratory and are within ±0.4% of the calculated values unless otherwise noted. Optical rotations were measured on a Perkin-Elmer 241 polarimeter at the sodium D-line ($\lambda = 589$ nm). Thin-layer chromatography was performed using J.T. Baker flex silica gel IB2-F, plastic-backed sheets with fluorescent indicator, visualizing with UV light at 254 nm and eluting with 4:1 hexanes–ethyl acetate unless otherwise noted. Column chromatography was carried out using silica gel 60, 230–400 mesh (J.T. Baker). All reactions were carried out under an inert atmosphere of argon unless otherwise indicated.

1,4-Bis(2-chloroethoxy)benzene (9).[19] Pyridine (29.4 mL, 364 mmol) was added to a mechanically stirred solution of 1,4-bis(hydroxyethoxy)benzene (**8**) (Aldrich; 30.0 g, 152 mmol) in CH_2Cl_2 (300 mL) at 0 °C. Next, thionyl chloride (25.4 mL, 348 mmol) was added dropwise such that the internal temperature did not exceed 5 °C.[20] This mixture was allowed to warm gradually to room temperature and was stirred overnight. Aqueous 2 N HCl (500 mL) was added slowly and the layers were separated. The aqueous layer was extracted with CH_2Cl_2 (3 × 75 mL) and the organic extracts were combined. The pooled organic extracts were then washed with aqueous 2 N HCl (2 × 200 mL), water (200 mL), 1 N NaOH (100 mL), and brine (100 mL). The organic extracts were then dried ($MgSO_4$), filtered, and evaporated to leave a tan solid that was recrystallized from ethanol to afford white crystals: 31.4 g, 88%; mp 90–91 °C; ^{1}H NMR ($CDCl_3$) δ 3.79 (t, 4 H, $ArOCH_2CH_2Cl$, $J = 6.0$ Hz), 4.19 (t, 4 H, $ArOCH_2CH_2Cl$, $J = 6.0$ Hz), 6.87 (s, 4 H, Ar*H*); CIMS *m/z* 235 ($M + H^+$).

1,4-Bis(2-chloroethoxy)-2,5-dibromobenzene (10).[11] Zinc chloride (38.2 g, 280 mmol) was added to a solution of **9** (27.5 g, 117 mmol) in acetic acid (280 mL). After enclosing the apparatus in aluminum foil to exclude light, bromine (39.3 g, 246 mmol) dissolved in acetic acid (55 mL) was added dropwise to the suspension over 1.5 h. The reaction was allowed to stir overnight, during which time a precipitate had formed. The reaction was diluted with aqueous saturated sodium thiosulfate (500 mL) and extracted with CH_2Cl_2 (5 × 200 mL). The organic layers were combined and washed with aqueous 1 N NaOH (1 × 200 mL), brine (100 mL), dried ($MgSO_4$), filtered, and evaporated to leave an off-white solid. Recrystallization from ethanol afforded a crystalline white product: 50.0 g, 91%; mp 120 °C (lit.[11] mp 119 °C); ^{1}H NMR ($CDCl_3$) δ 3.83 (t, 4 H, $ArOCH_2CH_2Cl$, $J = 6.3$ Hz), 4.23 (t, 4 H, $ArOCH_2CH_2Cl$, $J = 6.3$ Hz), 7.14 (s, 2 H, Ar*H*); CIMS *m/z* 391 ($M + H^+$).

2,3,6,7-Tetrahydrobenzo[1,2-*b*;4,5-*b*']difuran (7).[10] To a suspension of magnesium powder (Aldrich, −50 mesh, 99+%; 3.7 g, 152 mmol) in anhydrous THF (50 mL) was slowly added EtMgBr (3.4 mL, 10 mmol, 3 M solution in Et_2O).[21] An anhydrous THF solution (125 mL) of the dibrominated compound **10** (20.0 g, 51.0 mmol) was then added dropwise such that the internal reaction temperature did not exceed 35 °C. Upon completion of the addition, the reaction was heated at reflux for 3 h. The reaction was then cooled to room temperature and carefully poured into cold 1 N HCl (200 mL). Upon cessation of gas evolution, the mixture was extracted with Et_2O (3 × 300 mL). The organic layers were combined and washed with aqueous 1 N NaOH (4 × 75 mL), brine (50 mL), dried ($MgSO_4$), filtered, and concentrated by rotary evaporation to afford a tan solid. This was recrystallized from ethanol to afford off-white, platelike crystals: 6.5 g, 79%; mp 155 °C (lit.[11]

mp 155−156 °C); ^{1}H NMR ($CDCl_3$) δ 3.13 (t, 4 H, $ArOCH_2CH_2$, J = 8.5 Hz), 4.52 (t, 4 H, $ArOCH_2CH_2$, J = 8.5 Hz), 6.63 (s, 2 H, Ar*H*); CIMS *m/z* 163 (M + H$^+$).

(*R*)-*N*-Trifluoroacetylalanine ((*R*)-12).[12] The procedure of Curphey was followed exactly except for a slight modification of the acidic workup. Triethylamine (3.1 mL, 22 mmol) was added to a solution of D-alanine ((*R*)-**11**; 99+%) (2.0 g, 22 mmol) in MeOH (11 mL). After 5 min, ethyl trifluoroacetate (3.3 mL, 28 mmol) was added and the reaction was allowed to stir for 24 h. The solvent was removed by rotary evaporation and the residue that remained was dissolved in H_2O (35 mL) and acidified with concentrated HCl (4 mL). After stirring for 15 min, the mixture was extracted with ethyl acetate (4 × 30 mL) and the organic layers were combined and washed with brine (25 mL), dried ($MgSO_4$), filtered, and concentrated by rotary evaporation to leave a clear oil. After being subjected to high vacuum for 24 h, the clear oil solidified into a fluffy, hygroscopic solid: 2.7 g, 86%; mp 69 °C (lit.[12] mp 70−71 °C); ^{1}H NMR ($CDCl_3$) δ 1.58 (d, 3 H, $CHCH_3$, J = 7.5 Hz), 4.68 (p, 1 H, $CHCH_3$, J = 7.5 Hz), 6.87 (bs, 1 H, N*H*).

(*S*)-*N*-Trifluoroacetylalanine ((*S*)-12).[12] The title compound was prepared from L-alanine ((*S*)-**11**; 99%) as described for compound (*R*)-**12**: 87%; mp 70 °C (lit.[12] mp 70−71 °C); ^{1}H NMR ($CDCl_3$) δ 1.58 (d, 3 H, $CHCH_3$, J = 7.5 Hz), 4.68 (p, 1 H, $CHCH_3$, J = 7.5 Hz), 6.87 (bs, 1 H, N*H*).

(*R*)-(+)-*N*-Trifluoroacetyl-2,3,6,7-tetrahydro-4-alanylbenzo[1,2-*b*;4,5-*b*']difuran ((*R*)-14). Trifluoracetamide-protected D-alanine ((*R*)-**12**) (4.09 g, 22 mmol) was added to a pretared flask and placed under high vacuum for 24 h to remove any residual moisture. The flask was then reweighed to record an accurate weight of the starting material. Next, CH_2Cl_2 (100 mL) was added to the flask, followed by pyridine (2 drops) and the solution was cooled to 0 °C. Oxalyl chloride (4.3 mL, 49 mmol) was then added via syringe and the reaction was allowed to gradually warm to room temperature and stir for 3.5 h. The solvent and excess oxalyl chloride were removed by rotary evaporation at 35 °C to afford acid chloride (*R*)-**13**, which was not characterized. The heterocycle **7** (1.1 g, 6.6 mmol) was dissolved in CH_2Cl_2 (35 mL) and this solution was added slowly via dropping funnel to a suspension of $AlCl_3$ (2.4 g, 18.3 mmol) in CH_2Cl_2 (50 mL). This was followed by slow addition of the acid chloride (*R*)-**13** dissolved in CH_2Cl_2 (45 mL). The mixture was allowed to stir for 16 h, at which time TLC showed only one yellow spot. The reaction mixture was poured slowly onto ice to quench the reaction and the two phases were then separated. The aqueous layer was extracted with CH_2Cl_2 (4 × 75 mL) and the organic layers were combined and washed with cold, aqueous 1 N HCl (75 mL), H_2O (50 mL), and then saturated $NaHCO_3$ (2 × 50 mL). The organic solution was then dried ($MgSO_4$), filtered, and concentrated to leave a yellow solid that was recrystallized from methanol to afford fluffy, yellow crystals: 1.88 g, 86%; mp 209−210 °C; ^{1}H NMR ($CDCl_3$) δ 1.46 (d, 3 H, $CHCH_3$, J = 6.8 Hz), 3.21 (m, 2 H, $ArOCH_2CH_2$), 3.33 (p, 1 H, $ArOCH_2CH_2$, J = 8.5 Hz), 3.61 (p, 1 H, $ArOCH_2CH_2$, J = 9.0 Hz), 4.64 (m, 4 H, $ArOCH_2CH_2$), 5.62 (p, 1 H, $CHCH_3$, J = 6.8 Hz), 6.90 (s, 1 H, Ar*H*), 7.64 (bs, 1 H, N*H*); $[\alpha]_D$ = +56.0° (c = 0.01, CH_3CN); CIMS *m/z* 330 (M + H$^+$). Anal. ($C_{15}H_{14}F_3NO_4$) C, H, N.

(*S*)-(−)-*N*-Trifluoroacetyl-2,3,6,7-tetrahydro-4-alanylbenzo[1,2-*b*;4,5-*b*']difuran ((*S*)-14). The title compound was prepared from (*S*)-**12** as described for compound (*R*)-**14**: 89%; mp 210−211 °C; ^{1}H NMR ($CDCl_3$) δ 1.46 (d, 3 H, $CHCH_3$, J = 6.8 Hz), 3.21 (m, 2 H, $ArOCH_2CH_2$), 3.33 (p, 1 H, $ArOCH_2CH_2$, J = 8.5 Hz), 3.61 (p, 1 H, $ArOCH_2CH_2$, J = 9.0 Hz), 4.64 (m, 4 H, $ArOCH_2CH_2$), 5.62 (p, 1 H, $CHCH_3$, J = 6.8 Hz), 6.90 (s, 1 H, Ar*H*), 7.64 (bs, 1 H, N*H*); $[\alpha]_D$ = −56.1° (c = 0.01, CH_3CN); CIMS *m/z* 330 (M + H$^+$). Anal. ($C_{15}H_{14}F_3NO_4$) C, H, N.

(*R*)-(+)-*N*-Trifluoroacetyl-1-(2,3,6,7-tetrahydrobenzo-[1,2-*b*;4,5-*b*']difuran-4-yl)-2-aminopropane ((*R*)-15). Ketone (*R*)-**14** (0.94 g, 2.9 mmol) was dissolved in trifluoroacetic acid (9.4 mL) and then triethylsilane (2.3 mL, 14.5 mmol) was added. The mixture was heated at reflux for 6 h, at which time TLC showed no starting material. The reaction was cooled to room temperature followed by the very slow addition of saturated, aqueous $NaHCO_3$ solution until evolution of gas had ceased and the solution remained alkaline. The mixture was then extracted with Et_2O (4 × 75 mL), the organic layers combined and dried ($MgSO_4$), filtered and evaporated to leave a tan solid. The product was triturated with hexanes and the resulting suspension was then vacuum filtered to leave a white solid: 0.84 g, 92%; mp 139−140 °C; ^{1}H NMR ($CDCl_3$) δ 1.27 (d, 3 H, $CHCH_3$, J = 6.6 Hz), 2.75 (d, 2 H, $ArCH_2CH$, J = 6.0 Hz), 3.09 (t, 2 H, $ArOCH_2CH_2$, J = 8.6 Hz), 3.17 (t, 2 H, $ArOCH_2CH_2$, J = 8.7 Hz), 4.16 (p, 1 H, $ArCH_2CH$, J = 6.5 Hz), 4.54 (t, 2 H, $ArOCH_2CH_2$, J = 8.4 Hz), 4.56 (t, 2 H, $ArOCH_2CH_2$), 6.56 (s, 1 H, Ar*H*), 7.73 (bs, 1 H, N*H*); $[\alpha]_D$ = +8.80° (c = 0.081, CH_3CN); CIMS *m/z* 316 (M + H$^+$). Anal. ($C_{15}H_{16}F_3NO_3$) C, H, N.

(*S*)-(−)-*N*-Trifluoroacetyl-1-(2,3,6,7-tetrahydrobenzo-[1,2-*b*;4,5-*b*']difuran-4-yl)-2-aminopropane ((*S*)-15). The title compound was prepared from (*S*)-**14** as described for compound (*R*)-**15**: 94%; mp 139−140 °C; ^{1}H NMR ($CDCl_3$) δ 1.27 (d, 3 H, $CHCH_3$, J = 6.6 Hz), 2.75 (d, 2 H, $ArCH_2CH$, J = 6.0 Hz), 3.09 (t, 2 H, $ArOCH_2CH_2$, J = 8.6 Hz), 3.17 (t, 2 H, $ArOCH_2CH_2$, J = 8.7 Hz), 4.16 (p, 1 H, $ArCH_2CH$, J = 6.5 Hz), 4.54 (t, 2 H, $ArOCH_2CH_2$, J = 8.4 Hz), 4.56 (t, 2 H, $ArOCH_2CH_2$), 6.56 (s, 1 H, Ar*H*), 7.73 (bs, 1 H, N*H*); $[\alpha]_D$ = −8.76° (c = 0.069, CH_3CN); CIMS *m/z* 316 (M + H$^+$). Anal. ($C_{15}H_{16}F_3NO_3$) C, H, N.

Representative Procedure for Hydrolysis of Trifluoroacetamides: (*R*)-(−)-1-(2,3,6,7-Tetrahydrobenzo[1,2-*b*;4,5-*b*']difuran-4-yl)-2-aminopropane Hydrochloride ((*R*)-5a·HCl). The protected amine (*R*)-**15** (0.1 g, 0.3 mmol) was dissolved in MeOH (20 mL) and cooled to 0 °C. Aqueous 5 N NaOH (5 mL) was added to this solution and the mixture was allowed to stir overnight and was then diluted with Et_2O (50 mL). The phases were separated and the aqueous layer was extracted with Et_2O (3 × 15 mL). The organic layers were combined, dried ($MgSO_4$), filtered and evaporated to yield a tan oil. This oil was taken up in anhydrous Et_2O (15 mL) and filtered through glass wool. A slight excess of ethanolic 1 N HCl was added dropwise to the solution with vigorous stirring. The flask was then placed in a freezer overnight and the precipitate was collected by vacuum filtration. The resulting solid was recrystallized from *i*-PrOH to afford white, fluffy crystals: 0.073 g, 86%; mp 275−276 °C dec; ^{1}H NMR (D_2O) δ 1.28 (d, 3 H, $CHCH_3$, J = 6.9 Hz), 2.83 (d, 2 H, $ArCH_2CH$, J = 6.9 Hz), 3.13 (dt, 4 H, $ArOCH_2CH_2$, J = 7.8 Hz), 3.66 (m, 1 H, $ArCH_2CH$, J = 6.9 Hz), 4.55 (dt, 4 H, $ArOCH_2CH_2$, J = 9.0 Hz), 6.68 (s, 1 H, Ar*H*); $[\alpha]_D$ = −11.78° (c = 0.011, DMF); CIMS *m/z* 220 (M + H$^+$). Anal. ($C_{13}H_{18}ClNO_2$) C, H, N.

(*S*)-(+)-1-(2,3,6,7-Tetrahydrobenzo[1,2-*b*;4,5-*b*']difuran-4-yl)-2-aminopropane Hydrochloride ((*S*)-5a·HCl). The title compound was prepared from (*S*)-**15** as described for (*R*)-**5a·HCl**: 84%; mp 275−276 °C dec; ^{1}H NMR (D_2O) δ 1.28 (d, 3 H, $CHCH_3$, J = 6.9 Hz), 2.83 (d, 2 H, $ArCH_2CH$, J = 6.9 Hz), 3.13 (dt, 4 H, $ArOCH_2CH_2$, J = 7.8 Hz), 3.66 (m, 1 H, $ArCH_2CH$, J = 6.9 Hz), 4.55 (dt, 4 H, $ArOCH_2CH_2$, J = 9.0 Hz), 6.68 (s, 1 H, Ar*H*); $[\alpha]_D$ = +11.72° (c = 0.011, DMF); CIMS *m/z* 220 (M + H$^+$). Anal. ($C_{13}H_{18}ClNO_2$) C, H, N.

Representative Procedure for Aromatization of Substituted 2,3,6,7-Tetrahydrobenzo[1,2-*b*;4,5-*b*']difurans to Benzo[1,2-*b*;4,5-*b*']difurans: (*R*)-(+)-*N*-Trifluoroacetyl-1-(benzo[1,2-*b*;4,5-*b*']difuran-4-yl)-2-aminopropane ((*R*)-16). A solution of DDQ (0.42 g, 1.85 mmol) in dioxane (8 mL) was slowly added to a solution of protected amine (*R*)-**15** (0.20 g, 0.63 mmol) in dioxane (10 mL).[14] The solution was heated at reflux for 24 h, at which time TLC indicated reaction completion. The reaction was then cooled to room temperature and the precipitate that formed was removed by vacuum filtration. The filter cake was washed thoroughly with CH_2Cl_2 and then the solvents were removed by rotary evaporation. The brown oil that remained was subjected to column chromatography (4:1 hexanes−ethyl acetate as eluent) to afford a white solid product: 0.134 g, 64%; mp 150−151 °C; ^{1}H NMR ($CDCl_3$) δ 1.29 (d, 3 H, $CHCH_3$, J = 6.6 Hz), 3.38 (dd, 2 H, $ArCH_2CH$, J = 6.0, 3.0 Hz), 4.48 (m, 1 H, $ArCH_2CH$, J = 6.9 Hz), 6.54 (bs, 1 H, N*H*), 6.85 (d, 1 H, Ar*H*, J = 2.4 Hz), 6.90 (d, 1 H, Ar*H*, J

= 2.4 Hz), 7.58 (s, 1 H, ArH), 7.64 (d, 1 H, ArH, J = 2.4 Hz), 7.67 (d, 1 H, ArH, J = 2.1 Hz); $[\alpha]_D$ = +3.06° (c = 0.006, CH_3CN); CIMS m/z 312 ($M + H^+$). Anal. ($C_{15}H_{12}F_3NO_3$) C, H, N.

(*S*)-(−)-*N*-Trifluoroacetyl-1-(benzo[1,2-*b*;4,5-*b*']difuran-4-yl)-2-aminopropane ((*S*)-16). The title compound was prepared from (*S*)-**15** by the general procedure described for compound (*R*)-**16**: 58%; mp 152−153 °C; ^1H NMR ($CDCl_3$) δ 1.29 (d, 3 H, $CHCH_3$, J = 6.6 Hz), 3.38 (dd, 2 H, $ArCH_2CH$, J = 6.0, 3.0 Hz), 4.48 (m, 1 H, $ArCH_2CH$, J = 6.9 Hz), 6.54 (bs, 1 H, NH), 6.85 (d, 1 H, ArH, J = 2.4 Hz), 6.90 (d, 1 H, ArH, J = 2.4 Hz), 7.58 (s, 1 H, ArH), 7.64 (d, 1 H, ArH, J = 2.4 Hz), 7.67 (d, 1 H, ArH, J = 2.1 Hz); $[\alpha]_D$ = −3.04° (c = 0.006, CH_3CN); CIMS m/z 312 ($M + H^+$). Anal. ($C_{15}H_{12}F_3NO_3$) C, H, N.

(*R*)-(−)-1-(Benzo[1,2-*b*;4,5-*b*']difuran-4-yl)-2-aminopropane Hydrochloride ((*R*)-6a·HCl). The title compound was prepared from (*R*)-**16** by the general procedure described for compound (*R*)-**5a·HCl**: 81%; mp 269 °C dec; ^1H NMR (D_2O) δ 1.29 (d, 3 H, $CHCH_3$, J = 6.9 Hz), 3.36 (d, 2 H, $ArCH_2CH$, J = 6.9 Hz), 3.85 (m, 1 H, $ArCH_2CH$, J = 6.9 Hz), 6.94 (d, 1 H, ArH, J = 1.2 Hz), 6.98 (d, 1 H, ArH, J = 1.2 Hz), 7.64 (s, 1 H, ArH), 7.77 (s, 1 H, ArH), 7.78 (s, 1 H, ArH); $[\alpha]_D$ = −9.54° (c = 0.0102, DMF); CIMS m/z 216 ($M + H^+$). Anal. ($C_{13}H_{14}ClNO_2$) C, H, N.

(*S*)-(+)-1-(Benzo[1,2-*b*;4,5-*b*']difuran-4-yl)-2-aminopropane Hydrochloride ((*S*)-6a·HCl). The title compound was prepared from (*S*)-**16** by the general procedure described for compound (*R*)-**5a·HCl**: 82%; mp 270 °C dec; ^1H NMR (D_2O) δ 1.29 (d, 3 H, $CHCH_3$, J = 6.9 Hz), 3.36 (d, 2 H, $ArCH_2CH$, J = 6.9 Hz), 3.85 (m, 1 H, $ArCH_2CH$, J = 6.9 Hz), 6.94 (d, 1 H, ArH, J = 1.2 Hz), 6.98 (d, 1 H, ArH, J = 1.2 Hz), 7.64 (s, 1 H, ArH), 7.77 (s, 1 H, ArH), 7.78 (s, 1 H, ArH); $[\alpha]_D$ = +9.58° (c = 0.0102, DMF); CIMS m/z 216 ($M + H^+$). Anal. ($C_{13}H_{14}ClNO_2$) C, H, N.

(*R*)-(+)-*N*-Trifluoroacetyl-1-(8-bromo-2,3,6,7-tetrahydrobenzo[1,2-*b*;4,5-*b*']difuran-4-yl)-2-aminopropane ((*R*)-17). The protected amine (*R*)-**15** (1.1 g, 3.5 mmol) was dissolved in acetic acid (70 mL) and the flask was covered with aluminum foil to exclude light.[11] This solution was cooled to 15 °C and a solution of bromine (0.54 g, 3.5 mmol) in acetic acid (12 mL) was added dropwise. The reaction was allowed to warm to room temperature and stir for 4.5 h, at which time a precipitate had formed and TLC indicated the absence of starting material. The reaction was quenched by the addition of H_2O (100 mL) and extracted with CH_2Cl_2 (5 × 50 mL). The organic layers were combined, dried ($MgSO_4$), filtered, and evaporated to afford 1.0 g (79%) of the product as a white solid. Care should be taken to use not more than 1.0 equivalent of bromine in this procedure and to recrystallize the product if any impurities are observed, since we have noted that bromine can oxidize the dihydrofuran moieties to furans under some circumstances. An analytical sample was recrystallized from ethyl acetate−hexane: mp 201−202 °C; ^1H NMR ($CDCl_3$) δ 1.27 (d, 3 H, $CHCH_3$, J = 6.3 Hz), 2.71 (dd, 2 H, $ArCH_2CH$, J = 7.2, 1.5 Hz), 3.20 (t, 4 H, $ArOCH_2CH_2$, J = 8.7 Hz), 4.13 (p, 1 H, $ArCH_2CH$, J = 6.6 Hz), 4.59 (t, 2 H, $ArOCH_2CH_2$, J = 8.4 Hz), 4.65 (t, 2 H, $ArOCH_2CH_2$, J = 8.4 Hz), 7.47 (bs, 1 H, NH); $[\alpha]_D$ = +6.6° (c = 0.00445, CH_3CN); CIMS m/z 394 ($M + H^+$). Anal. ($C_{15}H_{13}BrF_3NO_3$) C, H, N.

(*S*)-(−)-*N*-Trifluoroacetyl-1-(8-bromo-2,3,6,7-tetrahydrobenzo[1,2-*b*;4,5-*b*']difuran-4-yl)-2-aminopropane ((*S*)-17). The title compound was prepared from (*S*)-**15** by the general procedure described for compound (*R*)-**17**: 82%; mp 201−202 °C; ^1H NMR ($CDCl_3$) δ 1.27 (d, 3 H, $CHCH_3$, J = 6.3 Hz), 2.71 (dd, 2 H, $ArCH_2CH$, J = 7.2, 1.5 Hz), 3.20 (t, 4 H, $ArOCH_2CH_2$, J = 8.7 Hz), 4.13 (p, 1 H, $ArCH_2CH$, J = 6.6 Hz), 4.59 (t, 2 H, $ArOCH_2CH_2$, J = 8.4 Hz), 4.65 (t, 2 H, $ArOCH_2CH_2$, J = 8.4 Hz), 7.47 (bs, 1 H, NH); $[\alpha]_D$ = −6.9° (c = 0.00445, CH_3CN); CIMS m/z 394 ($M + H^+$). Anal. ($C_{15}H_{15}BrF_3NO_3$) C, H, N.

(*R*)-(−)-1-(8-Bromo-2,3,6,7-tetrahydrobenzo[1,2-*b*;4,5-*b*']difuran-4-yl)-2-aminopropane Hydrochloride ((*R*)-5b·HCl). The title compound was prepared from (*R*)-**17** by the general procedure described for compound (*R*)-**5a·HCl**: 75%; mp 282−283 °C; ^1H NMR (D_2O) δ 1.27 (d, 3 H, $CHCH_3$, J = 6.3 Hz), 2.78 (dd, 2 H, $ArCH_2CH$, J = 7.2, 3.3 Hz), 3.14 (t, 2 H, $ArOCH_2CH_2$, J = 8.7 Hz), 3.23 (t, 2 H, $ArOCH_2CH_2$, J = 8.7 Hz), 3.63 (m, 1 H, $ArCH_2CH$, J = 6.9 Hz), 4.61 (q, 4 H, $ArOCH_2CH_2$, J = 8.7 Hz); $[\alpha]_D$ = −10.82° (c = 0.0089, DMF); CIMS m/z 297 ($M + H^+$). Anal. ($C_{13}H_{17}BrClNO_2$) C, H, N.

(*S*)-(+)-1-(8-Bromo-2,3,6,7-tetrahydrobenzo[1,2-*b*;4,5-*b*']difuran-4-yl)-2-aminopropane Hydrochloride ((*S*)-5b·HCl). The title compound was prepared from (*S*)-**17** by the general procedure described for compound (*R*)-**5a·HCl**: 78%; mp 282−283 °C; ^1H NMR (D_2O) δ 1.27 (d, 3 H, $CHCH_3$, J = 6.3 Hz), 2.78 (dd, 2 H, $ArCH_2CH$, J = 7.2, 3.3 Hz), 3.14 (t, 2 H, $ArOCH_2CH_2$, J = 8.7 Hz), 3.23 (t, 2 H, $ArOCH_2CH_2$, J = 8.7 Hz), 3.63 (m, 1 H, $ArCH_2CH$, J = 6.9 Hz), 4.61 (q, 4 H, $ArOCH_2CH_2$, J = 8.7 Hz); $[\alpha]_D$ = +10.80° (c = 0.0089, DMF); CIMS m/z 297 ($M + H^+$). Anal. ($C_{13}H_{17}BrClNO_2$) C, H, N.

(*R*)-(+)-*N*-Trifluoroacetyl-1-(8-bromobenzo[1,2-*b*;4,5-*b*']difuran-4-yl)-2-aminopropane ((*R*)-18). The title compound was prepared from (*R*)-**17** by the general procedure described for compound (*R*)-**16**: 68%; mp 215−216 °C; ^1H NMR ($CDCl_3$) δ 1.26 (d, 3 H, $CHCH_3$, J = 6.7 Hz), 3.35 (dd, 2 H, $ArCH_2CH$, J = 6.4, 3.3 Hz), 4.46 (m, 1 H, $ArCH_2CH$, J = 6.8 Hz), 6.41 (bs, 1 H, NH), 6.92 (d, 1 H, ArH, J = 2.2 Hz), 6.99 (d, 1 H, ArH, J = 2.2 Hz), 7.69 (d, 1 H, ArH, J = 2.2 Hz), 7.73 (d, 1 H, ArH, J = 2.3 Hz); $[\alpha]_D$ = +17.7° (c = 0.0075, CH_3CN); CIMS m/z 390 ($M + H^+$). Anal. ($C_{15}H_{11}BrF_3NO_3$) C, H, N.

(*S*)-(−)-*N*-Trifluoroacetyl-1-(8-bromobenzo[1,2-*b*;4,5-*b*']difuran-4-yl)-2-aminopropane ((*S*)-18). The title compound was prepared from (*S*)-**17** by the general procedure described for compound (*R*)-**16**: 64%; mp 214−215 °C; ^1H NMR ($CDCl_3$) δ 1.26 (d, 3 H, $CHCH_3$, J = 6.7 Hz), 3.35 (dd, 2 H, $ArCH_2CH$, J = 6.4, 3.3 Hz), 4.46 (m, 1 H, $ArCH_2CH$, J = 6.8 Hz), 6.41 (bs, 1 H, NH), 6.92 (d, 1 H, ArH, J = 2.2 Hz), 6.99 (d, 1 H, ArH, J = 2.2 Hz), 7.69 (d, 1 H, ArH, J = 2.2 Hz), 7.73 (d, 1 H, ArH, J = 2.3 Hz); $[\alpha]_D$ = −17.2° (c = 0.0075, CH_3CN); CIMS m/z 390 ($M + H^+$). Anal. ($C_{15}H_{11}BrF_3NO_3$) C, H, N.

(*R*)-(−)-1-(8-Bromobenzo[1,2-*b*;4,5-*b*']difuran-4-yl)-2-aminopropane Hydrochloride ((*R*)-6b·HCl). The title compound was prepared from (*R*)-**18** by the general procedure described for compound (*R*)-**5a·HCl**: 87%; mp 290 °C dec; ^1H NMR (D_2O) δ 1.23 (d, 3 H, $CHCH_3$, J = 6.6 Hz), 3.21 (d, 2 H, $ArCH_2CH$, J = 6.9 Hz), 3.74 (m, 1 H, $ArCH_2CH$, J = 6.9 Hz), 6.84 (d, 1 H, ArH, J = 2.1 Hz), 6.96 (d, 1 H, ArH, J = 2.4 Hz), 7.73 (d, 1 H, ArH, J = 2.4 Hz), 7.76 (s, 1 H, ArH, J = 2.4 Hz); $[\alpha]_D$ = −20.1° (c = 0.005, DMF); CIMS m/z 294 ($M + H^+$). Anal. ($C_{13}H_{13}BrClNO_2$) C, H, N.

(*S*)-(+)-1-(8-Bromobenzo[1,2-*b*;4,5-*b*']difuran-4-yl)-2-aminopropane Hydrochloride ((*S*)-6b·HCl). The title compound was prepared from (*S*)-**18** by the general procedure described for compound (*R*)-**5a·HCl**: 85%; mp 291 °C dec; ^1H NMR (D_2O) δ 1.23 (d, 3 H, $CHCH_3$, J = 6.6 Hz), 3.21 (d, 2 H, $ArCH_2CH$, J = 6.9 Hz), 3.74 (m, 1 H, $ArCH_2CH$, J = 6.9 Hz), 6.84 (d, 1 H, ArH, J = 2.1 Hz), 6.96 (d, 1 H, ArH, J = 2.4 Hz), 7.73 (d, 1 H, ArH, J = 2.4 Hz), 7.76 (s, 1 H, ArH, J = 2.4 Hz); $[\alpha]_D$ = +20.8° (c = 0.005, DMF); CIMS m/z 294 ($M + H^+$). Anal. ($C_{13}H_{13}BrClNO_2$) C, H, N.

(*R*)-(+)-*N*-Trifluoroacetyl-1-(8-trifluoromethyl-2,3,6,7-tetrahydrobenzo[1,2-*b*;4,5-*b*']difuran-4-yl)-2-aminopropane ((*R*)-19). Toluene (25 mL) was added to a flask fitted with a Dean−Stark trap and containing tetramethylammonium trifluoroacetate (1.2 g, 6.3 mmol), copper iodide (1.4 g, 7.1 mmol), and (*R*)-**17** (0.50 g, 1.3 mmol).[15] This mixture was brought to reflux for 4 h to azeotrope residual H_2O present in the starting materials. Next, anhydrous DMF (7.9 mL, 101.5 mmol) was added slowly with concomitant removal of toluene to bring the reaction temperature to 145 °C for 4 h. The reaction was monitored by ^{19}F NMR for the appearance of a second singlet. Upon completion, the reaction was cooled to room temperature, diluted with H_2O (100 mL) and extracted with CH_2Cl_2 (4 × 50 mL). The organic layers were combined, dried ($MgSO_4$), filtered, and evaporated to leave a white solid that was subjected to column chromatography (4:1 hexanes−ethyl acetate as eluent) to afford the title compound as white crystals: 0.35 g, 72%; mp 178−179 °C; ^1H NMR ($CDCl_3$) δ 1.28 (d, 3 H, $CHCH_3$, J = 6.3 Hz), 2.77 (t, 1 H, $ArCH_2CH$, J = 13.5

Hz), 2.78 (q, 1 H, ArCH_2CH, J = 12.9 Hz), 3.13 (t, 2 H, ArOCH$_2$CH_2, J = 8.7 Hz), 3.34 (t, 2 H, ArOCH$_2$CH_2, J = 8.7 Hz), 4.17 (m, 1 H, ArCH$_2$CH, J = 6.9 Hz), 4.59 (t, 2 H, ArOCH_2CH$_2$, J = 9.0 Hz), 4.67 (t, 2 H, ArOCH_2CH$_2$, J = 8.7 Hz), 7.40 (bs, 1 H, NH); $[\alpha]_D$ = +1.79° (c = 0.013, CH$_3$CN); CIMS m/z 384 (M + H$^+$). Anal. ($C_{16}H_{15}F_6NO_3$) C, H, N.

(*S*)-(−)-*N*-Trifluoroacetyl-1-(8-trifluoromethyl-2,3,6,7-tetrahydrobenzo[1,2-*b*;4,5-*b*']difuran-4-yl)-2-aminopropane ((*S*)-19). The title compound was prepared from (*S*)-**17** by the procedure described for compound (*R*)-**19**: 70%; mp 178−179 °C; ^{1}H NMR (CDCl$_3$) δ 1.28 (d, 3 H, CHCH_3, J = 6.3 Hz), 2.77 (t, 1 H, ArCH_2CH, J = 13.5 Hz), 2.78 (q, 1 H, ArCH_2CH, J = 12.9 Hz), 3.13 (t, 2 H, ArOCH$_2$CH_2, J = 8.7 Hz), 3.34 (t, 2 H, ArOCH$_2$CH_2, J = 8.7 Hz), 4.17 (m, 1 H, ArCH$_2$CH, J = 6.9 Hz), 4.59 (t, 2 H, ArOCH_2CH$_2$, J = 9.0 Hz), 4.67 (t, 2 H, ArOCH_2CH$_2$, J = 8.7 Hz), 7.40 (bs, 1 H, NH); $[\alpha]_D$ = −1.83° (c = 0.013, CH$_3$CN); CIMS m/z 384 (M + H$^+$). Anal. ($C_{16}H_{15}F_6NO_3$) C, H, N.

(*R*)-(−)-1-(8-Trifluoromethyl-2,3,6,7-tetrahydrobenzo[1,2-*b*;4,5-*b*']difuran-4-yl)-2-aminopropane Hydrochloride ((*R*)-5c·HCl). The title compound was prepared from (*R*)-**19** by the general procedure described for compound (*R*)-**5a·HCl**: 84%; mp 314−315 °C; ^{1}H NMR (D$_2$O) δ 1.27 (d, 3 H, CHCH_3, J = 7.2 Hz), 2.87 (m, 2 H, ArCH_2CH, J = 6.9 Hz), 3.18 (t, 2 H, ArOCH$_2$CH_2, J = 9.0 Hz), 3.33 (t, 2 H, ArOCH$_2$CH_2, J = 8.6 Hz), 3.69 (m, 1 H, ArCH$_2$CH, J = 6.6 Hz), 4.61 (q, 2 H, ArOCH_2CH$_2$, J = 8.7 Hz), 4.64 (q, 2 H, ArOCH_2CH$_2$, J = 8.7 Hz); $[\alpha]_D$ = −13.33° (c = 0.0097, DMF); CIMS m/z 288 (M + H$^+$). Anal. ($C_{14}H_{17}ClF_3NO_2$) C, H, N.

(*S*)-(+)-1-(8-Trifluoromethyl-2,3,6,7-tetrahydrobenzo[1,2-*b*;4,5-*b*']difuran-4-yl)-2-aminopropane Hydrochloride ((*S*)-5c·HCl). The title compound was prepared from (*S*)-**19** by the general procedure described for compound (*R*)-**5a·HCl**: 84%; mp 314−315 °C; ^{1}H NMR (D$_2$O) δ 1.27 (d, 3 H, CHCH_3, J = 7.2 Hz), 2.87 (m, 2 H, ArCH_2CH, J = 6.9 Hz), 3.18 (t, 2 H, ArOCH$_2$CH_2, J = 9.0 Hz), 3.33 (t, 2 H, ArOCH$_2$CH_2, J = 8.6 Hz), 3.69 (m, 1 H, ArCH$_2$CH, J = 6.6 Hz), 4.61 (q, 2 H, ArOCH_2CH$_2$, J = 8.7 Hz), 4.64 (q, 2 H, ArOCH_2CH$_2$, J = 8.7 Hz); $[\alpha]_D$ = +12.90° (c = 0.0097, DMF); CIMS m/z 288 (M + H$^+$). Anal. ($C_{14}H_{17}ClF_3NO_2$) C, H, N.

(*R*)-(+)-*N*-Trifluoroacetyl-1-(8-trifluoromethylbenzo[1,2-*b*;4,5-*b*']difuran-4-yl)-2-aminopropane ((*R*)-20). The title compound was prepared from (*R*)-**19** by the general procedure described for compound (*R*)-**16**: 74%; mp 170−171 °C; ^{1}H NMR (CDCl$_3$) δ 1.27 (d, 3 H, CHCH_3, J = 6.3 Hz), 3.35 (d, 2 H, ArCH_2CH, J = 6.0 Hz), 4.48 (m, 1 H, ArCH$_2$CH, J = 7.5 Hz), 6.39 (bs, 1 H, NH), 7.68 (d, 1 H, ArH, J = 2.4 Hz), 7.07 (p, 1 H, ArH, J = 1.8 Hz), 7.74 (d, 1 H, ArH, J = 2.4 Hz), 7.77 (d, 1 H, ArH, J = 2.1 Hz); $[\alpha]_D$ = +7.46° (c = 0.0025, CH$_3$CN); CIMS m/z 380 (M + H$^+$), 360. Anal. ($C_{16}H_{11}F_6NO_3$) C, H, N.

(*S*)-(−)-*N*-Trifluoroacetyl-1-(8-trifluoromethylbenzo[1,2-*b*;4,5-*b*']difuran-4-yl)-2-aminopropane ((*S*)-20). The title compound was prepared from (*S*)-**19** by the general procedure described for compound (*R*)-**16**: 75%; mp 170−171 °C; ^{1}H NMR (CDCl$_3$) δ 1.27 (d, 3 H, CHCH_3, J = 6.3 Hz), 3.35 (d, 2 H, ArCH_2CH, J = 6.0 Hz), 4.48 (m, 1 H, ArCH$_2$CH, J = 7.5 Hz), 6.39 (bs, 1 H, NH), 7.68 (d, 1 H, ArH, J = 2.4 Hz), 7.07 (p, 1 H, ArH, J = 1.8 Hz), 7.74 (d, 1 H, ArH, J = 2.4 Hz), 7.77 (d, 1 H, ArH, J = 2.1 Hz); $[\alpha]_D$ = −7.38° (c = 0.0025, CH$_3$CN); CIMS m/z 380 (M + H$^+$), 360. Anal. ($C_{16}H_{11}F_6NO_3$) C, H, N.

(*R*)-(−)-1-(8-Trifluoromethylbenzo[1,2-*b*;4,5-*b*']difuran-4-yl)-2-aminopropane Hydrochloride ((*R*)-6c·HCl). The title compound was prepared from (*R*)-**20** by the general procedure described for compound (*R*)-**5a·HCl**: 69%; mp 282 °C dec; ^{1}H NMR (D$_2$O) δ 1.28 (d, 3 H, CHCH_3, J = 6.6 Hz), 3.41 (d, 1 H, ArCH_2CH, J = 6.9 Hz), 3.42 (d, 1 H, ArCH_2CH, J = 6.3 Hz), 3.87 (m, 1 H, ArCH$_2$CH, J = 6.6 Hz), 7.08 (d, 1 H, ArH, J = 2.7 Hz), 7.13 (p, 1 H, ArH, J = 1.8 Hz), 7.87 (d, 1 H, ArH, J = 2.4 Hz), 7.90 (d, 1 H, ArH, J = 2.1 Hz); $[\alpha]_D$ = −33.49° (c = 0.0106, DMF); CIMS m/z 284 (M + H$^+$). Anal. ($C_{14}H_{13}ClF_3NO_2$) C, H, N.

(*S*)-(+)-1-(8-Trifluoromethylbenzo[1,2-*b*;4,5-*b*']difuran-4-yl)-2-aminopropane Hydrochloride ((*S*)-6c·HCl). The title compound was prepared from (*S*)-**20** by the general procedure described for compound (*R*)-**5a·HCl**: 71%; mp 283 °C dec; ^{1}H NMR (D$_2$O) δ 1.28 (d, 3 H, CHCH_3, J = 6.6 Hz), 3.41 (d, 1 H, ArCH_2CH, J = 6.9 Hz), 3.42 (d, 1 H, ArCH_2CH, J = 6.3 Hz), 3.87 (m, 1 H, ArCH$_2$CH, J = 6.6 Hz), 7.08 (d, 1 H, ArH, J = 2.7 Hz), 7.13 (p, 1 H, ArH, J = 1.8 Hz), 7.87 (d, 1 H, ArH, J = 2.4 Hz), 7.90 (d, 1 H, ArH, J = 2.1 Hz); $[\alpha]_D$ = +33.38° (c = 0.0106, DMF); CIMS m/z 284 (M + H$^+$). Anal. ($C_{14}H_{13}ClF_3NO_2$) C, H, N.

Chromatographic Studies. All HPLC analyses were performed on a Rainin Rabbit HPX high-performance liquid chromatograph with a Knauer variable wavelength detector set to observe at 254 nm. A 20-μL injection loop was used for sample injection. A flow rate of 1 mL/min of dichloromethane was used as the mobile phase through a 250- × 4.6-mm Alltech Silica column. Chromatographic parameters reported for each solute are averages of triplicate analyses.

Representative Procedure for Amine Derivitization:[22] *N*-Trifluoroacetyl-1-(8-bromo-2,3,6,7-tetrahydrobenzo[1,2-*b*;4,5-*b*']difuran-4-yl)-2-aminopropane ((*R* or *S*)-17). To confirm that the samples of product (*R*)- and (*S*)-**5b·HCl** that were used in pharmacological evaluation were not contaminated with side products of the aromatic bromination reaction used to make (*R* or *S*)-**17**, a sample of (*R*)-**5b·HCl** was converted to the *N*-trifluoroacetyl-protected compound. Trifluoroacetic anhydride (0.010 mL, 0.072 mmol) was added dropwise to a dichloromethane (0.4 mL) solution of (*R*)-**5b·HCl** (0.010 g, 0.030 mmol), triethylamine (0.014 mL, 0.105 mmol) and 4-(dimethylamino)pyridine (0.0003 g, 0.0024 mmol). The reaction was stirred for 4 h and then diluted with dichloromethane (4 mL), washed with aqueous 2 N HCl (2 mL), saturated NaHCO$_3$ (2 mL), dried (MgSO$_4$), filtered, and evaporated to leave a clear oil. HPLC analysis of this oil indicated that it was 99.5% pure and had a retention time of 7.10 min (±0.01 min). This procedure was repeated for a sample of (*S*)-**5b·HCl**. HPLC analysis of this product indicated a 99.3% purity and a retention time of 7.11 min (±0.02 min). None of the minor impurities observed in the HPLC data trace corresponded to the fully aromatic compound (*R*)-**18** which was likewise analyzed by HPLC and found to have a retention time of 4.98 min (±0.03 min) and a purity of 99.2%. These results indicate that careful addition of bromine to the reaction discussed above and recrystallization of the product led to pure compounds and that the pharmacological data were not confounded by potent impurities.

***N*-(1-Methyl-2-(8-trifluoromethylbenzo[1,2-*b*;4,5-*b*']difuran-4-yl)ethyl)-(*R*)-MTPA Amides.** To confirm that the integrity of the chiral center remained intact throughout the reactions used in the synthetic scheme, of which several might have potentially racemized the stereocenter, products (*R*)- and (*S*)-**6c·HCl** were converted to their corresponding MTPA amides using (*R*)-(−)-α-methoxy-α-(trifluoromethyl)phenylacetyl chloride[15] ((*R*)-MTPA-Cl: Fluka) to provide the pair of diastereomers for HPLC analysis. This was accomplished by the general procedure[22] used to make the trifluoroacetyl-protected compound discussed above, using 2.4 equiv of (*R*)-MPTA-Cl in place of the trifluoroacetic anhydride. The oils that were obtained were dissolved in dichloromethane to give equal concentrations of each solute. To be certain baseline separation could be accomplished using the HPLC conditions discussed above, an equimolar mixture of the pure amides was prepared by combining equal volumes of the two amide solutions and performing HPLC analysis on this mixture. Excellent resolution was obtained, with approximately 2.2 min of baseline separation between the two eluted diastereoisomers. The 2*R*,1′*S*-amide was analyzed by HPLC and found to be 99.4% pure, with a retention time of 11.69 min (±0.03 min). A very small peak that corresponded to the 2*R*,1′*R*-amide was observed however, which accounted for the other 0.6% of the injected sample. The 2*R*,1′*R*-amide was also analyzed by HPLC and found to be 100.0% pure, with a retention time of 13.95 min (±0.01 min). These results indicated that racemization had not occurred in the synthesis of these products. Further, because products (*R*)- and (*S*)-**6c·HCl** were subjected to all possible reaction conditions in the synthetic scheme, one may

deduce that all the other products are likewise enantiomerically pure. The small amount of the 2*R*,1′*R*-amide found in the 2*R*,1′*S*-amide most likely arose as a consequence of the slightly lower purity of the L-alanine starting material.

Pharmacology Methods. 1. Cell Culture. NIH-3T3 fibroblast cells stably transfected to express either the rat 5-HT_{2A} or 5-HT_{2C} receptor[23] were maintained in minimum essential medium, containing 10% dialyzed fetal bovine serum (Gibco BRL) and supplemented with L-glutamine, Pen/Strep, and Geneticin. The cells were cultured at 37 °C in a water saturated atmosphere of 95% air and 5% CO_2. For radioligand binding assays, cells were split into 100-mm² culture dishes when they reached 90% confluency. Upon reaching 100% confluency in the culture dishes, the cells were washed with sterile filtered phosphate-buffered solution and left to incubate in serum-free Opti-MEM for 5 h. After this incubation, the cells were harvested by centrifugation (15000*g*, 20 min) and placed immediately in a freezer at −80 °C until the assay was performed. For phosphoinositide hydrolysis experiments the cells were seeded into 24-well plates and assays were performed when 70% confluency was achieved.

2. Radioreceptor Competition Assays. For saturation assays, 0.125−6 nM [^{3}H]DOB or [^{125}I]DOI were used. The total volume of the assay was 250 μL. Nonspecific binding was defined in the presence of 10 μM cinanserin (rat 5-HT_{2A}-expressing cells) or 10 μM mianserin (rat 5-HT_{2C}-expressing cells). Competition binding experiments were carried out in a total volume of 500 μL with either 1.0 nM [^{3}H]DOB or 0.20 nM [^{125}I]DOI. Previously harvested cells were resuspended and added to each well containing assay buffer (50 mM Tris, 0.5 mM EDTA, 10 mM $MgCl_2$; pH = 7.4), radioligand, and new compound (or in the case of the saturation assays, cinanserin or mianserin). Incubation was carried out at 25 °C for 60 min and terminated by rapid filtration using a prechilled Packard 96-well harvester with GF/B Uni-filters that had been preincubated for 30 min in 0.3% polyethylenimine. The filters were rinsed using chilled wash buffer (10 mM Tris, 154 mM NaCl) and left to dry overnight. The following day, Microscint-O was added and radioactivity was determined using a TopCount (Packard) scintillation counter. GraphPad Prism (GraphPad Software, San Diego, CA) was used to analyze the saturation and competition binding curves.

3. Phosphoinositol Hydrolysis Studies in NIH-3T3 Cells Expressing the 5-HT_{2A} Receptor. Accumulation of inositol phosphates was determined using a modified version of a previously published protocol.[24] Briefly, cells expressing the rat 5-HT_{2A} receptor were labeled for 18−20 h in CRML medium containing 1.0 μCi/mL [^{3}H]*myo*-inositol. After pretreating the cells with 10 μM pargyline/10 mM LiCl for 15 min, the cells were placed in the presence of agonist for 30 min at 37 °C, under an atmosphere of 95% O_2 and 5% CO_2. The assay was terminated by aspirating the medium and adding 10 mM formic acid. After incubation for 16 h at 4 °C, the [^{3}H]inositol phosphates were separated from the cellular debris on Dowex-1 ion-exchange columns and eluted with 1.0 M ammonium formate and 0.10 M formic acid. The vials were counted for tritium using a TriCarb scintillation counter (Packard Instrument Corp.).

Acknowledgment. We thank S. Frescas and A. Monte for their helpful contributions in optimizing the synthesis of the benzodifuran nucleus. We also thank Dr. David Julius (UCSF) for his kind donation of the 5-$HT_{2A/2C}$ cell lines. This work was supported by Grant DA02189 from NIDA and by a grant from the Heffter Research Institute.

References

(1) Sanders-Bush, E.; Mayer, S. E. 5-Hydroxytryptamine (Serotonin) Receptor Agonists and Antagonists. In *The Pharmacological Basis of Therapeutics*, 9th ed.; Hardman, J. G., Limbird, L. E., Molinoff, P. B., Ruddon, R. W., Gilman, A. G., Eds.; McGraw-Hill: New York, 1996; pp 249−263.

(2) Aghajanian, G. K.; Marek, G. J. Serotonin-Glutamate Interactions: A New Target for Antipsychotic Drugs. *Neuropsychopharmacology* **1999**, *21*, S122−S1333.

(3) Roth, B. L.; Willins, D. L.; Kristiansen, K.; Kroeze, W. K. 5-Hydroxytryptamine$_2$−Family Receptors (5-Hydroxytryptamine$_{2A}$, 5-Hydroxytryptamine$_{2B}$, 5-Hydroxytryptamine$_{2C}$): Where Structure Meets Function. *Pharmacol. Ther.* **1998**, *79*, 231−257.

(4) Boess, F. G.; Martin, I. L. Molecular Biology of 5-HT Receptors. *Neuropharmacology* **1994**, *33*, 275−317.

(5) Monte, A. P.; Marona-Lewicka, D.; Kanthasamy, A.; Sanders-Bush, E.; Nichols, D. E. Stereoselective LSD-like Activity in a Series of d-Lysergic-Acid Amides of (*R*)-2-Aminoalkanes and (*S*)-2-Aminoalkanes. *J. Med. Chem.* **1995**, *38*, 958−966.

(6) Oberlender, R.; Ramachandran, P. V.; Johnson, M. P.; Huang, X.; Nichols, D. E. Effect of a Chiral 4-Alkyl Substituent in Hallucinogenic Amphetamines. *J. Med. Chem.* **1995**, *38*, 3593−3601.

(7) Monte, A. P.; Waldman, S. R.; Marona-Lewicka, D.; Wainscott, D. B.; Nelson, D. L.; Sanders-Bush, E.; Nichols, D. E. Dihydrobenzofuran Analogues of Hallucinogens. 4. Mescaline Derivatives. *J. Med. Chem.* **1997**, *40*, 2997−3008.

(8) Parker, M. A.; Marona-Lewicka, D.; Lucaites, V. L.; Nelson, D. L.; Nichols, D. E. A Novel (Benzodifuranyl)aminoalkane with Extremely Potent Activity at the 5-HT_{2A} Receptor. *J. Med. Chem.* **1998**, *41*, 5148−5149.

(9) Parker, M. A. Studies of Perceptiotropic Phenethylamines: Determinants of Affinity for the 5-HT_{2A} Receptor. Ph.D. Thesis, Purdue University, 1998.

(10) Blade-Font, A.; Rocabayera, T. M. Synthesis of Dihydrobenzofurans from Phenolic Mannich Bases and their Quaternized Derivatives. *J. Chem. Soc., Perkin Trans. 1* **1982**, *38*, 841−848.

(11) Monte, A. P.; Marona-Lewicka, D.; Parker, M. A.; Wainscott, D. B.; Nelson, D. L.; Nichols, D. E. Dihydrobenzofuran Analogues of Hallucinogens. 3. Models of 4-Substituted (2,5-Dimethoxyphenyl)alkylamine Derivatives with Rigidified Methoxy Groups. *J. Med. Chem.* **1996**, *39*, 2953−2961.

(12) Curphey, T. J. Trifluoroacetylation of Amino Acids and Peptides by Ethyl Trifluoroacetate. *J. Org. Chem.* **1979**, *44*, 2805−2807.

(13) Nordlander, J. E.; Payne, M. J.; Njoroge, F. G.; Balk, M. A.; Laikos, G. D.; Vishwanath, V. M. Friedel−Crafts Acylation with *N*-(Trifluoroacetyl)-α-amino Acid Chlorides. Application to the Preparation of β-Arylalkylamines and 3-Subsituted 1,2,3,4-Tetrahydroisoquinolines. *J. Org. Chem.* **1984**, *49*, 4107−4111.

(14) Moron, J.; Bisagni, E. Synthesis of 4-Methylfuro[3′,2′:5,6]benzofuro[3,2-c]pyridine. *J. Heterocycl. Chem.* **1986**, *23*, 1637−1639.

(15) Carr, G. E.; Chambers, R. D.; Holmes, T. F.; Parker, D. G. Sodium Perfluoroalkane Carboxylates as Sources of Perfluoroalkyl Groups. *J. Chem. Soc., Perkin Trans. 1* **1988**, *38*, 921−926.

(16) Dale, J. A.; Dull, D. L.; Mosher, H. S. α-Methoxy-α-trifluoromethylphenylacetic Acid, a Versatile Reagent for the Determination of Enantiomeric Composition of Alcohols and amines. *J. Org. Chem.* **1969**, *34*, 2543−2549.

(17) Makriyannis, A.; Knittel, J. Conformational-Analysis of Amphetamine in Solution Based on Unambiguous Assignment of the Diastereotopic Benzylic Protons in the H-1-NMR Spectra. *Tetrahedron Lett.* **1981**, *22*, 4631−4634.

(18) Nichols, D. E.; Frescas, S.; Marona-Lewicka, D.; Huang, X.; Roth, B. L.; Gudelsky, G. A.; Nash, J. F. 1-(2,5-Dimethoxy-4-(trifluoromethyl)phenyl)-2-aminopropane − A Potent Serotonin 5-$HT_{2A/2C}$ Agonist. *J. Med. Chem.* **1994**, *37*, 4346−4351.

(19) Siubesma, R. P.; Nolte, R. J. M. Synthesis of Concave Receptors Derived from Diphenylglycoluril. *Recl. Trav. Chim. Pays-Bas* **1993**, *112*, 643−647.

(20) Ellison, R. A.; Kotsonis, F. N. Complexation as a Factor in Metalation Reactions. Metalation of 1-Methoxy-2-phenoxyethane. *J. Org. Chem.* **1973**, *38*, 4192−4196.

(21) Alabaster, R. J.; Cottrell, I. F.; Marley, H.; Wright, S. H. B. The synthesis of 5-Substituted 2,3-Dihydrobenzofurans. *Synthesis* **1988**, 950−952.

(22) Jackson, P. T.; Kim, T.-Y.; Carr, P. W. Diastereomeric Selectivity of Carbon-Coated Zirconia Reversed-Phase Liquid Chromatographic Media. *Anal. Chem.* **1997**, *69*, 5011−5017.

(23) Julius, D.; Huang, K. N.; Livelli, T. J.; Axel, R.; Jessell, T. M. The 5HT$_2$ receptor defines a family of structurally distinct but functionally conserved serotonin receptors. *Proc. Natl. Acad. Sci. U.S.A.* **1990**, *87*, 928−932.

(24) Berg, K. A.; Clarke, W. P.; Sailstad, C.; Saltzman, A.; Maayani, S. Signal Transduction Differences Between 5-Hydroxytryptamine Type 2A and Type 2C Receptor Systems. *Mol. Pharmacol.* **1994**, *46*, 477−484.

JM000491Y